

Analytic Techniques for Calculating Two-Loop Yang–Mills Amplitudes

Adam R. Dalglish

Department of Physics
Swansea University

Primary supervisor
Dr Warren Perkins

Submitted to Swansea University in fulfilment of the requirements
for the degree of Doctor of Philosophy in Physics
2023

Copyright: The Author, Adam R. Dalglish, 2023.

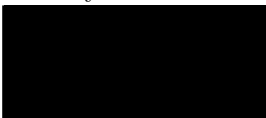
Distributed under the terms of a Creative Commons Attribution 4.0 License
(CC BY 4.0).

Abstract

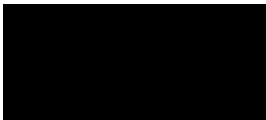
This thesis explores the use of analytic techniques for calculating pure Yang–Mills amplitudes. The main focus is on deriving two-loop amplitudes, representing the forefront of current efforts, using the methods of four-dimensional unitarity and augmented recursion. To this end, the two-loop all-plus helicity amplitudes are presented in full colour, for six and seven gluons. Results are analytic, compact expressions with manifest symmetries. A detailed discussion of augmented recursion is presented, including an algorithmic way to determine the required off-shell currents. Wider issues of the reduction of analytic results to simpler forms are also discussed, with various examples considered over one and two loops.

Declaration

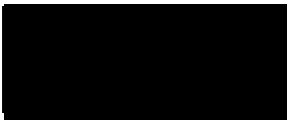
This work has not previously been accepted in substance for any degree and is not being concurrently submitted in candidature for any degree.

Signed  (20/02/2023)


This thesis is the result of my own investigations, except where otherwise stated. Other sources are acknowledged by footnotes giving explicit references. A bibliography is appended.

Signed  (20/02/2023)

I hereby give consent for my thesis, if accepted, to be available for photocopying and for inter-library loan, and for the title and summary to be made available to outside organisations.

Signed  (20/02/2023)

The University's ethical procedures have been followed and, where appropriate, that ethical approval has been granted.

Signed  (20/02/2023)

Contents

List of Tables	xiii
List of Figures	xv
1 Introduction	1
1.1 Yang–Mills Theory	2
1.2 Tree Amplitudes	6
1.3 One-loop Amplitudes	10
1.4 Two-loop Amplitudes	14
1.5 Thesis Outline	18
2 Foundations of Amplitude Techniques	21
2.1 Introduction	21
2.2 Colour Decomposition	22
2.2.1 Colour trace basis	23
2.2.2 Partial amplitudes	26
2.2.3 Decoupling identities	28
2.3 Spinor-Helicity Formalism	29
2.3.1 Spinor definitions	30
2.3.2 Using spinors in amplitudes	32
2.3.3 Little group scaling	33
3 The Six Gluon Two-Loop Amplitude	35
3.1 Introduction	35
3.2 Structure of the Amplitude	36
3.2.1 Colour decomposition	36
3.2.2 Singularity structure	39
3.3 Unitarity	41
3.4 Augmented Recursion	44

3.5	Rational Piece Reconstruction	47
3.5.1	Rational piece $R_{6:2,2}^{(2)}$	48
3.5.2	Rational piece $R_{6:4}^{(2)}$	51
3.6	Collinear Momentum Limits	55
3.7	Conclusions	57
4	The Seven Gluon Two-Loop Amplitude	59
4.1	Introduction	59
4.2	Full Colour Amplitudes	60
4.2.1	Decoupling identities	62
4.3	Structure of the Amplitude	64
4.4	Polylogarithmic Terms	64
4.4.1	Basis functions	66
4.4.2	$P_{7:1}$	69
4.4.3	$P_{7:2}$	70
4.4.4	$P_{7:3}$	71
4.4.5	$P_{7:4}$	74
4.4.6	$P_{7:1,1}$	76
4.4.7	$P_{7:1,2}$	78
4.4.8	$P_{7:1,3}$	81
4.4.9	$P_{7:2,2}$	83
4.4.10	$P_{7:1B}$	85
4.4.11	Validity checks	88
4.5	Rational Terms	89
4.5.1	Tree to two-loop factorisation	89
4.5.2	One-loop to one-loop factorisation	90
4.5.3	Non-factorising augmented recursion piece	91
4.5.4	Results and consistency checks	93
4.5.5	$R_{7:1}$	94
4.5.6	$R_{7:2}$	95
4.5.7	$R_{7:3}$	95
4.5.8	$R_{7:4}$	95
4.5.9	$R_{7:1,1}$	100
4.5.10	$R_{7:1,2}$	105
4.5.11	$R_{7:1,3}$	106
4.5.12	$R_{7:2,2}$	106

4.5.13	$R_{7:1B}$	107
4.6	Collinear Momentum Limits	109
4.7	Conclusions	110
5	Currents and their Integration	113
5.1	Introduction	113
5.2	Deriving Currents	114
5.2.1	Note about poles	116
5.2.2	A systematic method	116
5.3	The Two-Loop Five-Point Current	118
5.3.1	Previous result	119
5.3.2	New derivation	119
5.3.3	Checks with simplifying reference momentum	120
5.3.4	Checks with a general reference momentum	122
5.4	The Two-Loop Seven-Point Currents	127
5.4.1	The adjacent current	129
5.4.2	The singly non-adjacent current	130
5.4.3	The doubly non-adjacent current	131
5.5	Integrating Currents	131
5.5.1	Manipulations to aid integration	132
5.5.2	Feynman integration	134
5.5.3	Integration results	137
5.6	Conclusions	139
6	Reconstruction of Rational Functions	141
6.1	Introduction	141
6.2	Overview of the Method	142
6.2.1	Leading poles	142
6.2.2	Sub-leading poles	145
6.3	One-Loop Partial Amplitudes	146
6.3.1	Single-minus helicity $A_{5:2}^{(1)}(a^+, b^-, c^+, d^+, e^+)$	146
6.3.2	All-plus helicity $A_{5:2}^{(1)}(a^+, b^+, c^+, d^+, e^+)$	148
6.3.3	Single-minus helicity $A_{5:2}^{(1)}(a^-, b^+, c^+, d^+, e^+)$	149
6.3.4	Single-minus helicity $A_{6:4}^{(1)}(a^-, b^+, c^+, d^+, e^+, f^+)$	150
6.4	Seven-Point Two-Loop Rational Pieces	155

Contents

6.5	Seven-Point Rational Piece $R_{7:1,1}^{(2)}$	157
6.5.1	Augmented recursion output	157
6.5.2	Pole tests	158
6.5.3	Leading pole factorisations	158
6.5.4	Sub-leading pole fitting	170
6.6	Seven-Point Rational Piece $R_{7:4}^{(2)}$	176
6.6.1	Augmented recursion output	177
6.6.2	Pole tests	177
6.6.3	Leading pole factorisations	178
6.6.4	Sub-leading pole fitting	188
6.7	Conclusions	194
7	Conclusions	195

Acknowledgements

Many thanks to Dr Warren Perkins. His support and advice has been invaluable throughout my time at Swansea, especially through lockdowns and remote working.

Thanks also to Professor David Dunbar, whose perspective showed me other ways of thinking about amplitudes.

Thanks to Dr Joe Strong and Dr John Godwin for their help when I was getting started, and to Siddharth Pandey as well for the useful discussions.

List of Tables

1.1	Feynman rules for the propagator and vertices of pure Yang–Mills theory, in the axial gauge.	5
1.2	The number of Feynman diagrams required to calculate an amplitude in pure Yang–Mills theory, where n gluons interact.	6
1.3	Momentum dimensions and helicity state choices made in different dimensional regularisation schemes.	11
2.1	Colour-ordered Feynman rules for the propagator and vertices of pure Yang–Mills theory, in the axial gauge.	27
6.1	Results of numerical pole tests on $A_{6;4}^{(1)}(a^-, b^+, c^+; d^+, e^+, f^+)$, to find coinciding poles.	153
6.2	Approximate expression sizes for the seven-point rational pieces calculated using augmented recursion.	156
6.3	Results of numerical pole tests on $R_{7;4}^{(2)}(a^+, b^+, c^+; d^+, e^+, f^+)$, to find coinciding poles.	171
6.4	Results of numerical pole tests on $R_{7;4}^{(2)}(a^+, b^+, c^+; d^+, e^+, f^+)$, to find coinciding poles	189
6.5	Approximate expression sizes and evaluation times for the reconstructed seven-point rational pieces.	194

List of Figures

1.1	Diagrams depicting unitarity cutting.	13
3.1	The quad-cut four-dimensional unitarity diagrams which provide the coefficients of polylogarithms in $P_{6:\lambda}^{(2)}(1^+, 2^+, 3^+, 4^+, 5^+, 6^+)$	43
3.2	The augmented recursion diagram for the two-loop six-point rational piece. 46	
4.1	The quad-cut four-dimensional unitarity diagrams that determine the coefficients of polylogarithms in $P_{n:\lambda}^{(2)}(1^+, 2^+, \dots, n^+)$	65
4.2	The three unitarity structures that contribute to $P_{7:\lambda}^{(2)}(1^+, 2^+, \dots, 7^+)$, labelled with the number, r , of external momenta originating on the MHV tree amplitude.	67
4.3	The tree to two-loop factorisation, which gives rise to a simple pole in s_{ab} . 90	
4.4	The one-loop to one-loop factorisation, which gives rise to a simple pole in t_{abc}	91
4.5	The one-loop to one-loop factorisation that gives rise to double poles in s_{ab}	92
4.6	Augmented recursion diagram containing both double and simple s_{ab} pole contributions.	92

1 Introduction

The Standard Model of Particle Physics is the most successful theory of nature devised so far, with scattering amplitudes being the tool through which it makes its predictions in modern experiments. Describing three of the four fundamental forces and all the known particles, it successfully predicted the existence of the W and Z bosons, gluons, the top and charm quarks, as well as the most recently experimentally verified Higgs boson. The latter detection, at the Large Hadron Collider (LHC), relied heavily on perturbative amplitude calculations to set out the expected behaviour of the theory, which were then confirmed in high-energy scattering events. As the LHC, and future experiments, probe higher energy levels and greater precision, we will require scattering amplitudes to be calculated to correspondingly higher orders and numbers of particles [1, 2].

Although it is highly impressive in its scope and predictions, the Standard Model does not account for all phenomena. Most significantly, it does not contain the force of gravity, for which we must turn to general relativity. Cosmology also calls for some form of dark matter, to explain the form of the cosmic microwave background, galactic dynamics and gravitational lensing. In addition, some form of dark energy is expected to cause the accelerating expansion of the universe we see today.

The hope is that at higher energies, experiments may find deviations from the Standard Model that point towards a more complete theory, incorporating some or all of the above features. So far, no signs of postulated new physics, such as extra symmetry supersymmetry, have appeared. But some candidate particles for dark matter, such as certain types of weakly interacting massive particles, are of masses that should be produced in upcoming collision experiments if those theories are correct. In order to determine whether such events occur, the Standard Model prediction must be known precisely in order to compare to experiment. For that, we must calculate amplitudes.

The Standard Model is a gauge theory, with symmetry group $SU(3) \times SU(2) \times U(1)$. The portion $SU(2) \times U(1)$ contains the electroweak symmetry, which is partially broken by the Higgs mechanism, leaving a new $U(1)$ symmetry with the photon as its associated

gauge boson. The $SU(3)$ symmetry is that of QCD, or the strong interaction, and has the gluon as its force carrier. Particles with a colour charge interact under the strong interaction, with the strength of the strong coupling constant decreasing at higher energy scales [3]. This fact makes a perturbative approach appropriate when considering, for example, high-energy collider experiments.

The phenomenon of colour confinement means that particle colliders do not detect free quarks. Rather, they detect jets of strongly bound particles, produced from the energy put into separating two quarks bound by the strong force. While the photon is not charged under electromagnetism, the gluon does have a colour charge, which allows them to interact with each other. As a result, a theory with only gluons already has significant complexity. Calculating perturbative amplitudes in such a theory will be the topic of this thesis.

1.1 Yang–Mills Theory

Yang–Mills theories are quantum field theories based on non-abelian gauge groups [4]. Both the electroweak ($SU(2) \times U(1)$) and strong ($SU(3)$) interactions in the Standard Model fit this description. It is the gluons of the Standard Model that this thesis will investigate, but a more general symmetry group $SU(N_c)$ can be chosen with N_c colours, rather than the three of the Standard Model. In fact, further generalising to consider the group $U(N_c)$ will lead to additional useful identities when we come to inspect the colour structures of the resulting amplitudes. These will be described in detail in Chapter 2.

The Lagrangian of pure Yang–Mills is

$$\mathcal{L}_{YM} = -\frac{1}{4}\text{Tr}(F_{\mu\nu}F^{\mu\nu}), \quad (1.1)$$

where the field strength $F_{\mu\nu}$ is

$$F_{\mu\nu} = \partial_\mu A_\nu - \partial_\nu A_\mu - ig[A_\mu, A_\nu], \quad (1.2)$$

written in terms of the gauge field of the gluons, A_μ . Specifying the gauge group to be $U(N_c)$, the A_μ are Hermitian $N_c \times N_c$ matrices. (For an $SU(N_c)$ group, they would also be traceless.)

We can consider local transformations $U(x)$, where $U(x)$ is a matrix of the gauge group at each point in space. The transformation is applied to the gauge field according

to the rule

$$A_\mu(x) \rightarrow U(x)A_\mu(x)U^\dagger(x) + \frac{i}{g}U(x)\partial_\mu U^\dagger(x), \quad (1.3)$$

leading to the field strength tensor transforming as

$$F_{\mu\nu} \rightarrow U(x)F_{\mu\nu}U^\dagger(x). \quad (1.4)$$

With $U(x)$ being unitary, the Lagrangian is invariant under the transformation. The group $U(N_c)$ is a local symmetry of the Lagrangian.

Typically, the next step taken when analysing a theory is to consider infinitesimal gauge transformations, to gain an understanding of the generators of the Lie algebra. Expanding around the identity and showing matrix indices explicitly,

$$U_i^j(x) = \delta_i^j - ig\theta^a(x)(T^a)_i^j, \quad (1.5)$$

where $(T^a)_i^j$ are the generators of $U(N_c)$ and $\theta^a(x)$ are their small parameters. The generators are $N_c \times N_c$ Hermitian matrices, as a result of the the unitarity condition on $U_i^j(x)$. There is an implied sum over the repeated index $a = \{1, 2, \dots, N_c^2\}$, and the matrix indices run over $i, j = \{1, 2, \dots, N_c\}$. (For the case of an $SU(N_c)$ gauge group, the generators would also be traceless and as a result there would be one fewer entry in the sum over a .) The commutation relation of the generators,

$$[T^a, T^b] = if^{abc}T^c, \quad (1.6)$$

defines a structure constant f^{abc} for the gauge group, where a choice of normalisation has been made. With this, the gauge field and field strength tensor can be expanded in a basis of generators T^a as

$$\begin{aligned} (A_\mu)_i^j(x) &= A_\mu^a(x)(T^a)_i^j, \\ (F_{\mu\nu})_i^j(x) &= F_{\mu\nu}^a(x)(T^a)_i^j, \end{aligned} \quad (1.7)$$

which allows us to re-express the field strength via

$$F_{\mu\nu}^a = \partial_\mu A_\nu^a - \partial_\nu A_\mu^a + gf^{bca}A_\mu^b A_\nu^c. \quad (1.8)$$

The structure constant appears in the self-interacting term, so this constant of the colour algebra appears whenever interactions between gluons take place. Choosing a

1 Introduction

convenient basis for the generators such that

$$\mathrm{Tr}[T^a T^b] = \delta^{ab}, \quad (1.9)$$

it is possible to express the structure constants back in terms of generator matrices if desired, through

$$f^{abc} = -i\mathrm{Tr}[T^a [T^b, T^c]]. \quad (1.10)$$

The normalisation here is a result of previous choices.

With the Lagrangian of the theory specified, it is possible to write down Feynman rules for gluon interactions. A traditional way of calculating amplitudes would then be to draw all the allowed Feynman diagrams for the desired set of incoming and outgoing external states, interpreting each as an expression according to the rules. Evaluating each diagram, the sum yields the amplitude.

Such a procedure might begin as follows. First, the gauge is fixed according to the Faddeev–Popov procedure, to avoid problems in the path integral formulation. When making a gauge choice, ghosts are generally added to the Lagrangian and must also be included in the Feynman rules. However, the choice of axial gauge,

$$\mathcal{L}_{GF} = -\frac{1}{2\xi}(q^\mu A_\mu^a)^2, \quad (1.11)$$

is particularly convenient in pure Yang–Mills, as it leads to ghosts decoupling from gluons.¹ Light cone gauge can be used to fix the remaining ambiguities. The resulting Feynman rules are stated in Table 1.1, where ghosts have been ignored. External gluons require a polarisation state $\epsilon_\mu^\pm(p)$, where $p \cdot \epsilon^\pm(p) = 0$ and $p^2 = 0$, to be contracted with the propagators and vertices. Any loops in diagrams will contain momenta not fixed by the external particles, which should be integrated over.

To work in perturbation theory, the coupling constant of the theory must be small. With the constant $\alpha_s \equiv g^2/(4\pi)$ defined in terms of the Yang–Mills coupling g , the condition required for an expansion to be meaningful is that $\alpha_s < 1$. The values experienced in a collision at the LHC are, for example, around $\alpha_s(Q^2) \sim 0.1$ for an interaction energy of $Q \sim 1\mathrm{TeV}$ [3] and decrease with greater interaction energies.

¹It will also be appropriate for use with the spinor-helicity formalism introduced in later chapters, as the reference momentum introduced must have $q^2 = 0$. Where calculation techniques in the following chapters call for a reference momentum, they can also be identified with the same q .

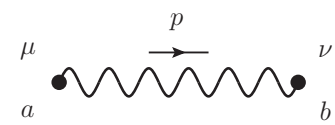
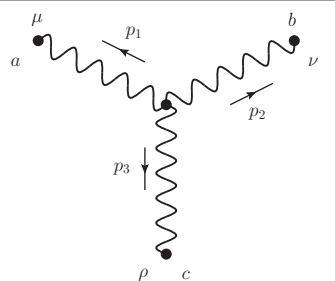
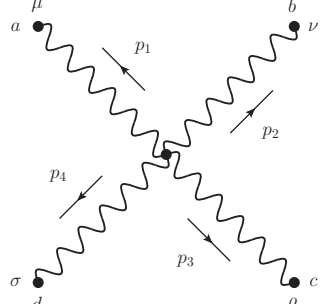
Propagator	
	$\Delta_{\mu\nu}^{ab}(p) = \frac{i\delta^{ab}}{p^2} \left(-\eta_{\mu\nu} + \frac{p_\mu q_\nu + q_\mu p_\nu}{p \cdot q} \right)$
Vertices	
	$V_{\mu\nu\rho}^{abc}(p_1, p_2, p_3) = igf^{abc} \left(\eta^{\mu\nu}(p_1 - p_2)^\rho \right. \\ \left. + \eta^{\nu\rho}(p_2 - p_3)^\mu \right. \\ \left. + \eta^{\rho\mu}(p_3 - p_1)^\nu \right)$
	$V_{\mu\nu\rho\sigma}^{abcd}(p_1, p_2, p_3, p_4) = \\ ig^2 \left(f^{abe} f^{cde} (\eta_{\mu\rho} \eta_{\nu\sigma} - \eta_{\mu\sigma} \eta_{\nu\rho}) \right. \\ \left. + f^{ace} f^{dbe} (\eta_{\mu\sigma} \eta_{\rho\nu} - \eta_{\mu\nu} \eta_{\rho\sigma}) \right. \\ \left. + f^{ade} f^{bce} (\eta_{\mu\nu} \eta_{\sigma\rho} - \eta_{\mu\rho} \eta_{\sigma\nu}) \right)$

Table 1.1: Feynman rules for the propagator and vertices of pure Yang–Mills theory, in the axial gauge. Ghosts decouple from gluons, so are not featured. In addition to these, each external particle will require a polarisation vector, and loop momenta should be integrated over.

Therefore it is acceptable to expand an n -gluon amplitude \mathcal{A}_n in terms of loop amplitudes, multiplying successive powers of this small constant. (The explicit definition of the expansion is chosen in Chapter 2.) The loop amplitudes, written $\mathcal{A}_n^{(\ell)}$, can be found in the Feynman diagram approach by evaluating all the valid diagrams featuring ℓ loops. The hierarchy of scale means that the $\ell = 0$ “tree” amplitudes are expected to give the largest contribution to the overall amplitude. They are also the simplest to calculate, so are generally obtained first. More precise predictions require calculations of higher loop numbers.

This procedure is intuitive, and works well for tree amplitudes with small numbers of interacting particles. However, the number of diagrams that must be evaluated grows exponentially as the number of interacting gluons, and number of loops, increases. Restricting only to tree amplitudes, the number of diagrams needed makes the calculation

1 Introduction

n	4	5	6	7	8	9	10
Tree	4	25	220	2485	34 300	559 405	10 525 900
One-loop				227 585			

Table 1.2: The number of Feynman diagrams required to calculate an amplitude in pure Yang–Mills theory, where n gluons interact [5].

become intractable for even a modest number of interacting gluons, and the situation is even worse at loop level, as illustrated in Table 1.2 [5]. Additionally, the diagrams corresponding to interactions of more gluons, or higher loops, will individually be longer, more complicated expressions. Clearly, other methods are needed for calculating more difficult amplitudes. A core issue with the Feynman diagram approach, which is suggestive of the way forward, is that each diagram is dependent on the gauge choice taken. In contrast, the overall amplitude must be gauge-invariant because it is an observable. The many diagrams must combine in some complex way to arrive at a gauge-invariant result, meaning significant effort will be needed to write that result in a simple, compact form. As an example, the choice of axial gauge means a reference momentum q has been introduced into every propagator, but must eventually cancel out of the result.

The issue of gauge invariance suggests that in general, the Feynman diagram approach is not a particularly efficient method for calculating amplitudes. It takes a Lagrangian of a theory, with no particular gauge dependence, then through laborious gauge-dependent intermediate steps arrives at a gauge-independent amplitude. A reasonable question to ask would be whether a derivation process could exist that dealt with gauge-invariant objects throughout, therefore avoiding introducing redundant gauge information that must be subject to cancellations and simplifications later.

1.2 Tree Amplitudes

A major step towards such a scheme was made in 1988 with ref. [6], where a new way of decomposing an amplitude on a basis of colour structures was presented. The key insight employed was to use the relation of eq. 1.10 to replace structure constants that arise from diagram vertices with traces of the generator matrices. Collecting together terms containing equivalent traces, it was found that amplitudes separated into kinematic functions multiplying distinct colour trace strings. Those kinematic functions, which are referred to in this thesis as “partial amplitudes”, are individually gauge-invariant. For tree amplitudes, only one type of partial amplitude occurred in the decomposition, with the difference between terms being solely one of leg ordering.

Calculations of that partial amplitude followed straightforwardly from “colour-ordered Feynman rules”, where the colour factors are stripped out of the usual Feynman rules and only diagrams with a particular cyclic order of legs are considered. The partial amplitudes showed further useful properties, such as being invariant under cyclic permutations of their arguments, matching the symmetry of their associated trace structure.

Later work on one-loop amplitudes [7] and above [8] would demonstrate how this colour trace decomposition works for general loop amplitudes. More types of trace structure appear at greater numbers of loops, due to the increased number of ways that the structure constants can combine in a diagram. The precise forms of these tree- and loop-level colour decompositions are deferred to the next chapter, along with the statement of the previously mentioned colour ordered Feynman rules. Colour trace decomposition is an important technology used up to the present, including in this thesis, so Section 2.2 is devoted to specifying it, and its consequences, in detail.

The choice of $U(N_c)$ as the Yang–Mills gauge symmetry group, rather than the more typically used $SU(N_c)$, also allows a procedure for obtaining identities relating different partial amplitudes, known as “decoupling identities”. (See Section 2.2 for its full description.) In ref. [7], the authors show how repeated application of one-loop decoupling identities allows any one-loop partial amplitude to be expressed in terms of a single “leading in colour” partial amplitude.² For two-loop and greater amplitudes, the leading in colour partial amplitude does not fully determine the amplitude. However, decoupling identities do still reduce the number of independent partial amplitudes needed to specify the “full colour” amplitude.³

We see that the colour trace decomposition contains redundancy, as shown by the existence of decoupling identities between the structures. In fact, those identities do not fully exhaust the redundancies between partial amplitudes. Additional relations were found in refs. [9, 10] for some specific one-loop amplitudes, by considering alternative ways of presenting the colour structure of an amplitude. Different types of colour decomposition have been developed, with purposes such as expressing the amplitude in terms of a minimal set of independent structures [11, 12].

²At one-loop, the partial amplitude multiplying the single colour trace is often referred to as “leading in colour”, due to it being accompanied by a factor of N_c , which is not present in the two-trace “sub-leading in colour” partial amplitudes. The terminology generalises straightforwardly to greater numbers of loops, where N_c^ℓ multiplies the leading in colour partial amplitude. Although this language might usually imply an expansion, N_c is not necessarily large in this thesis and all partial amplitudes are of importance.

³The term “full colour” is often used to emphasise that a complete loop amplitude is being referred to, rather than one of the partial amplitudes that constitute its colour decomposition.

1 Introduction

An early success in realising simple forms for Yang–Mills amplitudes came from Parke and Taylor, who postulated an n -point form for the maximally helicity violating (MHV) tree partial amplitude [13], which is the amplitude with two gluons of negative helicity and the rest of positive helicity. That form was later proved in ref. [14]. The result is particularly compact and possesses a cyclic denominator factor that is ubiquitous in later amplitude calculations, becoming known as the Parke–Taylor denominator.

Up until this point, amplitude calculations had been carried out in terms of the four-momenta of the external gluons. However, work by several authors established that amplitudes could be represented more compactly if spinors were used to represent the momenta of massless particles [15, 16, 17, 18], in what is known as the “spinor-helicity formalism”. Briefly, the approach taken is to replace each four-momentum p_i^μ with a pair of two-component spinors λ_i^α and $\tilde{\lambda}_i^{\dot{\alpha}}$, according to

$$p^{\dot{\alpha}\alpha} = p^\mu \bar{\sigma}_\mu^{\dot{\alpha}\alpha} = \tilde{\lambda}^{\dot{\alpha}} \lambda^\alpha. \quad (1.12)$$

The factor $\bar{\sigma}_\mu^{\dot{\alpha}\alpha} = (\mathbb{I}, \vec{\sigma})$ contains the Pauli matrices. Expressions can then be built out of Lorentz-invariant spinor products, defined

$$\begin{aligned} \langle ij \rangle &\equiv \lambda_i^\alpha \lambda_{j\alpha} = \epsilon_{\alpha\beta} \lambda_i^\alpha \lambda_j^\beta = -\langle ji \rangle, \\ [ij] &\equiv \tilde{\lambda}_{i\dot{\alpha}} \tilde{\lambda}_j^{\dot{\alpha}} = -\epsilon_{\dot{\alpha}\dot{\beta}} \tilde{\lambda}_i^{\dot{\alpha}} \tilde{\lambda}_j^{\dot{\beta}} = -[ji], \end{aligned} \quad (1.13)$$

where the Levi-Civita antisymmetric tensor raises and lowers spinor indices.

The spinor-helicity formalism is another technology of great importance to present-day work, and the work in this thesis. As such, a detailed discussion of its definitions and consequences is presented in Section 2.3 of the next chapter.

A key part of the efficiency improvement of the formalism comes from the fact that spinors can only represent null momenta, $\langle ii \rangle = [ii] = 0$. So the $p_i^2 = 0$ condition is built into the variables, rather than representing redundancy in the description, as it does in the four-momenta description of massless particles. Even so, some redundancy remains in the spinor notation, as expanded upon in Section 2.3.

Calculations in the new formalism yielded simple, often very symmetric results [6, 14].

A significant step forward in methods for calculating tree amplitudes efficiently came in 2005, with the description of Britto–Cachazo–Feng–Witten (BCFW) recursion [19]. This was not the first recursive technique developed, for example in ref. [14], Berends and Giele proved the Parke–Taylor result using a recursive technique, where the ingre-

dients were amplitudes with one off-shell leg. Later, the discovery of a way to transform Yang–Mills to twistor space [20] helped to motivate Cachazo–Svrcek–Witten (CSW) recursion, which presented a set of rules for constructing tree amplitudes from on-shell Feynman-type diagrams containing MHV amplitudes [21]. Due to the helicities of the ingredients, to construct an amplitude with q external legs of negative helicity required drawing diagrams with $q - 1$ MHV vertices.

BCFW recursion improved upon previous work by presenting a way to construct tree amplitudes from factorisations involving only two on-shell amplitudes. Treating an amplitude as a rational function of its momenta, a complex shift was applied to spinors in two of the momenta, introducing a new parameter z . The resulting expression is an analytic function, with corresponding properties to exploit. In particular, it was observed that the complex function will contain poles whenever z occurs in a (complex shifted) propagator factor. At the values of z where propagator momenta go on-shell, the shifted amplitude splits into two smaller on-shell amplitudes. Applying Cauchy’s residue theorem, it was shown that the original, unshifted amplitude can be rewritten as a sum of factorisations around such poles.

With recursive methods building amplitudes from smaller amplitudes, a natural question is what the smallest building blocks are. Somewhat surprisingly, these are the three-point tree amplitudes with helicities either MHV, $(- - +)$, or $\overline{\text{MHV}}$, $(+ + -)$. For real, null external momenta, these amplitudes vanish as a result of momentum conservation,

$$\begin{aligned} p_1^\mu + p_2^\mu + p_3^\mu &= 0, \\ \Rightarrow p_1 \cdot p_2 &= p_2 \cdot p_3 = p_3 \cdot p_1 = 0. \end{aligned} \tag{1.14}$$

The three momenta are collinear and there are no non-vanishing invariants out of which to build an amplitude. But by allowing the momentum spinors in an amplitude to take complex values in general, the spinors λ_i and $\tilde{\lambda}_i$ can be determined independently. Choosing either $\langle 12 \rangle = \langle 23 \rangle = \langle 31 \rangle = 0$ or $[12] = [23] = [31] = 0$ is sufficient to satisfy eq. 1.14, with the opposite set of spinor products allowed to remain non-zero. These three-point tree amplitudes can be found by considering the Parke–Taylor n -point result [13, 14] for $n = 3$, or can be identified (up to some constant) as the only possible structures with the correct helicities, built from the non-vanishing invariants. In the twistor space description of ref. [20], amplitudes become algebraic curves, and the three-point amplitudes appear as the special case of degree zero curves (points).

BCFW recursion has allowed huge steps to be taken in amplitude calculation. Prior

to the publication of its proof in terms of complex analysis, the postulated procedure was used to express many tree amplitudes in their most simple spinor-helicity forms [22]. Later, Risager demonstrated that CSW recursion is expressible as a particular application of BCFW recursion [23], albeit using an alternative momentum shift which involves three spinors. As will be seen in the discussion of loop amplitudes, its utility does not end at rational functions such as tree amplitudes. The logic of shifting an expression to become a complex analytic function, then exploiting that analyticity, is applicable to rational terms in any amplitude and continues to be used to great effect in work ongoing today.

1.3 One-loop Amplitudes

The step up from tree amplitudes in Yang–Mills, to one-loop amplitudes, represents a huge increase in complexity. Unlike the tree amplitudes, one-loop amplitudes in Yang–Mills are not necessarily finite, rational functions. Loop integrals occur, which give rise to logarithms and cannot be written as factorisations of smaller amplitudes as in BCFW recursion. Furthermore, both UV and IR divergences can occur in general in $D = 4$ dimensions. UV divergences relate to the region of an integration where the loop momentum becomes large, and occur when the overall power of momentum appearing in the integrand and measure is greater than or equal to zero. For example, they are present in the one- and two-point scalar integrals. IR divergences occur when the loop momentum becomes small, or collinear with null external momenta, and there are enough propagator factors that this outweighs the momentum factors in the measure. It is necessary to introduce a regularisation scheme to control the singularities that occur, with the common approach being to analytically continue the theory from taking place in four dimensions, to $D = 4 - 2\epsilon$ dimensions [24]. Calculations then give rise to poles in ϵ , when $\epsilon \rightarrow 0$, in place of divergences. Variations on this dimensional regularisation method exist, where different choices are made for the dimensions of the internal and external momenta, and the numbers of helicity states on spinors [25]. Table 1.3 summarises the choices made in the original scheme of 't Hooft and Veltman (HV) [24], the conventional dimensional regularisation scheme (CDR) [26] and the four-dimensional helicity scheme (FDH) [27]. The FDH scheme has the external states remain in four dimensions, as well as the Dirac algebra, while integrals are carried out in D dimensions. This is particularly convenient for amplitude calculations in the spinor-helicity formalism, because that four-dimensional technology continues to be applicable even when the chosen methodology exposes internal momentum states. In comparison,

		CDR	HV	FDH
External particles	Momentum dimension	$4 - 2\epsilon$	4	4
	Helicity states	$2 - 2\epsilon$	2	2
Internal particles	Momentum dimension	$4 - 2\epsilon$	$4 - 2\epsilon$	$4 - 2\epsilon$
	Helicity states	$2 - 2\epsilon$	$2 - 2\epsilon$	2

Table 1.3: Momentum dimensions and helicity state choices made in different dimensional regularisation schemes. Listed are Conventional Dimensional Reduction (CDR) [26], the 't Hooft-Veltman scheme (HV) [24] and the Four-Dimensional Helicity scheme (FDH) [27].

CDR is conceptually simpler, treating all momenta uniformly, but computationally more complicated due to the presence of ϵ -dimensional helicity states.

The difficulties posed by one-loop amplitudes would lead to a new technique of unitarity cutting [28], which forms one of the major strands to amplitude calculations up to the present day. The method is motivated by the idea that instead of considering the many distinct Feynman diagrams that contribute to a given loop amplitude, that amplitude should instead be thought of in terms of the types of loop integral that it can contain, of which there are far fewer. Crucially, it was realised by Passarino and Veltman [29] that any general one-loop tensor integral can be reduced to a sum of scalar box, triangle, bubble and tadpole integrals with rational coefficients, as well as a rational piece and terms of order ϵ . Hence a basis for any one-loop amplitude could be built out of readily evaluated integral functions, and the task of calculating a loop amplitude is converted to one of determining their coefficients. This was done by applying rules proposed earlier by Cutkosky [30] that allow propagators to be “cut”, or placed on-shell. Applying these unitarity cuts to propagators in a loop diagram breaks it into a product of rational tree diagrams. Then applying the same cuts to the amplitude’s expansion in terms of integral functions causes those functions not containing the cut propagators to vanish, and the rest to simplify. Equating the two forms yields information on the coefficients of the various integral functions present in the full amplitude. This procedure is explained in greater detail in Chapter 3. The unitarity method was first applied in the FDH scheme, where the spinor-helicity formalism makes evaluation of the cuts straightforward [28, 31]. The tree amplitudes encountered are on-shell, with the formerly internal legs treated like any external momentum. The drawback of the FDH approach, however, is that by considering internal momenta to be four-dimensional, rational and order ϵ information is missed and only the coefficients of the integral functions are “cut-constructible”. Any remaining information must be de-

1 Introduction

terminated through other methods, for example the rational terms being determined via collinear limits [32]. Alternatively, by carrying out unitarity cuts in the D -dimensional CDR scheme, various authors have more recently shown how it is possible to obtain the information to fully determine one-loop amplitudes [33, 34], albeit following more involved algebraic manipulations.

Early examples of unitarity used double propagator cuts to reduce a loop diagram to tree amplitudes. This is depicted in Figure 1.1. Each way of applying the two cuts produced constraints on the unknown coefficients in the integral basis. So by carrying out various cuts, a system of equations in the unknowns was produced, and could then be solved. The later development of generalised unitarity [35] improved upon the standard technique by showing the utility of applying more cuts at once to a diagram. A quadruple cut was shown to determine the coefficients of the corresponding box function in a natural way in terms of four tree amplitudes, which could be subtracted from the overall amplitude. Next, triple cuts determine the coefficients of triangle functions, and so on. The systematic nature of the process greatly helps calculation of loop amplitudes, and those pieces that are cut-constructible in the FDH scheme are particularly easily obtained through spinor-helicity manipulations. As before, the rational pieces missed by employing a four-dimensional unitarity approach can be obtained by applying generalised unitarity in D dimensions [36], or by other means.

Although one-loop amplitudes in general contain transcendental functions of the momenta, necessitating the use of one of the above unitarity procedures, there are specific exceptions to this story which can offer useful insights. In particular, the all-plus helicity and single-minus helicity amplitudes are fully rational at the one-loop level, which can be considered to be a result of them vanishing at tree level. Because of this, they are in theory amenable to techniques akin to those used to generate tree amplitudes, while also being structures that a four-dimensional unitarity procedure would entirely fail to generate. In ref. [37], an attempt was made to calculate some of these amplitudes using BCFW recursion, to investigate how factorisation techniques fare at the loop level. New behaviour was encountered, because one-loop amplitudes can contain double poles, going beyond the simple poles of tree amplitudes. Such double poles were captured by the recursion procedure in factorisations where one of the amplitudes is the one-loop three-point amplitude. However, the simple pole behaviour beneath this double pole is also required to complete the BCFW expression, but was not found to emerge from any factorisation. This reveals a limitation of factorisation methods, in that they can only determine the leading pole information. To complete the rational expression, the sub-leading coefficients of the Laurent expansion must be

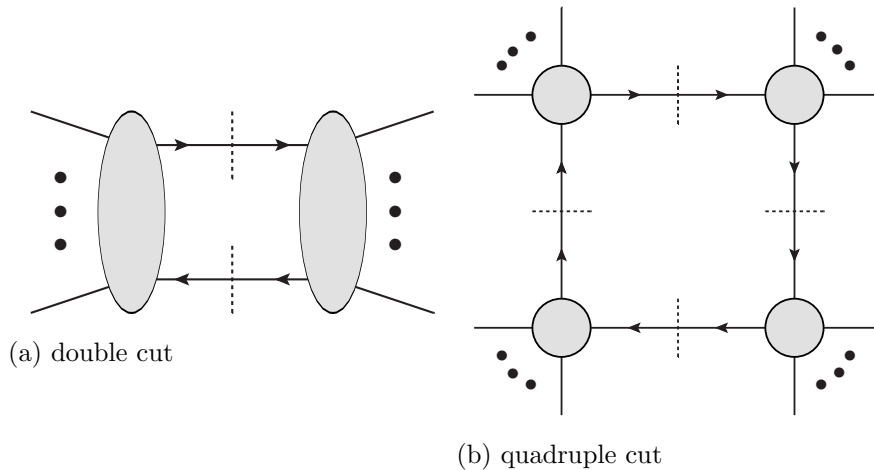


Figure 1.1: Diagrams depicting unitarity cutting. The dashed lines represent propagators being put on-shell, or “cut”, to reduce a loop diagram to a product of tree diagrams. Unitarity was originally carried out using double cuts [28]. Generalised unitarity introduced quadruple and triple cut diagrams to hone in on the coefficients of the box and triangle integrals, respectively [35].

obtained by other means.

Augmented recursion is one such technique, presenting a way to obtain the sub-leading information in the rational part of an amplitude. It was demonstrated for various one-loop amplitudes in Yang–Mills (and gravity) [38, 39, 40], and provides an alternative treatment for the channels which produce double pole terms in recursive methods such as BCFW. Rather than drawing a factorisation involving a three-point one-loop amplitude as BCFW would suggest, the double pole contributions are re-drawn as diagrams featuring an off-shell loop, which once integrated over captures both the leading and sub-leading Laurent coefficients. One side of those loops are structures that are akin to amplitudes with two legs taken off-shell, known as currents. For the calculation to be carried out in the language of spinor-helicity objects, it is necessary to define a way to represent off-shell momenta with spinors, which individually can only represent null momenta. That issue was solved with the axial gauge formalism, which represents non-null momenta in terms of the usual null spinors, as well as a new reference momentum [41]. For the channels that produce only simple poles, BCFW recursion can be used as it is for tree amplitudes, with no further complications. We see that with the introduction of a reference momentum, and calculation of off-shell currents, the procedure

is not gauge-invariant like earlier recursion or unitarity procedures. The particular choice of axial gauge means that ghosts do not occur in the calculation of purely gluon amplitudes, but the reference momentum will appear. Choosing augmented recursion also allows four-dimensional spinor-helicity to continue being used, the simplicity of which may make up for the gauge-dependent step, if compared to a gauge-invariant but D -dimensional approach. Regardless of method used, in the final result, a gauge-independent amplitude must emerge, meaning the overall cancellation of the axial gauge reference momentum can be used as a consistency check of the augmented recursion procedure.

1.4 Two-loop Amplitudes

With generalised unitarity and various recursive techniques giving a good handle on one-loop amplitudes, two-loop amplitudes presented the next major challenge to theoreticians. At the same time, collider experiments continued to probe greater energies and better precision, so field theory predictions at higher orders in perturbation theory were also desirable from a phenomenological perspective. Compared to the advances in techniques required between tree and one-loop amplitudes, the jump to two-loop amplitudes does not present such a significant challenge in principle. The techniques required are extensions of those already seen. For example, unitarity can be applied at two loops, although the number of possible cuts to two-loop diagrams is greater. (A maximally cut four-point two-loop diagram requires seven cuts, rather than the quadruple cuts of a one-loop diagram, for example.) A corresponding basis of two-loop integral functions is also required, in general. Carrying out unitarity cuts in D dimensions would fully determine the amplitude. However, the greater complexity of two loops may make four-dimensional unitarity the more practical choice above a certain number of points.

Catani presented a general form for the IR divergent piece of two-loop amplitudes in ref. [42]. (The UV divergences were removed in the $\overline{\text{MS}}$ scheme, by a renormalisation of the coupling constant.) The singularities appear in factorisation structures that involve lower loop amplitudes multiplied by ϵ -pole-containing operator functions. It was known that one-loop amplitudes have divergences in $1/\epsilon^2$ and $1/\epsilon$, multiplied by the tree-level amplitude [43]. In comparison, two-loop amplitudes are more complex, containing poles up to $1/\epsilon^4$ in general. Those terms with poles in $1/\epsilon^4$, $1/\epsilon^3$ and $1/\epsilon^2$ are fully specified, but there is also a non-universal $\mathcal{O}(1/\epsilon)$ piece multiplying the tree-level amplitude, which must be determined for the specific amplitude of interest. The

discovery of a universal factorisation formula for two-loop singularities demonstrates an impressive simplicity in these amplitudes, and provided a valuable validity check for all derivations of full amplitudes that followed.

The first two-loop pure Yang–Mills amplitude to be obtained was the four-point amplitude, calculated for all-plus helicity in ref. [44]. The authors carried out the calculation using D -dimensional unitarity, in the HV scheme where internal cut propagators are considered to be in $D = 4 - 2\epsilon$ dimensions, but external legs remain in four dimensions. It was found that diagrams containing up to four cuts were required to obtain all integral coefficients, an increase on the two required for one-loop unitarity. (One-loop generalised unitarity does make use of up to quadruple cuts, but this is for reasons of calculational simplicity. The same one-loop unitarity result can be obtained through application of only double cuts, as was done historically.) The form of the divergence structure was found to be similar to that expected for a one-loop amplitude [43]. This matched the prediction of Catani [42], with the simplicity being a result of the tree-level all-plus amplitude vanishing. Since all-plus and single-minus helicity amplitudes vanish at tree level for any number of gluons, the simpler two-loop divergence structure can be expected to be a general occurrence for either of those helicity choices, at any number of points.

Following papers calculated the full four-point two-loop amplitude for all helicity choices, in various dimensional regularisation schemes: in CDR [45], then in HV and FDH [8]. In ref. [46], the amplitudes were calculated again, but with additional orders in the dimensional regulator (up to $\mathcal{O}(\epsilon^2)$), which are required by future higher loop calculations.

The five gluon two-loop amplitude is a further step up in difficulty, so its calculation proceeded in pieces. Most, but not all, of its structures have now been obtained. As the simplest structure, the all-plus leading in colour partial amplitude was calculated first, using a generalised unitarity procedure [47]. The authors used a novel variation on the D -dimensional unitarity procedure where the tree amplitudes used in integrand reduction are six-dimensional. The extra dimensions accommodate the -2ϵ -dimensional information of the $D = 4 - 2\epsilon$ integral, and allow a six-dimensional spinor-helicity formalism [48] to be used. That derivation also benefitted from the previously identified one-loop-like singularity structure, and due to the colour structure, only diagrams with a planar momentum arrangement are required. The full colour all-plus partial amplitude was derived soon after [49], using a method that still avoided evaluating the tricky non-planar pieces. Instead, BCJ relations [50], which allow the legs of a four-point tree amplitude to be interchanged, were used to express non-planar cuts in terms of planar

ones.

Due to the number of contributions to the derivation method, and complexity of the resulting expressions, the previous five-point results were not particularly simple. More efficient ways of stating the results were required to make them human-readable, so that interesting properties or symmetries may become manifest. In ref. [51], such a step was taken for the leading in colour partial amplitude. The authors produced a set of planar two-loop master integrals, with which the result of ref. [47] was re-expressed in a compact, analytic form that can be stated in a few lines. The same partial amplitude was then re-calculated using an alternative method of four-dimensional unitarity and augmented recursion [52]. Carrying out generalised unitarity in the FDH scheme, so that the amplitudes appearing are four-dimensional and can be expressed in terms of spinors, many potential unitarity cut diagrams vanish. Those diagrams that remain are only those containing an uncut one-loop amplitude, with the maximal number of non-vanishing cuts being four, as in the one-loop case. All diagrams where both loops are cut give zero contribution, and this is easily seen without calculation when working in the spinor-helicity formalism. The unitarity procedure effectively reduces to a one-loop one, but with an all-plus one-loop amplitude inserted as a vertex in the cut diagrams. What remains of the amplitude, the rational piece missed by four-dimensional unitarity, was obtained through augmented recursion. That step, too, required at most one-loop integration. The authors arrived at compact form matching ref. [51], but without requiring laborious two-loop integration.

A compact form for the full colour all-plus amplitude followed in ref. [53], which continued with the master integral approach by computing those additional two-loop integrals needed for non-planar structures. The same full colour amplitude was also re-calculated using four-dimensional unitarity and augmented recursion [54]. To obtain a full colour result, the constituent amplitudes in the unitarity and recursion diagrams were each dressed with their full colour structures, and a new current, appearing in some non-planar arrangements, was calculated.

The single-minus helicity leading in colour partial amplitude was obtained in ref. [55], using a finite fields technique to perform integrand reduction onto a basis of pentagon integral functions. The finite field approach is a recent development, first proposed in ref. [56] as an efficient computational procedure for applying integration by parts identities to integrand reduction. The rationale is that as amplitude calculations become harder, there is a tendency for symbolic expressions in intermediate steps to become increasingly large, particularly in D -dimensional techniques, so avoiding symbolic evaluation can be beneficial. For the single-minus amplitude, what this means is that

rather than working with unwieldy analytic expressions, the calculation was performed numerically over a finite field arithmetic. After multiple evaluations of that algorithm, an analytic form for the result was then reconstructed. Following on from that success, the remaining leading in colour helicity configurations were obtained in [57], also using finite field numerical methods. Although the leading in colour parts of the two-loop five-point amplitude have now all been presented, calculating the partial amplitudes that complete the full colour results with one or two negative helicity gluons represents an open challenge.

Six gluons with two loops is the level at which some of the previous derivation methods become prohibitively difficult to carry out, given the step up in complexity. As is generally the case, the all-plus helicity amplitude was the first focus of research, being the simplest structure. It is also the only helicity choice that has been found in an analytic form for pure Yang–Mills to date. The first six-point all-plus calculation, of the leading in colour partial amplitude, was performed in ref. [58], using the methods of four-dimensional unitarity and augmented recursion. The full colour all-plus amplitude was then completed in ref. [59], using a colour dressed form of the previous paper’s methodology. (And the contributions to ref. [59] by the author of this thesis are detailed in Chapter 3.) The analytic form expressed in the paper is remarkably simple, considering the complexity, and number, of contributions to the derivation procedure. The approach benefits greatly from the way that it reduces the unitarity problem to one analogous to a one-loop calculation. For this helicity choice, the complexity of four-dimensional unitarity tends to scale with gluon number like a one-loop problem. On the other hand, a method based on D -dimensional unitarity, where genuine two-loop cuts are organised and evaluated, will tend to feature a complexity that scales accordingly. Either approach should reach the same answer following various cancellations and simplifications, but if the intermediate steps feature excessive complexity then this can be a barrier to performing the calculation with that methodology. Six-point happens to be the arena where calculations begin to fill the available resources of a typical desktop computer, and with that comes an increased focus on efficient methods that leverage symmetries of the problem to avoid complex intermediate stages.

Despite the mounting complexity, a seven-point partial amplitude was also derived recently. Again using four-dimensional helicity and augmented recursion, the all-plus leading in colour structure was determined in ref. [60] and presented in a compact, analytic form. Using a D -dimensional unitarity approach, a numerical form was then published for the full colour all-plus amplitude [61], confirming the previous result, and

presenting new sub-leading in colour partial amplitudes. Finally, the full colour amplitude was determined independently in a compact, analytic form using four-dimensional helicity and augmented recursion [62]. (A detailed account of this derivation appears in Chapter 4 of this thesis.)

The availability of compact analytic amplitude forms has also allowed some authors to look to n -point generalisations of certain structures. An n -point expression for the all-plus single colour trace, N_c -independent partial amplitude was conjectured in [63], satisfying various consistency conditions. The proposed form was arrived at by inspection of the previously found analytic results for four, five and six points. That an expression for a general number of gluons could be found from a few examples of specific compact, analytic forms is a perfect demonstration of the value to theoreticians of performing these calculations. The conjecture was recently found to hold up to nine points, tested numerically in ref. [61].

Another impressive recent achievement is the derivation of an n -point form for the non-rational (divergent and polylogarithmic) parts of the all-plus helicity two-loop amplitude, for all colour structures [62]. That result represents the completion of the four-dimensional unitarity scheme's application to two-loop all-plus amplitudes. Further derivations of pure Yang–Mills amplitudes of this type need only focus on the rational piece, for which techniques such as augmented recursion are applicable.

1.5 Thesis Outline

This thesis is structured as follows:

Chapter 2 provides further technical detail and elaboration on the key technologies used in Yang–Mills amplitude calculations and in this thesis. First, colour trace decomposition will be explicitly defined for tree, one-loop and two-loop amplitudes. There is a discussion of the various symmetry properties that occur in the partial amplitudes that arise. Decoupling identities, which form a large part of the reasoning behind extending the symmetry of Yang–Mills to $U(N_c)$, will be derived. Following that, the spinor-helicity formalism will be described in detail. The use of spinors will be further justified, and additional definitions relevant to the rest of the work will be made. There is also discussion of the freedoms remaining in the spinor description of variables, including Schouten identities and a useful little group scaling.

In Chapter 3, the method for deriving the full colour two-loop six-point all-plus helicity Yang–Mills amplitude is set out. By applying a colour trace decomposition to the $U(N_c)$ gauge theory, photon decoupling identities between the partial amplitudes act as

validity checks. The calculation is separated into parts, handled by different methods. Divergent and polylogarithmic terms are determined by four-dimensional unitarity, the procedure for which takes a particularly simple form with only one-loop cuts required. The remaining terms are rational, so can be generated through a recursive method. Due to the presence of double poles in momenta, augmented recursion is required. The final amplitude results obtained are those previously published in ref. [59] and are the product of collaboration. Chapter 3 therefore focuses on the contribution of the author of this thesis. In particular, explicit results for two of the partial amplitude rational pieces are derived in a compact analytic form, and their validity is tested.

Chapter 4 presents the derivation of the full colour all-plus helicity amplitude with seven gluons, in a compact, analytic form. This involves re-deriving the previously identified leading in colour partial amplitude and confirming the form of the single trace N_c -independent piece, as well as calculating the other colour structures for the first time. Non-rational parts are derived using four-dimensional unitarity, finding agreement with the n -point polylogarithmic result [62]. For the rational parts, augmented recursion is used. That process requires two new seven-point currents, in addition to the one used in the leading in colour calculation. Finally, the result is reduced to a compact analytic form. The derivation of currents and the reconstruction of the analytic result are both topics in their own right, which deserve further elaboration. So they are skipped over in the seven-point explanation, to be presented in detail and with additional context in the following two chapters. The expressions found have also been described in ref. [62], together with other work carried out in collaboration.

A detailed account of currents and their integration is provided in Chapter 5. When the intended use is in augmented recursion, it is not necessary in general to calculate all the terms in a current, only those that contribute to the residue after integration and a complex shift has been applied. Currents with unnecessary terms omitted are sometimes called “good enough” currents, and the main result presented in this chapter is an intuitive new way of thinking about deriving them. The procedure is algorithmic, so suitable for automation, which may aid future calculations of more complicated currents. As verification, the previously found five-point one-loop current is re-derived in the new methodology. Seven-point one-loop currents, used in the derivation of the seven-point two-loop amplitude of Chapter 4, are also presented. Finally, the integration of current diagrams in augmented recursion is described in detail. Various useful integral results are arrived at, which are applicable in general calculations.

In Chapter 6, techniques to simplify rational analytic results emerging from augmented recursion (and elsewhere) are discussed and applied. While recursive proce-

1 Introduction

dures lead to far simpler expressions than directly evaluating Feynman diagrams, their complexity does still grow with the number of gluons involved, necessitating simplification. The increasing number of terms involved, as well as the presence of a reference momentum in augmented recursion results, are two challenges that are addressed. To improve the compactness of recursion results, the smallest available versions of the one-loop ingredients are desirable. New forms of several one-loop amplitudes are determined with fewer terms, and are in some cases manifestly free of spurious poles for the first time.⁴ A process of reconstruction is applied to two of the partial amplitudes of the two-loop seven-point calculation of Chapter 4. By identifying the leading poles from direct factorisations, and comparing the sub-leading poles to an ansatz basis, sizeable expressions are reduced to very compact, symmetric functions.

⁴Spurious poles are those factors which appear in a denominator of a particular statement of an amplitude, but due to overall cancellations do not lead to singular behaviour when they become small.

2 Foundations of Amplitude Techniques

2.1 Introduction

In this chapter, two major technologies in the calculation of amplitudes are described. Specifically, these apply to the loop amplitudes $\mathcal{A}_n^{(\ell)}$ which appear in the perturbative expansion of the complete amplitude,

$$\mathcal{A}_n = g^{n-2} \sum_{\ell \geq 0} a^\ell \mathcal{A}_n^{(\ell)}, \quad (2.1)$$

where the constant $a \equiv g^2 e^{-\epsilon \gamma_E} / (4\pi)^{2-\epsilon}$ contains the Yang–Mills coupling g , the Euler–Mascheroni constant γ_E and the small parameter ϵ introduced by dimensional regularisation.¹

The first technology, colour trace decomposition was proposed as a way to separate the colour degrees of freedom from the kinematic degrees of freedom in a loop amplitude. By manipulating the colour factors into a standard form, the calculation can focus on finding only the kinematic functions, which inherit additional useful properties from the decomposition.

The second technology, spinor-helicity formalism is an alternative, arguably more natural, choice of variables in which to present an amplitude for massless particles. Instead of working with the Minkowski four-momenta of the external gluons, each gluon is associated with two Weyl bispinors.² These spinors automatically encode the null condition of the momenta, so lead to simpler amplitude expressions.

Both rest on the standard definitions related to Yang–Mills theory, which are made in Chapter 1. However, the following techniques (and the unitarity and recursive techniques described in Chapters 3 and 4) mean that the traditional ways of deriving amplitudes, such as the Feynman rules of Table 1.1 are no longer the best route forward. We also choose a symmetry group for our theory that moves beyond direct

¹Loop integrals in four dimensions may diverge, so they are regularised by analytically continuing the integration dimension to $D = 4 - 2\epsilon$.

²In group theory terms, the vector transforming under $SO^+(1,3)$ is replaced by two spinors, each transforming in one of the $SL(2, \mathbb{C})$ covers of $SO^+(1,3)$.

investigation of the Standard Model. The Yang–Mills symmetry is often generalised from the three-colour $SU(3)$ of the strong force, to $SU(N_c)$ with an arbitrary number of colour charges, which this thesis further extends to $U(N_c)$. The reasons for doing so are expanded upon in the following sections.

2.2 Colour Decomposition

Colour trace decomposition is the procedure through which loop amplitudes are separated into a number of individually gauge-invariant structures, according to the types of colour structures which appear with them. Historically, this was first carried out for tree amplitudes [6], then one-loop amplitudes [7] and later two-loop amplitudes [8].

The chosen colour basis is written in terms of traces of the generators of the colour symmetry, $(T^a)_j^i$. In earlier work, amplitudes were calculated using Feynman rules that made use of structure constants f^{abc} (such as those in Table 1.1). Colour decomposition required these constants to be rewritten in terms of the generator matrices using

$$f^{abc} = -i(\text{Tr}[T^a T^b T^c] - \text{Tr}[T^a T^c T^b]). \quad (2.2)$$

Applying that change to a Feynman diagram, strings of (traced over) generators are obtained. Colour indices related to external legs will appear once each, with a single factor of $\{T^1, T^2, \dots\}$ donated by the vertex receiving the external $\{p_1, p_2, \dots\}$ momentum. For internal propagators, the associated colour indices will appear contracted in pairs, with a factor of T^a occurring in both vertices ending the internal p_a momentum. Completeness relations can then be applied to the pairs of generators which appear contracted over their colour indices, simplifying the expressions.

Working with colour generators in an $SU(N_c)$ theory, the completeness relation reads

$$\sum_a (T^a)_j^i (T^a)_l^k = \delta_l^i \delta_j^k - \frac{1}{N_c} \delta_j^i \delta_l^k. \quad (2.3)$$

The final term is present to enforce the traceless property of the generators. Extending the symmetry group to $U(N_c)$, as is done in this thesis, allows the application of the simpler completeness relation

$$\sum_a (T^a)_j^i (T^a)_l^k = \delta_l^i \delta_j^k, \quad (2.4)$$

which makes the handling of generator strings very straightforward. Those paired generators are removed from the expressions, leading to the sewing together of trace factors in some cases, and the introduction of factors of $\delta_i^i = N_c$ in others. Considering the ways that traces can appear gives the possible combinations

$$\begin{aligned}\mathrm{Tr}[XT^a]\mathrm{Tr}[T^aY] &= X_i^j(T^a)_j^i(T^a)_k^l Y_l^k = X_i^j \delta_k^i \delta_j^l Y_l^k = \mathrm{Tr}[XY], \\ \mathrm{Tr}[XT^a T^a Y] &= X_i^j(T^a)_j^k(T^a)_k^l Y_l^i = X_i^j \delta_k^k \delta_j^l Y_l^i = N_c \mathrm{Tr}[XY], \\ \mathrm{Tr}[XT^a Y T^a] &= X_i^j(T^a)_j^k Y_k^l(T^a)_l^i = X_i^j \delta_l^k \delta_j^i Y_k^l = \mathrm{Tr}[X]\mathrm{Tr}[Y],\end{aligned}\tag{2.5}$$

where X and Y represent some general generator strings. Summation over repeated indices is implied. For tree amplitudes, only the first of the three relations is needed, and it is found that only single traces, containing a colour generator for each external gluon, appear in the colour basis. Loop amplitudes require all three relations to establish their colour structures, which can contain multiple colour traces in the same term. In fact, for an ℓ -loop amplitude, the generators can form into up to $\ell + 1$ separate traces.

2.2.1 Colour trace basis

The colour trace decomposition will now be defined for tree, one-loop and two-loop amplitudes. In each case, the function $\mathcal{A}_n^{(\ell)}$ on the left is the ℓ -loop, n gluon amplitude, which contains both the kinematic and colour information. The expansion then pulls out the colour structures explicitly, defining a number of new, purely kinematic functions known as partial amplitudes. In this thesis, the complete amplitude will be referred to as a ‘‘full colour’’ amplitude, to ensure clarity when individual partial amplitudes are also mentioned.

Tree amplitudes can be written in the colour trace basis as [6]

$$\mathcal{A}_n^{(0)}(1, 2, \dots, n) = \sum_{S_n/\mathcal{P}_{n:1}} \mathrm{Tr}[T^{a_1} \dots T^{a_n}] A_{n:1}^{(0)}(a_1, \dots, a_n),\tag{2.6}$$

where the functions $A_{n:1}^{(0)}(a_1, \dots, a_n)$ are partial amplitudes. The matrices T^a are generators in the fundamental representation of the symmetry group, which we choose to be $U(N_c)$, but could also be interpreted as $SU(N_c)$ without requiring any modification to the expansion. The summation is over non-cyclic permutations of the external momentum labels. These are denoted using $S_n/\mathcal{P}_{n:1}$, where S_n is the full group of

2 Foundations of Amplitude Techniques

permutations of n elements and

$$\mathcal{P}_{n:1} = Z_n(a_1, a_2, \dots, a_n) \quad (2.7)$$

is the cyclic group of n elements. The partial amplitudes have a number of notable features. They are functions of the external momenta only, and are individually gauge-invariant. They also possess a cyclic $\mathcal{P}_{n:1}$ symmetry in their arguments, matching the symmetry of the trace structure.

For one-loop amplitudes, generator matrices join up to form either a single trace and a factor of N_c , or two separate traces, in [7]

$$\begin{aligned} \mathcal{A}_n^{(1)}(1, 2, \dots, n) &= N_c \sum_{S_n/\mathcal{P}_{n:1}} \text{Tr}[T^{a_1} \dots T^{a_n}] A_{n:1}^{(1)}(a_1, \dots, a_n) \\ &+ \sum_{r=2}^{\lfloor n/2 \rfloor + 1} \sum_{S_n/\mathcal{P}_{n:r}} \text{Tr}[T^{a_1} \dots T^{a_{r-1}}] \text{Tr}[T^{b_r} \dots T^{b_n}] A_{n:r}^{(1)}(a_1, \dots, a_{r-1}; b_r, \dots, b_n). \end{aligned} \quad (2.8)$$

The partial amplitude $A_{n:1}^{(1)}$ can be called “leading in colour”, because of its associated factor of N_c . It possesses the same cyclic symmetries as, and could be considered analogous to, the $A_{n:1}^{(0)}$ of the tree decomposition. The partial amplitude $A_{n:r}^{(1)}$ possesses a new symmetry of its arguments, encountered at one-loop level and above, in connection with the cyclic symmetries of two trace strings. Explicitly, the group $\mathcal{P}_{n:r}$ which describes these is

$$\mathcal{P}_{n:r} = Z_{r-1}(a_1, \dots, a_{r-1}) \times Z_{n-r+1}(b_r, \dots, b_n) \times G_{n:r}, \quad (2.9)$$

where

$$G_{n:r} = \begin{cases} Z_2(\{a_1, \dots, a_{r-1}\}, \{b_r, \dots, b_n\}), & \text{if } (r-1) = n/2, \\ 1, & \text{otherwise.} \end{cases} \quad (2.10)$$

An additional Z_2 symmetry is present when the traces are the same length, which interchanges the full sets of their momentum labels. Note that $r \neq 1$, and that by convention, the traces are arranged shortest to longest, so the label r ranges over $r = \{2, 3, \dots, \lfloor n/2 \rfloor + 1\}$. The $S_n/\mathcal{P}_{n:r}$ sum is over permutations of the momentum labels, up to the cyclic symmetries of the traces, so that each allowed colour trace

structure appears once in the overall expansion.

Two-loop amplitudes can be expanded in the colour trace basis as [54]

$$\begin{aligned}
\mathcal{A}_n^{(2)}(1, 2, \dots, n) &= N_c^2 \sum_{S_n/\mathcal{P}_{n:1}} \text{Tr}[T^{a_1} \dots T^{a_n}] A_{n:1}^{(2)}(a_1, \dots, a_n) \\
&\quad + N_c \sum_{r=2}^{\lfloor n/2 \rfloor + 1} \sum_{S_n/\mathcal{P}_{n:r}} \text{Tr}[T^{a_1} \dots T^{a_{r-1}}] \text{Tr}[T^{b_r} \dots T^{b_n}] A_{n:r}^{(2)}(a_1, \dots, a_{r-1}; b_r, \dots, b_n) \\
&\quad + \sum_{s=1}^{\lfloor n/3 \rfloor} \sum_{t=s}^{\lfloor (n-s)/2 \rfloor} \sum_{S_n/\mathcal{P}_{n:s,t}} \text{Tr}[T^{a_1} \dots T^{a_s}] \text{Tr}[T^{b_{s+1}} \dots T^{b_{s+t}}] \text{Tr}[T^{c_{s+t+1}} \dots T^{c_n}] \\
&\quad \quad \quad \times A_{n:s,t}^{(2)}(a_1, \dots, a_s; b_{s+1}, \dots, b_{s+t}; c_{s+t+1}, \dots, c_n) \\
&\quad + \sum_{S_n/\mathcal{P}_{n:1}} \text{Tr}[T^{a_1} \dots T^{a_n}] A_{n:1B}^{(2)}(a_1, \dots, a_n). \tag{2.11}
\end{aligned}$$

In addition to the leading in colour partial amplitude $A_{n:1}^{(2)}$ and the two-trace partial amplitudes $A_{n:r}^{(2)}$, there also appear three-trace partial amplitudes $A_{n:s,t}^{(2)}$ and a new single-trace N_c -independent partial amplitude $A_{n:1B}^{(2)}$. A new symmetry type is defined, describing the symmetries of the three-trace terms and their partial amplitudes,

$$\mathcal{P}_{n:s,t} = Z_s(a_1, \dots, a_s) \times Z_t(b_{s+1}, \dots, b_{s+t}) \times Z_{n-s-t}(c_{s+t+1}, \dots, c_n) \times G_{n:s,t}, \tag{2.12}$$

where

$$G_{n:s,t} = \begin{cases} S_3(\{a_1, \dots, a_s\}, \{b_{s+1}, \dots, b_{s+t}\}, \{c_{s+t+1}, \dots, c_n\}), & \text{if } s = t = n/3, \\ Z_2(\{a_1, \dots, a_s\}, \{b_{s+1}, \dots, b_{s+t}\}), & \text{if } s = t \neq n/3, \\ Z_2(\{b_{s+1}, \dots, b_{s+t}\}, \{c_{s+t+1}, \dots, c_n\}), & \text{if } s \neq t = (n - s - t), \\ 1, & \text{otherwise.} \end{cases} \tag{2.13}$$

The final factor accounts for traces occurring that are of the same length, so can be interchanged. The conventional way of labelling the partial amplitudes has the trace groups ordered in ascending length, which imposes a condition $s \leq t \leq (n - s - t)$ on the labels.

The above colour expansions are valid for a $U(N_c)$ symmetry group. To obtain the $SU(N_c)$ version, it is sufficient to remove those terms containing factors of $\text{Tr}[T^a]$.

2 Foundations of Amplitude Techniques

(The $SU(N_c)$ generators are traceless, so these pieces vanish.) Specifically, the partial amplitudes $A_{n:2}^{(1)}$, $A_{n:2}^{(2)}$ and $A_{n:1,t}^{(2)}$ do not appear. The partial amplitudes that appear in the $SU(N_c)$ expansion are therefore a subset of those appearing in the $U(N_c)$ expansion.

It can be useful to be able to refer to a partial amplitude of a general type, for which we will use $A_{n:\lambda}^{(\ell)}$ in future sections. The label λ is a stand-in for any of the previously defined colour structures, out of those allowed at the specified ℓ -loop, n -point level.

2.2.2 Partial amplitudes

Having carried out colour decomposition on an amplitude, the partial amplitudes become the objects of interest. They possess a number of notable properties. As previously mentioned, each is an individually gauge-invariant function of the kinematic variables.

Symmetries are inherited from their associated colour trace structure, so the partial amplitude $A_{n:\lambda}^{(\ell)}$ will be invariant under permutations of its momenta in the group $\mathcal{P}_{n:\lambda}$.³

A flip symmetry also appears in the arguments of the partial amplitudes, which inverts each trace grouping of momentum labels according to

$$\begin{aligned}
 A_{n:1}^{(2)}(a_1, \dots, a_n) &= (-1)^n A_{n:1}^{(2)}(a_n, \dots, a_1), \\
 A_{n:r}^{(2)}(a_1, \dots, a_{r-1}; b_r, \dots, b_n) &= (-1)^n A_{n:r}^{(2)}(a_{r-1}, \dots, a_1; b_n, \dots, b_r), \\
 A_{n:s,t}^{(2)}(a_1, \dots, a_s; b_{s+1}, \dots, b_{s+t}; c_{s+t+1}, \dots, c_n) \\
 &= (-1)^n A_{n:s,t}^{(2)}(a_s, \dots, a_1; b_{s+t}, \dots, b_{s+1}; c_n, \dots, c_{s+t+1}), \\
 A_{n:1B}^{(2)}(a_1, \dots, a_n) &= (-1)^n A_{n:1B}^{(2)}(a_n, \dots, a_1).
 \end{aligned} \tag{2.14}$$

The expressions for two-loop partial amplitudes are shown, but the pattern generalises straightforwardly. This particular symmetry can be traced back to the Feynman rules, and emerges as a consequence of symmetries in the vertex rules.

An understanding of the form taken by the colour trace basis allows the construction of a version of the Feynman rules that is ‘‘colour ordered’’. These are most useful when working with tree amplitudes, due to the smaller number of diagrams required, and can be used to describe how to construct the partial amplitude $A_{n:1}^{(0)}$ directly, rather than the full colour amplitude $\mathcal{A}_n^{(0)}$. Whereas a standard Feynman diagram approach would

³The notation $\mathcal{P}_{n:\lambda}$ is used to refer to any of the previously defined symmetries $\mathcal{P}_{n:1}$, $\mathcal{P}_{n:r}$ or $\mathcal{P}_{n:s,t}$, with a general colour structure label λ .

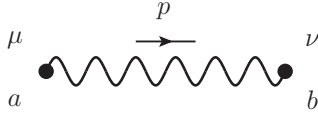
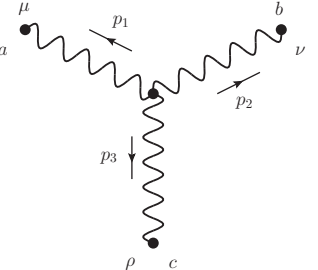
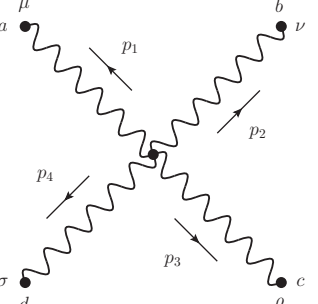
Propagator (colour ordered)	
	$\Delta_{\mu\nu}^c(p) = \frac{i}{p^2} \left(-\eta_{\mu\nu} + \frac{p_\mu q_\nu + q_\mu p_\nu}{p \cdot q} \right)$
Vertices (colour ordered)	
	$V_{\mu\nu\rho}^c(p_1, p_2, p_3) = ig \left(\eta^{\mu\nu} (p_1 - p_2)^\rho + \eta^{\nu\rho} (p_2 - p_3)^\mu + \eta^{\rho\mu} (p_3 - p_1)^\nu \right)$
	$V_{\mu\nu\rho\sigma}^c(p_1, p_2, p_3, p_4) = ig^2 (2\eta_{\mu\rho}\eta_{\nu\sigma} - \eta_{\mu\nu}\eta_{\rho\sigma} - \eta_{\mu\sigma}\eta_{\nu\rho})$

Table 2.1: Colour-ordered Feynman rules for the propagator and vertices of pure Yang–Mills theory, in the axial gauge. Colour factors no longer appear in the propagator or vertices. The rules give rise to a partial amplitude, when diagrams of a particular external leg ordering are drawn.

require diagrams with each possible permutation of external legs to be considered, the colour-ordered rules require only diagrams with a fixed cyclic ordering of legs, as these are the ones that contribute to a certain partial amplitude. By stripping out the colour factors from the usual Feynman rules, such that those factors form the expected traces of colour generators, laborious matrix manipulations are also avoided.

Table 2.1 collects the new ingredients for the colour-ordered Feynman rules. Both vertices show a symmetry under the reversal of their momentum labelling, justifying the earlier claim on the origin of the flip symmetry of the partial amplitudes.

2.2.3 Decoupling identities

As a consequence of extending the symmetry group of Yang–Mills theory to $U(N_c)$, beyond the $SU(N_c)$ more commonly seen, various relations occur between the partial amplitudes. These are known as “decoupling identities” and a procedure for generating them is as follows.

The $U(N_c)$ group possesses one more generator than $SU(N_c)$, reflecting the possibility for elements of the group to have non-zero traces. It is convenient to choose the extra generator of the $U(N_c)$ theory so that it lies in the $U(1)$ part of $U(N_c)$, taking the form of the $N_c \times N_c$ unit matrix in the fundamental representation. Then the rest of the generators can be identical to those used in the $SU(N_c)$ theory. Physically, the interpretation is that by going from $SU(N_c)$ to $U(N_c)$, a photon state with no overall colour is introduced to the theory. We expect such a state to decouple from the $N_c^2 - 1$ standard gluons, meaning any amplitude describing gluons interacting with photons should be vanishing.

Applying this fact to the colour decomposition, one or more generators can be replaced with the $U(1)$ generator explicitly, via $T^a \rightarrow T^{U(1)} = \mathbb{I}$. With such a choice, the full colour trace decomposition becomes equal to zero and traces involving that $T^{U(1)}$ simplify somewhat. The coefficients of each new type of colour trace present can be consolidated, yielding sums of partial amplitudes that must equal zero individually, to satisfy the overall vanishing of the amplitude. Each of these sums multiplying a certain colour trace is known as a decoupling identity. At tree level, the only identity found is

$$A_n^{(0)}(1, 2, 3, \dots, n) + A_n^{(0)}(2, 1, 3, \dots, n) + \dots + A_n^{(0)}(2, 3, \dots, 1, n) = 0, \quad (2.15)$$

originally observed when the first tree-level partial amplitudes were calculated [6] as a symmetry in addition to the cyclic permutation and flip symmetries of the momenta. The identity relates $n - 1$ versions of the single type of partial amplitude that occurs at tree level.

At one-loop level, there are more types of partial amplitude and more decoupling relations. It is possible to re-write any one-loop partial amplitude in terms of the leading in colour structure, by repeated application of those identities [7]. For higher loop levels, the leading in colour partial amplitude is no longer sufficient to describe the entire amplitude, but decoupling identities do allow a smaller subset of the partial amplitudes to describe the whole set.

In general, identities can contain a mixture of partial amplitudes, including both structures that are present in the $SU(N_c)$ expansion, and those that are exclusive to

the $U(N_c)$ theory. This gives a strong justification for calculating the $U(N_c)$ -specific partial amplitudes, even if $SU(N_c)$ is ultimately the theory of interest: they are consistent gauge-invariant structures, which are required to produce cancellations with the $SU(N_c)$ structures when unphysical photon states are considered.

This thesis makes use of the colour trace basis in its calculations. Other types of colour decomposition also exist, with uses such as expressing the information of the partial amplitudes in terms of fully independent structures [11, 12]. We calculate all the partial amplitudes associated with a $U(N_c)$ Yang–Mills theory, so that decoupling identities between them can be used as a validity check on the results.

2.3 Spinor-Helicity Formalism

The spinor-helicity formalism is a way of restating amplitude calculations in terms of spinor variables, rather than the usual four-momentum kinematics. This brings a number of benefits, particularly when working in theories of massless particles, and is central to many modern amplitude techniques. The formalism was originally set out in a series of papers by several authors [15, 16, 17, 18], the key steps of which we summarise in this section.

As a first step, the conversion from four-momenta to spinors can be motivated by constructing 2×2 matrices from the momenta,

$$p^{\alpha\dot{\alpha}} = p^\mu \bar{\sigma}_\mu^{\alpha\dot{\alpha}} = \begin{pmatrix} p^0 + p^3 & p^1 - ip^2 \\ p^1 + ip^2 & p^0 - p^3 \end{pmatrix}, \quad (2.16)$$

where

$$\bar{\sigma}_\mu^{\alpha\dot{\alpha}} = (\mathbb{I}, \vec{\sigma}). \quad (2.17)$$

The matrix is indexed with the spinor indices α and $\dot{\alpha}$, and the Pauli matrices $(\sigma_i)^{\alpha\dot{\alpha}}$ are used in the conversion. For massless particles such as the gluons of Yang–Mills theory, their momenta are null, meaning $p^2 = 0$. In terms of the above matrix, this is equivalent to $p^{\alpha\dot{\alpha}}$ having zero determinant. In general, a 2×2 matrix would have rank 2, but one with zero determinant has rank 1 or less. Therefore the momentum matrix

2 Foundations of Amplitude Techniques

can be represented as a single product,

$$p^{\alpha\dot{\alpha}} = \lambda^\alpha \tilde{\lambda}^{\dot{\alpha}}, \quad (2.18)$$

where λ and $\tilde{\lambda}$ are recognised to be Weyl spinors in the $(1/2, 0)$ and $(0, 1/2)$ representations of the Lorentz group, respectively.

2.3.1 Spinor definitions

An explicit form for the two spinors can be written down for completeness, although it will not be necessary to return to four-momentum components in spinor-helicity calculations. We have

$$\lambda^\alpha = \frac{h}{\sqrt{p_0 - p_3}} \begin{pmatrix} p_0 - p_3 \\ -p_1 - ip_2 \end{pmatrix} \quad (2.19)$$

and

$$\tilde{\lambda}^{\dot{\alpha}} = \frac{h^{-1}}{\sqrt{p_0 - p_3}} \begin{pmatrix} p_0 - p_3 \\ -p_1 + ip_2 \end{pmatrix}, \quad (2.20)$$

where there is still some freedom in these definitions, contained in the choice of value h . (That leads to a little group scaling, discussed in Subsection 2.3.3.) If it is assumed that momenta are real, then the two types of spinor are related by complex conjugation. However, momenta are usually considered to be complex-valued in spinor-helicity calculations, leading to independent spinors and allowing techniques such as BCFW recursion [19] to be used.

Amplitudes themselves can then be considered functions of the spinors $\{\lambda_i, \tilde{\lambda}_i\}$, where i ranges over the external momenta, rather than the four-momenta. Expressions are built out of Lorentz-invariant spinor products, defined

$$\begin{aligned} \langle ij \rangle &\equiv \lambda_i^\alpha \lambda_{j\alpha} = \epsilon_{\alpha\beta} \lambda_i^\alpha \lambda_j^\beta = -\langle ji \rangle, \\ [ij] &\equiv \tilde{\lambda}_{i\dot{\alpha}} \tilde{\lambda}_j^{\dot{\alpha}} = -\epsilon_{\dot{\alpha}\dot{\beta}} \tilde{\lambda}_i^{\dot{\alpha}} \tilde{\lambda}_j^{\dot{\beta}} = -[ji], \end{aligned} \quad (2.21)$$

where the antisymmetric Levi-Civita tensor is used to raise and lower spinor indices.

Further useful structures can be defined in terms of spinors and spinor products. The

common Mandelstam variable s_{ij} is expressed as

$$s_{ij} \equiv (p_i + p_j)^2 = 2p_i \cdot p_j = \langle i j \rangle [j i] \quad (2.22)$$

and in this thesis we also define a three-particle momentum factor

$$t_{ijk} \equiv (p_i + p_j + p_k)^2 = s_{ij} + s_{jk} + s_{ki}, \quad (2.23)$$

for later convenience. A way of compacting the notation, by joining two spinor products of opposite type, is also suggestive of how one can convert between full four-momentum factors and their spinors if desired,

$$[i|j|k\rangle \equiv [i j] \langle j k \rangle = \tilde{\lambda}_i^{\dot{\alpha}} p_{j\mu} \bar{\sigma}_{\dot{\alpha}\alpha}^{\mu} \lambda_k^{\alpha}. \quad (2.24)$$

A pair of polarisation definitions can now be made for historical purposes, although these do not tend to be used explicitly when applying modern spinor-helicity amplitude techniques. The polarisation vectors of external gluon legs can be rewritten using the helicity spinors [18], as

$$(\epsilon_i^+)_{\mu} = \frac{[q_i | \gamma_{\mu} | p_i \rangle}{\sqrt{2} [p_i q_i]} \quad (2.25)$$

and

$$(\epsilon_i^-)_{\mu} = -\frac{[p_i | \gamma_{\mu} | q_i \rangle}{\sqrt{2} \langle p_i q_i \rangle}, \quad (2.26)$$

where the momentum q_i is a reference momentum, which the final amplitude will have no dependence on. The γ_{μ} are Dirac matrices. The helicity spinor polarisation states obey all the required relations, such as being orthogonal to the momentum of their gluon,

$$(p_i)^{\mu} (\epsilon_i^{\pm})_{\mu} = 0, \quad (2.27)$$

and being mutually orthogonal,

$$(\epsilon_i^{\pm})_{\mu} (\epsilon_i^{\mp})^{*\mu} = (\epsilon_i^{\pm})_{\mu} (\epsilon_i^{\pm})^{\mu} = 0. \quad (2.28)$$

2 Foundations of Amplitude Techniques

Constructing Feynman diagrams using these spinor states, and the other colour-ordered rules of Table 2.1, is one way of obtaining partial amplitudes directly in a spinor-helicity form. However, that has been superseded by recursive methods, which build a desired amplitude from products of amplitudes with fewer legs. (See Chapters 3 and 4 for an in-depth discussion.)

2.3.2 Using spinors in amplitudes

One of the earliest demonstrations of the efficiency of the spinor-helicity formalism comes from the statement of the “maximally helicity violating”, or MHV, tree amplitude. (The amplitude featuring two gluons of negative helicity, and the rest positive.) The original result by Parke and Taylor [13] was proved in a compact spinor form [14] to be

$$A_n^{(0)}(1^+, \dots, i^-, \dots, j^-, \dots, n^+) = \frac{\langle ij \rangle^4}{\langle 12 \rangle \langle 23 \rangle \dots \langle (n-1)n \rangle \langle n1 \rangle}, \quad (2.29)$$

where here $\{i, j\}$ are taken to be the two gluons with negative helicity, and the remainder have positive helicity. One notable feature, beyond the impressive simplicity, is that only spinors of the type λ_i appear in the expression. That the $\tilde{\lambda}_i$ can be wholly absent from some expressions demonstrates how helicity spinors are a natural choice of variables for the system.

The simplest possible amplitudes, which form the basis for recursive procedures, are the three-point trees. This may be unexpected, as these are all vanishing when considering real four-momenta. With momentum conservation enforcing $p_1 + p_2 + p_3 = 0$, there is no non-vanishing momentum invariant out of which to build any structure. ($s_{12} = (p_1 + p_2)^2 = p_3^2 = 0$ etc.) However, if the choice is made to allow complex spinors in the momentum representation, then only one of the pair $\langle 12 \rangle$ or $[12]$ need to equal zero to satisfy $s_{12} = \langle 12 \rangle [21] = 0$. That way, we can obtain both MHV and $\overline{\text{MHV}}$ amplitudes, respectively,

$$A_3^{(0)}(1^-, 2^-, 3^+) = \frac{\langle 12 \rangle^3}{\langle 23 \rangle \langle 31 \rangle} \quad (2.30)$$

and

$$A_3^{(0)}(1^+, 2^+, 3^-) = -\frac{[12]^3}{[23][31]}, \quad (2.31)$$

where either $[1\,2] = [2\,3] = [3\,1] = 0$, or in the alternative case $\langle 1\,2 \rangle = \langle 2\,3 \rangle = \langle 3\,1 \rangle = 0$. These can be considered a special case of the Parke–Taylor result (eq. 2.29) for $n = 3$, or can be identified as the only allowed structures with the particular non-vanishing spinor products (see Subsection 2.3.3).

Why are such compact expressions for amplitudes possible in the spinor-helicity formalism? One reason is that spinors can only represent null momenta, having $\langle i\,i \rangle = [i\,i] = 0$. This makes them a natural choice when describing massless gluons, because the mass condition is built into the variables. In a four-momentum picture, there exists some additional redundancy in the variables of the amplitude expression, which must be fixed with the additional constraints $p_i^2 = 0$.

However, some redundancy does remain in the spinor-helicity notation. Schouten identities exist between the spinor products,

$$\begin{aligned} \langle i\,j \rangle \langle k\,l \rangle + \langle i\,k \rangle \langle l\,j \rangle + \langle i\,l \rangle \langle j\,k \rangle &= 0, \\ [i\,j] [k\,l] + [i\,k] [l\,j] + [i\,l] [j\,k] &= 0. \end{aligned} \tag{2.32}$$

2.3.3 Little group scaling

The explicit spinor definitions made in eq. 2.19 contain a freedom to choose some overall factor, which we denote with a constant h . Although this means an ambiguity when moving from four-momenta to spinors, it also gives rise to a beneficial little group scaling. Re-scaling the spinors by some constant α , so $h \rightarrow \alpha h$, the spinors relating to a particular gluon transform as

$$\lambda_i \rightarrow \alpha \lambda_i \quad \text{and} \quad \tilde{\lambda}_i \rightarrow \alpha^{-1} \tilde{\lambda}_i, \tag{2.33}$$

which leaves the momentum, $p_i = \lambda_i \tilde{\lambda}_i$, invariant. Considering a whole amplitude expression, it will contain as variables a spinor pair for each external gluon, which can each be separately re-scaled by some α_i . The powers of α_i which emerge from the amplitude under re-scaling depend on how many factors of the λ_i and $\tilde{\lambda}_i$ appear in the numerator and denominator. The overall exponent can be considered to be a “spinor weight” for that gluon.

Inspection of the spinor-helicity Feynman rules shows that only the external polarisation vectors contain spinors not paired into momenta, so only external gluons have non-zero weight under little group scaling. Spinor-helicity versions of the polarisation states also allow the scaling of any given momentum to be anticipated. Based on the

2 Foundations of Amplitude Techniques

helicities of the external momenta, it is found that

$$\mathcal{A}_n(1, \dots, i^\pm, \dots, n) \rightarrow \alpha^{\mp 2} \mathcal{A}_n(1, \dots, i^\pm, \dots, n), \quad (2.34)$$

after applying a scaling $h \rightarrow \alpha h$ to the spinors $\{\lambda_i, \tilde{\lambda}_i\}$.

In other words, we find that for any amplitude, a spinor weight can be assigned to each leg according to its helicity. A leg with positive helicity has overall weight -2 , and a leg with negative helicity has overall weight $+2$. These must be fulfilled by the spinors in the amplitude, which individually have the spinor weights:

- $+1$ for λ_i spinors in the numerator,
- -1 for $\tilde{\lambda}_i$ spinors in the numerator,
- -1 for λ_i spinors in the denominator,
- $+1$ for $\tilde{\lambda}_i$ spinors in the denominator.

This provides powerful constraints on the possible forms of amplitudes. In the simplest case, the three-point trees are fully determined, up to an overall constant, by their little group scaling.

3 The Six Gluon Two-Loop Amplitude

3.1 Introduction

Perturbative scattering amplitudes are an essential tool, both in comparing theory to experiment, and for inspecting symmetries of that theory that may not be apparent from the Lagrangian. We chose Yang–Mills as a focus, because it can give insight into the Standard Model of Particle Physics, both being gauge theories, and particularly into the behaviour of gluons of the strong force.

Currently, there is interest in predictions for two-loop amplitudes, or “Next-to-Next-to-Leading Order” (NNLO) predictions, which are of relevance to the energy scales and precision probed at the LHC [1, 2]. This represents the cutting edge of analytic Yang–Mills amplitude calculations. Significant progress has been made towards calculating all tree and one-loop amplitudes, but two-loop amplitudes present challenges that have not all been overcome. To proceed, amplitudes are separated into components which are calculated separately. Generally, this means making a specific choice of helicities for the external gluons, and colour decomposing the amplitude into “partial amplitudes” each multiplying a particular colour structure. (See Section 2.2 for details on this procedure.) All-plus helicity, being the most symmetric, tends to be the easiest calculation so the most progress has been made here. The partial amplitude multiplying a single colour trace and an N_c^2 factor is particularly simple, often being referred to as “leading in colour” and calculated before the other colour structures.

Prior research relating to two-loop amplitudes, also discussed in Chapter 1, guides the work undertaken in this chapter. Most structures of the five gluon amplitude have now been calculated: the all-plus leading in colour partial amplitude was first calculated using a generalised unitarity procedure [47, 49] (then presented more compactly in ref. [51]). It was re-derived using a simpler method of four-dimensional unitarity and augmented recursion in ref. [52], which is the method we use. Later, the remaining all-plus colour structures were calculated in refs. [53, 54], completing the all-plus amplitude. The single-minus helicity leading in colour partial amplitude was obtained in ref. [55] and the remaining leading in colour helicity configurations were obtained in ref. [57],

3 The Six Gluon Two-Loop Amplitude

both using finite field numerical methods.

For six gluons at two loops, the leading in colour all-plus partial amplitude (which we denote with $A_{6:1}^{(2)}(1^+, 2^+, 3^+, 4^+, 5^+, 6^+)$) was computed in ref. [58] using four-dimensional unitarity and augmented recursion.

In this chapter, we describe how all the partial amplitudes $A_{6:\lambda}^{(2)}(1^+, 2^+, 3^+, 4^+, 5^+, 6^+)$ of the full all-plus amplitude are calculated. The final results are a product of collaboration and were previously published in ref. [59]. As such, the emphasis of this chapter is on the work performed by the author of this thesis, and the explicit results contained within are those elements obtained by this author. For a complete statement of the amplitude, the reader is directed to the related paper.

The next section describes how an amplitude is decomposed according to colour trace structures, then into different types of function each with their own derivation process. The following sections contain overviews of the methods of unitarity cutting and augmented recursion. Finally, it is demonstrated how compact forms for the rational terms are reconstructed, then how the amplitude can be validated using collinear limit testing.

3.2 Structure of the Amplitude

We outline how a full colour amplitude is divided into parts, to be treated separately in later sections. The colour decomposition process, and the spinor-helicity formalism used throughout, was set out in Chapter 2.

3.2.1 Colour decomposition

Working in perturbative Yang–Mills, we can expand an ℓ -loop amplitude with n gluons in terms of its colour structures, as detailed in Section 2.2. A general statement of the colour trace decomposition is [6, 7, 8],

$$\mathcal{A}_n^{(\ell)} = \sum_{\lambda} A_{n:\lambda}^{(\ell)} C_{\lambda}, \quad (3.1)$$

where the $A_{n:\lambda}^{(\ell)}$ are known as partial amplitudes, and the C_{λ} contain traces over the $SU(N_c)$ (or $U(N_c)$) colour symmetry generator matrices, as well as factors of N_c . A general label λ is used to refer to the various types of colour structure which occur.

For the specific case of interest, the two-loop six-point amplitude, the $U(N_c)$ colour decomposition is [54]

$$\begin{aligned}
\mathcal{A}_6^{(2)}(1, 2, 3, 4, 5, 6) = & N_c^2 \sum_{S_6/\mathcal{P}_{6:1}} \text{Tr}[T^{a_1} T^{a_2} T^{a_3} T^{a_4} T^{a_5} T^{a_6}] A_{6:1}^{(2)}(a_1, a_2, a_3, a_4, a_5, a_6) \\
& + N_c \sum_{S_6/\mathcal{P}_{6:2}} \text{Tr}[T^{a_1}] \text{Tr}[T^{a_2} T^{a_3} T^{a_4} T^{a_5} T^{a_6}] A_{6:2}^{(2)}(a_1; a_2, a_3, a_4, a_5, a_6) \\
& + N_c \sum_{S_6/\mathcal{P}_{6:3}} \text{Tr}[T^{a_1} T^{a_2}] \text{Tr}[T^{a_3} T^{a_4} T^{a_5} T^{a_6}] A_{6:3}^{(2)}(a_1, a_2; a_3, a_4, a_5, a_6) \\
& + N_c \sum_{S_6/\mathcal{P}_{6:4}} \text{Tr}[T^{a_1} T^{a_2} T^{a_3}] \text{Tr}[T^{a_4} T^{a_5} T^{a_6}] A_{6:4}^{(2)}(a_1, a_2, a_3; a_4, a_5, a_6) \\
& + \sum_{S_6/\mathcal{P}_{6:1,1}} \text{Tr}[T^{a_1}] \text{Tr}[T^{a_2}] \text{Tr}[T^{a_3} T^{a_4} T^{a_5} T^{a_6}] A_{6:1,1}^{(2)}(a_1; a_2; a_3, a_4, a_5, a_6) \\
& + \sum_{S_6/\mathcal{P}_{6:1,2}} \text{Tr}[T^{a_1}] \text{Tr}[T^{a_2} T^{a_3}] \text{Tr}[T^{a_4} T^{a_5} T^{a_6}] A_{6:1,2}^{(2)}(a_1; a_2, a_3; a_4, a_5, a_6) \\
& + \sum_{S_6/\mathcal{P}_{6:2,2}} \text{Tr}[T^{a_1} T^{a_2}] \text{Tr}[T^{a_3} T^{a_4}] \text{Tr}[T^{a_5} T^{a_6}] A_{6:2,2}^{(2)}(a_1, a_2; a_3, a_4; a_5, a_6) \\
& + \sum_{S_6/\mathcal{P}_{6:1}} \text{Tr}[T^{a_1} T^{a_2} T^{a_3} T^{a_4} T^{a_5} T^{a_6}] A_{6:1B}^{(2)}(a_1, a_2, a_3, a_4, a_5, a_6),
\end{aligned} \tag{3.2}$$

where the T^a are the generator matrices of the colour symmetry. Each sum is over the permutations (S_6) of the momentum labels $\{a_1, a_2, \dots, a_6\}$, up to the cyclic and interchange symmetries of the trace structures ($\mathcal{P}_{6:\lambda}$).

The partial amplitudes $A_{6:\lambda}^{(2)}$ are gauge-invariant objects, with cyclic and interchange symmetries $\mathcal{P}_{6:\lambda}$ in their momentum arguments that match those of the associated trace

3 The Six Gluon Two-Loop Amplitude

structures. In full,

$$\begin{aligned}
\mathcal{P}_{6:1} &= Z_6(1, 2, 3, 4, 5, 6), \\
\mathcal{P}_{6:2} &= Z_5(2, 3, 4, 5, 6), \\
\mathcal{P}_{6:3} &= Z_2(1, 2) \times Z_4(3, 4, 5, 6), \\
\mathcal{P}_{6:4} &= Z_3(1, 2, 3) \times Z_3(4, 5, 6) \times Z_2(\{1, 2, 3\}, \{4, 5, 6\}), \\
\mathcal{P}_{6:1,1} &= Z_2(1, 2) \times Z_4(3, 4, 5, 6), \\
\mathcal{P}_{6:1,2} &= Z_2(2, 3) \times Z_3(4, 5, 6), \\
\mathcal{P}_{6:2,2} &= Z_2(1, 2) \times Z_2(3, 4) \times Z_2(5, 6) \times S_3(\{1, 2\}, \{3, 4\}, \{5, 6\}), \\
\mathcal{P}_{6:1B} &= \mathcal{P}_{6:1} = Z_6(1, 2, 3, 4, 5, 6).
\end{aligned} \tag{3.3}$$

The colour decomposition of eq. 3.2 is written for a $U(N_c)$ gauge theory, however it is also applicable with a smaller $SU(N_c)$ gauge group. In that case, generators must be traceless, so terms involving $\text{Tr}[T^a]$ vanish. The specifically $SU(N_c)$ partial amplitudes $A_{6:1}^{(2)}$, $A_{6:3}^{(2)}$, $A_{6:4}^{(2)}$, $A_{6:2,2}^{(2)}$ and $A_{6:1B}^{(2)}$ remain.

Even if the aim is to ultimately calculate amplitudes in an $SU(N_c)$ theory, the partial amplitudes found exclusively in $U(N_c)$ are useful to derive. Dependence in the complete set of partial amplitudes means that decoupling identities exist, as discussed in Section 2.2. For example, choosing to set $T^1 \rightarrow T^{U(1)} = \mathbb{I}$ and inspecting the coefficient of $N_c^2 \text{Tr}[T^2 T^3 T^4 T^5 T^6]$, there is

$$\begin{aligned}
&A_{6:2}^{(2)}(1; 2, 3, 4, 5, 6) + A_{6:1}^{(2)}(1, 2, 3, 4, 5, 6) + A_{6:1}^{(2)}(2, 1, 3, 4, 5, 6) \\
&+ A_{6:1}^{(2)}(2, 3, 1, 4, 5, 6) + A_{6:1}^{(2)}(2, 3, 4, 1, 5, 6) + A_{6:1}^{(2)}(2, 3, 4, 5, 1, 6) = 0.
\end{aligned} \tag{3.4}$$

With the same generator choice, inspecting the coefficients of $\text{Tr}[T^2 T^3 T^4 T^5 T^6]$ that do not contain N_c^2 gives another identity,

$$\begin{aligned}
&A_{6:1B}^{(2)}(1, 2, 3, 4, 5, 6) + A_{6:1B}^{(2)}(2, 1, 3, 4, 5, 6) + A_{6:1B}^{(2)}(2, 3, 1, 4, 5, 6) \\
&+ A_{6:1B}^{(2)}(2, 3, 4, 1, 5, 6) + A_{6:1B}^{(2)}(2, 3, 4, 5, 1, 6) = 0.
\end{aligned} \tag{3.5}$$

While the former can be used to determine the $U(N_c)$ partial amplitude $A_{6:2}^{(2)}$ from the leading in colour, the latter relates only to $A_{6:1B}^{(2)}$.

By calculating all $U(N_c)$ structures independently, the decoupling identities between partial amplitudes can be used as a powerful consistency check on the results.

3.2.2 Singularity structure

We will use dimensional regularisation when presenting the amplitude, to control the singularities that occur in both IR and UV regions. When the dimension is analytically continued to $D = 4 - 2\epsilon$, divergences are replaced by poles in ϵ . Various schemes exist to carry out the calculation, of which we use the four-dimensional helicity scheme [27].

As the singular structures of these partial amplitudes are known in general [42], we can subdivide ours into terms that contain divergences $U_{n:\lambda}^{(2)}$, or those that are finite $F_{n:\lambda}^{(2)}$,

$$A_{n:\lambda}^{(2)} = U_{n:\lambda}^{(2)} + F_{n:\lambda}^{(2)} + \mathcal{O}(\epsilon). \quad (3.6)$$

Following the lead of ref. [42], the UV divergences can be removed by expressing the bare coupling in terms of the running coupling defined in the $\overline{\text{MS}}$ scheme. The amplitude $A_{n:\lambda}^{(2)}$ above could be considered the renormalised form, although this has no bearing on the finite pieces $F_{n:\lambda}^{(2)}$, which are the focus of this work. In general, we would expect to see soft IR divergences and collinear IR divergences appearing in $U_{n:\lambda}^{(2)}$, with contributions up to $1/\epsilon^4$ [42]. However, due to the all-plus tree amplitude vanishing with our choice of all-plus helicity, the new divergent factor that appears in a general two-loop amplitude does not get to contribute. As such, poles have at most $1/\epsilon^2$ as in the one-loop case.

We note that the vanishing tree amplitude, and finiteness of the one-loop amplitude, mean that any regularisation scheme dependence appears only at $\mathcal{O}(\epsilon)$ in the two-loop all-plus amplitude. Both the divergent piece and finite piece are regularisation scheme independent [42].

The form of the IR singular structure for an all-plus two-loop amplitude was presented in a colour trace basis in [54], which we reproduce here (with some notational changes): define

$$I_{i,j} \equiv -\frac{(s_{ij})^{-\epsilon}}{\epsilon^2} \quad (3.7)$$

and for a list $S = \{a_1, a_2, \dots, a_s\}$,

$$I_r[S] = I_r[\{a_1, a_2, \dots, a_s\}] \equiv \sum_{i=1}^s I_{a_i, a_{i+1}}, \quad (3.8)$$

3 The Six Gluon Two-Loop Amplitude

where $I_{a_s, a_{s+1}} \equiv I_{a_s, a_1}$ is included in the sum. Also

$$\begin{aligned} I_j[S_1, S_2] &= I_j[\{a_1, a_2, \dots, a_s\}, \{b_1, b_2, \dots, b_t\}] \equiv (I_{a_1, a_s} + I_{b_1, b_t} - I_{a_1, b_1} - I_{a_s, b_t}), \\ I_k[S_1, S_2] &= I_k[\{a_1, a_2, \dots, a_s\}, \{b_1, b_2, \dots, b_t\}] \equiv (I_{a_1, b_t} + I_{b_1, a_s} - I_{a_1, b_1} - I_{a_s, b_t}), \end{aligned} \quad (3.9)$$

so that

$$I_r[S_1 \oplus S_2] = I_r[S_1] + I_r[S_2] + I_k[S_1, S_2] - I_j[S_1, S_2], \quad (3.10)$$

where $\{a_1, a_2, \dots, a_s\} \oplus \{b_1, b_2, \dots, b_t\} = \{a_1, a_2, \dots, a_s, b_1, b_2, \dots, b_t\}$.

For two-loop all-plus partial amplitudes, we have

$$\begin{aligned} U_{n:1}^{(2)}(S) &= A_{n:1}^{(1)}(S) \times I_r[S], \\ U_{n:r}^{(2)}(S_1; S_2) &= A_{n:r}^{(1)}(S_1; S_2) \times (I_r[S_1] + I_r[S_2]) \\ &\quad + \sum_{S'_1 \in C(S_1)} \sum_{S'_2 \in C(S_2)} A_{n:1}^{(1)}(S'_1 \oplus S'_2) \times I_j[S'_1, S'_2], \\ U_{n:s,t}^{(2)}(S_1; S_2; S_3) &= \sum_{S'_2 \in C(S_2)} \sum_{S'_3 \in C(S_3)} A_{n:r}^{(1)}(S'_1; S'_2 \oplus S'_3) \times I_j[S'_2, S'_3] \\ &\quad + \sum_{S'_1 \in C(S_1)} \sum_{S'_3 \in C(S_3)} A_{n:r}^{(1)}(S'_2; S'_1 \oplus S'_3) \times I_j[S'_1, S'_3] \\ &\quad + \sum_{S'_1 \in C(S_1)} \sum_{S'_2 \in C(S_2)} A_{n:r}^{(1)}(S'_3; S'_1 \oplus S'_2) \times I_j[S'_1, S'_2], \\ U_{n:1B}^{(2)}(S) &= \sum_{U(S)} A_{n:r}^{(1)}(S'_1; S'_2) \times I_k[S'_1, S'_2], \end{aligned} \quad (3.11)$$

where $C(S)$ is the set of cyclic permutations of S . $U(S)$ is the set of all distinct pairs of lists (S'_1, S'_2) such that $S'_1 \oplus S'_2 \in S$ (and the size of S'_i is greater than one). For our six-point amplitude specifically, we need

$$\begin{aligned} U(\{1, 2, 3, 4, 5, 6\}) &= \left\{ (\{1, 2, 3\}, \{4, 5, 6\}), (\{2, 3, 4\}, \{5, 6, 1\}), \right. \\ &\quad (\{3, 4, 5\}, \{6, 1, 2\}), (\{1, 2\}, \{3, 4, 5, 6\}), \\ &\quad (\{2, 3\}, \{4, 5, 6, 1\}), (\{3, 4\}, \{5, 6, 1, 2\}), \\ &\quad (\{4, 5\}, \{6, 1, 2, 3\}), (\{5, 6\}, \{1, 2, 3, 4\}), \\ &\quad \left. (\{6, 1\}, \{2, 3, 4, 5\}) \right\}, \end{aligned} \quad (3.12)$$

for example.

Having dealt with the singularities, we turn to the finite remainder function $F_{n:\lambda}^{(2)}$. This can be separated into polylogarithmic terms $P_{n:\lambda}^{(2)}$ and rational terms $R_{n:\lambda}^{(2)}$,

$$F_{n:\lambda}^{(2)} = P_{n:\lambda}^{(2)} + R_{n:\lambda}^{(2)}. \quad (3.13)$$

We can calculate the polylogarithmic piece using four-dimensional unitarity and the rational piece using augmented recursion.

3.3 Unitarity

It was shown by Passarino and Veltman [29] that a one-loop amplitude can be decomposed in terms of n -point scalar integral functions I_n^i ,

$$\mathcal{A}_n^{(1)} = \sum_i a_i I_4^i + \sum_j b_j I_3^j + \sum_k c_k I_2^k + \mathcal{R}_n + \mathcal{O}(\epsilon), \quad (3.14)$$

where a_i, b_j, c_k are rational coefficients and \mathcal{R}_n is a rational remainder. This provides a convenient way to calculate an amplitude, because the integral functions are relatively simple and may be re-used once calculated. What remains is determining the rational coefficients that appear, for which the unitarity technique [28, 31] was developed. This proceeds by considering making cuts to propagators in the loop amplitude, to reduce it to a basis of box, triangle and bubble integrals. The coefficients of the reduction are the amplitudes that remain after propagators have been cut and their momenta put on-shell.

For example, as the first step of following the generalised unitarity procedure [35], four cuts are made to the amplitude. This means choosing four propagators in the loop integrals to replace with delta functions that nullify their momenta,

$$\frac{1}{P^2} \rightarrow \delta^4(P^2), \quad (3.15)$$

where $P = \ell + p_i + \dots$ contains the loop momentum and some external momenta. The outcome is that every contribution to eq. 3.14 vanishes, except the particular integral function I_4^i matching the cut choice, which becomes the identity. The coefficient a_i is then equal to the amplitude with those four cuts applied, which can be represented as a product of four tree amplitudes with their (previously internal) momenta determined

3 The Six Gluon Two-Loop Amplitude

by the cut conditions. (See Figure 3.1 for a graphical example that will be used later.) Once the box function coefficients are determined in this way, three cuts can be made to find the triangle coefficients, and so on.

We will use the technique of four-dimensional unitarity cuts [64] to obtain the polylogarithmic pieces of the partial amplitudes. Due to the constraints of helicity in four dimensions, any set of unitarity cuts that cut both loops will create a vanishing coefficient [65, 60]. Therefore, one of the loops can be treated like a vertex insertion for the purposes of unitarity and our calculation can be analogous to that of a one-loop amplitude.

Previous work has used D -dimensional unitarity techniques to obtain two-loop amplitudes [47, 51]. The four-dimensional method differs in that the spinor-helicity formalism may be used straightforwardly, allowing for simpler calculations. We also do not need to consider two-loop integrals, because the unitarity procedure simplifies for all-plus helicity amplitudes in four dimensions. The trade-off in our method is that four-dimensional unitarity does not capture the rational piece, which we calculate separately by recursion methods, and the singularity structure is only found to $\mathcal{O}(\epsilon^0)$.

For finding $P_{6:\lambda}^{(2)}$, we need only consider the box integrals in eq. 3.14, shown in Figure 3.1. The bubble integrals are shown to have zero coefficient in ref. [64] and the triangle integrals contribute to $U_{6:\lambda}^{(2)}$ only. The box integrals can be separated into contributions to $U_{6:\lambda}^{(2)}$ and to $P_{6:\lambda}^{(2)}$ [54],

$$I_4^{2me}(S, T, K_2^2, K_4^2) = I_4^{2me} \Big|_{IR} - \frac{2}{ST - K_2^2 K_4^2} F^{2m}(S, T, K_2^2, K_4^2), \quad (3.16)$$

where F^{2m} is a dimensionless function of polylogarithms. The superscript label of I_4^{2me} indicates a box integral with two opposite corners “massive”. (Possessing more than one external momentum each.) Combining all the singular terms, the IR piece is again obtained, but truncated to $\mathcal{O}(\epsilon^0)$ [65, 54]:

$$\left(\sum_i a_i I_{4,i}^{2me} \Big|_{IR} + \sum_j b_j I_{3,j} \right)_{n:\lambda} = U_{n:\lambda}^{(2),\epsilon^0}(1^+, 2^+, \dots, n^+). \quad (3.17)$$

The function $U_{n:\lambda}^{(2),\epsilon^0}$ can be promoted to its all- ϵ form to find agreement with the full singularity structure.

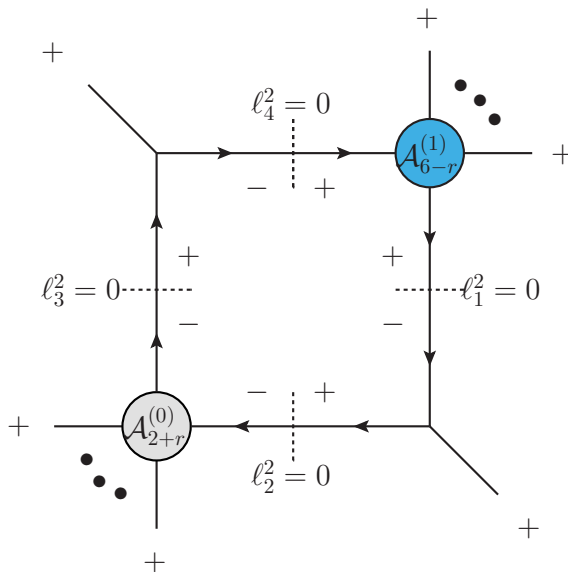


Figure 3.1: The quad-cut four-dimensional unitarity diagrams which provide the coefficients of polylogarithms in $P_{6:\lambda}^{(2)}(1^+, 2^+, 3^+, 4^+, 5^+, 6^+)$. The one-loop amplitude (blue) acts like an insertion, due to the helicity choice. Colour dressing the four amplitudes is necessary to obtain the full colour result, and each of $r = \{1, 2\}$ should be evaluated.

The polylogarithmic piece can therefore be expressed as

$$P_{6:\lambda}^{(2)} = \sum_i c_\lambda^i F_i^{2m}, \quad (3.18)$$

where the c_λ^i are rational coefficients found by drawing unitarity cuts. The F_i^{2m} are box functions containing dilogarithms and logarithms squared, obtained from evaluating the box integral itself [65],

$$\begin{aligned} F^{2m}(S, T, K_2^2, K_4^2) = & \text{Li}_2\left(1 - \frac{K_2^2}{S}\right) + \text{Li}_2\left(1 - \frac{K_2^2}{T}\right) + \text{Li}_2\left(1 - \frac{K_4^2}{S}\right) \\ & + \text{Li}_2\left(1 - \frac{K_4^2}{T}\right) - \text{Li}_2\left(1 - \frac{K_2^2 K_4^2}{ST}\right) + \frac{1}{2} \ln^2\left(\frac{S}{T}\right), \end{aligned} \quad (3.19)$$

and when $K_2^2 = 0$,

$$F^{2m}(S, T, 0, K_4^2) = \text{Li}_2\left(1 - \frac{K_4^2}{S}\right) + \text{Li}_2\left(1 - \frac{K_4^2}{T}\right) + \frac{1}{2} \ln^2\left(\frac{S}{T}\right) + \frac{\pi^2}{6}. \quad (3.20)$$

3 The Six Gluon Two-Loop Amplitude

The full results for $P_{6;\lambda}^{(2)}$, in terms of rational coefficients and the above functions, are found in ref. [59] as derived by this author's collaborators.

3.4 Augmented Recursion

The rational pieces of the amplitude, $R_{6;\lambda}^{(2)}$, are then determined using a procedure of augmented recursion. The technique is an extension of an earlier recursive method, which we first outline.

Tree amplitudes are fully rational, and Britto, Cachazo, Feng and Witten showed how these can be obtained recursively from lower-point amplitudes by treating the amplitude as a function of complex momenta, and investigating its pole structure [19]. For BCFW recursion, a complex shift is applied to two of the gluon momenta, p_1 and p_2 , shifting the spinors as

$$\begin{aligned}\tilde{\lambda}_1 &\rightarrow \tilde{\lambda}_1(z) = \tilde{\lambda}_1 - z\tilde{\lambda}_2, \\ \lambda_2 &\rightarrow \lambda_2(z) = \lambda_2 + z\lambda_1,\end{aligned}\tag{3.21}$$

where z is a new complex variable. The momenta $\hat{p}_1(z)$ and $\hat{p}_2(z)$, containing the shifted spinors, remain on-shell and overall momentum conservation is preserved. The rational amplitude can now be considered to be a complex function $R(z)$.

Applying Cauchy's theorem to $R(z)/z$ over a contour at infinity, and assuming that $R(z)$ vanishes at large $|z|$, gives

$$R(0) = - \sum_{z_{ij} \neq 0} \text{Res} \left[\frac{R(z)}{z} \right] \Big|_{z_{ij}},\tag{3.22}$$

where z_{ij} are the positions of poles in $R(z)$. $R(0)$ is the original unshifted function that we wish to find. For tree amplitudes $R^{(tree)}$, considering their Feynman diagram decomposition shows us that they will only contain simple poles, appearing as a result of (shifted) propagators

$$\begin{aligned}\frac{1}{\hat{p}_{ij}^2(z)} &\equiv \frac{1}{(p_i + \dots + \hat{p}_1(z) + \dots + p_j)^2} \\ &= \frac{1}{p_{ij}^2 - z\langle 2|p_{ij}|1 \rangle} = \frac{1}{z - z_{ij}} \frac{(-1)}{\langle 2|p_{ij}|1 \rangle},\end{aligned}\tag{3.23}$$

where

$$z_{ij} = \frac{p_{ij}^2}{\langle 2|p_{ij}|1\rangle}. \quad (3.24)$$

When a particular propagator goes on-shell, the structures on either side can be written as lower-point amplitudes,

$$\lim_{z \rightarrow z_{ij}} R^{(tree)}(z) = \frac{(-1)}{\langle 2|p_{ij}|1\rangle} \sum_{h=\pm 1} R_L^h(z_{ij}) \frac{1}{z - z_{ij}} R_R^{-h}(z_{ij}), \quad (3.25)$$

where R_L and R_R are amplitudes and the superscript $\pm h$ is shorthand for the helicity on the p_{ij} leg entering the propagator. Comparing to a Laurent expansion around the pole z_{ij} ,

$$R^{(tree)}(z) = \frac{a_{-1}^{(ij)}}{z - z_{ij}} + \mathcal{O}((z - z_{ij})^0), \quad (3.26)$$

we identify the residue as these amplitudes and see that eq. 3.22 becomes

$$R^{(tree)} = - \sum_{z_{ij} \neq 0} \frac{a_{-1}^{(ij)}}{z_{ij}} = \sum_{z_{ij} \neq 0} \sum_{h=\pm 1} R_L^h(z_{ij}) \frac{1}{p_{ij}^2} R_R^{-h}(z_{ij}). \quad (3.27)$$

That is, the desired amplitude can be determined entirely by its factorisations into smaller (complex-shifted) amplitudes. The BCFW procedure allows the easy calculation of any tree amplitude, which can be built up recursively from the simplest amplitudes (the three-point tree amplitudes).

For two-loop amplitudes as approached in this thesis, the situation is more complex. The amplitudes are no longer purely rational, also containing polylogarithmic terms emerging from loop integrals. The BCFW argument about shifted propagators does not apply to these terms. (They were instead calculated using unitarity cutting in Section 3.3.) Eq. 3.22 does still apply to the rational piece $R_{n:\lambda}^{(2)}$, however there is now the possibility of double poles occurring. If we Laurent expand our rational piece,

$$R_{n:\lambda}^{(2)}(z) = \frac{a_{-2}^{(ij)}}{(z - z_{ij})^2} + \frac{a_{-1}^{(ij)}}{(z - z_{ij})} + \mathcal{O}((z - z_{ij})^0), \quad (3.28)$$

3 The Six Gluon Two-Loop Amplitude

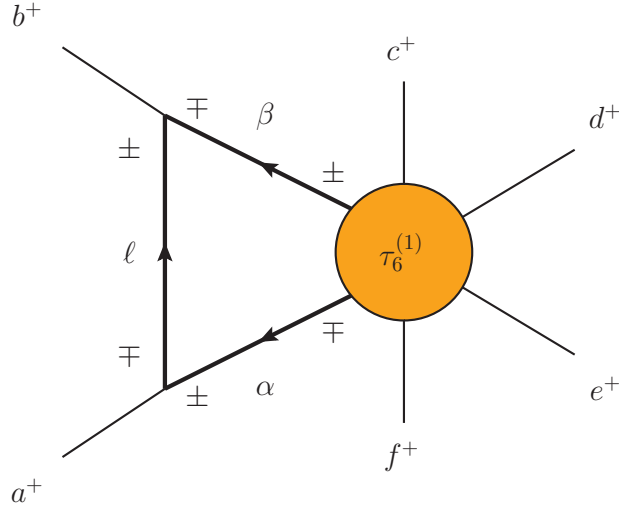


Figure 3.2: The augmented recursion diagram for the two-loop six-point rational piece. It generates both the double and simple s_{ab} poles, for use in recursion. An explicit loop integral must be carried out over off-shell internal propagators, marked with thick lines. A current, which is a structure with two off-shell legs, is involved.

then the residues in eq. 3.22 are

$$\text{Res}\left[\frac{R(z)}{z}\right]\Big|_{z_{ij}} = -\frac{a_{-2}}{z_{ij}^2} + \frac{a_{-1}}{z_{ij}}. \quad (3.29)$$

However, only the residue of the leading pole can be found by a straightforward factorisation. The sub-leading pole receives non-factorising contributions, meaning we must find these through other means.

Augmented recursion provides a way to capture both the leading and sub-leading pole information, by drawing diagrams involving partially off-shell objects known as currents [52]. To illustrate this, the diagram required for the six-point calculation is presented in Figure 3.2. Carrying out the loop integral over the internal off-shell momenta, both leading and sub-leading poles are obtained and can be used in the recursion procedure in an analogous way to a factorisation diagram. Generating the current required, which is an object similar to an amplitude with two off-shell legs, is non-trivial and we describe that process in detail in Chapter 5. The difficulty of representing off-shell momenta with spinors is overcome by using an axial gauge formalism [66, 41, 67], which introduces a reference momentum into the derivation.

To obtain each colour structure $R_{6,\lambda}^{(2)}$, all possible factorisations (in the case of sim-

ple poles) and augmented recursion diagrams (in the case of double poles) must be identified, and their components dressed with colour. An appropriate complex shift is required, such that the expression vanishes at large z as required by the contour integral. In this case, the Risager shift [23],

$$\begin{aligned}
 \lambda_1 &\rightarrow \lambda_{\hat{1}}(z) = \lambda_1 + z[23]\lambda_\eta, \\
 \lambda_2 &\rightarrow \lambda_{\hat{2}}(z) = \lambda_2 + z[31]\lambda_\eta, \\
 \lambda_3 &\rightarrow \lambda_{\hat{3}}(z) = \lambda_3 + z[12]\lambda_\eta,
 \end{aligned}
 \tag{3.30}$$

has this property, but requires the introduction of a reference spinor, λ_η . Finally, the residue is taken to obtain the rational piece results.

The output expressions are analytic and can be confirmed to follow the decoupling identities, possess all the expected symmetries, and are not affected by varying the reference momentum. However, they still contain occurrences of the reference momentum (both that introduced by the axial gauge formalism and by the complex shift) in their explicit forms. Having been constructed via recursion from multiple complicated objects, the rational pieces contain many terms and are hard to work with, showing none of their symmetries in a manifest way.

The next section demonstrates how these expressions can be reconstructed to obtain simpler, analytic forms with manifest symmetries and no remaining reference spinors. Doing so is desirable from a theoretical viewpoint, to better view and understand the properties of the theory. And from a practical viewpoint, optimising the expressions allows them to be evaluated more rapidly in numerical applications.

3.5 Rational Piece Reconstruction

The results of the augmented recursion procedure are analytic, but large and inefficient, rational piece expressions. Symmetries are not manifest, and a reference momentum appears throughout despite the functions being independent of it overall. To resolve these issues and obtain a compact, readable form, the rational pieces are reconstructed.

At this stage, the part of the derivation based on complex analyticity is complete. However, thinking about poles is still useful for understanding the structure of the amplitude. This thesis refers to “ t -poles” and “ s -poles”, which are denominator factors of t_{ijk} and s_{ij} , respectively. These diverge when the momenta involved become small or collinear. “Angle bracket poles” and “square bracket poles”, relating to $\langle ij \rangle$ and $[ij]$, also occur and diverge when their spinors become collinear. Note the different usage of

3 The Six Gluon Two-Loop Amplitude

“poles” to in the recursion process, where divergence happens due to a specific value of a complex shift.

The reconstruction method chosen is to consider the leading poles and sub-leading poles of the rational pieces separately.

Following a cutting-type argument, the leading poles can be written in terms of factorisations where the pole appears explicitly in a propagator. Unlike in BCFW recursion, the factorisations are used directly, rather than applying a complex shift to certain momenta. To obtain all pole types, a sum must be taken over all momentum arrangements. However, where a factorisation happens to include another leading pole, care must be taken not to double count that overlap between the factorisations. As with previous stages in the derivation, the factorisations should be dressed with colour in order to obtain the contributions to all partial amplitudes.

Subtracting the leading piece from the known rational piece expression, the remaining sub-leading poles can be identified, using pole tests where the function is evaluated numerically on a kinematic point chosen to make that pole blow up. Having removed the leading structures, what is found should be relatively simple, and can be fitted to a suitable compact ansatz. If necessary, the form of the ansatz can be further constrained by using pole tests where multiple poles become large simultaneously. The scaling of the overall numerical result, against the individual poles, reveals how many of those poles can occur together in a term.

The procedure is considered in greater detail in Chapter 6. Its use is now demonstrated for the colour structures $R_{6:2,2}^{(2)}$ and $R_{6:4}^{(2)}$.

3.5.1 Rational piece $R_{6:2,2}^{(2)}$

The six-point rational piece $R_{6:2,2}^{(2)}(1^+, 2^+, 3^+, 4^+, 5^+, 6^+)$ has simple angle bracket poles, as well as multiparticle t_{abc} -type poles. Those t -poles will be considered to be the leading pole structure, to be determined from factorisations. Although the angle bracket poles are also technically leading poles, several appear in each term, so attempting to untangle the overlap between factorisations would be impractical.

Colour dressing the factorisation

$$\mathcal{A}_4^{(1)}(a^+, b^+, c^+, -k_{abc}^+) - \frac{i}{t_{abc}} - \mathcal{A}_4^{(1)}(k_{abc}^-, d^+, e^+, f^+), \quad (3.31)$$

summing over permutations of external momenta, then extracting the coefficient of the relevant colour trace structure $\text{Tr}[T^a T^b] \text{Tr}[T^c T^d] \text{Tr}[T^e T^f]$ returns one type of factorisation for $R_{6:2,2}^{(2)}$. The different versions can be written under a sum, which matches the

expected symmetry of the colour structure,

$$\frac{1}{4} \sum_{\mathcal{P}_{6:2,2}} A_{4:3}^{(1)}(a^+, b^+; c^+, -k_{abc}^+) \frac{i}{t_{abc}} A_{4:3}^{(1)}(k_{abc}^-, d^+; e^+, f^+). \quad (3.32)$$

That the cyclic symmetries of the partial amplitude can be made to appear as a manifest sum over a basis function is quite a general feature when working with leading pole factorisations. In this case, the factorisation provided a sum over $Z_2(c, d) \times S_3(\{a, b\}, \{c, d\}, \{e, f\})$, which was promoted to the full $\mathcal{P}_{6:2,2}$ by recognising that the basis is invariant under $Z_2(a, b)$ and $Z_2(e, f)$ due to the symmetries of its constituent amplitudes. Inserting sums over those symmetries, with corresponding factors of $1/2$ as normalisation, allows the leading poles to be written in this compact, manifestly symmetric form.

Evaluating the basis, we have

$$\begin{aligned} B_{6:2,2}^{(lead)} &= \frac{1}{4} A_{4:3}^{(1)}(a^+, b^+; c^+, -k_{abc}^+) \frac{i}{t_{abc}} A_{4:3}^{(1)}(k_{abc}^-, d^+; e^+, f^+) \\ &= \frac{1}{4} (-2i) \frac{[c k_{abc}]^2}{\langle a b \rangle \langle b a \rangle} \frac{i}{t_{abc}} (2i) \frac{\langle k_{abc} | e f | k_{abc} \rangle}{\langle d e \rangle \langle e f \rangle \langle f d \rangle} \\ &= \frac{i}{t_{abc}} \frac{[e f] [c | k_{abc} | e] [c | k_{abc} | f]}{\langle a b \rangle^2 \langle d e \rangle \langle e f \rangle \langle f d \rangle} + \mathcal{O}(t_{abc}^0), \end{aligned} \quad (3.33)$$

where the k_{abc} appearing in spinor products are “nullified” in the axial gauge formalism [41], then are paired up to form non-null momentum factors. It is sufficient to know that the extra terms created this way are $\mathcal{O}(t_{abc}^0)$, so do not affect the leading pole piece. (Further detail on nullified momenta is in Chapter 5.)

We note that there is no $\langle a b \rangle^2$ double pole in the partial amplitude itself, but one does appear in the factorisation. This is considered to be a “spurious” structure, because it implies the presence of pole behaviour that the amplitude does not possess. Therefore it should be removed, so that misleading “poles” do not appear in the final result. If not removed in the factorisation stage, the spurious pole must also appear in the sub-leading fitting stage to give an overall cancellation.

One manipulation that removes the spurious pole is to introduce factors of a genuine pole, $\langle b c \rangle$, to the numerator and denominator. Then carrying out a Schouten identity

3 The Six Gluon Two-Loop Amplitude

with a k_{abc} -containing numerator factor,

$$\begin{aligned}
B_{6:2,2}^{(lead)} &= \frac{i}{t_{abc}} \frac{[e f] [c|k_{abc}|e] [c|k_{abc}|f] \langle b c \rangle}{\langle a b \rangle^2 \langle b c \rangle \langle d e \rangle \langle e f \rangle \langle f d \rangle} \\
&= -\frac{i}{t_{abc}} \frac{[e f] [c|k_{abc}|e]}{\langle a b \rangle^2 \langle b c \rangle \langle d e \rangle \langle e f \rangle \langle f d \rangle} ([c|k_{abc}|b] \langle c f \rangle + [c|k_{abc}|c] \langle f b \rangle) \\
&= -\frac{i}{t_{abc}} \frac{[e f] [c|k_{abc}|e]}{\langle a b \rangle^2 \langle b c \rangle \langle d e \rangle \langle e f \rangle \langle f d \rangle} ([c a] \langle a b \rangle \langle c f \rangle + (t_{abc} - s_{ab}) \langle f b \rangle) \\
&= -\frac{i}{t_{abc}} \frac{[e f] [c|k_{abc}|e] ([c a] \langle e f \rangle - [b a] \langle f b \rangle)}{\langle a b \rangle \langle b c \rangle \langle d e \rangle \langle e f \rangle \langle f d \rangle} + \mathcal{O}(t_{abc}^0) \\
&= \frac{i}{t_{abc}} \frac{[e f] [c|k_{abc}|e] [a|k_{abc}|f]}{\langle a b \rangle \langle b c \rangle \langle d e \rangle \langle e f \rangle \langle f d \rangle} + \mathcal{O}(t_{abc}^0), \tag{3.34}
\end{aligned}$$

a form for the leading poles is obtained that is compact and manifestly free of spurious poles.

For the ansatz fitting stage, pole tests find that the sub-leading terms contain only simple poles $\langle a b \rangle$, $\langle b c \rangle$, and those that are equivalent to these under the $\mathcal{P}_{6:2,2}$ symmetry. Choosing an ansatz basis with these poles, placed under a $\mathcal{P}_{6:2,2}$ sum to ensure a symmetric result, a fit is easily obtained.

The full rational piece result, incorporating the leading poles from factorisations and sub-leading poles from ansatz fitting, is [59]

$$R_{6:2,2}^{(2)}(a, b, c, d, e, f) = \sum_{\mathcal{P}_{6:2,2}} i \frac{G_{6:2,2}^{lead}(a, b, c, d, e, f) + G_{6:2,2}^{sub}(a, b, c, d, e, f)}{\langle a b \rangle \langle b c \rangle \langle c a \rangle \langle d e \rangle \langle e f \rangle \langle f d \rangle}, \tag{3.35}$$

where

$$\begin{aligned}
G_{6:2,2}^{lead}(a, b, c, d, e, f) &= \frac{\langle b|k_{abc}f|d \rangle [b|ck_{abc}|d]}{t_{abc}}, \\
G_{6:2,2}^{sub}(a, b, c, d, e, f) &= s_{ad}[e|k_{bc}|e] - s_{ac}[e|k_{fa}|e] - s_{ae}s_{af} - s_{ae}s_{cd}. \tag{3.36}
\end{aligned}$$

The final form is manifestly symmetric, free of spurious poles, and contains only the physical gluon momenta. Very few terms are required to describe the full behaviour, which is a significant simplification compared to the tens or hundreds present in the expression produced by augmented recursion.

3.5.2 Rational piece $R_{6:4}^{(2)}$

The six-point rational piece $R_{6:4}^{(2)}(1^+, 2^+, 3^+, 4^+, 5^+, 6^+)$ contains multiparticle poles t_{abc} , double poles $\langle ab \rangle^2$, and all those equivalent under the $\mathcal{P}_{6:4}$ symmetry. Poles in $\langle cd \rangle$ are also present, but are at most simple.

To find all the leading poles, both types of factorisation that can occur must be considered. Schematically, these are

$$\begin{aligned} & \mathcal{A}_4^{(1)}(a^+, b^+, c^+, -k_{abc}^+) - \frac{i}{t_{abc}} - \mathcal{A}_4^{(1)}(k_{abc}^-, d^+, e^+, f^+), \\ & \mathcal{A}_3^{(1)}(a^+, b^+, -k_{ab}^+) - \frac{i}{s_{ab}} - \mathcal{A}_5^{(1)}(k_{ab}^-, c^+, d^+, e^+, f^+), \end{aligned} \quad (3.37)$$

where the three-point one-loop amplitude provides the second factor of s_{ab} in the double poles. Summing over colour dressed, distinct permutations, the relevant structures are those accompanying $N_c \text{Tr}[T^a T^b T^c] \text{Tr}[T^d T^e T^f]$. The specific factorisations to evaluate are

$$\begin{aligned} & \sum_{\mathcal{P}_{6:4}} \frac{1}{3} A_{4:1}^{(1)}(a^+, b^+, c^+, -k_{abc}^+) \frac{i}{t_{abc}} A_{4:2}^{(1)}(k_{abc}^-; d^+, e^+, f^+), \\ & \sum_{\mathcal{P}_{6:4}} \frac{1}{3} A_{4:1}^{(1)}(a^+, b^+, c^+, -k_{abc}^-) \frac{i}{t_{abc}} A_{4:2}^{(1)}(k_{abc}^+; d^+, e^+, f^+), \\ & \sum_{\mathcal{P}_{6:4}} \frac{1}{9} A_{4:2}^{(1)}(-k_{abc}^+; a^+, b^+, c^+) \frac{i}{t_{abc}} A_{4:2}^{(1)}(k_{abc}^-; d^+, e^+, f^+), \\ & \sum_{\mathcal{P}_{6:4}} \frac{1}{3} A_{3:1}^{(1)}(a^+, b^+; -k_{ab}^+) \frac{i}{s_{ab}} A_{5:3}^{(1)}(k_{ab}^-, c^+; d^+, e^+, f^+), \end{aligned} \quad (3.38)$$

which can again be treated as a basis appearing under a $\mathcal{P}_{6:4}$ sum.

Treating each basis piece separately in turn, the first contribution gives rise to

$$\begin{aligned} B_{6:4}^1 &= \frac{1}{3} A_{4:1}^{(1)}(a^+, b^+, c^+, -k_{abc}^+) \frac{i}{t_{abc}} A_{4:2}^{(1)}(k_{abc}^-; d^+, e^+, f^+) \\ &= \frac{1}{3} (-1) \frac{i}{3} \frac{[ab][ck_{abc}]}{\langle ab \rangle \langle ck_{abc} \rangle} \frac{i}{t_{abc}} (-1) \frac{i \langle k_{abc} | de | k_{abc} \rangle}{\langle de \rangle \langle ef \rangle \langle fd \rangle} \\ &= -\frac{i}{9} \frac{1}{t_{abc}} \frac{[ab][ck_{abc}de|k_{abc}]}{\langle ab \rangle \langle ck_{abc} \rangle \langle de \rangle \langle ef \rangle \langle fd \rangle}, \end{aligned} \quad (3.39)$$

where the $\langle ck_{abc} \rangle$ represents a new type of spurious pole. It is common for the nullified propagator momentum to appear in factorisation denominators, so one of the main tasks in assembling leading pole factorisations is dealing with spurious poles such as

3 The Six Gluon Two-Loop Amplitude

this. At six-point, the issue can be resolved trivially by introducing a square bracket spinor product to pair with the spurious pole. Choosing outer momenta that cancel against the factor of k_{abc} within,

$$\begin{aligned}
B_{6:4}^1 &= -\frac{i}{9} \frac{1}{t_{abc}} \frac{[a b] [c | k_{abc} d e | k_{abc}] [k_{abc} a]}{\langle a b \rangle \langle c | k_{abc} | a \rangle \langle d e \rangle \langle e f \rangle \langle f d \rangle} + \mathcal{O}(t_{abc}^0) \\
&= -\frac{i}{9} \frac{1}{t_{abc}} \frac{[a b] [c | k_{abc} d e k_{abc} | a]}{\langle a b \rangle \langle c | b | a \rangle \langle d e \rangle \langle e f \rangle \langle f d \rangle} + \mathcal{O}(t_{abc}^0) \\
&= -\frac{i}{9} \frac{1}{t_{abc}} \frac{[c | k_{abc} d e k_{abc} | a]}{\langle a b \rangle \langle b c \rangle \langle d e \rangle \langle e f \rangle \langle f d \rangle} + \mathcal{O}(t_{abc}^0), \tag{3.40}
\end{aligned}$$

the piece is rendered free of spurious poles.

The second contribution can be evaluated similarly,

$$\begin{aligned}
B_{6:4}^2 &= \frac{1}{3} A_{4:1}^{(1)}(a^+, b^+, c^+, -k_{abc}^-) \frac{i}{t_{abc}} A_{4:2}^{(1)}(k_{abc}^+; d^+, e^+, f^+) \\
&= \frac{1}{3} \frac{i}{3} \frac{s_{ac} [a c]^2}{\langle a b \rangle \langle b c \rangle [c k_{abc}] [k_{abc} a] t_{abc}} (-1) \frac{i [k_{abc} | d e | k_{abc}]}{\langle d e \rangle \langle e f \rangle \langle f d \rangle} \\
&= \frac{i}{9} \frac{1}{t_{abc}} \frac{s_{ac} [a c]^2}{\langle a b \rangle \langle b c \rangle [c | k_{abc} | b] [a | k_{abc} | b]} \frac{\langle b | k_{abc} d e k_{abc} | b \rangle}{\langle d e \rangle \langle e f \rangle \langle f d \rangle} + \mathcal{O}(t_{abc}^0) \\
&= \frac{i}{9} \frac{1}{t_{abc}} \frac{s_{ac}}{\langle a b \rangle^2 \langle b c \rangle^2} \frac{\langle b | k_{abc} d e k_{abc} | b \rangle}{\langle d e \rangle \langle e f \rangle \langle f d \rangle} + \mathcal{O}(t_{abc}^0), \tag{3.41}
\end{aligned}$$

with two spurious double poles occurring. Making use of the $[e | k_{abc} | b]$ remaining in the numerator,

$$\begin{aligned}
B_{6:4}^2 &= \frac{i}{9} \frac{1}{t_{abc}} \frac{s_{ac}}{\langle a b \rangle^2 \langle b c \rangle^2} \frac{\langle d e \rangle [d | k_{abc} | b] [e | k_{abc} | b]}{\langle d e \rangle \langle e f \rangle \langle f d \rangle} \\
&= \frac{i}{9} \frac{1}{t_{abc}} \frac{s_{ac}}{\langle a b \rangle^2 \langle b c \rangle^2} \frac{\langle d e \rangle [d | k_{abc} | b]}{\langle d e \rangle \langle e f \rangle \langle f d \rangle} ([e a] \langle a b \rangle + [e c] \langle c b \rangle) \\
&= \frac{i}{9} \frac{1}{t_{abc}} \frac{\langle d e \rangle}{\langle d e \rangle \langle e f \rangle \langle f d \rangle} \left(\frac{s_{ac} [e a] [d | k_{abc} | b]}{\langle a b \rangle \langle b c \rangle^2} - \frac{s_{ac} [e c] [d | k_{abc} | b]}{\langle a b \rangle^2 \langle b c \rangle} \right) \\
&= \frac{i}{9} \frac{1}{t_{abc}} \frac{\langle d e \rangle}{\langle d e \rangle \langle e f \rangle \langle f d \rangle} s_{ac} \left(\frac{[e a] [d a]}{\langle b c \rangle^2} - \frac{[e a] [d c]}{\langle a b \rangle \langle b c \rangle} - \frac{[e c] [d a]}{\langle a b \rangle \langle b c \rangle} + \frac{[e c] [d c]}{\langle a b \rangle^2} \right), \tag{3.42}
\end{aligned}$$

the number of spurious poles in a term is reduced. Recognising that this basis lives under a $\mathcal{P}_{6:4}$ sum, a $Z_3(a, b, c)$ rotation can be made to bring one spurious pole type to

match the other. Then recombining the terms,

$$\begin{aligned}
 s_{ac} \left(\frac{[e a][d a]}{\langle b c \rangle^2} + \frac{[e c][d c]}{\langle a b \rangle^2} \right) &\rightarrow \frac{s_{cb}[e c][d c]}{\langle a b \rangle^2} + \frac{s_{ac}[e c][d c]}{\langle a b \rangle^2} \\
 &= \frac{(s_{bc} + s_{ca})[e c][d c]}{\langle a b \rangle^2} \\
 &= \frac{(t_{abc} - s_{ab})[e c][d c]}{\langle a b \rangle^2} \\
 &= \frac{[a b][e c][d c]}{\langle a b \rangle} + \mathcal{O}(t_{abc}), \tag{3.43}
 \end{aligned}$$

the remaining spurious pole cancels. Redefining the basis function,

$$\begin{aligned}
 B_{6:4}^2 &= \frac{i}{9} \frac{1}{t_{abc}} \frac{\langle d e \rangle}{\langle d e \rangle \langle e f \rangle \langle f d \rangle} \left(-s_{ac} \frac{[e a][d c]}{\langle a b \rangle \langle b c \rangle} - s_{ac} \frac{[e c][d a]}{\langle a b \rangle \langle b c \rangle} + \frac{[a b][e c][d c]}{\langle a b \rangle} \right) \\
 &= \frac{i}{9} \frac{1}{t_{abc}} \frac{1}{\langle a b \rangle \langle b c \rangle \langle d e \rangle \langle e f \rangle \langle f d \rangle} (s_{ac}[c|d e|a] + s_{ac}[a|d e|c] - [a|b c d e|c]) \tag{3.44}
 \end{aligned}$$

captures the poles of interest.

The third contribution is comparatively straightforward,

$$\begin{aligned}
 B_{6:4}^3 &= \frac{1}{9} A_{4:2}^{(1)}(-k_{abc}^+; a^+, b^+, c^+) \frac{i}{t_{abc}} A_{4:2}^{(1)}(k_{abc}^-; d^+, e^+, f^+) \\
 &= \frac{1}{9} \frac{i[k_{abc}|ab|k_{abc}]}{\langle a b \rangle \langle b c \rangle \langle c a \rangle} \frac{i}{t_{abc}} (-1) \frac{i\langle k_{abc}|d e|k_{abc} \rangle}{\langle d e \rangle \langle e f \rangle \langle f d \rangle} \\
 &= \frac{i}{9} \frac{1}{t_{abc}} \frac{\langle a b \rangle [b|k_{abc} d e k_{abc}|a]}{\langle a b \rangle \langle b c \rangle \langle c a \rangle \langle d e \rangle \langle e f \rangle \langle f d \rangle}, \tag{3.45}
 \end{aligned}$$

containing no spurious poles from the start.

The fourth contribution is also free of spurious poles,

$$\begin{aligned}
 B_{6:4}^4 &= \frac{1}{3} A_{3:1}^{(1)}(a^+, b^+; -k_{ab}^+) \frac{i}{s_{ab}} A_{5:3}^{(1)}(k_{ab}^-; c^+; d^+, e^+, f^+) \\
 &= \frac{1}{3} \frac{i[a b][b k_{ab}][k_{ab} a]}{3 s_{ab}} \frac{i}{s_{ab}} \left(\sum_{Z_3(d,e,f)} \frac{i(\langle k_{ab}|c d|k_{ab} \rangle + \langle k_{ab}|e f|k_{ab} \rangle)}{\langle c d \rangle \langle d e \rangle \langle e f \rangle \langle f c \rangle} \right) \\
 &= - \sum_{Z_3(d,e,f)} \frac{1}{9} \frac{[a b]}{s_{ab}^2} \frac{([b|k_{ab} c d k_{ab}|a] + [b|k_{ab} e f k_{ab}|a])}{\langle c d \rangle \langle d e \rangle \langle e f \rangle \langle f c \rangle}. \tag{3.46}
 \end{aligned}$$

The $Z_3(d, e, f)$ sum is duplicated in the overall $\mathcal{P}_{6:4}$ sum, so can be replaced with a

3 The Six Gluon Two-Loop Amplitude

factor of 3,

$$B_{6:4}^4 = -\frac{1}{3} \frac{[ab]}{\langle ab \rangle^2} \frac{(\langle a|cd|b \rangle + \langle a|ef|b \rangle)}{\langle cd \rangle \langle de \rangle \langle ef \rangle \langle fc \rangle}. \quad (3.47)$$

With the four pieces of $B_{6:4}$, a compact basis for the leading poles has been identified. Subtracting from the augmented recursion result leaves only sub-leading poles, to be fitted to an ansatz. An ansatz is prepared, with a basis of

$$\frac{G_1}{\langle ab \rangle \langle bc \rangle \langle ca \rangle \langle de \rangle \langle ef \rangle \langle fd \rangle} + \frac{G_2}{\langle ab \rangle \langle cd \rangle \langle de \rangle \langle ef \rangle \langle fc \rangle} \quad (3.48)$$

under a $\mathcal{P}_{6:4}$ sum. The G_1, G_2 represent numerators of terms with the correct spinor weights and unknown coefficients. These denominators are chosen to match the structures that appear in the leading pole terms, which are postulated to be present throughout the rational piece.

The fitting is successful, validating that choice. With the fitting result included, the full partial amplitude rational piece can then be written compactly as

$$R_{6:4}^{(2)}(a, b, c, d, e, f) = \frac{i}{36} \sum_{\mathcal{P}_{6:4}} \left(\frac{G_{6:4}^1(a, b, c, d, e, f) + G_{6:4}^2(a, b, c, d, e, f)}{\langle ab \rangle \langle bc \rangle \langle ca \rangle \langle de \rangle \langle ef \rangle \langle fd \rangle} + \frac{G_{6:4}^3(a, b, c, d, e, f) + G_{6:4}^4(a, b, c, d, e, f)}{\langle ab \rangle \langle cd \rangle \langle de \rangle \langle ef \rangle \langle fc \rangle} \right), \quad (3.49)$$

with

$$\begin{aligned} G_{6:4}^1(a, b, c, d, e, f) &= 4 \frac{\langle e|k_{abc}a|b \rangle [e|dk_{abc}|b]}{t_{abc}}, \\ G_{6:4}^2(a, b, c, d, e, f) &= s_{ad}^2 + 106s_{ab}s_{ad} + 102[a|bcd|a] - 4[a|bde|a] - 4[a|dbe|a], \\ G_{6:4}^3(a, b, c, d, e, f) &= -\frac{[ab]}{\langle ab \rangle} (\langle a|cd|b \rangle + \langle a|ef|b \rangle), \\ G_{6:4}^4(a, b, c, d, e, f) &= [a|cd|b] + [a|ef|b]. \end{aligned} \quad (3.50)$$

This compact form is a significantly simpler expression than the form produced by augmented recursion. Reference momenta have been removed, and the cyclic symmetries are guaranteed by the overall sum.

The remaining partial amplitudes can be found in ref. [59] in their compact, reconstructed forms. This completes the derivation of the two-loop six-point all-plus helicity full colour amplitude. The partial amplitudes possess all the expected symmetries and

satisfy the decoupling identities. An additional test on the result's validity is carried out in the next section.

3.6 Collinear Momentum Limits

Collinear momentum limits are a powerful validity check of amplitude results. These entail taking two momenta to be parallel, with the particular choice used here being $a \rightarrow zK$, $b \rightarrow (1-z)K$. The expected behaviour in this limit is that the amplitude reduces to lower point amplitudes multiplied by splitting functions.

The general behaviour for a two-loop collinear limit is [68]

$$\mathcal{A}_n^{(2)}(\dots, a^{\lambda_a}, b^{\lambda_b}, \dots) \xrightarrow{a||b} \sum_{\lambda=\pm} \left(\text{Split}_{-\lambda}^{(0)}(z; a^{\lambda_a}, b^{\lambda_b}) \mathcal{A}_{n-1}^{(2)}(\dots, K^\lambda, \dots) \right. \\ \left. + \text{Split}_{-\lambda}^{(1)}(z; a^{\lambda_a}, b^{\lambda_b}) \mathcal{A}_{n-1}^{(1)}(\dots, K^\lambda, \dots) \right. \\ \left. + \text{Split}_{-\lambda}^{(2)}(z; a^{\lambda_a}, b^{\lambda_b}) \mathcal{A}_{n-1}^{(0)}(\dots, K^\lambda, \dots) \right), \quad (3.51)$$

where $\text{Split}_h^{(\ell)}$ are splitting functions of differing loop level ℓ and helicity h . Working with all-plus helicity amplitudes, the tree amplitudes $\mathcal{A}_{n-1}^{(0)}$ are zero, leading to simplification.

An example of such testing was carried out in detail for the five-point leading in colour partial amplitude, $A_{5;1}^{(2)}(a^+, b^+, c^+, d^+, e^+)$, in ref. [52]. Extending the procedure to be able to test the full colour result is straightforward. Amplitudes on either side of eq. 3.51 should be interpreted as the full, colour-dressed forms. In order for the colour structures to be consistent, each splitting function must also be accompanied by a colour trace of $\text{Tr}[T^a T^b T^K]$. Those colour traces can be joined to those of the lower-point amplitudes using unitary relations,

$$\text{Tr}[T^a T^b T^K] \text{Tr}[T^K T^c \dots T^d] = \text{Tr}[T^a T^b T^c \dots T^d], \quad (3.52)$$

and the collinear limits re-expressed in terms of partial amplitudes by inspecting the coefficients of a certain colour structure. Immediately from this, we see that certain collinear limits can be predicted to be zero: any limit where the collinear momenta a and b are not adjacent in the partial amplitude, and in the same colour trace, cannot have any corresponding structure in terms of splitting functions.

Unlike when testing cyclic symmetries or decoupling identities, the divergent, polylog-

3 The Six Gluon Two-Loop Amplitude

arithmetic and rational parts of the amplitude cannot be treated separately in a collinear limit test. The contributions interact, with finite terms relating to $P_{5:\lambda}^{(2)}$ and $R_{5:\lambda}^{(2)}$ emerging from the divergent piece $U_{6:\lambda'}^{(2)}$ in the limit. The most straightforward route therefore is to test the collinear limits numerically on the full amplitude, on multiple numerical points and with high precision.

Doing so, relations are obtained for each partial amplitude. The six-point result is found to satisfy them, as required. Namely,

$$\begin{aligned}
A_{6:1}^{(2)}(a, b, c, d, e, f) &\xrightarrow{a\parallel b} \text{Split}_-^{(0)}(z; a^+, b^+) A_{5:1}^{(2)}(K^+, c, d, e, f) \\
&\quad + \text{Split}_+^{(1)}(z; a^+, b^+) A_{5:1}^{(1)}(K^-, c, d, e, f) \\
&\quad + \text{Split}_-^{(1)}(z; a^+, b^+) A_{5:1}^{(1)}(K^+, c, d, e, f), \\
A_{6:1}^{(2)}(a, b, c, d, e, f) &\xrightarrow{a\parallel c} 0, \\
A_{6:3}^{(2)}(a, b; c, d, e, f) &\xrightarrow{a\parallel b} \text{Split}_-^{(0)}(z; a^+, b^+) A_{5:2}^{(2)}(K^+; c, d, e, f) \\
&\quad + \text{Split}_+^{(1)}(z; a^+, b^+) A_{5:2}^{(1)}(K^-; c, d, e, f) \\
&\quad + \text{Split}_-^{(1)}(z; a^+, b^+) A_{5:2}^{(1)}(K^+; c, d, e, f), \\
A_{6:3}^{(2)}(a, b; c, d, e, f) &\xrightarrow{b\parallel c} 0, \\
A_{6:2,2}^{(2)}(a, b; c, d; e, f) &\xrightarrow{a\parallel b} \text{Split}_-^{(0)}(z; a^+, b^+) A_{5:1,2}^{(2)}(K^+; c, d; e, f), \\
A_{6:2,2}^{(2)}(a, b, c, d, e, f) &\xrightarrow{b\parallel c} 0
\end{aligned} \tag{3.53}$$

and so on, for the remaining partial amplitudes. As expected from the colour structure arguments, a collinear limit is zero if it involves non-adjacent momenta, or momenta belonging to different cyclic colour trace groupings. In the case of the non-vanishing limits, a partial amplitude splits into the equivalent lower-point amplitudes with $a+b \rightarrow K$, with appropriate splitting functions. (The ‘‘equivalent’’ five-point partial amplitude meaning the one where the cyclic group containing the collinear momentum is one entry smaller compared to the six-point partial amplitude of interest.) There are no triple-trace or N_c -independent single-trace partial amplitudes at one-loop level, so for those collinear limits only the two-loop amplitude appears on the right hand side. One-loop amplitudes contain leading in colour and sub-leading in colour structures, so two-loop partial amplitudes with those structures can also split into one-loop lower-point partial amplitudes.

3.7 Conclusions

We have calculated an analytic form for the full colour six-point two-loop Yang–Mills amplitude for gluons of all-plus helicity. The final result is a product of collaboration, with the results presented in this chapter being those of this author. The full expression is available in ref. [59].

The method employed was to decompose the amplitude into its gauge-invariant colour components, known as partial amplitudes. Each of these can be separated into pieces depending on the types of function involved. The polylogarithmic finite piece was derived using four-dimensional unitarity cuts, for which the problem simplifies to a one-loop one. An augmented recursion procedure was then used to calculate the rational terms not captured by unitarity. This technique goes beyond BCFW recursion by using current diagrams to describe sub-leading pole behaviour.

A procedure of reconstruction was employed to remove occurrences of reference momenta and express the result in a more efficient form. The leading poles were re-derived by hand, from a handful of factorisations. Results tend to be manifestly symmetric, often showing a surprising simplicity when compared to intermediate steps. Ansatzes are used to fit the remaining sub-leading poles, allowing the same symmetries to be enforced. The ability to reduce complicated amplitude expressions to simpler forms will be increasingly useful when working with greater numbers of gluons, so we devote Chapter 6 to developing the topic further.

The final six-point partial amplitudes obtained are compact, free of spurious poles or reference momenta, and show their cyclic symmetries explicitly. Validity checks such as decoupling identities, which inter-relate the partial amplitudes, and collinear momentum limits, which relate the amplitude to those of a lower point, are successful. Therefore high confidence can be placed in the results and the methodology employed to achieve them. The natural next step is to perform the procedure for the more challenging case of seven gluons, which is carried out in Chapter 4.

4 The Seven Gluon Two-Loop Amplitude

4.1 Introduction

Following the successful calculation of the six-point two-loop amplitude with all-plus helicity in the previous chapter, we will move on to calculating the amplitude with one further gluon: the full colour seven-point two-loop all-plus helicity amplitude. As before, the goal will be to find a compact, analytic form. Once again, this result has utility in high-precision experimental tests of the Standard Model and in investigating the symmetries of the theory. Additionally, obtaining another compact full colour amplitude using the same procedure allows the methodology itself to be improved and its suitability to more difficult calculations to be assessed. Any patterns that can be identified in the set of results may also present clues towards a general n -point two-loop amplitude form.

For six gluons at the two-loop level, only the all-plus amplitude has been computed (leading in colour [58], then full colour [59]), using four-dimensional unitarity and augmented recursion as described in Chapter 3. The seven gluon all-plus leading in colour partial amplitude has also been calculated using this methodology [60]. An n -point expression for the all-plus single colour trace, N_c^0 partial amplitude was conjectured in [63], satisfying various consistency conditions.

This chapter presents a compact analytic form for the two-loop seven gluon all-plus amplitude, at full colour, $\mathcal{A}_7^{(2)}(1^+, 2^+, 3^+, 4^+, 5^+, 6^+, 7^+)$. This involves re-deriving the leading colour piece and confirming the structure of the single trace N_c -independent piece, as well as deriving the remaining partial amplitudes for the first time. We use the method of four-dimensional unitarity [28, 31, 35] to obtain the polylogarithmic parts of these results in a simple way. Due to the presence of double poles in momenta, augmented recursion [39] is used to obtain the rational parts.

We will structure the chapter as follows: the next section describes the colour decomposition of the seven-point amplitude and lists the decoupling identities that arise between partial amplitudes. The following section describes the separation into pieces

4 The Seven Gluon Two-Loop Amplitude

to be treated with differing techniques. The method of four-dimensional unitarity is then carried out, followed by the resulting polylogarithmic contributions to the partial amplitudes. Augmented recursion will then be presented in detail, however the intermediate steps of generating the required currents will be omitted, to be covered in Chapter 5. This is done to maintain the flow of the present calculation, as the topic of currents is a somewhat separate one that requires its own in-depth treatment. Finally, the rational piece results are presented in a compact, analytic form. The process of reconstruction used to obtain the particularly simple version stated here is the topic of Chapter 6, so the detailed method used is postponed to that chapter.

4.2 Full Colour Amplitudes

The colour trace decomposition was specified for general tree, one-loop and two-loop amplitudes in Section 2.2. For the current task of a seven-point two-loop amplitude, we now provide an explicit decomposition. As before, our notation is inclusive of both the $SU(N_c)$ and $U(N_c)$ theories, allowing for the structures of both symmetry choices to be present. While the structures of $SU(N_c)$ may be of more interest experimentally, the partial amplitudes exclusive to the $U(N_c)$ symmetry still play a useful role in our calculations as consistent gauge-invariant objects that take part in overall decoupling identities.

At the two-loop level, the seven-point amplitude has an expansion [54]

$$\begin{aligned}
 \mathcal{A}_7^{(2)}(1, 2, 3, 4, 5, 6, 7) = & \\
 & N_c^2 \sum_{S_7/\mathcal{P}_{7:1}} \text{Tr}[T^{a_1} T^{a_2} T^{a_3} T^{a_4} T^{a_5} T^{a_6} T^{a_7}] A_{7:1}^{(2)}(a_1, a_2, a_3, a_4, a_5, a_6, a_7) \\
 & + N_c \sum_{S_7/\mathcal{P}_{7:2}} \text{Tr}[T^{a_1}] \text{Tr}[T^{a_2} T^{a_3} T^{a_4} T^{a_5} T^{a_6} T^{a_7}] A_{7:2}^{(2)}(a_1; a_2, a_3, a_4, a_5, a_6, a_7) \\
 & + N_c \sum_{S_7/\mathcal{P}_{7:3}} \text{Tr}[T^{a_1} T^{a_2}] \text{Tr}[T^{a_3} T^{a_4} T^{a_5} T^{a_6} T^{a_7}] A_{7:3}^{(2)}(a_1, a_2; a_3, a_4, a_5, a_6, a_7) \\
 & + N_c \sum_{S_7/\mathcal{P}_{7:4}} \text{Tr}[T^{a_1} T^{a_2} T^{a_3}] \text{Tr}[T^{a_4} T^{a_5} T^{a_6} T^{a_7}] A_{7:4}^{(2)}(a_1, a_2, a_3; a_4, a_5, a_6, a_7) \\
 & + \sum_{S_7/\mathcal{P}_{7:1,1}} \text{Tr}[T^{a_1}] \text{Tr}[T^{a_2}] \text{Tr}[T^{a_3} T^{a_4} T^{a_5} T^{a_6} T^{a_7}] A_{7:1,1}^{(2)}(a_1; a_2; a_3, a_4, a_5, a_6, a_7) \\
 & + \sum_{S_7/\mathcal{P}_{7:1,2}} \text{Tr}[T^{a_1}] \text{Tr}[T^{a_2} T^{a_3}] \text{Tr}[T^{a_4} T^{a_5} T^{a_6} T^{a_7}] A_{7:1,2}^{(2)}(a_1; a_2, a_3; a_4, a_5, a_6, a_7) \\
 & + \sum_{S_7/\mathcal{P}_{7:1,3}} \text{Tr}[T^{a_1}] \text{Tr}[T^{a_2} T^{a_3} T^{a_4}] \text{Tr}[T^{a_5} T^{a_6} T^{a_7}] A_{7:1,3}^{(2)}(a_1; a_2, a_3, a_4; a_5, a_6, a_7) \\
 & + \sum_{S_7/\mathcal{P}_{7:2,2}} \text{Tr}[T^{a_1} T^{a_2}] \text{Tr}[T^{a_3} T^{a_4}] \text{Tr}[T^{a_5} T^{a_6} T^{a_7}] A_{7:2,2}^{(2)}(a_1, a_2; a_3, a_4; a_5, a_6, a_7) \\
 & + \sum_{S_7/\mathcal{P}_{7:1}} \text{Tr}[T^{a_1} T^{a_2} T^{a_3} T^{a_4} T^{a_5} T^{a_6} T^{a_7}] A_{7:1B}^{(2)}(a_1, a_2, a_3, a_4, a_5, a_6, a_7) \quad (4.1)
 \end{aligned}$$

in a colour trace basis. The T^a are generators in the fundamental representation of $U(N_c)$ (or $SU(N_c)$) and the partial amplitudes $A_{7:1}^{(2)}$, $A_{7:r}^{(2)}$, $A_{7:s,t}^{(2)}$ and $A_{7:1B}^{(2)}$ are individually gauge-invariant functions. The symmetry factors $\mathcal{P}_{7:1}$, $\mathcal{P}_{7:r}$ and $\mathcal{P}_{7:s,t}$ in each case describe the symmetries of cycling the arguments of the trace structures, or interchanging two trace structures when they are of equal length, as previously defined in Chapter 2. The partial amplitudes themselves are invariant under the relevant $\mathcal{P}_{7:1}$, $\mathcal{P}_{7:r}$ or $\mathcal{P}_{7:s,t}$.

4 The Seven Gluon Two-Loop Amplitude

Specifically, the symmetry factors appearing in the seven-point expansion are

$$\begin{aligned}
\mathcal{P}_{7:1} &= Z_7(1, 2, 3, 4, 5, 6, 7), \\
\mathcal{P}_{7:2} &= Z_6(2, 3, 4, 5, 6, 7), \\
\mathcal{P}_{7:3} &= Z_2(1, 2) \times Z_5(3, 4, 5, 6, 7), \\
\mathcal{P}_{7:4} &= Z_3(1, 2, 3) \times Z_4(4, 5, 6, 7), \\
\mathcal{P}_{7:1,1} &= Z_5(3, 4, 5, 6, 7) \times Z_2(\{1\}, \{2\}), \\
\mathcal{P}_{7:1,2} &= Z_2(2, 3) \times Z_4(4, 5, 6, 7), \\
\mathcal{P}_{7:1,3} &= Z_3(2, 3, 4) \times Z_3(5, 6, 7) \times Z_2(\{2, 3, 4\}, \{5, 6, 7\}), \\
\mathcal{P}_{7:2,2} &= Z_2(1, 2) \times Z_2(3, 4) \times Z_3(5, 6, 7) \times Z_2(\{1, 2\}, \{3, 4\}), \\
\mathcal{P}_{7:1B} &= \mathcal{P}_{7:1} = Z_7(1, 2, 3, 4, 5, 6, 7).
\end{aligned} \tag{4.2}$$

The sums in the expansion are then over all permutations of the legs, up to these symmetries, written as $S_7/\mathcal{P}_{7:\lambda}$.

In the $SU(N_c)$ theory, factors of $\text{Tr}[T^a]$ vanish, so those terms would not appear in the above expansions. We also note that this is not the only possible colour decomposition; others exist [12] and may be more useful for certain tasks.

4.2.1 Decoupling identities

As discussed in Section 2.2, decoupling identities exist between the partial amplitudes in $U(N_c)$ Yang–Mills theory. In full, the two-loop seven-point amplitude possesses five $SU(N_c)$ partial amplitudes: $A_{7:1}^{(2)}$, $A_{7:3}^{(2)}$, $A_{7:4}^{(2)}$, $A_{7:2,2}^{(2)}$ and $A_{7:1B}^{(2)}$. It has four purely $U(N_c)$ partial amplitudes: $A_{7:2}^{(2)}$, $A_{7:1,1}^{(2)}$, $A_{7:1,2}^{(2)}$ and $A_{7:1,3}^{(2)}$.

The following decoupling identities can be derived, inter-relating both sets:

$$\begin{aligned}
&R_{7:1}^{(2)}(1, 2, 3, 4, 5, 6, 7) + R_{7:1}^{(2)}(1, 3, 4, 5, 6, 7, 2) + R_{7:1}^{(2)}(1, 4, 5, 6, 7, 2, 3) \\
&+ R_{7:1}^{(2)}(1, 5, 6, 7, 2, 3, 4) + R_{7:1}^{(2)}(1, 6, 7, 2, 3, 4, 5) + R_{7:1}^{(2)}(1, 7, 2, 3, 4, 5, 6) \\
&\quad + R_{7:2}^{(2)}(1; 2, 3, 4, 5, 6, 7) = 0,
\end{aligned} \tag{4.3}$$

$$\begin{aligned}
&R_{7:1,1}^{(2)}(1; 2; 3, 4, 5, 6, 7) + R_{7:2}^{(2)}(2; 1, 3, 4, 5, 6, 7) + R_{7:2}^{(2)}(2; 1, 4, 5, 6, 7, 3) \\
&+ R_{7:2}^{(2)}(2; 1, 5, 6, 7, 3, 4) + R_{7:2}^{(2)}(2; 1, 6, 7, 3, 4, 5) + R_{7:2}^{(2)}(2; 1, 7, 3, 4, 5, 6) \\
&\quad + R_{7:3}^{(2)}(1, 2; 3, 4, 5, 6, 7) = 0,
\end{aligned} \tag{4.4}$$

$$\begin{aligned}
& R_{7:1,2}^{(2)}(1; 2, 3; 4, 5, 6, 7) + R_{7:3}^{(2)}(2, 3; 1, 4, 5, 6, 7) + R_{7:3}^{(2)}(2, 3; 1, 5, 6, 7, 4) \\
& + R_{7:3}^{(2)}(2, 3; 1, 6, 7, 4, 5) + R_{7:3}^{(2)}(2, 3; 1, 7, 4, 5, 6) + R_{7:4}^{(2)}(1, 2, 3; 4, 5, 6, 7) \\
& + R_{7:4}^{(2)}(1, 3, 2; 4, 5, 6, 7) = 0, \quad (4.5)
\end{aligned}$$

$$\begin{aligned}
& R_{7:1,3}^{(2)}(1; 2, 3, 4; 5, 6, 7) + R_{7:4}^{(2)}(2, 3, 4; 1, 5, 6, 7) + R_{7:4}^{(2)}(2, 3, 4; 1, 6, 7, 5) \\
& + R_{7:4}^{(2)}(2, 3, 4; 1, 7, 5, 6) + R_{7:4}^{(2)}(5, 6, 7; 1, 2, 3, 4) + R_{7:4}^{(2)}(5, 6, 7; 1, 3, 4, 2) \\
& + R_{7:4}^{(2)}(5, 6, 7; 1, 4, 2, 3) = 0, \quad (4.6)
\end{aligned}$$

$$\begin{aligned}
& R_{7:1,1}^{(2)}(2; 3; 1, 4, 5, 6, 7) + R_{7:1,1}^{(2)}(2; 3; 1, 5, 6, 7, 4) + R_{7:1,1}^{(2)}(2; 3; 1, 6, 7, 4, 5) \\
& + R_{7:1,1}^{(2)}(2; 3; 1, 7, 4, 5, 6) + R_{7:1,2}^{(2)}(2; 1, 3; 4, 5, 6, 7) + R_{7:1,2}^{(2)}(3; 1, 2; 4, 5, 6, 7) = 0, \quad (4.7)
\end{aligned}$$

$$\begin{aligned}
& R_{7:1,2}^{(2)}(2; 3, 4; 1, 5, 6, 7) + R_{7:1,2}^{(2)}(2; 3, 4; 1, 6, 7, 5) + R_{7:1,2}^{(2)}(2; 3, 4; 1, 7, 5, 6) \\
& + R_{7:1,3}^{(2)}(2; 1, 3, 4; 5, 6, 7) + R_{7:1,3}^{(2)}(2; 1, 4, 3; 5, 6, 7) + R_{7:2,2}^{(2)}(1, 2; 3, 4; 5, 6, 7) = 0, \quad (4.8)
\end{aligned}$$

$$\begin{aligned}
& R_{7:2,2}^{(2)}(2, 3; 4, 5; 1, 6, 7) + R_{7:2,2}^{(2)}(2, 3; 4, 5; 1, 7, 6) + R_{7:2,2}^{(2)}(2, 3; 6, 7; 1, 4, 5) \\
& + R_{7:2,2}^{(2)}(2, 3; 6, 7; 1, 5, 4) + R_{7:2,2}^{(2)}(4, 5; 6, 7; 1, 2, 3) + R_{7:2,2}^{(2)}(4, 5; 6, 7; 1, 3, 2) = 0 \quad (4.9)
\end{aligned}$$

and

$$\begin{aligned}
& R_{7:1B}^{(2)}(1, 2, 3, 4, 5, 6, 7) + R_{7:1B}^{(2)}(1, 3, 4, 5, 6, 7, 2) + R_{7:1B}^{(2)}(1, 4, 5, 6, 7, 2, 3) \\
& + R_{7:1B}^{(2)}(1, 5, 6, 7, 2, 3, 4) + R_{7:1B}^{(2)}(1, 6, 7, 2, 3, 4, 5) + R_{7:1B}^{(2)}(1, 7, 2, 3, 4, 5, 6) = 0. \quad (4.10)
\end{aligned}$$

The decoupling identities do not fully exhaust the relations between structures in this colour decomposition. Further relations have been derived explicitly for four, five and six gluons [10, 69], by exploiting remaining redundancy in the colour trace decomposition.

We will independently calculate all nine $U(N_c)$ partial amplitudes with our methodology, then use the above decoupling identities as a consistency check on the results.

4.3 Structure of the Amplitude

Each partial amplitude can be further separated according to its singularity structures, so that an efficient derivation method can be applied to each piece. This process was described in greater detail in the previous chapter, in Section 3.2.2.

General forms for the singular terms, which we denote as $U_{7:\lambda}^{(2)}$ for the seven-point amplitude, were determined in ref. [42]. They take a particularly simple form due to the vanishing of the all-plus helicity tree amplitude. Of the finite terms, both polylogarithmic pieces, $P_{7:\lambda}^{(2)}$, and rational pieces, $R_{7:\lambda}^{(2)}$, are encountered. In total,

$$A_{7:\lambda}^{(2)} = U_{7:\lambda}^{(2)} + P_{7:\lambda}^{(2)} + R_{7:\lambda}^{(2)} + \mathcal{O}(\epsilon). \quad (4.11)$$

Four-dimensional unitarity cuts are employed to calculate the polylogarithms $P_{7:\lambda}^{(2)}$. Augmented recursion is used to obtain the rational contribution $R_{7:\lambda}^{(2)}$.

4.4 Polylogarithmic Terms

As previously discussed for the six-point amplitude in Section 3.3, loop amplitudes can be decomposed in terms of n -point scalar integral functions and a rational remainder [29]. Unitarity techniques were developed to identify the coefficients of these integral functions, by making cuts to propagators in the loop integral [28, 31].

For the seven-point calculation, the approach of generalised unitarity [35] is used again. The momenta inside the unitarity cuts are treated as four-dimensional [64], rather than the more general D dimensions of dimensional regularisation. This simplifies the procedure, particularly for all-plus helicity amplitudes. No non-vanishing cut diagrams exist where both loops are cut simultaneously, so the procedure is essentially a one-loop calculation with an extra one-loop amplitude as a vertex [65, 60].

The drawback of working with four-dimensional cuts is that they do not capture the rational piece of the amplitude, or any $\mathcal{O}(\epsilon)$ terms. Four-dimensional unitarity is used in this derivation only to find the polylogarithmic terms $P_{7:\lambda}^{(2)}$, so this is not an issue here.

It has been shown that bubble integrals have zero coefficient [64] and triangle integrals only contribute to divergences in $U_{7:\lambda}^{(2)}$ [65, 54]. Therefore quadruple cuts, relating to box integrals, are the only diagrams that need to be evaluated. These are shown in Figure 4.1. These are also the most convenient, as the four conditions freeze the loop momentum.

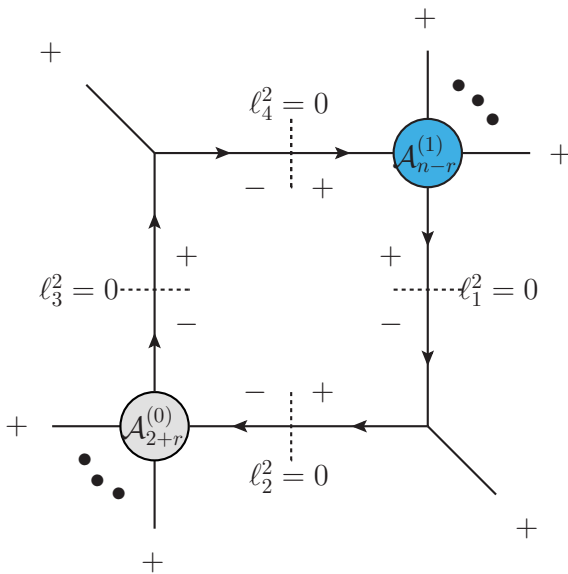


Figure 4.1: The quad-cut four-dimensional unitarity diagrams that determine the coefficients of polylogarithms in $P_{n:\lambda}^{(2)}(1^+, 2^+, \dots, n^+)$. At all-plus helicity, only diagrams where the one-loop amplitude (blue) acts like an insertion are non-vanishing. To obtain the full colour result, the four amplitudes must be dressed with colour.

4.4.1 Basis functions

The box function F^{2m} , resulting from the general scalar box integral [65], is defined in eqs. 3.19 and 3.20 in Section 3.3. We can expand the polylogarithmic piece in terms of it as

$$P_{7;\lambda}^{(2)} = \sum_i c_\lambda^i F_i^{2m}, \quad (4.12)$$

where the rational coefficients c_λ^i are determined only by the quadruple cuts.

Three types of cut diagrams occur, shown in Figure 4.2. Each four-amplitude factorisation is written out in full colour, then colour traces combine according to the $U(N_c)$ identity

$$(T^a)_{i_1}^{j_1} (T^a)_{i_2}^{j_2} = \delta_{i_1}^{j_2} \delta_{i_2}^{j_1}, \quad (4.13)$$

so that

$$\begin{aligned} \text{Tr}[T^1 \dots T^2 T^k] \times \text{Tr}[T^k T^3 \dots T^4] &= \text{Tr}[T^1 \dots T^2 T^3 \dots T^4], \\ \text{Tr}[T^1 \dots T^2 T^k] \times \text{Tr}[T^k] &= \text{Tr}[T^1 \dots T^2], \\ \text{Tr}[T^k] \times \text{Tr}[T^k] &= N_c. \end{aligned} \quad (4.14)$$

Summing over all distinct ways of permuting the external legs of the factorisation yields all the colour-dressed quadruple cuts. (Here, “distinct” means permutations of $\{1, 2, \dots, 7\}$, up to permutations of legs on the same amplitude.) For each partial amplitude, the cuts to be evaluated can be read off as the coefficients of the relevant trace structure. In all but the $P_{7;1B}$ case, we see a $\mathcal{P}_{7;\lambda}$ sum naturally arise. Factoring this out makes the symmetry of the partial amplitude explicit.

Four types of factorisation appear, for which general coefficient functions can be defined. Borrowing the notation of ref. [62] for convenience, the box function is redefined in terms of sets of arguments as

$$\begin{aligned} F(a, b; A_1; A_2) &= F^{2m}(K_{aA_1}^2, K_{A_1b}^2, K_{A_1}^2, K_{A_2}^2), \\ F(a, b; 0, A_2) &= F(a, b; A_1, 0) = 0. \end{aligned} \quad (4.15)$$

In the following definitions, sets of momenta occur and are denoted by capitals S, T . The symbol K_X refers to the momentum that sums all elements of the set X . Finally,

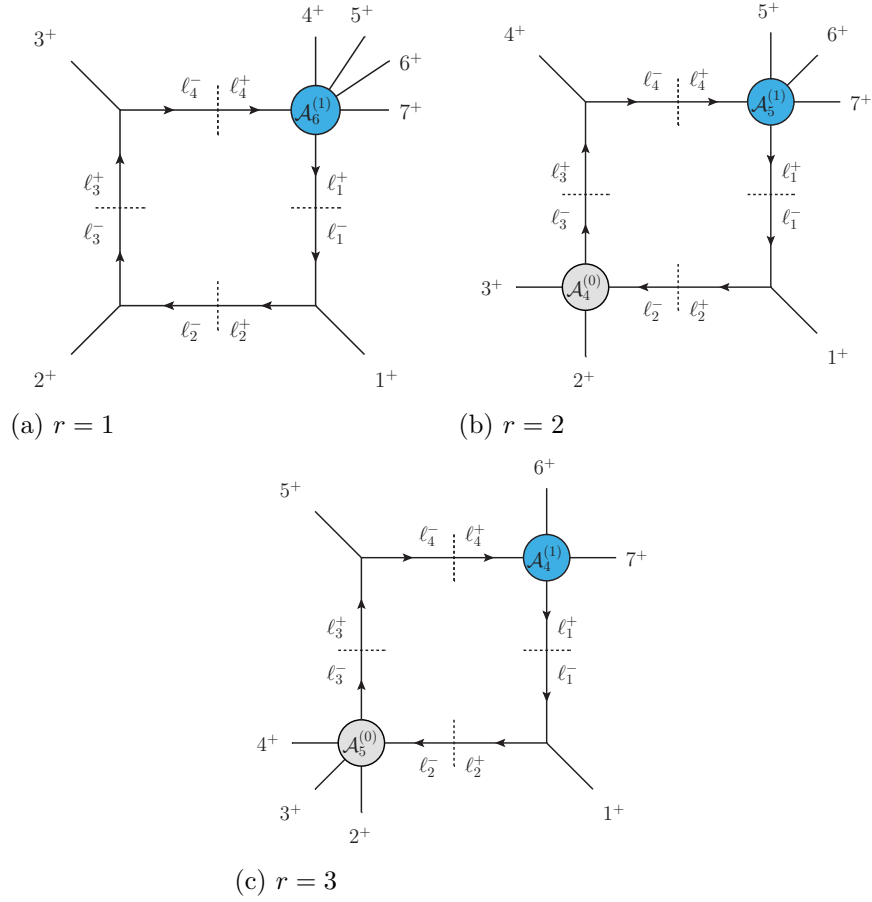


Figure 4.2: The three unitarity structures that contribute to $P_{7;\lambda}^{(2)}(1^+, 2^+, \dots, 7^+)$, labelled with the number, r , of external momenta originating on the MHV tree amplitude. All amplitudes are colour dressed. A sum over distinct permutations of the external legs must be taken to obtain all diagrams.

the momentum K_4 is defined to be $K_4 = K_{T_1} + K_{T_2}$ when a coefficient involves the sets T_1 and T_2 , or $K_4 = K_{T_1} + K_{T_2} + K_{t_3}$ when a momentum t_3 has also been specified.

The Parke–Talyor factor appears repeatedly, defined for arguments in terms of sets X, \dots, Y as

$$\begin{aligned} C_{PT}(X, \dots, Y) &= C_{PT}(X \oplus \dots \oplus Y) \\ &= \frac{1}{\langle x_1 x_2 \rangle \langle x_2 x_3 \rangle \cdots \langle y_{m-1} y_m \rangle \langle y_m x_1 \rangle}, \end{aligned} \quad (4.16)$$

where the elements of the sets $X = \{x_1, x_2, \dots, x_n\}$, \dots , $Y = \{y_1, y_2, \dots, y_m\}$ have

4 The Seven Gluon Two-Loop Amplitude

been joined into one set to form the cycle in the denominator. The spinor structure

$$\text{tr}_-[ijkl] \equiv \langle i j \rangle [j k] \langle k l \rangle [l i] \quad (4.17)$$

also appears.

Each coefficient arises from a different generalised quad-cut diagram. With the above definitions, and reproducing the notation of ref. [62], they take the forms

$$\begin{aligned} & C_1(a, b, S_1, S_2, T_1, T_2) \\ &= A_{|S_1 \oplus S_2|}^{(0)}(k^-, S_1, l^-, S_2) A_3^{(0)}(a^+, k^+, j^-) A_3^{(0)}(l^+, b^+, i^-) A^{(1)}(i^+, T_1, j^+, T_2) \\ &= \frac{i}{3} \langle a b \rangle^2 C_{PT}(a, S_1, b, S_2) C_{PT}(b, T_1, a, T_2) \\ &\quad \times \left(\frac{\langle b | T_1 T_2 | b \rangle \langle a | T_1 T_2 | a \rangle}{\langle a b \rangle^2} + \sum_{u < v < w < x \in K_4} \text{tr}_-[uvwx] + \sum_{u < v \in T_1} \frac{K_4^2 \langle b | uv | a \rangle + \langle a | T_2 uv K_4 | b \rangle}{\langle b a \rangle} \right. \\ &\quad + \sum_{u < v \in T_2} \frac{\langle b | K_4 uv T_2 | a \rangle}{\langle b a \rangle} + \sum_{u < v < w \in K_4} \frac{\langle b | uvw K_4 | a \rangle}{\langle a b \rangle} + \sum_{u < v < w \in T_1} \frac{\langle b | K_4 uvw | a \rangle}{\langle a b \rangle} \\ &\quad \left. + \sum_{u < v < w \in T_2} \frac{\langle a | uvw K_4 | b \rangle}{\langle b a \rangle} \right) \times F(a, b; S_1 \oplus S_2; T_1 \oplus T_2), \quad (4.18) \end{aligned}$$

$$\begin{aligned} & C_2(a, b, S_1, S_2, T_1, T_2, T_3) \\ &= A_{|S_1 \oplus S_2|}^{(0)}(k^-, S_1, l^-, S_2) A_3^{(0)}(a^+, k^+, j^-) A_3^{(0)}(l^+, b^+, i^-) A^{(1)}(i^+, T_1, j^+, T_2; T_3) \\ &= 2i \langle a b \rangle^2 C_{PT}(b, T_1, a, T_2) C_{PT}(T_3) C_{PT}(a, S_1, b, S_2) \times \left(K_{T_3}^2 \right)^2 \\ &\quad \times F(a, b; S_1 \oplus S_2; T_1 \oplus T_2 \oplus T_3), \quad (4.19) \end{aligned}$$

$$\begin{aligned} & C_3(a, b, S_1, S_2, T_1, T_2) \\ &= A_{|S_1 \oplus S_2|}^{(0)}(k^-, S_1, l^-, S_2) A_3^{(0)}(a^+, k^+, j^-) A_3^{(0)}(l^+, b^+, i^-) A^{(1)}(i^+, T_1; j^+, T_2) \\ &= 2i \langle a | K_{T_2} K_{T_1} | b \rangle^2 C_{PT}(a S_1 b S_2) C_{PT}(b T_1) C_{PT}(T_2 a) \\ &\quad \times F(a, b; S_1 \oplus S_2; T_1 \oplus T_2) \quad (4.20) \end{aligned}$$

and

$$\begin{aligned}
 & C_4(a, b, S_1, S_2, T_1, T_2, t_3) \\
 &= A_{|S_1 \oplus S_2|}^{(0)}(k^-, S_1, l^-, S_2) A_3^{(0)}(a^+, k^+, j^-) A_3^{(0)}(l^+, b^+, i^-) A^{(1)}(t_3; i^+, T_1, j^+, T_2) \\
 &= i \langle ab \rangle^2 C_{PT}(a, S_1, b, S_2) C_{PT}(b, T_1, a, T_2) \\
 &\quad \times \left(\frac{[t_3|K_4|a][t_3|(K_{T_1} - K_{T_2})|b]}{\langle ab \rangle} + 2[t_3|T_2 T_1|t_3] + \sum_{v < w \in K_4} [t_3|vw|t_3] \right) \\
 &\quad \times F(a, b; S_1 \oplus S_2; T_1 \oplus T_2 \oplus t_3). \tag{4.21}
 \end{aligned}$$

The polylogarithmic pieces of each partial amplitude are expressed in terms of these general functions in the following subsections.

In our results, the external on-shell momenta $\{1, 2, \dots, 7\}$ will always be of positive helicity. We omit writing an explicit helicity designation for brevity. The helicities of the ℓ_i match those depicted in Figure 4.2. A negative sign will appear on one of each ℓ_i pair to account for propagator direction, potentially introducing an overall factor of (-1) in the factorisation.

4.4.2 $\mathcal{P}_{7:1}$

For the first partial amplitude, the cuts to evaluate can be written schematically as

$$\text{cut}_{7:1}^{r=1} = A_{6:1}^{(1)}(4, 5, 6, 7, \ell_1, \ell_4) A_3^{(0)}(1, \ell_2, \ell_1) A_3^{(0)}(2, \ell_3, \ell_2) A_3^{(0)}(\ell_3, 3, \ell_4), \tag{4.22}$$

$$\text{cut}_{7:1}^{r=2} = A_{5:1}^{(1)}(5, 6, 7, \ell_1, \ell_4) A_3^{(0)}(1, \ell_2, \ell_1) A_3^{(0)}(\ell_3, 4, \ell_4) A_4^{(0)}(2, 3, \ell_3, \ell_2) \tag{4.23}$$

and

$$\text{cut}_{7:1}^{r=3} = A_{4:1}^{(1)}(6, 7, \ell_1, \ell_4) A_3^{(0)}(1, \ell_2, \ell_1) A_3^{(0)}(\ell_3, 5, \ell_4) A_5^{(0)}(2, 3, 4, \ell_3, \ell_2), \tag{4.24}$$

where ℓ_i are the on-shell cut momenta. The label $r = 1, 2, 3$ indicates which factorisation structure of Figure 4.2 resolves to a given contribution, once colour dressing is applied. The full cut diagram actually yields all permutations of the above structures under a $\mathcal{P}_{7:1}$ sum, which must be applied to the basis to complete the polylogarithmic piece.

4 The Seven Gluon Two-Loop Amplitude

Evaluating the cuts, we find a straightforward correspondence to the first general coefficient function. The result is simple and has a manifest symmetry,

$$\begin{aligned}
P_{7:1}^{(2)}(1, 2, 3, 4, 5, 6, 7) = \sum_{\mathcal{P}_{7:1}} & \left(C_1(1, 3, \{2\}, \{\}, \{4, 5, 6, 7\}, \{\}) \right. \\
& + C_1(1, 4, \{2, 3\}, \{\}, \{5, 6, 7\}, \{\}) \\
& \left. + C_1(1, 5, \{2, 3, 4\}, \{\}, \{6, 7\}, \{\}) \right). \quad (4.25)
\end{aligned}$$

4.4.3 $\mathcal{P}_{7:2}$

The cuts to evaluate can be written schematically as

$$\begin{aligned}
\text{cut}_{7:2}^{r=1} = & A_{6:1}^{(1)}(2, 3, 4, 5, \ell_1, \ell_4) A_3^{(0)}(1, \ell_2, \ell_3) A_3^{(0)}(6, \ell_2, \ell_1) A_3^{(0)}(\ell_3, 7, \ell_4) \\
& + A_{6:1}^{(1)}(2, 3, 4, 5, \ell_1, \ell_4) A_3^{(0)}(1, \ell_1, \ell_2) A_3^{(0)}(6, \ell_3, \ell_2) A_3^{(0)}(\ell_3, 7, \ell_4) \\
& + A_{6:1}^{(1)}(1, \ell_4, 2, 3, 4, \ell_1) A_3^{(0)}(5, \ell_2, \ell_1) A_3^{(0)}(6, \ell_3, \ell_2) A_3^{(0)}(\ell_3, 7, \ell_4) \\
& + A_{6:2}^{(1)}(1; 2, 3, 4, \ell_1, \ell_4) A_3^{(0)}(5, \ell_2, \ell_1) A_3^{(0)}(6, \ell_3, \ell_2) A_3^{(0)}(\ell_3, 7, \ell_4) \\
& + A_{6:1}^{(1)}(2, 3, 4, 5, \ell_1, \ell_4) A_3^{(0)}(6, \ell_2, \ell_1) A_3^{(0)}(7, \ell_3, \ell_2) A_3^{(0)}(\ell_3, \ell_4, 1), \quad (4.26)
\end{aligned}$$

$$\begin{aligned}
\text{cut}_{7:2}^{r=2} = & A_{5:1}^{(1)}(2, 3, 4, \ell_1, \ell_4) A_3^{(0)}(5, \ell_2, \ell_1) A_3^{(0)}(\ell_3, 7, \ell_4) A_4^{(0)}(1, \ell_2, 6, \ell_3) \\
& + A_{5:1}^{(1)}(2, 3, 4, \ell_1, \ell_4) A_3^{(0)}(1, \ell_1, \ell_2) A_3^{(0)}(\ell_3, 7, \ell_4) A_4^{(0)}(5, 6, \ell_3, \ell_2) \\
& + A_{5:1}^{(1)}(1, \ell_4, 2, 3, \ell_1) A_3^{(0)}(4, \ell_2, \ell_1) A_3^{(0)}(\ell_3, 7, \ell_4) A_4^{(0)}(5, 6, \ell_3, \ell_2) \\
& + A_{5:2}^{(1)}(1; 2, 3, \ell_1, \ell_4) A_3^{(0)}(4, \ell_2, \ell_1) A_3^{(0)}(\ell_3, 7, \ell_4) A_4^{(0)}(5, 6, \ell_3, \ell_2) \\
& + A_{5:1}^{(1)}(2, 3, 4, \ell_1, \ell_4) A_3^{(0)}(5, \ell_2, \ell_1) A_3^{(0)}(\ell_3, \ell_4, 1) A_4^{(0)}(6, 7, \ell_3, \ell_2) \quad (4.27)
\end{aligned}$$

and

$$\begin{aligned}
\text{cut}_{7:2}^{r=3} = & A_{4:1}^{(1)}(2, 3, \ell_1, \ell_4) A_3^{(0)}(4, \ell_2, \ell_1) A_3^{(0)}(\ell_3, 7, \ell_4) A_5^{(0)}(1, \ell_2, 5, 6, \ell_3) \\
& + A_{4:1}^{(1)}(2, 3, \ell_1, \ell_4) A_3^{(0)}(1, \ell_1, \ell_2) A_3^{(0)}(\ell_3, 7, \ell_4) A_5^{(0)}(4, 5, 6, \ell_3, \ell_2) \\
& + A_{4:1}^{(1)}(1, \ell_4, 2, \ell_1) A_3^{(0)}(3, \ell_2, \ell_1) A_3^{(0)}(\ell_3, 7, \ell_4) A_5^{(0)}(4, 5, 6, \ell_3, \ell_2) \\
& + A_{4:2}^{(1)}(1; 2, \ell_1, \ell_4) A_3^{(0)}(3, \ell_2, \ell_1) A_3^{(0)}(\ell_3, 7, \ell_4) A_5^{(0)}(4, 5, 6, \ell_3, \ell_2) \\
& + A_{4:1}^{(1)}(2, 3, \ell_1, \ell_4) A_3^{(0)}(4, \ell_2, \ell_1) A_3^{(0)}(\ell_3, \ell_4, 1) A_5^{(0)}(5, 6, 7, \ell_3, \ell_2), \quad (4.28)
\end{aligned}$$

where ℓ_i are the on-shell cut momenta. A $\mathcal{P}_{7:2}$ sum must then be applied to this basis.

Evaluating the cuts, the full result takes the form

$$P_{7:2}^{(2)}(1, 2, 3, 4, 5, 6, 7) = \sum_{\mathcal{P}_{7:2}} \left(P_{7:2}^{(2),r=1} + P_{7:2}^{(2),r=2} + P_{7:2}^{(2),r=3} \right), \quad (4.29)$$

where

$$\begin{aligned} P_{7:2}^{(2),r=1} = & -C_1(1, 7, \{6\}, \{\}, \{2, 3, 4, 5\}, \{\}) + C_1(5, 7, \{6\}, \{\}, \{2, 3, 4\}, \{1\}) \\ & - C_1(6, 1, \{7\}, \{\}, \{2, 3, 4, 5\}, \{\}) + C_1(6, 7, \{\}, \{1\}, \{2, 3, 4, 5\}, \{\}) \\ & + C_4(5, 7, \{6\}, \{\}, \{2, 3, 4\}, \{\}, 1), \end{aligned} \quad (4.30)$$

$$\begin{aligned} P_{7:2}^{(2),r=2} = & -C_1(1, 7, \{5, 6\}, \{\}, \{2, 3, 4\}, \{\}) + C_1(4, 7, \{5, 6\}, \{\}, \{2, 3\}, \{1\}) \\ & - C_1(5, 1, \{6, 7\}, \{\}, \{2, 3, 4\}, \{\}) + C_1(5, 7, \{6\}, \{1\}, \{2, 3, 4\}, \{\}) \\ & + C_4(4, 7, \{5, 6\}, \{\}, \{2, 3\}, \{\}, 1) \end{aligned} \quad (4.31)$$

and

$$\begin{aligned} P_{7:2}^{(2),r=3} = & -C_1(1, 7, \{4, 5, 6\}, \{\}, \{2, 3\}, \{\}) + C_1(3, 7, \{4, 5, 6\}, \{\}, \{2\}, \{1\}) \\ & - C_1(4, 1, \{5, 6, 7\}, \{\}, \{2, 3\}, \{\}) + C_1(4, 7, \{5, 6\}, \{1\}, \{2, 3\}, \{\}) \\ & + C_4(3, 7, \{4, 5, 6\}, \{\}, \{2\}, \{\}, 1). \end{aligned} \quad (4.32)$$

4.4.4 $\mathbf{P}_{7:3}$

The cuts to evaluate can be written schematically as

$$\begin{aligned} \text{cut}_{7:3}^{r=1} = & \frac{1}{2} A_{6:3}^{(1)}(1, 2; 3, 4, \ell_1, \ell_4) A_3^{(0)}(5, \ell_2, \ell_1) A_3^{(0)}(6, \ell_3, \ell_2) A_3^{(0)}(\ell_3, 7, \ell_4) \\ & + A_{6:1}^{(1)}(3, 4, 5, 6, \ell_1, \ell_4) A_3^{(0)}(1, \ell_1, \ell_2) A_3^{(0)}(2, \ell_2, \ell_3) A_3^{(0)}(\ell_3, 7, \ell_4) \\ & + A_{6:1}^{(1)}(1, \ell_4, 3, 4, 5, \ell_1) A_3^{(0)}(2, \ell_2, \ell_3) A_3^{(0)}(6, \ell_2, \ell_1) A_3^{(0)}(\ell_3, 7, \ell_4) \\ & + A_{6:1}^{(1)}(1, \ell_4, 3, 4, 5, \ell_1) A_3^{(0)}(2, \ell_1, \ell_2) A_3^{(0)}(6, \ell_3, \ell_2) A_3^{(0)}(\ell_3, 7, \ell_4) \\ & + A_{6:1}^{(1)}(1, 2, \ell_4, 3, 4, \ell_1) A_3^{(0)}(5, \ell_2, \ell_1) A_3^{(0)}(6, \ell_3, \ell_2) A_3^{(0)}(\ell_3, 7, \ell_4) \\ & + A_{6:1}^{(1)}(3, 4, 5, 6, \ell_1, \ell_4) A_3^{(0)}(1, \ell_2, \ell_3) A_3^{(0)}(7, \ell_2, \ell_1) A_3^{(0)}(\ell_3, \ell_4, 2) \\ & + A_{6:1}^{(1)}(3, 4, 5, 6, \ell_1, \ell_4) A_3^{(0)}(1, \ell_1, \ell_2) A_3^{(0)}(7, \ell_3, \ell_2) A_3^{(0)}(\ell_3, \ell_4, 2) \\ & + A_{6:1}^{(1)}(1, \ell_4, 3, 4, 5, \ell_1) A_3^{(0)}(6, \ell_2, \ell_1) A_3^{(0)}(7, \ell_3, \ell_2) A_3^{(0)}(\ell_3, \ell_4, 2), \end{aligned} \quad (4.33)$$

4 The Seven Gluon Two-Loop Amplitude

$$\begin{aligned}
\text{cut}_{7:3}^{r=2} = & \frac{1}{2} A_{5:3}^{(1)}(1, 2; 3, \ell_1, \ell_4) A_3^{(0)}(4, \ell_2, \ell_1) A_3^{(0)}(\ell_3, 7, \ell_4) A_4^{(0)}(5, 6, \ell_3, \ell_2) \\
& + A_{5:1}^{(1)}(3, 4, 5, \ell_1, \ell_4) A_3^{(0)}(6, \ell_2, \ell_1) A_3^{(0)}(\ell_3, 7, \ell_4) A_4^{(0)}(1, 2, \ell_2, \ell_3) \\
& + A_{5:1}^{(1)}(3, 4, 5, \ell_1, \ell_4) A_3^{(0)}(6, \ell_2, \ell_1) A_3^{(0)}(\ell_3, \ell_4, 2) A_4^{(0)}(1, \ell_2, 7, \ell_3) \\
& + A_{5:1}^{(1)}(3, 4, 5, \ell_1, \ell_4) A_3^{(0)}(1, \ell_1, \ell_2) A_3^{(0)}(\ell_3, 7, \ell_4) A_4^{(0)}(2, \ell_2, 6, \ell_3) \\
& + A_{5:1}^{(1)}(1, \ell_4, 3, 4, \ell_1) A_3^{(0)}(5, \ell_2, \ell_1) A_3^{(0)}(\ell_3, 7, \ell_4) A_4^{(0)}(2, \ell_2, 6, \ell_3) \\
& + A_{5:1}^{(1)}(1, \ell_4, 3, 4, \ell_1) A_3^{(0)}(2, \ell_1, \ell_2) A_3^{(0)}(\ell_3, 7, \ell_4) A_4^{(0)}(5, 6, \ell_3, \ell_2) \\
& + A_{5:1}^{(1)}(1, 2, \ell_4, 3, \ell_1) A_3^{(0)}(4, \ell_2, \ell_1) A_3^{(0)}(\ell_3, 7, \ell_4) A_4^{(0)}(5, 6, \ell_3, \ell_2) \\
& + A_{5:1}^{(1)}(3, 4, 5, \ell_1, \ell_4) A_3^{(0)}(1, \ell_1, \ell_2) A_3^{(0)}(\ell_3, \ell_4, 2) A_4^{(0)}(6, 7, \ell_3, \ell_2) \\
& + A_{5:1}^{(1)}(1, \ell_4, 3, 4, \ell_1) A_3^{(0)}(5, \ell_2, \ell_1) A_3^{(0)}(\ell_3, \ell_4, 2) A_4^{(0)}(6, 7, \ell_3, \ell_2) \quad (4.34)
\end{aligned}$$

and

$$\begin{aligned}
\text{cut}_{7:3}^{r=3} = & \frac{1}{2} A_{4:3}^{(1)}(1, 2; \ell_1, \ell_4) A_3^{(0)}(3, \ell_2, \ell_1) A_3^{(0)}(\ell_3, 7, \ell_4) A_5^{(0)}(4, 5, 6, \ell_3, \ell_2) \\
& + A_{4:1}^{(1)}(3, 4, \ell_1, \ell_4) A_3^{(0)}(5, \ell_2, \ell_1) A_3^{(0)}(\ell_3, 7, \ell_4) A_5^{(0)}(1, 2, \ell_2, 6, \ell_3) \\
& + A_{4:1}^{(1)}(3, 4, \ell_1, \ell_4) A_3^{(0)}(5, \ell_2, \ell_1) A_3^{(0)}(\ell_3, \ell_4, 2) A_5^{(0)}(1, \ell_2, 6, 7, \ell_3) \\
& + A_{4:1}^{(1)}(3, 4, \ell_1, \ell_4) A_3^{(0)}(1, \ell_1, \ell_2) A_3^{(0)}(\ell_3, 7, \ell_4) A_5^{(0)}(2, \ell_2, 5, 6, \ell_3) \\
& + A_{4:1}^{(1)}(1, \ell_4, 3, \ell_1) A_3^{(0)}(4, \ell_2, \ell_1) A_3^{(0)}(\ell_3, 7, \ell_4) A_5^{(0)}(2, \ell_2, 5, 6, \ell_3) \\
& + A_{4:1}^{(1)}(1, \ell_4, 3, \ell_1) A_3^{(0)}(2, \ell_1, \ell_2) A_3^{(0)}(\ell_3, 7, \ell_4) A_5^{(0)}(4, 5, 6, \ell_3, \ell_2) \\
& + A_{4:1}^{(1)}(1, 2, \ell_4, \ell_1) A_3^{(0)}(3, \ell_2, \ell_1) A_3^{(0)}(\ell_3, 7, \ell_4) A_5^{(0)}(4, 5, 6, \ell_3, \ell_2) \\
& + A_{4:1}^{(1)}(3, 4, \ell_1, \ell_4) A_3^{(0)}(1, \ell_1, \ell_2) A_3^{(0)}(\ell_3, \ell_4, 2) A_5^{(0)}(5, 6, 7, \ell_3, \ell_2) \\
& + A_{4:1}^{(1)}(1, \ell_4, 3, \ell_1) A_3^{(0)}(4, \ell_2, \ell_1) A_3^{(0)}(\ell_3, \ell_4, 2) A_5^{(0)}(5, 6, 7, \ell_3, \ell_2), \quad (4.35)
\end{aligned}$$

where ℓ_i are the on-shell cut momenta. A $\mathcal{P}_{7:3}$ sum must then be applied to this basis.

Evaluating the cuts, we have

$$P_{7:3}^{(2)}(1, 2, 3, 4, 5, 6, 7) = \sum_{\mathcal{P}_{7:3}} \left(P_{7:3}^{(2),r=1} + P_{7:3}^{(2),r=2} + P_{7:3}^{(2),r=3} \right), \quad (4.36)$$

where

$$\begin{aligned}
 P_{7:3}^{(2),r=1} = & \frac{1}{2}C_2(5, 7, \{6\}, \{\}, \{3, 4\}, \{\}, \{1, 2\}) + C_1(1, 2, \{7\}, \{\}, \{3, 4, 5, 6\}, \{\}) \\
 & - C_1(1, 7, \{\}, \{2\}, \{3, 4, 5, 6\}, \{\}) - C_1(2, 7, \{6\}, \{\}, \{3, 4, 5\}, \{1\}) \\
 & + C_1(5, 7, \{6\}, \{\}, \{3, 4\}, \{1, 2\}) - C_1(6, 2, \{7\}, \{\}, \{3, 4, 5\}, \{1\}) \\
 & + C_1(6, 7, \{\}, \{2\}, \{3, 4, 5\}, \{1\}) - C_1(7, 2, \{\}, \{1\}, \{3, 4, 5, 6\}, \{\}), \quad (4.37)
 \end{aligned}$$

$$\begin{aligned}
 P_{7:3}^{(2),r=2} = & \frac{1}{2}C_2(4, 7, \{5, 6\}, \{\}, \{3\}, \{\}, \{1, 2\}) + C_1(1, 2, \{6, 7\}, \{\}, \{3, 4, 5\}, \{\}) \\
 & - C_1(1, 7, \{6\}, \{2\}, \{3, 4, 5\}, \{\}) - C_1(2, 7, \{5, 6\}, \{\}, \{3, 4\}, \{1\}) \\
 & + C_1(4, 7, \{5, 6\}, \{\}, \{3\}, \{1, 2\}) - C_1(5, 2, \{6, 7\}, \{\}, \{3, 4\}, \{1\}) \\
 & + C_1(5, 7, \{6\}, \{2\}, \{3, 4\}, \{1\}) - C_1(6, 2, \{7\}, \{1\}, \{3, 4, 5\}, \{\}) \\
 & + C_1(6, 7, \{\}, \{1, 2\}, \{3, 4, 5\}, \{\}) \quad (4.38)
 \end{aligned}$$

and

$$\begin{aligned}
 P_{7:3}^{(2),r=3} = & \frac{1}{2}C_2(3, 7, \{4, 5, 6\}, \{\}, \{\}, \{\}, \{1, 2\}) + C_1(1, 2, \{5, 6, 7\}, \{\}, \{3, 4\}, \{\}) \\
 & - C_1(1, 7, \{5, 6\}, \{2\}, \{3, 4\}, \{\}) - C_1(2, 7, \{4, 5, 6\}, \{\}, \{3\}, \{1\}) \\
 & + C_1(3, 7, \{4, 5, 6\}, \{\}, \{\}, \{1, 2\}) - C_1(4, 2, \{5, 6, 7\}, \{\}, \{3\}, \{1\}) \\
 & + C_1(4, 7, \{5, 6\}, \{2\}, \{3\}, \{1\}) - C_1(5, 2, \{6, 7\}, \{1\}, \{3, 4\}, \{\}) \\
 & + C_1(5, 7, \{6\}, \{1, 2\}, \{3, 4\}, \{\}). \quad (4.39)
 \end{aligned}$$

4.4.5 $P_{7:4}$

The cuts to evaluate can be written schematically as

$$\begin{aligned}
 \text{cut}_{7:4}^{r=1} = & \frac{1}{3} A_{6:4}^{(1)}(1, 2, 3; 4, \ell_1, \ell_4) A_3^{(0)}(5, \ell_2, \ell_1) A_3^{(0)}(6, \ell_3, \ell_2) A_3^{(0)}(\ell_3, 7, \ell_4) \\
 & + \frac{1}{4} A_{6:3}^{(1)}(\ell_1, \ell_4; 4, 5, 6, 7) A_3^{(0)}(1, \ell_2, \ell_1) A_3^{(0)}(2, \ell_3, \ell_2) A_3^{(0)}(\ell_3, 3, \ell_4) \\
 & + A_{6:1}^{(1)}(1, \ell_4, 4, 5, 6, \ell_1) A_3^{(0)}(2, \ell_2, \ell_3) A_3^{(0)}(3, \ell_1, \ell_2) A_3^{(0)}(\ell_3, 7, \ell_4) \\
 & + A_{6:1}^{(1)}(1, 2, \ell_4, 4, 5, \ell_1) A_3^{(0)}(3, \ell_2, \ell_3) A_3^{(0)}(6, \ell_2, \ell_1) A_3^{(0)}(\ell_3, 7, \ell_4) \\
 & + A_{6:1}^{(1)}(1, 2, \ell_4, 4, 5, \ell_1) A_3^{(0)}(3, \ell_1, \ell_2) A_3^{(0)}(6, \ell_3, \ell_2) A_3^{(0)}(\ell_3, 7, \ell_4) \\
 & + A_{6:1}^{(1)}(1, 2, 3, \ell_4, 4, \ell_1) A_3^{(0)}(5, \ell_2, \ell_1) A_3^{(0)}(6, \ell_3, \ell_2) A_3^{(0)}(\ell_3, 7, \ell_4) \\
 & + A_{6:1}^{(1)}(4, 5, 6, 7, \ell_1, \ell_4) A_3^{(0)}(2, \ell_2, \ell_3) A_3^{(0)}(3, \ell_1, \ell_2) A_3^{(0)}(\ell_3, \ell_4, 1) \\
 & + A_{6:1}^{(1)}(1, \ell_4, 4, 5, 6, \ell_1) A_3^{(0)}(3, \ell_2, \ell_3) A_3^{(0)}(7, \ell_2, \ell_1) A_3^{(0)}(\ell_3, \ell_4, 2) \\
 & + A_{6:1}^{(1)}(1, \ell_4, 4, 5, 6, \ell_1) A_3^{(0)}(3, \ell_1, \ell_2) A_3^{(0)}(7, \ell_3, \ell_2) A_3^{(0)}(\ell_3, \ell_4, 2) \\
 & + A_{6:1}^{(1)}(1, 2, \ell_4, 4, 5, \ell_1) A_3^{(0)}(6, \ell_2, \ell_1) A_3^{(0)}(7, \ell_3, \ell_2) A_3^{(0)}(\ell_3, \ell_4, 3), \tag{4.40}
 \end{aligned}$$

$$\begin{aligned}
 \text{cut}_{7:4}^{r=2} = & \frac{1}{3} A_{5:3}^{(1)}(\ell_1, \ell_4; 1, 2, 3) A_3^{(0)}(4, \ell_2, \ell_1) A_3^{(0)}(\ell_3, 7, \ell_4) A_4^{(0)}(5, 6, \ell_3, \ell_2) \\
 & + A_{5:1}^{(1)}(4, 5, 6, \ell_1, \ell_4) A_3^{(0)}(3, \ell_1, \ell_2) A_3^{(0)}(\ell_3, 7, \ell_4) A_4^{(0)}(1, 2, \ell_2, \ell_3) \\
 & + A_{5:1}^{(1)}(1, \ell_4, 4, 5, \ell_1) A_3^{(0)}(6, \ell_2, \ell_1) A_3^{(0)}(\ell_3, 7, \ell_4) A_4^{(0)}(2, 3, \ell_2, \ell_3) \\
 & + A_{5:1}^{(1)}(4, 5, 6, \ell_1, \ell_4) A_3^{(0)}(7, \ell_2, \ell_1) A_3^{(0)}(\ell_3, \ell_4, 1) A_4^{(0)}(2, 3, \ell_2, \ell_3) \\
 & + A_{5:1}^{(1)}(1, \ell_4, 4, 5, \ell_1) A_3^{(0)}(3, \ell_1, \ell_2) A_3^{(0)}(\ell_3, 7, \ell_4) A_4^{(0)}(2, \ell_2, 6, \ell_3) \\
 & + A_{5:1}^{(1)}(4, 5, 6, \ell_1, \ell_4) A_3^{(0)}(3, \ell_1, \ell_2) A_3^{(0)}(\ell_3, \ell_4, 1) A_4^{(0)}(2, \ell_2, 7, \ell_3) \\
 & + A_{5:1}^{(1)}(1, 2, \ell_4, 4, \ell_1) A_3^{(0)}(5, \ell_2, \ell_1) A_3^{(0)}(\ell_3, 7, \ell_4) A_4^{(0)}(3, \ell_2, 6, \ell_3) \\
 & + A_{5:1}^{(1)}(1, \ell_4, 4, 5, \ell_1) A_3^{(0)}(6, \ell_2, \ell_1) A_3^{(0)}(\ell_3, \ell_4, 2) A_4^{(0)}(3, \ell_2, 7, \ell_3) \\
 & + A_{5:1}^{(1)}(1, 2, \ell_4, 4, \ell_1) A_3^{(0)}(3, \ell_1, \ell_2) A_3^{(0)}(\ell_3, 7, \ell_4) A_4^{(0)}(5, 6, \ell_3, \ell_2) \\
 & + A_{5:1}^{(1)}(1, 2, 3, \ell_4, \ell_1) A_3^{(0)}(4, \ell_2, \ell_1) A_3^{(0)}(\ell_3, 7, \ell_4) A_4^{(0)}(5, 6, \ell_3, \ell_2) \\
 & + A_{5:1}^{(1)}(1, \ell_4, 4, 5, \ell_1) A_3^{(0)}(3, \ell_1, \ell_2) A_3^{(0)}(\ell_3, \ell_4, 2) A_4^{(0)}(6, 7, \ell_3, \ell_2) \\
 & + A_{5:1}^{(1)}(1, 2, \ell_4, 4, \ell_1) A_3^{(0)}(5, \ell_2, \ell_1) A_3^{(0)}(\ell_3, \ell_4, 3) A_4^{(0)}(6, 7, \ell_3, \ell_2) \tag{4.41}
 \end{aligned}$$

and

$$\begin{aligned}
 \text{cut}_{7:4}^{r=3} = & A_{4:1}^{(1)}(4, 5, \ell_1, \ell_4) A_3^{(0)}(6, \ell_2, \ell_1) A_3^{(0)}(\ell_3, 7, \ell_4) A_5^{(0)}(1, 2, 3, \ell_2, \ell_3) \\
 & + A_{4:1}^{(1)}(4, 5, \ell_1, \ell_4) A_3^{(0)}(3, \ell_1, \ell_2) A_3^{(0)}(\ell_3, 7, \ell_4) A_5^{(0)}(1, 2, \ell_2, 6, \ell_3) \\
 & + A_{4:1}^{(1)}(1, \ell_4, 4, \ell_1) A_3^{(0)}(5, \ell_2, \ell_1) A_3^{(0)}(\ell_3, 7, \ell_4) A_5^{(0)}(2, 3, \ell_2, 6, \ell_3) \\
 & + A_{4:1}^{(1)}(4, 5, \ell_1, \ell_4) A_3^{(0)}(6, \ell_2, \ell_1) A_3^{(0)}(\ell_3, \ell_4, 1) A_5^{(0)}(2, 3, \ell_2, 7, \ell_3) \\
 & + A_{4:1}^{(1)}(1, \ell_4, 4, \ell_1) A_3^{(0)}(3, \ell_1, \ell_2) A_3^{(0)}(\ell_3, 7, \ell_4) A_5^{(0)}(2, \ell_2, 5, 6, \ell_3) \\
 & + A_{4:1}^{(1)}(4, 5, \ell_1, \ell_4) A_3^{(0)}(3, \ell_1, \ell_2) A_3^{(0)}(\ell_3, \ell_4, 1) A_5^{(0)}(2, \ell_2, 6, 7, \ell_3) \\
 & + A_{4:1}^{(1)}(1, 2, \ell_4, \ell_1) A_3^{(0)}(4, \ell_2, \ell_1) A_3^{(0)}(\ell_3, 7, \ell_4) A_5^{(0)}(3, \ell_2, 5, 6, \ell_3) \\
 & + A_{4:1}^{(1)}(1, \ell_4, 4, \ell_1) A_3^{(0)}(5, \ell_2, \ell_1) A_3^{(0)}(\ell_3, \ell_4, 2) A_5^{(0)}(3, \ell_2, 6, 7, \ell_3) \\
 & + A_{4:1}^{(1)}(1, 2, \ell_4, \ell_1) A_3^{(0)}(3, \ell_1, \ell_2) A_3^{(0)}(\ell_3, 7, \ell_4) A_5^{(0)}(4, 5, 6, \ell_3, \ell_2) \\
 & + A_{4:1}^{(1)}(1, \ell_4, 4, \ell_1) A_3^{(0)}(3, \ell_1, \ell_2) A_3^{(0)}(\ell_3, \ell_4, 2) A_5^{(0)}(5, 6, 7, \ell_3, \ell_2) \\
 & + A_{4:1}^{(1)}(1, 2, \ell_4, \ell_1) A_3^{(0)}(4, \ell_2, \ell_1) A_3^{(0)}(\ell_3, \ell_4, 3) A_5^{(0)}(5, 6, 7, \ell_3, \ell_2), \tag{4.42}
 \end{aligned}$$

where ℓ_i are the on-shell cut momenta. A $\mathcal{P}_{7:4}$ sum must then be applied to this basis.

Evaluating the cuts, we have

$$P_{7:4}^{(2)}(1, 2, 3, 4, 5, 6, 7) = \sum_{\mathcal{P}_{7:4}} \left(P_{7:4}^{(2),r=1} + P_{7:4}^{(2),r=2} + P_{7:4}^{(2),r=3} \right), \tag{4.43}$$

where

$$\begin{aligned}
 P_{7:4}^{(2),r=1} = & \frac{1}{4} C_2(1, 3, \{2\}, \{\}, \{\}, \{\}, \{4, 5, 6, 7\}) + \frac{1}{3} C_2(5, 7, \{6\}, \{\}, \{4\}, \{\}, \{1, 2, 3\}) \\
 & + C_1(3, 1, \{\}, \{2\}, \{4, 5, 6, 7\}, \{\}) + C_1(3, 2, \{7\}, \{\}, \{4, 5, 6\}, \{1\}) \\
 & - C_1(3, 7, \{\}, \{2\}, \{4, 5, 6\}, \{1\}) - C_1(3, 7, \{6\}, \{\}, \{4, 5\}, \{1, 2\}) \\
 & + C_1(5, 7, \{6\}, \{\}, \{4\}, \{1, 2, 3\}) - C_1(6, 3, \{7\}, \{\}, \{4, 5\}, \{1, 2\}) \\
 & + C_1(6, 7, \{\}, \{3\}, \{4, 5\}, \{1, 2\}) - C_1(7, 2, \{\}, \{3\}, \{4, 5, 6\}, \{1\}), \tag{4.44}
 \end{aligned}$$

4 The Seven Gluon Two-Loop Amplitude

$$\begin{aligned}
P_{7:4}^{(2),r=2} = & \frac{1}{3}C_2(4, 7, \{5, 6\}, \{\}, \{\}, \{\}, \{1, 2, 3\}) + C_1(3, 1, \{7\}, \{2\}, \{4, 5, 6\}, \{\}) \\
& + C_1(3, 2, \{6, 7\}, \{\}, \{4, 5\}, \{1\}) - C_1(3, 7, \{\}, \{1, 2\}, \{4, 5, 6\}, \{\}) \\
& - C_1(3, 7, \{6\}, \{2\}, \{4, 5\}, \{1\}) - C_1(3, 7, \{5, 6\}, \{\}, \{4\}, \{1, 2\}) \\
& + C_1(4, 7, \{5, 6\}, \{\}, \{\}, \{1, 2, 3\}) - C_1(5, 3, \{6, 7\}, \{\}, \{4\}, \{1, 2\}) \\
& + C_1(5, 7, \{6\}, \{3\}, \{4\}, \{1, 2\}) - C_1(6, 2, \{7\}, \{3\}, \{4, 5\}, \{1\}) \\
& + C_1(6, 7, \{\}, \{2, 3\}, \{4, 5\}, \{1\}) - C_1(7, 1, \{\}, \{2, 3\}, \{4, 5, 6\}, \{\}) \quad (4.45)
\end{aligned}$$

and

$$\begin{aligned}
P_{7:4}^{(2),r=3} = & C_1(3, 1, \{6, 7\}, \{2\}, \{4, 5\}, \{\}) + C_1(3, 2, \{5, 6, 7\}, \{\}, \{4\}, \{1\}) \\
& - C_1(3, 7, \{6\}, \{1, 2\}, \{4, 5\}, \{\}) - C_1(3, 7, \{5, 6\}, \{2\}, \{4\}, \{1\}) \\
& - C_1(3, 7, \{4, 5, 6\}, \{\}, \{\}, \{1, 2\}) - C_1(4, 3, \{5, 6, 7\}, \{\}, \{\}, \{1, 2\}) \\
& + C_1(4, 7, \{5, 6\}, \{3\}, \{\}, \{1, 2\}) - C_1(5, 2, \{6, 7\}, \{3\}, \{4\}, \{1\}) \\
& + C_1(5, 7, \{6\}, \{2, 3\}, \{4\}, \{1\}) - C_1(6, 1, \{7\}, \{2, 3\}, \{4, 5\}, \{\}) \\
& + C_1(6, 7, \{\}, \{1, 2, 3\}, \{4, 5\}, \{\}). \quad (4.46)
\end{aligned}$$

4.4.6 $P_{7:1,1}$

The cuts to evaluate can be written schematically as

$$\begin{aligned}
\text{cut}_{7:1,1}^{r=1} = & A_{6:2}^{(1)}(1; 3, 4, 5, \ell_1, \ell_4)A_3^{(0)}(2, \ell_2, \ell_3)A_3^{(0)}(6, \ell_2, \ell_1)A_3^{(0)}(\ell_3, 7, \ell_4) \\
& + A_{6:2}^{(1)}(1; 3, 4, 5, \ell_1, \ell_4)A_3^{(0)}(2, \ell_1, \ell_2)A_3^{(0)}(6, \ell_3, \ell_2)A_3^{(0)}(\ell_3, 7, \ell_4) \\
& + A_{6:2}^{(1)}(1; 2, \ell_4, 3, 4, \ell_1)A_3^{(0)}(5, \ell_2, \ell_1)A_3^{(0)}(6, \ell_3, \ell_2)A_3^{(0)}(\ell_3, 7, \ell_4) \\
& + A_{6:2}^{(1)}(1; 3, 4, 5, \ell_1, \ell_4)A_3^{(0)}(6, \ell_2, \ell_1)A_3^{(0)}(7, \ell_3, \ell_2)A_3^{(0)}(\ell_3, \ell_4, 2), \quad (4.47)
\end{aligned}$$

$$\begin{aligned}
\text{cut}_{7:1,1}^{r=2} = & A_{5:2}^{(1)}(1; 3, 4, \ell_1, \ell_4)A_3^{(0)}(5, \ell_2, \ell_1)A_3^{(0)}(\ell_3, 7, \ell_4)A_4^{(0)}(2, \ell_2, 6, \ell_3) \\
& + A_{5:2}^{(1)}(1; 3, 4, \ell_1, \ell_4)A_3^{(0)}(2, \ell_1, \ell_2)A_3^{(0)}(\ell_3, 7, \ell_4)A_4^{(0)}(5, 6, \ell_3, \ell_2) \\
& + A_{5:2}^{(1)}(1; 2, \ell_4, 3, \ell_1)A_3^{(0)}(4, \ell_2, \ell_1)A_3^{(0)}(\ell_3, 7, \ell_4)A_4^{(0)}(5, 6, \ell_3, \ell_2) \\
& + A_{5:2}^{(1)}(1; 3, 4, \ell_1, \ell_4)A_3^{(0)}(5, \ell_2, \ell_1)A_3^{(0)}(\ell_3, \ell_4, 2)A_4^{(0)}(6, 7, \ell_3, \ell_2) \quad (4.48)
\end{aligned}$$

and

$$\begin{aligned}
\text{cut}_{7:1,1}^{r=3} &= A_{4:2}^{(1)}(1; 3, \ell_1, \ell_4) A_3^{(0)}(4, \ell_2, \ell_1) A_3^{(0)}(\ell_3, 7, \ell_4) A_5^{(0)}(2, \ell_2, 5, 6, \ell_3) \\
&\quad + A_{4:2}^{(1)}(1; 3, \ell_1, \ell_4) A_3^{(0)}(2, \ell_1, \ell_2) A_3^{(0)}(\ell_3, 7, \ell_4) A_5^{(0)}(4, 5, 6, \ell_3, \ell_2) \\
&\quad + A_{4:2}^{(1)}(1; 2, \ell_4, \ell_1) A_3^{(0)}(3, \ell_2, \ell_1) A_3^{(0)}(\ell_3, 7, \ell_4) A_5^{(0)}(4, 5, 6, \ell_3, \ell_2) \\
&\quad + A_{4:2}^{(1)}(1; 3, \ell_1, \ell_4) A_3^{(0)}(4, \ell_2, \ell_1) A_3^{(0)}(\ell_3, \ell_4, 2) A_5^{(0)}(5, 6, 7, \ell_3, \ell_2), \quad (4.49)
\end{aligned}$$

where ℓ_i are the on-shell cut momenta. A $\mathcal{P}_{7:1,1}$ sum must then be applied to this basis.

Evaluating the cuts, we have

$$P_{7:1,1}^{(2)}(1, 2, 3, 4, 5, 6, 7) = \sum_{\mathcal{P}_{7:1,1}} \left(P_{7:1,1}^{(2),r=1} + P_{7:1,1}^{(2),r=2} + P_{7:1,1}^{(2),r=3} \right), \quad (4.50)$$

where

$$\begin{aligned}
P_{7:1,1}^{(2),r=1} &= -C_4(2, 7, \{6\}, \{\}, \{3, 4, 5\}, \{\}, 1) + C_4(5, 7, \{6\}, \{\}, \{3, 4\}, \{2\}, 1) \\
&\quad - C_4(6, 2, \{7\}, \{\}, \{3, 4, 5\}, \{\}, 1) + C_4(6, 7, \{\}, \{2\}, \{3, 4, 5\}, \{\}, 1), \quad (4.51)
\end{aligned}$$

$$\begin{aligned}
P_{7:1,1}^{(2),r=2} &= -C_4(2, 7, \{5, 6\}, \{\}, \{3, 4\}, \{\}, 1) + C_4(4, 7, \{5, 6\}, \{\}, \{3\}, \{2\}, 1) \\
&\quad - C_4(5, 2, \{6, 7\}, \{\}, \{3, 4\}, \{\}, 1) + C_4(5, 7, \{6\}, \{2\}, \{3, 4\}, \{\}, 1) \quad (4.52)
\end{aligned}$$

and

$$\begin{aligned}
P_{7:1,1}^{(2),r=3} &= -C_4(2, 7, \{4, 5, 6\}, \{\}, \{3\}, \{\}, 1) + C_4(3, 7, \{4, 5, 6\}, \{\}, \{\}, \{2\}, 1) \\
&\quad - C_4(4, 2, \{5, 6, 7\}, \{\}, \{3\}, \{\}, 1) + C_4(4, 7, \{5, 6\}, \{2\}, \{3\}, \{\}, 1). \quad (4.53)
\end{aligned}$$

4.4.7 $P_{7:1,2}$

The cuts to evaluate can be written schematically as

$$\begin{aligned}
\text{cut}_{7:1,2}^{r=1} = & \frac{1}{4} A_{6:3}^{(1)}(\ell_1, \ell_4; 4, 5, 6, 7) A_3^{(0)}(2, \ell_2, \ell_3) A_3^{(0)}(3, \ell_1, \ell_2) A_3^{(0)}(\ell_3, 1, \ell_4) \\
& + \frac{1}{4} A_{6:3}^{(1)}(\ell_1, \ell_4; 4, 5, 6, 7) A_3^{(0)}(1, \ell_3, \ell_2) A_3^{(0)}(3, \ell_1, \ell_2) A_3^{(0)}(\ell_3, \ell_4, 2) \\
& + \frac{1}{4} A_{6:3}^{(1)}(\ell_1, \ell_4; 4, 5, 6, 7) A_3^{(0)}(1, \ell_2, \ell_1) A_3^{(0)}(3, \ell_2, \ell_3) A_3^{(0)}(\ell_3, \ell_4, 2) \\
& + \frac{1}{2} A_{6:3}^{(1)}(2, 3; 4, 5, \ell_1, \ell_4) A_3^{(0)}(1, \ell_2, \ell_3) A_3^{(0)}(6, \ell_2, \ell_1) A_3^{(0)}(\ell_3, 7, \ell_4) \\
& + \frac{1}{2} A_{6:3}^{(1)}(2, 3; 4, 5, \ell_1, \ell_4) A_3^{(0)}(1, \ell_1, \ell_2) A_3^{(0)}(6, \ell_3, \ell_2) A_3^{(0)}(\ell_3, 7, \ell_4) \\
& + \frac{1}{2} A_{6:3}^{(1)}(2, 3; 1, \ell_4, 4, \ell_1) A_3^{(0)}(5, \ell_2, \ell_1) A_3^{(0)}(6, \ell_3, \ell_2) A_3^{(0)}(\ell_3, 7, \ell_4) \\
& + \frac{1}{2} A_{6:3}^{(1)}(2, 3; 4, 5, \ell_1, \ell_4) A_3^{(0)}(6, \ell_2, \ell_1) A_3^{(0)}(7, \ell_3, \ell_2) A_3^{(0)}(\ell_3, \ell_4, 1) \\
& + A_{6:2}^{(1)}(1; 4, 5, 6, \ell_1, \ell_4) A_3^{(0)}(2, \ell_2, \ell_3) A_3^{(0)}(3, \ell_1, \ell_2) A_3^{(0)}(\ell_3, 7, \ell_4) \\
& + A_{6:2}^{(1)}(1; 2, \ell_4, 4, 5, \ell_1) A_3^{(0)}(3, \ell_2, \ell_3) A_3^{(0)}(6, \ell_2, \ell_1) A_3^{(0)}(\ell_3, 7, \ell_4) \\
& + A_{6:2}^{(1)}(1; 2, \ell_4, 4, 5, \ell_1) A_3^{(0)}(3, \ell_1, \ell_2) A_3^{(0)}(6, \ell_3, \ell_2) A_3^{(0)}(\ell_3, 7, \ell_4) \\
& + A_{6:2}^{(1)}(1; 2, 3, \ell_4, 4, \ell_1) A_3^{(0)}(5, \ell_2, \ell_1) A_3^{(0)}(6, \ell_3, \ell_2) A_3^{(0)}(\ell_3, 7, \ell_4) \\
& + A_{6:2}^{(1)}(1; 4, 5, 6, \ell_1, \ell_4) A_3^{(0)}(3, \ell_2, \ell_3) A_3^{(0)}(7, \ell_2, \ell_1) A_3^{(0)}(\ell_3, \ell_4, 2) \\
& + A_{6:2}^{(1)}(1; 4, 5, 6, \ell_1, \ell_4) A_3^{(0)}(3, \ell_1, \ell_2) A_3^{(0)}(7, \ell_3, \ell_2) A_3^{(0)}(\ell_3, \ell_4, 2) \\
& + A_{6:2}^{(1)}(1; 2, \ell_4, 4, 5, \ell_1) A_3^{(0)}(6, \ell_2, \ell_1) A_3^{(0)}(7, \ell_3, \ell_2) A_3^{(0)}(\ell_3, \ell_4, 3), \tag{4.54}
\end{aligned}$$

$$\begin{aligned}
 \text{cut}_{7:1,2}^{r=2} = & \frac{1}{2} A_{5:3}^{(1)}(2, 3; 4, \ell_1, \ell_4) A_3^{(0)}(5, \ell_2, \ell_1) A_3^{(0)}(\ell_3, 7, \ell_4) A_4^{(0)}(1, \ell_2, 6, \ell_3) \\
 & + \frac{1}{2} A_{5:3}^{(1)}(2, 3; 4, \ell_1, \ell_4) A_3^{(0)}(1, \ell_1, \ell_2) A_3^{(0)}(\ell_3, 7, \ell_4) A_4^{(0)}(5, 6, \ell_3, \ell_2) \\
 & + \frac{1}{2} A_{5:3}^{(1)}(2, 3; 1, \ell_4, \ell_1) A_3^{(0)}(4, \ell_2, \ell_1) A_3^{(0)}(\ell_3, 7, \ell_4) A_4^{(0)}(5, 6, \ell_3, \ell_2) \\
 & + \frac{1}{2} A_{5:3}^{(1)}(2, 3; 4, \ell_1, \ell_4) A_3^{(0)}(5, \ell_2, \ell_1) A_3^{(0)}(\ell_3, \ell_4, 1) A_4^{(0)}(6, 7, \ell_3, \ell_2) \\
 & + A_{5:2}^{(1)}(1; 4, 5, \ell_1, \ell_4) A_3^{(0)}(6, \ell_2, \ell_1) A_3^{(0)}(\ell_3, 7, \ell_4) A_4^{(0)}(2, 3, \ell_2, \ell_3) \\
 & + A_{5:2}^{(1)}(1; 4, 5, \ell_1, \ell_4) A_3^{(0)}(3, \ell_1, \ell_2) A_3^{(0)}(\ell_3, 7, \ell_4) A_4^{(0)}(2, \ell_2, 6, \ell_3) \\
 & + A_{5:2}^{(1)}(1; 2, \ell_4, 4, \ell_1) A_3^{(0)}(5, \ell_2, \ell_1) A_3^{(0)}(\ell_3, 7, \ell_4) A_4^{(0)}(3, \ell_2, 6, \ell_3) \\
 & + A_{5:2}^{(1)}(1; 4, 5, \ell_1, \ell_4) A_3^{(0)}(6, \ell_2, \ell_1) A_3^{(0)}(\ell_3, \ell_4, 2) A_4^{(0)}(3, \ell_2, 7, \ell_3) \\
 & + A_{5:2}^{(1)}(1; 2, \ell_4, 4, \ell_1) A_3^{(0)}(3, \ell_1, \ell_2) A_3^{(0)}(\ell_3, 7, \ell_4) A_4^{(0)}(5, 6, \ell_3, \ell_2) \\
 & + A_{5:2}^{(1)}(1; 2, 3, \ell_4, \ell_1) A_3^{(0)}(4, \ell_2, \ell_1) A_3^{(0)}(\ell_3, 7, \ell_4) A_4^{(0)}(5, 6, \ell_3, \ell_2) \\
 & + A_{5:2}^{(1)}(1; 4, 5, \ell_1, \ell_4) A_3^{(0)}(3, \ell_1, \ell_2) A_3^{(0)}(\ell_3, \ell_4, 2) A_4^{(0)}(6, 7, \ell_3, \ell_2) \\
 & + A_{5:2}^{(1)}(1; 2, \ell_4, 4, \ell_1) A_3^{(0)}(5, \ell_2, \ell_1) A_3^{(0)}(\ell_3, \ell_4, 3) A_4^{(0)}(6, 7, \ell_3, \ell_2) \tag{4.55}
 \end{aligned}$$

and

$$\begin{aligned}
 \text{cut}_{7:1,2}^{r=3} = & \frac{1}{2} A_{4:3}^{(1)}(2, 3; \ell_1, \ell_4) A_3^{(0)}(4, \ell_2, \ell_1) A_3^{(0)}(\ell_3, 7, \ell_4) A_5^{(0)}(1, \ell_2, 5, 6, \ell_3) \\
 & + \frac{1}{2} A_{4:3}^{(1)}(2, 3; \ell_1, \ell_4) A_3^{(0)}(1, \ell_1, \ell_2) A_3^{(0)}(\ell_3, 7, \ell_4) A_5^{(0)}(4, 5, 6, \ell_3, \ell_2) \\
 & + \frac{1}{2} A_{4:3}^{(1)}(2, 3; \ell_1, \ell_4) A_3^{(0)}(4, \ell_2, \ell_1) A_3^{(0)}(\ell_3, \ell_4, 1) A_5^{(0)}(5, 6, 7, \ell_3, \ell_2) \\
 & + A_{4:2}^{(1)}(1; 4, \ell_1, \ell_4) A_3^{(0)}(5, \ell_2, \ell_1) A_3^{(0)}(\ell_3, 7, \ell_4) A_5^{(0)}(2, 3, \ell_2, 6, \ell_3) \\
 & + A_{4:2}^{(1)}(1; 4, \ell_1, \ell_4) A_3^{(0)}(3, \ell_1, \ell_2) A_3^{(0)}(\ell_3, 7, \ell_4) A_5^{(0)}(2, \ell_2, 5, 6, \ell_3) \\
 & + A_{4:2}^{(1)}(1; 2, \ell_4, \ell_1) A_3^{(0)}(4, \ell_2, \ell_1) A_3^{(0)}(\ell_3, 7, \ell_4) A_5^{(0)}(3, \ell_2, 5, 6, \ell_3) \\
 & + A_{4:2}^{(1)}(1; 4, \ell_1, \ell_4) A_3^{(0)}(5, \ell_2, \ell_1) A_3^{(0)}(\ell_3, \ell_4, 2) A_5^{(0)}(3, \ell_2, 6, 7, \ell_3) \\
 & + A_{4:2}^{(1)}(1; 2, \ell_4, \ell_1) A_3^{(0)}(3, \ell_1, \ell_2) A_3^{(0)}(\ell_3, 7, \ell_4) A_5^{(0)}(4, 5, 6, \ell_3, \ell_2) \\
 & + A_{4:2}^{(1)}(1; 4, \ell_1, \ell_4) A_3^{(0)}(3, \ell_1, \ell_2) A_3^{(0)}(\ell_3, \ell_4, 2) A_5^{(0)}(5, 6, 7, \ell_3, \ell_2) \\
 & + A_{4:2}^{(1)}(1; 2, \ell_4, \ell_1) A_3^{(0)}(4, \ell_2, \ell_1) A_3^{(0)}(\ell_3, \ell_4, 3) A_5^{(0)}(5, 6, 7, \ell_3, \ell_2), \tag{4.56}
 \end{aligned}$$

where ℓ_i are the on-shell cut momenta. A $\mathcal{P}_{7:1,2}$ sum must then be applied to this basis.

4 The Seven Gluon Two-Loop Amplitude

Evaluating the cuts, we have

$$P_{7:1,2}^{(2)}(1, 2, 3, 4, 5, 6, 7) = \sum_{\mathcal{P}_{7:1,2}} \left(P_{7:1,2}^{(2),r=1} + P_{7:1,2}^{(2),r=2} + P_{7:1,2}^{(2),r=3} \right), \quad (4.57)$$

where

$$\begin{aligned} P_{7:1,2}^{(2),r=1} = & -\frac{1}{4}C_2(1, 2, \{\}, \{3\}, \{\}, \{\}, \{4, 5, 6, 7\}) - \frac{1}{4}C_2(3, 1, \{\}, \{2\}, \{\}, \{\}, \{4, 5, 6, 7\}) \\ & + \frac{1}{4}C_2(3, 2, \{1\}, \{\}, \{\}, \{\}, \{4, 5, 6, 7\}) - \frac{1}{2}C_2(1, 7, \{6\}, \{\}, \{4, 5\}, \{\}, \{2, 3\}) \\ & + \frac{1}{2}C_2(5, 7, \{6\}, \{\}, \{4\}, \{1\}, \{2, 3\}) - \frac{1}{2}C_2(6, 1, \{7\}, \{\}, \{4, 5\}, \{\}, \{2, 3\}) \\ & + \frac{1}{2}C_2(6, 7, \{\}, \{1\}, \{4, 5\}, \{\}, \{2, 3\}) + C_4(3, 2, \{7\}, \{\}, \{4, 5, 6\}, \{\}, 1) \\ & - C_4(3, 7, \{\}, \{2\}, \{4, 5, 6\}, \{\}, 1) - C_4(3, 7, \{6\}, \{\}, \{4, 5\}, \{2\}, 1) \\ & + C_4(5, 7, \{6\}, \{\}, \{4\}, \{2, 3\}, 1) - C_4(6, 3, \{7\}, \{\}, \{4, 5\}, \{2\}, 1) \\ & + C_4(6, 7, \{\}, \{3\}, \{4, 5\}, \{2\}, 1) - C_4(7, 2, \{\}, \{3\}, \{4, 5, 6\}, \{\}, 1), \end{aligned} \quad (4.58)$$

$$\begin{aligned} P_{7:1,2}^{(2),r=2} = & -\frac{1}{2}C_2(1, 7, \{5, 6\}, \{\}, \{4\}, \{\}, \{2, 3\}) + \frac{1}{2}C_2(4, 7, \{5, 6\}, \{\}, \{\}, \{1\}, \{2, 3\}) \\ & - \frac{1}{2}C_2(5, 1, \{6, 7\}, \{\}, \{4\}, \{\}, \{2, 3\}) + \frac{1}{2}C_2(5, 7, \{6\}, \{1\}, \{4\}, \{\}, \{2, 3\}) \\ & + C_4(3, 2, \{6, 7\}, \{\}, \{4, 5\}, \{\}, 1) - C_4(3, 7, \{6\}, \{2\}, \{4, 5\}, \{\}, 1) \\ & - C_4(3, 7, \{5, 6\}, \{\}, \{4\}, \{2\}, 1) + C_4(4, 7, \{5, 6\}, \{\}, \{\}, \{2, 3\}, 1) \\ & - C_4(5, 3, \{6, 7\}, \{\}, \{4\}, \{2\}, 1) + C_4(5, 7, \{6\}, \{3\}, \{4\}, \{2\}, 1) \\ & - C_4(6, 2, \{7\}, \{3\}, \{4, 5\}, \{\}, 1) + C_4(6, 7, \{\}, \{2, 3\}, \{4, 5\}, \{\}, 1) \end{aligned} \quad (4.59)$$

and

$$\begin{aligned} P_{7:1,2}^{(2),r=3} = & -\frac{1}{2}C_2(1, 7, \{4, 5, 6\}, \{\}, \{\}, \{\}, \{2, 3\}) + -\frac{1}{2}C_2(4, 1, \{5, 6, 7\}, \{\}, \{\}, \{\}, \{2, 3\}) \\ & + \frac{1}{2}C_2(4, 7, \{5, 6\}, \{1\}, \{\}, \{\}, \{2, 3\}) + C_4(3, 2, \{5, 6, 7\}, \{\}, \{4\}, \{\}, 1) \\ & - C_4(3, 7, \{5, 6\}, \{2\}, \{4\}, \{\}, 1) - C_4(3, 7, \{4, 5, 6\}, \{\}, \{\}, \{2\}, 1) \\ & - C_4(4, 3, \{5, 6, 7\}, \{\}, \{\}, \{2\}, 1) + C_4(4, 7, \{5, 6\}, \{3\}, \{\}, \{2\}, 1) \\ & - C_4(5, 2, \{6, 7\}, \{3\}, \{4\}, \{\}, 1) + C_4(5, 7, \{6\}, \{2, 3\}, \{4\}, \{\}, 1). \end{aligned} \quad (4.60)$$

4.4.8 $P_{7:1,3}$

The cuts to evaluate can be written schematically as

$$\begin{aligned}
 \text{cut}_{7:1,3}^{r=1} = & \frac{1}{3} A_{6:4}^{(1)}(2, 3, 4; 5, \ell_1, \ell_4) A_3^{(0)}(1, \ell_2, \ell_3) A_3^{(0)}(6, \ell_2, \ell_1) A_3^{(0)}(\ell_3, 7, \ell_4) \\
 & + \frac{1}{3} A_{6:4}^{(1)}(2, 3, 4; 5, \ell_1, \ell_4) A_3^{(0)}(1, \ell_1, \ell_2) A_3^{(0)}(6, \ell_3, \ell_2) A_3^{(0)}(\ell_3, 7, \ell_4) \\
 & + \frac{1}{3} A_{6:4}^{(1)}(1, \ell_4, \ell_1; 2, 3, 4) A_3^{(0)}(5, \ell_2, \ell_1) A_3^{(0)}(6, \ell_3, \ell_2) A_3^{(0)}(\ell_3, 7, \ell_4) \\
 & + \frac{1}{3} A_{6:4}^{(1)}(2, 3, 4; 5, \ell_1, \ell_4) A_3^{(0)}(6, \ell_2, \ell_1) A_3^{(0)}(7, \ell_3, \ell_2) A_3^{(0)}(\ell_3, \ell_4, 1) \\
 & + A_{6:2}^{(1)}(1; 2, 3, \ell_4, 5, \ell_1) A_3^{(0)}(4, \ell_2, \ell_3) A_3^{(0)}(6, \ell_2, \ell_1) A_3^{(0)}(\ell_3, 7, \ell_4) \\
 & + A_{6:2}^{(1)}(1; 2, 3, \ell_4, 5, \ell_1) A_3^{(0)}(4, \ell_1, \ell_2) A_3^{(0)}(6, \ell_3, \ell_2) A_3^{(0)}(\ell_3, 7, \ell_4) \\
 & + A_{6:2}^{(1)}(1; 2, 3, 4, \ell_4, \ell_1) A_3^{(0)}(5, \ell_2, \ell_1) A_3^{(0)}(6, \ell_3, \ell_2) A_3^{(0)}(\ell_3, 7, \ell_4) \\
 & + A_{6:2}^{(1)}(1; 2, 3, \ell_4, 5, \ell_1) A_3^{(0)}(6, \ell_2, \ell_1) A_3^{(0)}(7, \ell_3, \ell_2) A_3^{(0)}(\ell_3, \ell_4, 4), \tag{4.61}
 \end{aligned}$$

$$\begin{aligned}
 \text{cut}_{7:1,3}^{r=2} = & \frac{1}{3} A_{5:3}^{(1)}(\ell_1, \ell_4; 2, 3, 4) A_3^{(0)}(5, \ell_2, \ell_1) A_3^{(0)}(\ell_3, 7, \ell_4) A_4^{(0)}(1, \ell_2, 6, \ell_3) \\
 & + \frac{1}{3} A_{5:3}^{(1)}(\ell_1, \ell_4; 2, 3, 4) A_3^{(0)}(1, \ell_1, \ell_2) A_3^{(0)}(\ell_3, 7, \ell_4) A_4^{(0)}(5, 6, \ell_3, \ell_2) \\
 & + \frac{1}{3} A_{5:3}^{(1)}(\ell_1, \ell_4; 2, 3, 4) A_3^{(0)}(5, \ell_2, \ell_1) A_3^{(0)}(\ell_3, \ell_4, 1) A_4^{(0)}(6, 7, \ell_3, \ell_2) \\
 & + \frac{1}{2} A_{5:2}^{(1)}(1; 2, \ell_4, 5, \ell_1) A_3^{(0)}(6, \ell_2, \ell_1) A_3^{(0)}(\ell_3, 7, \ell_4) A_4^{(0)}(3, 4, \ell_2, \ell_3) \\
 & + \frac{1}{2} A_{5:2}^{(1)}(1; 2, \ell_4, 5, \ell_1) A_3^{(0)}(4, \ell_1, \ell_2) A_3^{(0)}(\ell_3, 7, \ell_4) A_4^{(0)}(3, \ell_2, 6, \ell_3) \\
 & + \frac{1}{2} A_{5:2}^{(1)}(1; 2, \ell_4, 5, \ell_1) A_3^{(0)}(4, \ell_1, \ell_2) A_3^{(0)}(\ell_3, \ell_4, 3) A_4^{(0)}(6, 7, \ell_3, \ell_2) \\
 & + \frac{1}{2} A_{5:2}^{(1)}(1; 2, \ell_4, 5, \ell_1) A_3^{(0)}(6, \ell_2, \ell_1) A_3^{(0)}(\ell_3, \ell_4, 3) A_4^{(0)}(4, \ell_2, 7, \ell_3) \\
 & + A_{5:2}^{(1)}(1; 2, 3, \ell_4, \ell_1) A_3^{(0)}(5, \ell_2, \ell_1) A_3^{(0)}(\ell_3, 7, \ell_4) A_4^{(0)}(4, \ell_2, 6, \ell_3) \\
 & + A_{5:2}^{(1)}(1; 2, 3, \ell_4, \ell_1) A_3^{(0)}(4, \ell_1, \ell_2) A_3^{(0)}(\ell_3, 7, \ell_4) A_4^{(0)}(5, 6, \ell_3, \ell_2) \\
 & + A_{5:2}^{(1)}(1; 2, 3, \ell_4, \ell_1) A_3^{(0)}(5, \ell_2, \ell_1) A_3^{(0)}(\ell_3, \ell_4, 4) A_4^{(0)}(6, 7, \ell_3, \ell_2) \tag{4.62}
 \end{aligned}$$

4 The Seven Gluon Two-Loop Amplitude

and

$$\begin{aligned}
\text{cut}_{7:1,3}^{r=3} &= A_{4:2}^{(1)}(1; 2, \ell_4, \ell_1) A_3^{(0)}(5, \ell_2, \ell_1) A_3^{(0)}(\ell_3, 7, \ell_4) A_5^{(0)}(3, 4, \ell_2, 6, \ell_3) \\
&\quad + A_{4:2}^{(1)}(1; 2, \ell_4, \ell_1) A_3^{(0)}(4, \ell_1, \ell_2) A_3^{(0)}(\ell_3, 7, \ell_4) A_5^{(0)}(3, \ell_2, 5, 6, \ell_3) \\
&\quad + A_{4:2}^{(1)}(1; 2, \ell_4, \ell_1) A_3^{(0)}(5, \ell_2, \ell_1) A_3^{(0)}(\ell_3, \ell_4, 3) A_5^{(0)}(4, \ell_2, 6, 7, \ell_3) \\
&\quad + A_{4:2}^{(1)}(1; 2, \ell_4, \ell_1) A_3^{(0)}(4, \ell_1, \ell_2) A_3^{(0)}(\ell_3, \ell_4, 3) A_5^{(0)}(5, 6, 7, \ell_3, \ell_2), \tag{4.63}
\end{aligned}$$

where ℓ_i are the on-shell cut momenta. A $\mathcal{P}_{7:1,3}$ sum must then be applied to this basis.

Evaluating the cuts, we have

$$P_{7:1,3}^{(2)}(1, 2, 3, 4, 5, 6, 7) = \sum_{\mathcal{P}_{7:1,3}} \left(P_{7:1,3}^{(2),r=1} + P_{7:1,3}^{(2),r=2} + P_{7:1,3}^{(2),r=3} \right), \tag{4.64}$$

where

$$\begin{aligned}
P_{7:1,3}^{(2),r=1} &= -\frac{1}{3} C_2(1, 7, \{6\}, \{\}, \{5\}, \{\}, \{2, 3, 4\}) + \frac{1}{3} C_2(5, 7, \{6\}, \{\}, \{\}, \{1\}, \{2, 3, 4\}) \\
&\quad - \frac{1}{3} C_2(6, 1, \{7\}, \{\}, \{5\}, \{\}, \{2, 3, 4\}) + \frac{1}{3} C_2(6, 7, \{\}, \{1\}, \{5\}, \{\}, \{2, 3, 4\}) \\
&\quad - C_4(4, 7, \{6\}, \{\}, \{5\}, \{2, 3\}, 1) + C_4(5, 7, \{6\}, \{\}, \{\}, \{2, 3, 4\}, 1) \\
&\quad - C_4(6, 4, \{7\}, \{\}, \{5\}, \{2, 3\}, 1) + C_4(6, 7, \{\}, \{4\}, \{5\}, \{2, 3\}, 1), \tag{4.65}
\end{aligned}$$

$$\begin{aligned}
P_{7:1,3}^{(2),r=2} &= -\frac{1}{3} C_2(1, 7, \{5, 6\}, \{\}, \{\}, \{\}, \{2, 3, 4\}) - \frac{1}{3} C_2(5, 1, \{6, 7\}, \{\}, \{\}, \{\}, \{2, 3, 4\}) \\
&\quad + \frac{1}{3} C_2(5, 7, \{6\}, \{1\}, \{\}, \{\}, \{2, 3, 4\}) + \frac{1}{2} C_4(4, 3, \{6, 7\}, \{\}, \{5\}, \{2\}, 1) \\
&\quad - \frac{1}{2} C_4(4, 7, \{6\}, \{3\}, \{5\}, \{2\}, 1) - \frac{1}{2} C_4(6, 3, \{7\}, \{4\}, \{5\}, \{2\}, 1) \\
&\quad + \frac{1}{2} C_4(6, 7, \{\}, \{3, 4\}, \{5\}, \{2\}, 1) - C_4(4, 7, \{5, 6\}, \{\}, \{\}, \{2, 3\}, 1) \\
&\quad - C_4(5, 4, \{6, 7\}, \{\}, \{\}, \{2, 3\}, 1) + C_4(5, 7, \{6\}, \{4\}, \{\}, \{2, 3\}, 1) \tag{4.66}
\end{aligned}$$

and

$$\begin{aligned}
P_{7:1,3}^{(2),r=3} &= C_4(4, 3, \{5, 6, 7\}, \{\}, \{\}, \{2\}, 1) - C_4(4, 7, \{5, 6\}, \{3\}, \{\}, \{2\}, 1) \\
&\quad - C_4(5, 3, \{6, 7\}, \{4\}, \{\}, \{2\}, 1) + C_4(5, 7, \{6\}, \{3, 4\}, \{\}, \{2\}, 1). \tag{4.67}
\end{aligned}$$

4.4.9 $P_{7:2,2}$

The cuts to evaluate can be written schematically as

$$\begin{aligned}
 \text{cut}_{7:2,2}^{r=1} = & \frac{1}{3} A_{6:4}^{(1)}(1, \ell_1, \ell_4; 5, 6, 7) A_3^{(0)}(3, \ell_2, \ell_3) A_3^{(0)}(4, \ell_1, \ell_2) A_3^{(0)}(\ell_3, 2, \ell_4) \\
 & + \frac{1}{3} A_{6:4}^{(1)}(1, \ell_1, \ell_4; 5, 6, 7) A_3^{(0)}(2, \ell_3, \ell_2) A_3^{(0)}(4, \ell_1, \ell_2) A_3^{(0)}(\ell_3, \ell_4, 3) \\
 & + \frac{1}{3} A_{6:4}^{(1)}(1, \ell_1, \ell_4; 5, 6, 7) A_3^{(0)}(2, \ell_2, \ell_1) A_3^{(0)}(4, \ell_2, \ell_3) A_3^{(0)}(\ell_3, \ell_4, 3) \\
 & + \frac{1}{2} A_{6:3}^{(1)}(1, 2; 5, 6, \ell_1, \ell_4) A_3^{(0)}(3, \ell_2, \ell_3) A_3^{(0)}(4, \ell_1, \ell_2) A_3^{(0)}(\ell_3, 7, \ell_4) \\
 & + \frac{1}{2} A_{6:3}^{(1)}(1, 2; 3, \ell_4, 5, \ell_1) A_3^{(0)}(4, \ell_2, \ell_3) A_3^{(0)}(6, \ell_2, \ell_1) A_3^{(0)}(\ell_3, 7, \ell_4) \\
 & + \frac{1}{2} A_{6:3}^{(1)}(1, 2; 3, \ell_4, 5, \ell_1) A_3^{(0)}(4, \ell_1, \ell_2) A_3^{(0)}(6, \ell_3, \ell_2) A_3^{(0)}(\ell_3, 7, \ell_4) \\
 & + \frac{1}{2} A_{6:3}^{(1)}(1, 2; 3, 4, \ell_4, \ell_1) A_3^{(0)}(5, \ell_2, \ell_1) A_3^{(0)}(6, \ell_3, \ell_2) A_3^{(0)}(\ell_3, 7, \ell_4) \\
 & + \frac{1}{2} A_{6:3}^{(1)}(1, 2; 5, 6, \ell_1, \ell_4) A_3^{(0)}(4, \ell_2, \ell_3) A_3^{(0)}(7, \ell_2, \ell_1) A_3^{(0)}(\ell_3, \ell_4, 3) \\
 & + \frac{1}{2} A_{6:3}^{(1)}(1, 2; 5, 6, \ell_1, \ell_4) A_3^{(0)}(4, \ell_1, \ell_2) A_3^{(0)}(7, \ell_3, \ell_2) A_3^{(0)}(\ell_3, \ell_4, 3) \\
 & + \frac{1}{2} A_{6:3}^{(1)}(1, 2; 3, \ell_4, 5, \ell_1) A_3^{(0)}(6, \ell_2, \ell_1) A_3^{(0)}(7, \ell_3, \ell_2) A_3^{(0)}(\ell_3, \ell_4, 4), \tag{4.68}
 \end{aligned}$$

$$\begin{aligned}
 \text{cut}_{7:2,2}^{r=2} = & \frac{1}{3} A_{5:3}^{(1)}(\ell_1, \ell_4; 5, 6, 7) A_3^{(0)}(3, \ell_2, \ell_1) A_3^{(0)}(\ell_3, 4, \ell_4) A_4^{(0)}(1, 2, \ell_2, \ell_3) \\
 & + \frac{1}{3} A_{5:3}^{(1)}(\ell_1, \ell_4; 5, 6, 7) A_3^{(0)}(2, \ell_1, \ell_2) A_3^{(0)}(\ell_3, 4, \ell_4) A_4^{(0)}(1, \ell_2, 3, \ell_3) \\
 & + \frac{1}{2} A_{5:3}^{(1)}(1, 2; 5, \ell_1, \ell_4) A_3^{(0)}(6, \ell_2, \ell_1) A_3^{(0)}(\ell_3, 7, \ell_4) A_4^{(0)}(3, 4, \ell_2, \ell_3) \\
 & + \frac{1}{2} A_{5:3}^{(1)}(1, 2; 5, \ell_1, \ell_4) A_3^{(0)}(4, \ell_1, \ell_2) A_3^{(0)}(\ell_3, 7, \ell_4) A_4^{(0)}(3, \ell_2, 6, \ell_3) \\
 & + \frac{1}{2} A_{5:3}^{(1)}(1, 2; 3, \ell_4, \ell_1) A_3^{(0)}(5, \ell_2, \ell_1) A_3^{(0)}(\ell_3, 7, \ell_4) A_4^{(0)}(4, \ell_2, 6, \ell_3) \\
 & + \frac{1}{2} A_{5:3}^{(1)}(1, 2; 5, \ell_1, \ell_4) A_3^{(0)}(6, \ell_2, \ell_1) A_3^{(0)}(\ell_3, \ell_4, 3) A_4^{(0)}(4, \ell_2, 7, \ell_3) \\
 & + \frac{1}{2} A_{5:3}^{(1)}(1, 2; 3, \ell_4, \ell_1) A_3^{(0)}(4, \ell_1, \ell_2) A_3^{(0)}(\ell_3, 7, \ell_4) A_4^{(0)}(5, 6, \ell_3, \ell_2) \\
 & + \frac{1}{2} A_{5:3}^{(1)}(1, 2; 5, \ell_1, \ell_4) A_3^{(0)}(4, \ell_1, \ell_2) A_3^{(0)}(\ell_3, \ell_4, 3) A_4^{(0)}(6, 7, \ell_3, \ell_2) \\
 & + \frac{1}{2} A_{5:3}^{(1)}(1, 2; 3, \ell_4, \ell_1) A_3^{(0)}(5, \ell_2, \ell_1) A_3^{(0)}(\ell_3, \ell_4, 4) A_4^{(0)}(6, 7, \ell_3, \ell_2) \tag{4.69}
 \end{aligned}$$

4 The Seven Gluon Two-Loop Amplitude

and

$$\begin{aligned}
\text{cut}_{7:2,2}^{r=3} &= \frac{1}{2} A_{4:3}^{(1)}(1, 2; \ell_1, \ell_4) A_3^{(0)}(5, \ell_2, \ell_1) A_3^{(0)}(\ell_3, 7, \ell_4) A_5^{(0)}(3, 4, \ell_2, 6, \ell_3) \\
&+ \frac{1}{2} A_{4:3}^{(1)}(1, 2; \ell_1, \ell_4) A_3^{(0)}(4, \ell_1, \ell_2) A_3^{(0)}(\ell_3, 7, \ell_4) A_5^{(0)}(3, \ell_2, 5, 6, \ell_3) \\
&+ \frac{1}{2} A_{4:3}^{(1)}(1, 2; \ell_1, \ell_4) A_3^{(0)}(5, \ell_2, \ell_1) A_3^{(0)}(\ell_3, \ell_4, 3) A_5^{(0)}(4, \ell_2, 6, 7, \ell_3) \\
&+ \frac{1}{2} A_{4:3}^{(1)}(1, 2; \ell_1, \ell_4) A_3^{(0)}(4, \ell_1, \ell_2) A_3^{(0)}(\ell_3, \ell_4, 3) A_5^{(0)}(5, 6, 7, \ell_3, \ell_2), \quad (4.70)
\end{aligned}$$

where ℓ_i are the on-shell cut momenta. A $\mathcal{P}_{7:2,2}$ sum must then be applied to this basis.

Evaluating the cuts, we have

$$P_{7:2,2}^{(2)}(1, 2, 3, 4, 5, 6, 7) = \sum_{\mathcal{P}_{7:2,2}} \left(P_{7:2,2}^{(2),r=1} + P_{7:2,2}^{(2),r=2} + P_{7:2,2}^{(2),r=3} \right), \quad (4.71)$$

where

$$\begin{aligned}
P_{7:2,2}^{(2),r=1} &= -\frac{1}{3} C_2(2, 3, \{\}, \{4\}, \{1\}, \{\}, \{5, 6, 7\}) - \frac{1}{3} C_2(4, 2, \{\}, \{3\}, \{1\}, \{\}, \{5, 6, 7\}) \\
&+ \frac{1}{3} C_2(4, 3, \{2\}, \{\}, \{1\}, \{\}, \{5, 6, 7\}) + \frac{1}{2} C_2(4, 3, \{7\}, \{\}, \{5, 6\}, \{\}, \{1, 2\}) \\
&- \frac{1}{2} C_2(4, 7, \{\}, \{3\}, \{5, 6\}, \{\}, \{1, 2\}) - \frac{1}{2} C_2(4, 7, \{6\}, \{\}, \{5\}, \{3\}, \{1, 2\}) \\
&+ \frac{1}{2} C_2(5, 7, \{6\}, \{\}, \{\}, \{3, 4\}, \{1, 2\}) - \frac{1}{2} C_2(6, 4, \{7\}, \{\}, \{5\}, \{3\}, \{1, 2\}) \\
&+ \frac{1}{2} C_2(6, 7, \{\}, \{4\}, \{5\}, \{3\}, \{1, 2\}) - \frac{1}{2} C_2(7, 3, \{\}, \{4\}, \{5, 6\}, \{\}, \{1, 2\}), \quad (4.72)
\end{aligned}$$

$$\begin{aligned}
P_{7:2,2}^{(2),r=2} &= -\frac{1}{3} C_2(2, 4, \{3\}, \{1\}, \{\}, \{\}, \{5, 6, 7\}) + \frac{1}{3} C_2(3, 4, \{\}, \{1, 2\}, \{\}, \{\}, \{5, 6, 7\}) \\
&+ \frac{1}{2} C_2(4, 3, \{6, 7\}, \{\}, \{5\}, \{\}, \{1, 2\}) - \frac{1}{2} C_2(4, 7, \{6\}, \{3\}, \{5\}, \{\}, \{1, 2\}) \\
&- \frac{1}{2} C_2(4, 7, \{5, 6\}, \{\}, \{\}, \{3\}, \{1, 2\}) - \frac{1}{2} C_2(5, 4, \{6, 7\}, \{\}, \{\}, \{3\}, \{1, 2\}) \\
&+ \frac{1}{2} C_2(5, 7, \{6\}, \{4\}, \{\}, \{3\}, \{1, 2\}) - \frac{1}{2} C_2(6, 3, \{7\}, \{4\}, \{5\}, \{\}, \{1, 2\}) \\
&+ \frac{1}{2} C_2(6, 7, \{\}, \{3, 4\}, \{5\}, \{\}, \{1, 2\}) \quad (4.73)
\end{aligned}$$

and

$$\begin{aligned}
 P_{7:2,2}^{(2),r=3} &= \frac{1}{2}C_2(4, 3, \{5, 6, 7\}, \{\}, \{\}, \{\}, \{1, 2\}) - \frac{1}{2}C_2(4, 7, \{5, 6\}, \{3\}, \{\}, \{\}, \{1, 2\}) \\
 &\quad - \frac{1}{2}C_2(5, 3, \{6, 7\}, \{4\}, \{\}, \{\}, \{1, 2\}) + \frac{1}{2}C_2(5, 7, \{6\}, \{3, 4\}, \{\}, \{\}, \{1, 2\}).
 \end{aligned} \tag{4.74}$$

4.4.10 $\mathbf{P}_{7:1B}$

The cuts to evaluate can be written schematically as

$$\begin{aligned}
 \text{cut}_{7:1B}^{r=1} &= A_{6:4}^{(1)}(1, 2, \ell_1; 4, 5, \ell_4)A_3^{(0)}(6, \ell_2, \ell_3)A_3^{(0)}(7, \ell_1, \ell_2)A_3^{(0)}(\ell_3, 3, \ell_4) \\
 &\quad + A_{6:4}^{(1)}(1, 2, \ell_1; 5, 6, \ell_4)A_3^{(0)}(3, \ell_3, \ell_2)A_3^{(0)}(7, \ell_1, \ell_2)A_3^{(0)}(\ell_3, 4, \ell_4) \\
 &\quad + A_{6:4}^{(1)}(1, 2, \ell_1; 5, 6, \ell_4)A_3^{(0)}(3, \ell_2, \ell_1)A_3^{(0)}(7, \ell_2, \ell_3)A_3^{(0)}(\ell_3, 4, \ell_4) \\
 &\quad + A_{6:4}^{(1)}(1, 2, \ell_1; 6, 7, \ell_4)A_3^{(0)}(3, \ell_2, \ell_1)A_3^{(0)}(4, \ell_3, \ell_2)A_3^{(0)}(\ell_3, 5, \ell_4) \\
 &\quad + A_{6:3}^{(1)}(1, \ell_4; 4, 5, 6, \ell_1)A_3^{(0)}(2, \ell_2, \ell_3)A_3^{(0)}(3, \ell_1, \ell_2)A_3^{(0)}(\ell_3, 7, \ell_4) \\
 &\quad + A_{6:3}^{(1)}(1, \ell_4; 3, 4, 5, \ell_1)A_3^{(0)}(2, \ell_2, \ell_3)A_3^{(0)}(6, \ell_2, \ell_1)A_3^{(0)}(\ell_3, 7, \ell_4) \\
 &\quad + A_{6:3}^{(1)}(1, \ell_4; 3, 4, 5, \ell_1)A_3^{(0)}(2, \ell_1, \ell_2)A_3^{(0)}(6, \ell_3, \ell_2)A_3^{(0)}(\ell_3, 7, \ell_4) \\
 &\quad + A_{6:3}^{(1)}(1, \ell_4; 2, 3, 4, \ell_1)A_3^{(0)}(5, \ell_2, \ell_1)A_3^{(0)}(6, \ell_3, \ell_2)A_3^{(0)}(\ell_3, 7, \ell_4) \\
 &\quad + A_{6:3}^{(1)}(1, \ell_4; 5, 6, 7, \ell_1)A_3^{(0)}(3, \ell_2, \ell_3)A_3^{(0)}(4, \ell_1, \ell_2)A_3^{(0)}(\ell_3, \ell_4, 2) \\
 &\quad + A_{6:3}^{(1)}(1, \ell_4; 4, 5, 6, \ell_1)A_3^{(0)}(3, \ell_2, \ell_3)A_3^{(0)}(7, \ell_2, \ell_1)A_3^{(0)}(\ell_3, \ell_4, 2) \\
 &\quad + A_{6:3}^{(1)}(1, \ell_4; 4, 5, 6, \ell_1)A_3^{(0)}(3, \ell_1, \ell_2)A_3^{(0)}(7, \ell_3, \ell_2)A_3^{(0)}(\ell_3, \ell_4, 2) \\
 &\quad + A_{6:3}^{(1)}(1, \ell_4; 3, 4, 5, \ell_1)A_3^{(0)}(6, \ell_2, \ell_1)A_3^{(0)}(7, \ell_3, \ell_2)A_3^{(0)}(\ell_3, \ell_4, 2) \\
 &\quad + A_{6:4}^{(1)}(1, 2, \ell_1; 3, 4, \ell_4)A_3^{(0)}(6, \ell_2, \ell_3)A_3^{(0)}(7, \ell_1, \ell_2)A_3^{(0)}(\ell_3, \ell_4, 5) \\
 &\quad + A_{6:4}^{(1)}(1, 2, \ell_1; 4, 5, \ell_4)A_3^{(0)}(3, \ell_3, \ell_2)A_3^{(0)}(7, \ell_1, \ell_2)A_3^{(0)}(\ell_3, \ell_4, 6) \\
 &\quad + A_{6:4}^{(1)}(1, 2, \ell_1; 4, 5, \ell_4)A_3^{(0)}(3, \ell_2, \ell_1)A_3^{(0)}(7, \ell_2, \ell_3)A_3^{(0)}(\ell_3, \ell_4, 6) \\
 &\quad + A_{6:4}^{(1)}(1, 2, \ell_1; 5, 6, \ell_4)A_3^{(0)}(3, \ell_2, \ell_1)A_3^{(0)}(4, \ell_3, \ell_2)A_3^{(0)}(\ell_3, \ell_4, 7),
 \end{aligned} \tag{4.75}$$

4 The Seven Gluon Two-Loop Amplitude

$$\begin{aligned}
\text{cut}_{7:1B}^{r=2} = & A_{5:3}^{(1)}(1, \ell_1; 5, 6, \ell_4) A_3^{(0)}(7, \ell_1, \ell_2) A_3^{(0)}(\ell_3, 4, \ell_4) A_4^{(0)}(2, 3, \ell_3, \ell_2) \\
& + A_{5:3}^{(1)}(1, \ell_1; 4, 5, \ell_4) A_3^{(0)}(7, \ell_1, \ell_2) A_3^{(0)}(\ell_3, \ell_4, 6) A_4^{(0)}(2, 3, \ell_3, \ell_2) \\
& + A_{5:3}^{(1)}(1, \ell_1; 4, 5, \ell_4) A_3^{(0)}(7, \ell_1, \ell_2) A_3^{(0)}(\ell_3, 3, \ell_4) A_4^{(0)}(2, \ell_3, 6, \ell_2) \\
& + A_{5:3}^{(1)}(1, \ell_1; 3, 4, \ell_4) A_3^{(0)}(7, \ell_1, \ell_2) A_3^{(0)}(\ell_3, \ell_4, 5) A_4^{(0)}(2, \ell_3, 6, \ell_2) \\
& + A_{5:3}^{(1)}(1, \ell_1; 6, 7, \ell_4) A_3^{(0)}(2, \ell_2, \ell_1) A_3^{(0)}(\ell_3, 5, \ell_4) A_4^{(0)}(3, 4, \ell_3, \ell_2) \\
& + A_{5:3}^{(1)}(1, \ell_1; 5, 6, \ell_4) A_3^{(0)}(2, \ell_2, \ell_1) A_3^{(0)}(\ell_3, \ell_4, 7) A_4^{(0)}(3, 4, \ell_3, \ell_2) \\
& + A_{5:3}^{(1)}(1, \ell_1; 5, 6, \ell_4) A_3^{(0)}(2, \ell_2, \ell_1) A_3^{(0)}(\ell_3, 4, \ell_4) A_4^{(0)}(3, \ell_3, 7, \ell_2) \\
& + A_{5:3}^{(1)}(1, \ell_1; 4, 5, \ell_4) A_3^{(0)}(2, \ell_2, \ell_1) A_3^{(0)}(\ell_3, \ell_4, 6) A_4^{(0)}(3, \ell_3, 7, \ell_2) \\
& + A_{5:3}^{(1)}(1, \ell_1; 3, 4, \ell_4) A_3^{(0)}(7, \ell_1, \ell_2) A_3^{(0)}(\ell_3, 2, \ell_4) A_4^{(0)}(5, 6, \ell_2, \ell_3) \\
& + A_{5:3}^{(1)}(1, \ell_1; 2, 3, \ell_4) A_3^{(0)}(7, \ell_1, \ell_2) A_3^{(0)}(\ell_3, \ell_4, 4) A_4^{(0)}(5, 6, \ell_2, \ell_3) \\
& + A_{5:3}^{(1)}(1, \ell_1; 4, 5, \ell_4) A_3^{(0)}(2, \ell_2, \ell_1) A_3^{(0)}(\ell_3, 3, \ell_4) A_4^{(0)}(6, 7, \ell_2, \ell_3) \\
& + A_{5:3}^{(1)}(1, \ell_1; 3, 4, \ell_4) A_3^{(0)}(2, \ell_2, \ell_1) A_3^{(0)}(\ell_3, \ell_4, 5) A_4^{(0)}(6, 7, \ell_2, \ell_3)
\end{aligned} \tag{4.76}$$

and

$$\begin{aligned}
 \text{cut}_{7:1B}^{r=3} = & A_{4:3}^{(1)}(1, \ell_1; 6, \ell_4) A_3^{(0)}(7, \ell_1, \ell_2) A_3^{(0)}(\ell_3, 5, \ell_4) A_5^{(0)}(2, 3, 4, \ell_3, \ell_2) \\
 & + A_{4:3}^{(1)}(1, \ell_1; 5, \ell_4) A_3^{(0)}(7, \ell_1, \ell_2) A_3^{(0)}(\ell_3, \ell_4, 6) A_5^{(0)}(2, 3, 4, \ell_3, \ell_2) \\
 & + A_{4:3}^{(1)}(1, \ell_1; 5, \ell_4) A_3^{(0)}(7, \ell_1, \ell_2) A_3^{(0)}(\ell_3, 4, \ell_4) A_5^{(0)}(2, 3, \ell_3, 6, \ell_2) \\
 & + A_{4:3}^{(1)}(1, \ell_1; 4, \ell_4) A_3^{(0)}(7, \ell_1, \ell_2) A_3^{(0)}(\ell_3, \ell_4, 5) A_5^{(0)}(2, 3, \ell_3, 6, \ell_2) \\
 & + A_{4:3}^{(1)}(1, \ell_1; 4, \ell_4) A_3^{(0)}(7, \ell_1, \ell_2) A_3^{(0)}(\ell_3, 3, \ell_4) A_5^{(0)}(2, \ell_3, 5, 6, \ell_2) \\
 & + A_{4:3}^{(1)}(1, \ell_1; 3, \ell_4) A_3^{(0)}(7, \ell_1, \ell_2) A_3^{(0)}(\ell_3, \ell_4, 4) A_5^{(0)}(2, \ell_3, 5, 6, \ell_2) \\
 & + A_{4:3}^{(1)}(1, \ell_1; 7, \ell_4) A_3^{(0)}(2, \ell_2, \ell_1) A_3^{(0)}(\ell_3, 6, \ell_4) A_5^{(0)}(3, 4, 5, \ell_3, \ell_2) \\
 & + A_{4:3}^{(1)}(1, \ell_1; 6, \ell_4) A_3^{(0)}(2, \ell_2, \ell_1) A_3^{(0)}(\ell_3, \ell_4, 7) A_5^{(0)}(3, 4, 5, \ell_3, \ell_2) \\
 & + A_{4:3}^{(1)}(1, \ell_1; 6, \ell_4) A_3^{(0)}(2, \ell_2, \ell_1) A_3^{(0)}(\ell_3, 5, \ell_4) A_5^{(0)}(3, 4, \ell_3, 7, \ell_2) \\
 & + A_{4:3}^{(1)}(1, \ell_1; 5, \ell_4) A_3^{(0)}(2, \ell_2, \ell_1) A_3^{(0)}(\ell_3, \ell_4, 6) A_5^{(0)}(3, 4, \ell_3, 7, \ell_2) \\
 & + A_{4:3}^{(1)}(1, \ell_1; 5, \ell_4) A_3^{(0)}(2, \ell_2, \ell_1) A_3^{(0)}(\ell_3, 4, \ell_4) A_5^{(0)}(3, \ell_3, 6, 7, \ell_2) \\
 & + A_{4:3}^{(1)}(1, \ell_1; 4, \ell_4) A_3^{(0)}(2, \ell_2, \ell_1) A_3^{(0)}(\ell_3, \ell_4, 5) A_5^{(0)}(3, \ell_3, 6, 7, \ell_2) \\
 & + A_{4:3}^{(1)}(1, \ell_1; 3, \ell_4) A_3^{(0)}(7, \ell_1, \ell_2) A_3^{(0)}(\ell_3, 2, \ell_4) A_5^{(0)}(4, 5, 6, \ell_2, \ell_3) \\
 & + A_{4:3}^{(1)}(1, \ell_1; 2, \ell_4) A_3^{(0)}(7, \ell_1, \ell_2) A_3^{(0)}(\ell_3, \ell_4, 3) A_5^{(0)}(4, 5, 6, \ell_2, \ell_3) \\
 & + A_{4:3}^{(1)}(1, \ell_1; 4, \ell_4) A_3^{(0)}(2, \ell_2, \ell_1) A_3^{(0)}(\ell_3, 3, \ell_4) A_5^{(0)}(5, 6, 7, \ell_2, \ell_3) \\
 & + A_{4:3}^{(1)}(1, \ell_1; 3, \ell_4) A_3^{(0)}(2, \ell_2, \ell_1) A_3^{(0)}(\ell_3, \ell_4, 4) A_5^{(0)}(5, 6, 7, \ell_2, \ell_3), \tag{4.77}
 \end{aligned}$$

where ℓ_i are the on-shell cut momenta. In this case these are all the cuts required, rather than a basis for a sum. A simple sum cannot be factored out of these terms.

Evaluating the cuts, we have

$$P_{7:1B}^{(2)}(1, 2, 3, 4, 5, 6, 7) = \left(P_{7:1B}^{(2),r=1} + P_{7:1B}^{(2),r=2} + P_{7:1B}^{(2),r=3} \right), \tag{4.78}$$

where

$$\begin{aligned}
P_{7:1B}^{(2),r=1} = & -C_3(2, 7, \{6\}, \{\}, \{1\}, \{3, 4, 5\}) + C_3(3, 2, \{7\}, \{\}, \{1\}, \{4, 5, 6\}) \\
& + C_3(3, 4, \{\}, \{7\}, \{5, 6\}, \{1, 2\}) + C_3(3, 5, \{4\}, \{\}, \{6, 7\}, \{1, 2\}) \\
& - C_3(3, 6, \{\}, \{7\}, \{4, 5\}, \{1, 2\}) - C_3(3, 7, \{\}, \{2\}, \{1\}, \{4, 5, 6\}) \\
& - C_3(3, 7, \{4\}, \{\}, \{5, 6\}, \{1, 2\}) + C_3(4, 2, \{\}, \{3\}, \{1\}, \{5, 6, 7\}) \\
& + C_3(5, 7, \{6\}, \{\}, \{1\}, \{2, 3, 4\}) - C_3(6, 2, \{7\}, \{\}, \{1\}, \{3, 4, 5\}) \\
& + C_3(6, 7, \{\}, \{2\}, \{1\}, \{3, 4, 5\}) - C_3(7, 2, \{\}, \{3\}, \{1\}, \{4, 5, 6\}) \\
& - C_3(7, 3, \{\}, \{6\}, \{4, 5\}, \{1, 2\}) - C_3(7, 4, \{3\}, \{\}, \{5, 6\}, \{1, 2\}) \\
& + C_3(7, 5, \{\}, \{6\}, \{3, 4\}, \{1, 2\}) + C_3(7, 6, \{3\}, \{\}, \{4, 5\}, \{1, 2\}), \quad (4.79)
\end{aligned}$$

$$\begin{aligned}
P_{7:1B}^{(2),r=2} = & C_3(2, 3, \{\}, \{6, 7\}, \{4, 5\}, \{1\}) + C_3(2, 4, \{3\}, \{7\}, \{5, 6\}, \{1\}) \\
& - C_3(2, 5, \{\}, \{6, 7\}, \{3, 4\}, \{1\}) + C_3(2, 5, \{3, 4\}, \{\}, \{6, 7\}, \{1\}) \\
& - C_3(2, 6, \{3\}, \{7\}, \{4, 5\}, \{1\}) - C_3(2, 7, \{3, 4\}, \{\}, \{5, 6\}, \{1\}) \\
& - C_3(7, 2, \{\}, \{5, 6\}, \{3, 4\}, \{1\}) - C_3(7, 3, \{2\}, \{6\}, \{4, 5\}, \{1\}) \\
& + C_3(7, 4, \{\}, \{5, 6\}, \{2, 3\}, \{1\}) - C_3(7, 4, \{2, 3\}, \{\}, \{5, 6\}, \{1\}) \\
& + C_3(7, 5, \{2\}, \{6\}, \{3, 4\}, \{1\}) + C_3(7, 6, \{2, 3\}, \{\}, \{4, 5\}, \{1\}) \quad (4.80)
\end{aligned}$$

and

$$\begin{aligned}
P_{7:1B}^{(2),r=3} = & C_3(2, 3, \{\}, \{5, 6, 7\}, \{4\}, \{1\}) - C_3(2, 4, \{\}, \{5, 6, 7\}, \{3\}, \{1\}) \\
& + C_3(2, 4, \{3\}, \{6, 7\}, \{5\}, \{1\}) - C_3(2, 5, \{3\}, \{6, 7\}, \{4\}, \{1\}) \\
& + C_3(2, 5, \{3, 4\}, \{7\}, \{6\}, \{1\}) - C_3(2, 6, \{3, 4\}, \{7\}, \{5\}, \{1\}) \\
& + C_3(2, 6, \{3, 4, 5\}, \{\}, \{7\}, \{1\}) - C_3(2, 7, \{3, 4, 5\}, \{\}, \{6\}, \{1\}) \\
& - C_3(7, 2, \{\}, \{4, 5, 6\}, \{3\}, \{1\}) + C_3(7, 3, \{\}, \{4, 5, 6\}, \{2\}, \{1\}) \\
& - C_3(7, 3, \{2\}, \{5, 6\}, \{4\}, \{1\}) + C_3(7, 4, \{2\}, \{5, 6\}, \{3\}, \{1\}) \\
& - C_3(7, 4, \{2, 3\}, \{6\}, \{5\}, \{1\}) + C_3(7, 5, \{2, 3\}, \{6\}, \{4\}, \{1\}) \\
& - C_3(7, 5, \{2, 3, 4\}, \{\}, \{6\}, \{1\}) + C_3(7, 6, \{2, 3, 4\}, \{\}, \{5\}, \{1\}). \quad (4.81)
\end{aligned}$$

4.4.11 Validity checks

We confirm that the polylog results $P_{7:\lambda}^{(2)}$ satisfy the decoupling identities. The explicit $\mathcal{P}_{7:\lambda}$ sums in all pieces except $P_{7:1B}^{(2)}$ ensure that the expected cyclic symmetries in

momenta are present. The $P_{7:1B}^{(2)}$ piece also has the expected cyclic symmetry, despite not having an explicit $\mathcal{P}_{7:1}$ sum. This result agrees with the n -point result in ref. [62].

4.5 Rational Terms

We now turn to calculating the remaining rational pieces of the partial amplitudes, $R_{7:\lambda}^{(2)}$. The procedure used is augmented recursion [52], which was described in Section 3.4 for the six-point amplitude calculation. This method builds on the technique of Britto, Cachazo, Feng and Witten, who demonstrated how a rational tree amplitude could be determined recursively from lower-point amplitudes [19]. However, for two-loop amplitudes there is the possibility of double poles occurring. The simple poles beneath double poles are not accessible via factorisations and can instead be obtained from augmented recursion diagrams involving currents.

As before, the original BCFW complex shift does not lead to $R(z)$ vanishing as $|z|$ becomes large [52], so cannot be used here. Therefore we make use of the Risager shift [23], defined in eq. 3.30, which does have this property.

Applying the Risager shift to $R_{7:\lambda}^{(2)}$ excites three types of pole structure:

- tree to two-loop factorisations;
- one-loop to one-loop factorisations where the propagator is a sum of three momenta (giving rise to at most simple poles);
- “one-loop to one-loop” non-factorising structures where the pole is a sum of two momenta (giving rise to double and simple poles).

The first two situations cause only simple poles, so can be treated with BCFW recursion. The third situation introduces the double pole complication that we treat with augmented recursion. We now address these three contributions to $R_{7:\lambda}^{(2)}$ in turn.

4.5.1 Tree to two-loop factorisation

The first contributions considered are factorisations involving a lower-point two-loop amplitude. These lead to simple pole propagators, so BCFW recursion can be used. The only such (non-vanishing) diagram is shown in Figure 4.3. Note that the factorisation is dressed with colour, so all $R_{6:\lambda}^{(2)}$ partial amplitudes are present and will contribute to different $R_{7:\lambda}^{(2)}$ structures. We have also adopted general momentum labels $\{a, b, c, d, e, f, g\}$ to avoid confusion with the specific shifted set $\{\hat{1}, \hat{2}, \hat{3}, 4, 5, 6, 7\}$.

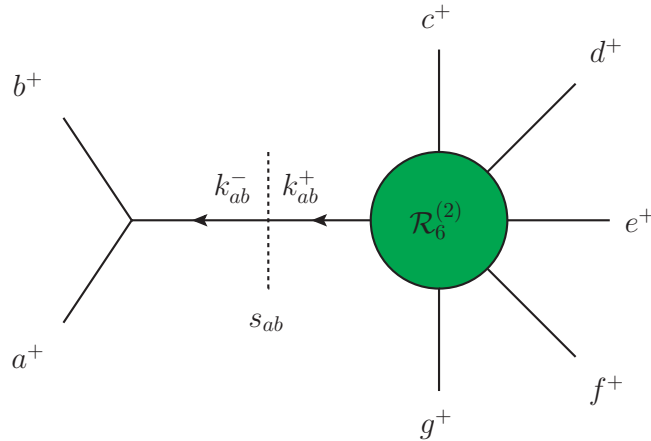


Figure 4.3: The tree to two-loop factorisation, which gives rise to a simple pole in s_{ab} . The two-loop rational piece $\mathcal{R}_6^{(2)}$, and three-point tree amplitude, are dressed with colour.

The BCFW residue will pick up contributions whenever $\{a, b\}$ is assigned one or two of the shifted momenta $\{\hat{1}, \hat{2}, \hat{3}\}$, because there will be a value of z for which $s_{ab} \rightarrow 0$. Therefore we collect all distinct momentum assignments of this diagram, discarding those where $\{a, b\}$ does not contain a shifted momentum. For each diagram $R_i(z)$, the residue $\text{Res}[R_i(z)/z]$ is taken for the value of z which causes the shifted propagator to vanish. The sum of these residues contributes to $R_{7;\lambda}^{(2)}$, according to eq. 3.22.

4.5.2 One-loop to one-loop factorisation

The next contributions considered are factorisations between two one-loop amplitudes, such that the propagator is a sum of three external momenta. These lead to simple poles, so BCFW recursion can again be used. Two helicity configurations are allowed, shown in Figure 4.4. The one-loop rational pieces involved are colour dressed, to find the contributions to each $R_{7;\lambda}^{(2)}$ structure.

Any external leg assignment where the shifted momenta are split across the two amplitudes will contribute to the BCFW residue. We collect all distinct diagrams with this property. For each diagram $R_j(z)$, the residue $\text{Res}[R_j(z)/z]$ is taken for the value of z which causes the shifted propagator to vanish. The sum of these residues contributes to $R_{7;\lambda}^{(2)}$, according to eq. 3.22.

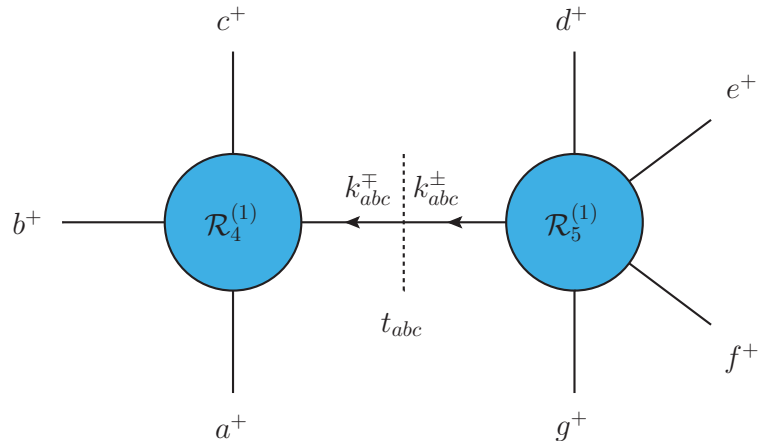


Figure 4.4: The one-loop to one-loop factorisation, which gives rise to a simple pole in t_{abc} . The rational pieces $\mathcal{R}_4^{(1)}$ and $\mathcal{R}_5^{(1)}$ are dressed with colour.

4.5.3 Non-factorising augmented recursion piece

The final contributions to consider are more complicated, being those that give rise to both double and simple poles. Naively, we may wish to draw the one-loop to one-loop factorisation that gives rise to double s_{ab} poles, shown in Figure 4.5, then proceed with BCFW recursion. However, this would miss any simple s_{ab} poles originating from similar but non-factorising structures. We require all pole information to evaluate the residue in eq. 3.22, so a different approach must be taken.

Following the procedure of augmented recursion [52], we draw a diagram containing both the leading double poles and sub-leading simple poles, Figure 4.6. The augmented recursion diagram contains the structure shown in Figure 4.5, occurring when the current factorises into a three-point tree and six-point loop, but also non-factorising structures that provide simple poles once integrated.

A current $\tau_7^{(1)}$ has been introduced, which is an object like an amplitude but with two off-shell legs. The spinor-helicity formalism only accommodates on-shell spinors, so we use an axial gauge construction for off-shell internal momenta [66, 41, 67]. The diagram is not a factorisation and the loop integral must be carried out. Deriving and integrating currents is a relatively in-depth procedure, which could be considered its own topic entirely. Therefore we discuss the detailed handling of the seven-point currents in Chapter 5, rather than interrupting this chapter with a lengthy aside.

As with the simple pole diagrams, we must colour dress the parts of the augmented recursion diagram to obtain results for all seven-point colour structures. The

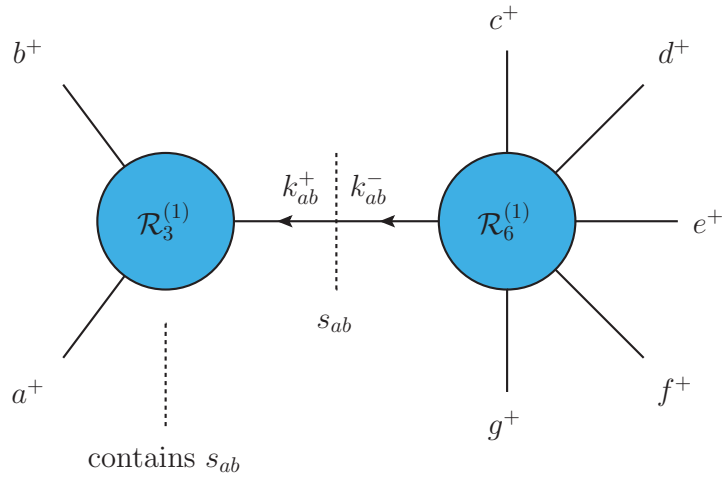


Figure 4.5: The one-loop to one-loop factorisation that gives rise to double poles in s_{ab} . Although the propagator only provides one factor of $1/s_{ab}$, an additional factor is present in the three-point amplitude. We do not evaluate this diagram, instead opting for augmented recursion.

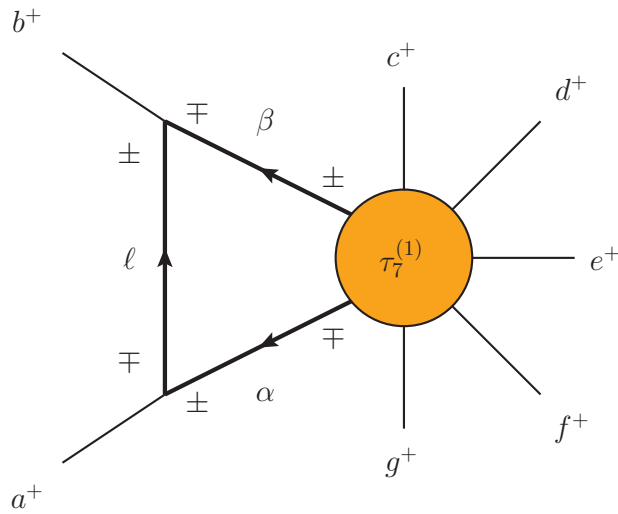


Figure 4.6: Augmented recursion diagram containing both double and simple s_{ab} pole contributions. The structure on the right is a current – an extension of an amplitude that has two off-shell legs. Thick lines are off-shell propagators, over which a loop integral must be carried out.

colour-dressed current contains multiple configurations of the external legs, including new currents that have not been required in previous work. The leading in colour rational piece $R_{7:1}^{(2)}$ required only $\tau_{7:1}^{(1)}(\alpha^-, \beta^+, c^+, d^+, e^+, f^+, g^+)$ for its derivation in ref. [60]. Exploiting symmetries and decoupling identities allows us to reduce the number of distinct currents appearing in our problem. We arrive at two new currents, $\tau_{7:1}^{(1)}(\alpha^-, c^+, \beta^+, d^+, e^+, f^+, g^+)$ and $\tau_{7:1}^{(1)}(\alpha^-, c^+, d^+, \beta^+, e^+, f^+, g^+)$, to derive and integrate. They are presented explicitly in Chapter 5.

With a complete set of integrated currents, what remains is to collect all distinct diagrams where at least one shifted leg appears in $\{a, b\}$. As previously, we calculate a residue $\text{Res}[R_k(z)/z]$ for each diagram $R_k(z)$, at the value of z for which the shifted $s_{ab} \rightarrow 0$. The sum of all these residues contributes to $R_{7:\lambda}^{(2)}$, via eq. 3.22.

4.5.4 Results and consistency checks

The sum of all recursion contributions for each colour trace structure gives us the partial amplitude rational pieces $R_{7:\lambda}^{(2)}$.

We confirm that the results are independent of the choice of Risager shift spinor λ_η , which is strong evidence that the procedure was successful and that an appropriate shift was chosen. (If $R(z)$ did not vanish as $|z|$ became large, as eq. 3.22 requires it to, then a λ_η dependence would likely remain [52].) The result is also independent of the reference spinor introduced with the axial gauge formalism. That the result is gauge-invariant as expected, despite this gauge-dependent intermediate step, is another strong consistency check. We find that the rational pieces $R_{7:\lambda}^{(2)}$ have the correct cyclic symmetries $\mathcal{P}_{7:\lambda}$ in their arguments. The rational pieces also satisfy all decoupling identities.

The augmented recursion procedure involves combining a large number of contributions at the seven-point level, leading to results with many terms (although orders of magnitude fewer than would be generated with a Feynman diagram approach). There is room for a large degree of simplification, although at this point the amplitude has been obtained and any further work is only an improvement in its representation. A procedure of reconstruction is set out in Chapter 6 and applied to the seven-point amplitude found. (We postpone the detail until then.)

The resulting compact, analytic $R_{7:\lambda}^{(2)}$ results are presented in the following subsections, organised by partial amplitude.

4.5.5 $R_{7:1}$

We confirm the result from ref. [60] and reproduce that form here for completeness,

$$R_{7:1}(a, b, c, d, e, f, g) = \frac{i}{9} \sum_{\mathcal{P}_{7:1}} \frac{G_{7:1}^1 + G_{7:1}^2 + G_{7:1}^3 + G_{7:1}^4 + G_{7:1}^5 + G_{7:1}^6 + G_{7:1}^7}{\langle a b \rangle \langle b c \rangle \langle c d \rangle \langle d e \rangle \langle e f \rangle \langle f g \rangle \langle g a \rangle}, \quad (4.82)$$

where

$$G_{7:1}^1 = \frac{\langle g a \rangle}{t_{abc} t_{efg}} \left(\frac{\langle c d \rangle [e g] [d | k_{abc} | e] [a | k_{abc} | e] [c | k_{abc} | f]}{\langle e f \rangle} \right. \\ - \frac{\langle d e \rangle [c a] [d | k_{efg} | c] [g | k_{efg} | c] [e | k_{efg} | b]}{\langle b c \rangle} \\ + \frac{\langle e f \rangle \langle c d \rangle [c a] [f g] [e | k_{efg} | a] [d | k_{efg} | b]}{\langle a b \rangle} \\ \left. - \frac{\langle b c \rangle \langle d e \rangle [e g] [a b] [c | k_{abc} | g] [d | k_{abc} | f]}{\langle f g \rangle} \right), \quad (4.83)$$

$$G_{7:1}^2 = \frac{1}{t_{abc} t_{efg}} s_{cd} s_{de} \langle g a \rangle [g | k_{efg} k_{abc} | a], \quad (4.84)$$

$$G_{7:1}^3 = \frac{1}{t_{cde}} \left(s_{ce} \left(\frac{s_{ef} \langle c | k_{ab} k_{fga} | d \rangle}{\langle c d \rangle} - \frac{s_{bc} \langle e | k_{fd} k_{gab} | d \rangle}{\langle d e \rangle} \right) \right. \\ + \frac{\langle e f \rangle \langle b c \rangle [f b] [c | k_{cde} | g] [e | k_{cde} | a]}{\langle g a \rangle} \\ + \frac{\langle b c \rangle [c | k_{cde} | b] [e | k_{cde} | a] [b | k_{fg} | e]}{\langle a b \rangle} \\ \left. + \frac{\langle e f \rangle [e | k_{cde} | f] [c | k_{cde} | g] [f | k_{ab} | c]}{\langle f g \rangle} \right), \quad (4.85)$$

$$G_{7:1}^4 = \frac{[g a]}{\langle g a \rangle} \langle g e \rangle \langle a e \rangle \left(\frac{[d e]}{\langle d e \rangle} \langle d g \rangle \langle d a \rangle + \frac{[e f]}{\langle e f \rangle} \langle f g \rangle \langle f a \rangle \right), \quad (4.86)$$

$$G_{7:1}^5 = \frac{1}{t_{cde}} \left([c e] (\langle e f \rangle [d f] \langle c | k_{ab} k_{fga} | d \rangle + \langle b c \rangle [d b] \langle e | k_{fg} k_{gab} | d \rangle) \right. \\ \left. + \langle b c \rangle \langle e f \rangle (2 \langle g a \rangle [c e] [f g] [a b] + [b f] [e | k_{ab} k_{fg} | c]) \right), \quad (4.87)$$

$$G_{7:1}^6 = \frac{1}{\langle g a \rangle} (\langle g | f k_{bc} | a \rangle t_{efg} - \langle a | b k_{ef} | g \rangle t_{abc}) \quad (4.88)$$

and

$$\begin{aligned} G_{7:1}^7 = & s_{bf}^2 - 2s_{ga}^2 - 3s_{db}s_{df} + 4s_{da}s_{dg} - 6s_{ac}s_{eg} + 7(s_{eb}s_{fc} + s_{ea}s_{gc}) + s_{ab}s_{fg} \\ & + 3s_{fa}s_{gb} + s_{ce}(s_{cf} + s_{eb} - 4(s_{ab} + s_{fg} + s_{ga}) + 5(s_{dg} + s_{ad})) \\ & + 4[e|bcf|e] - 2[f|gab|f] + 3[g|baf|g] + 2[g|cea|g]. \end{aligned} \quad (4.89)$$

4.5.6 $R_{7:2}$

Expressed in terms of the leading in colour partial amplitude, via a decoupling identity, we have

$$\begin{aligned} R_{7:2}(a; b, c, d, e, f, g) = & -R_{7:1}(a, b, c, d, e, f, g) - R_{7:1}(a, c, d, e, f, g, b) \\ & - R_{7:1}(a, d, e, f, g, b, c) - R_{7:1}(a, e, f, g, b, c, d) \\ & - R_{7:1}(a, f, g, b, c, d, e) - R_{7:1}(a, g, b, c, d, e, f) \\ = & - \sum_{Z_6(bcdefg)} R_{7:1}(a, b, c, d, e, f, g). \end{aligned} \quad (4.90)$$

4.5.7 $R_{7:3}$

The first new $SU(N_c)$ rational piece to be calculated is $R_{7:3}$. Using the decoupling identity, we can express it in terms of the previously defined partial amplitude and the new $R_{7:1,1}$,

$$\begin{aligned} R_{7:3}(a, b; c, d, e, f, g) = & -R_{7:1,1}(a; b; c, d, e, f, g) - R_{7:2}(b; a, c, d, e, f, g) \\ & - R_{7:2}(b; a, d, e, f, g, c) - R_{7:2}(b; a, e, f, g, c, d) \\ & - R_{7:2}(b; a, f, g, c, d, e) - R_{7:2}(b; a, g, c, d, e, f) \\ = & -R_{7:1,1}(a; b; c, d, e, f, g) - \sum_{Z_5(cdefg)} R_{7:2}(b; a, c, d, e, f, g). \end{aligned} \quad (4.91)$$

We make this choice because $R_{7:1,1}$ contains only simple poles whereas $R_{7:3}$ also contains double poles, so the former can be stated more compactly.

4.5.8 $R_{7:4}$

The second new $SU(N_c)$ partial amplitude to be calculated is $R_{7:4}$. The result obtained from augmented recursion is analytic, however the manifestly symmetric form presented

4 The Seven Gluon Two-Loop Amplitude

here required some additional work to obtain in such a compact form. That process of reconstruction is described in Chapter 6, after which we obtain

$$R_{7:4}(a, b, c; d, e, f, g) = \sum_{\mathcal{P}_{7:4}} B_{7:4}(a, b, c, d, e, f, g), \quad (4.92)$$

where the basis

$$\begin{aligned} B_{7:4}(a, b, c, d, e, f, g) = & B_{7:4}^{(ts)} + B_{7:4}^{(t1)} + B_{7:4}^{(t2)} + B_{7:4}^{(t3)} \\ & + B_{7:4}^{(t4)} + B_{7:4}^{(s1)} + B_{7:4}^{(s2)} \end{aligned} \quad (4.93)$$

can be divided into various denominator structures:

$$\begin{aligned} B_{7:4}^{(ts)} = & \frac{2i}{9} \frac{s_{df}}{\langle fg \rangle^2 t_{fgd}} \frac{[de]^2}{\langle ab \rangle \langle bc \rangle \langle ca \rangle} \\ & - \frac{2i}{9} \frac{s_{ef}}{\langle fg \rangle^2 t_{efg}} \frac{[ed]^2}{\langle ab \rangle \langle bc \rangle \langle ca \rangle}, \end{aligned} \quad (4.94)$$

$$\begin{aligned} B_{7:4}^{(t1)} = & -\frac{1}{9} \frac{i}{t_{abc}} \frac{1}{\langle bc \rangle \langle ca \rangle} \frac{1}{\langle de \rangle \langle ef \rangle \langle fg \rangle \langle gd \rangle} \\ & ([a|k_{abc}|e][b|k_{abc}|d][de] + [a|k_{abc}|e]s_{fg}[be] \\ & + [b|k_{fg}|d]s_{fg}[ad] + s_{fg}\langle fg \rangle [ag][bf] \\ & + \langle ef \rangle \langle fg \rangle [af][bf][eg]), \end{aligned} \quad (4.95)$$

$$\begin{aligned} B_{7:4}^{(t2)} = & \frac{1}{9} \frac{i}{t_{abc}} \frac{[ab]}{\langle ab \rangle \langle bc \rangle \langle ca \rangle} \frac{1}{\langle de \rangle \langle dg \rangle \langle ef \rangle \langle fg \rangle} \\ & ([f|k_{abc}|b]\langle ag \rangle \langle ef \rangle [eg] - [f|k_{abc}|b]\langle ad \rangle \langle ef \rangle [de] \\ & + [g|k_{abc}|b]s_{ef}\langle ag \rangle - [d|k_{abc}|a][g|k_{abc}|b]\langle dg \rangle), \end{aligned} \quad (4.96)$$

$$\begin{aligned}
 B_{7:4}^{(t3)} &= \frac{1}{9} \frac{i}{t_{efg}} \frac{1}{\langle ef \rangle \langle fg \rangle} \\
 &\quad \left(\frac{([e|k_{efg}|b][g|k_{efg}|c][bc] + [e|k_{efg}|a][g|k_{efg}|d][da])}{\langle ab \rangle \langle bc \rangle \langle cd \rangle \langle da \rangle} \right. \\
 &\quad + \frac{([e|k_{efg}|a][g|k_{efg}|c][ca] + [e|k_{efg}|b][g|k_{efg}|d][db])}{\langle ad \rangle \langle bc \rangle \langle ca \rangle \langle db \rangle} \\
 &\quad \left. + \frac{([e|k_{efg}|a][g|k_{efg}|b][ab] + [e|k_{efg}|c][g|k_{efg}|d][dc])}{\langle ab \rangle \langle bd \rangle \langle ca \rangle \langle dc \rangle} \right), \quad (4.97)
 \end{aligned}$$

$$\begin{aligned}
 B_{7:4}^{(t4)} &= \frac{2i}{9} \frac{1}{t_{efg}} \frac{1}{\langle ab \rangle \langle bc \rangle \langle ca \rangle} \\
 &\quad \left(\frac{[fg][de]^2}{\langle fg \rangle} + 2 \frac{[eg][dg][de]\langle eg \rangle}{\langle ef \rangle \langle fg \rangle} \right), \quad (4.98)
 \end{aligned}$$

$$\begin{aligned}
 B_{7:4}^{(s1)} &= -\frac{i}{3} \frac{[ab]}{\langle ab \rangle^2} \frac{1}{\langle cd \rangle \langle de \rangle \langle ef \rangle \langle fg \rangle \langle gc \rangle} \\
 &\quad (-\langle bc|g|a \rangle + \langle bd|e|a \rangle + \langle bd|f|a \rangle + \langle b|e|f|a \rangle) \quad (4.99)
 \end{aligned}$$

and

$$\begin{aligned}
 B_{7:4}^{(s2)} &= 6i \frac{1}{\langle fg \rangle^2} \frac{1}{\langle ab \rangle \langle bc \rangle \langle ca \rangle} \frac{G_{7:4}^1}{\langle de \rangle \langle ef \rangle \langle gd \rangle \langle ad \rangle} \\
 &\quad + \frac{i}{8} \frac{1}{\langle fg \rangle^2} \frac{G_{7:4}^2 + G_{7:4}^3 + G_{7:4}^4}{\langle ab \rangle \langle bc \rangle \langle ca \rangle} \frac{1}{\langle de \rangle \langle ef \rangle \langle gd \rangle} \frac{1}{\langle ae \rangle}. \quad (4.100)
 \end{aligned}$$

The numerators in the latter piece can be written

$$\begin{aligned}
 G_{7:4}^1 &= \langle af \rangle \langle bd \rangle \langle bf \rangle \langle dg \rangle [bd][bf] + \langle af \rangle \langle bd \rangle \langle cg \rangle \langle df \rangle [bf][cd] \\
 &\quad + \langle af \rangle \langle bf \rangle \langle cd \rangle \langle dg \rangle [bd][cf] + \langle af \rangle \langle cd \rangle \langle cf \rangle \langle dg \rangle [cd][cf] \\
 &\quad + 2 \langle af \rangle \langle bf \rangle \langle de \rangle \langle dg \rangle [bf][de] - \langle af \rangle \langle be \rangle \langle df \rangle \langle dg \rangle [bf][de] \\
 &\quad + 2 \langle ae \rangle \langle cg \rangle \langle df \rangle^2 [cf][de] - \langle af \rangle \langle ce \rangle \langle df \rangle \langle dg \rangle [cf][de] \\
 &\quad - \langle af \rangle \langle bf \rangle \langle de \rangle \langle dg \rangle [be][df] - \langle ae \rangle \langle cg \rangle \langle df \rangle^2 [ce][df] \\
 &\quad + \langle ae \rangle \langle df \rangle \langle dg \rangle \langle ef \rangle [de][ef], \quad (4.101)
 \end{aligned}$$

4 The Seven Gluon Two-Loop Amplitude

$$\begin{aligned}
G_{7:4}^2 = & -12 \langle a g \rangle \langle b d \rangle \langle b f \rangle \langle c e \rangle [b c] [b d] + 44 \langle a g \rangle \langle b d \rangle \langle b f \rangle \langle e d \rangle [b d]^2 \\
& - 32 \langle a f \rangle \langle b d \rangle^2 \langle e g \rangle [b d]^2 + 138 \langle a g \rangle \langle b e \rangle \langle b f \rangle \langle c e \rangle [b c] [b e] \\
& - 138 \langle a g \rangle \langle b e \rangle \langle b f \rangle \langle e d \rangle [b d] [b e] - 740 \langle a f \rangle \langle b d \rangle \langle b e \rangle \langle e g \rangle [b d] [b e] \\
& - 70 \langle a f \rangle \langle b e \rangle^2 \langle e g \rangle [b e]^2 + 12 \langle a f \rangle \langle b d \rangle \langle b f \rangle \langle e g \rangle [b d] [b f] \\
& + 646 \langle a f \rangle \langle b e \rangle \langle b f \rangle \langle e g \rangle [b e] [b f] + 8 \langle a g \rangle \langle b f \rangle \langle b g \rangle \langle e d \rangle [b d] [b g] \\
& - 32 \langle a g \rangle \langle b d \rangle \langle b g \rangle \langle e f \rangle [b d] [b g] + 36 \langle a g \rangle \langle b d \rangle \langle b f \rangle \langle e g \rangle [b d] [b g] \\
& - 138 \langle a g \rangle \langle b e \rangle \langle b f \rangle \langle e g \rangle [b e] [b g] + 8 \langle a g \rangle \langle b d \rangle \langle c f \rangle \langle e d \rangle [b d] [c d] \\
& - 12 \langle a f \rangle \langle b d \rangle \langle c g \rangle \langle e d \rangle [b d] [c d] + 36 \langle a d \rangle \langle b d \rangle \langle c g \rangle \langle e f \rangle [b d] [c d] \\
& - 32 \langle a f \rangle \langle b d \rangle \langle c d \rangle \langle e g \rangle [b d] [c d] - 54 \langle a f \rangle \langle b d \rangle \langle c e \rangle \langle e g \rangle [b e] [c d] \\
& - 8 \langle a f \rangle \langle b f \rangle \langle c g \rangle \langle e d \rangle [b f] [c d] - 24 \langle a g \rangle \langle b d \rangle \langle c f \rangle \langle e f \rangle [b f] [c d] \\
& + 32 \langle a f \rangle \langle b d \rangle \langle c g \rangle \langle e f \rangle [b f] [c d] - 40 \langle a f \rangle \langle c d \rangle \langle c g \rangle \langle e d \rangle [c d]^2 \\
& + 40 \langle a d \rangle \langle c d \rangle \langle c g \rangle \langle e f \rangle [c d]^2 + 24 \langle a g \rangle \langle b f \rangle \langle c e \rangle^2 [b c] [c e] \\
& - 48 \langle a g \rangle \langle b e \rangle \langle c f \rangle \langle e d \rangle [b d] [c e] - 106 \langle a f \rangle \langle b e \rangle \langle c g \rangle \langle e d \rangle [b d] [c e] \\
& + 690 \langle a d \rangle \langle b e \rangle \langle c g \rangle \langle e f \rangle [b d] [c e] - 710 \langle a f \rangle \langle b d \rangle \langle c e \rangle \langle e g \rangle [b d] [c e] \\
& + 40 \langle a e \rangle \langle b e \rangle \langle c g \rangle \langle e f \rangle [b e] [c e] - 70 \langle a f \rangle \langle b e \rangle \langle c e \rangle \langle e g \rangle [b e] [c e] \\
& - 40 \langle a g \rangle \langle b e \rangle \langle c f \rangle \langle e f \rangle [b f] [c e] + 560 \langle a f \rangle \langle b e \rangle \langle c g \rangle \langle e f \rangle [b f] [c e], \quad (4.102)
\end{aligned}$$

$$\begin{aligned}
G_{7:4}^3 = & 54 \langle a f \rangle \langle b f \rangle \langle c e \rangle \langle e g \rangle [b f] [c e] - 24 \langle a g \rangle \langle b g \rangle \langle c e \rangle \langle e f \rangle [b g] [c e] \\
& - 108 \langle a f \rangle \langle b e \rangle \langle c g \rangle \langle e g \rangle [b g] [c e] - 104 \langle a f \rangle \langle c e \rangle \langle c g \rangle \langle e d \rangle [c d] [c e] \\
& + 108 \langle a e \rangle \langle c f \rangle \langle c g \rangle \langle e d \rangle [c d] [c e] + 664 \langle a d \rangle \langle c e \rangle \langle c g \rangle \langle e f \rangle [c d] [c e] \\
& - 24 \langle a f \rangle \langle c d \rangle \langle c e \rangle \langle e g \rangle [c d] [c e] - 14 \langle a e \rangle \langle c e \rangle \langle c g \rangle \langle e f \rangle [c e]^2 \\
& + 706 \langle a f \rangle \langle b f \rangle \langle c e \rangle \langle e g \rangle [b e] [c f] + 44 \langle a f \rangle \langle c f \rangle \langle c g \rangle \langle e d \rangle [c d] [c f] \\
& + 8 \langle a f \rangle \langle c d \rangle \langle c g \rangle \langle e f \rangle [c d] [c f] - 52 \langle a d \rangle \langle c f \rangle \langle c g \rangle \langle e f \rangle [c d] [c f] \\
& + 536 \langle a f \rangle \langle c e \rangle \langle c g \rangle \langle e f \rangle [c e] [c f] - 652 \langle a e \rangle \langle c f \rangle \langle c g \rangle \langle e f \rangle [c e] [c f] \\
& - 16 \langle a f \rangle \langle c e \rangle \langle c f \rangle \langle e g \rangle [c e] [c f] + 8 \langle a g \rangle \langle b g \rangle \langle c f \rangle \langle e d \rangle [b d] [c g] \\
& - 8 \langle a g \rangle \langle b g \rangle \langle c d \rangle \langle e f \rangle [b d] [c g] - 4 \langle a f \rangle \langle c g \rangle^2 \langle e d \rangle [c d] [c g] \\
& + 4 \langle a d \rangle \langle c g \rangle^2 \langle e f \rangle [c d] [c g] + 54 \langle a e \rangle \langle c g \rangle^2 \langle e f \rangle [c e] [c g] \\
& - 108 \langle a f \rangle \langle c e \rangle \langle c g \rangle \langle e g \rangle [c e] [c g] - 32 \langle a f \rangle \langle b f \rangle \langle d g \rangle \langle e d \rangle [b d] [d f] \\
& - 32 \langle a f \rangle \langle b f \rangle \langle d g \rangle \langle e f \rangle [b f] [d f] + 32 \langle a f \rangle \langle b f \rangle \langle d f \rangle \langle e g \rangle [b f] [d f] \\
& - 8 \langle a f \rangle \langle b f \rangle \langle d g \rangle \langle e g \rangle [b g] [d f] - 231 \langle a f \rangle \langle c g \rangle \langle d f \rangle \langle e d \rangle [c d] [d f] \\
& + 8 \langle a f \rangle \langle c f \rangle \langle d g \rangle \langle e d \rangle [c d] [d f] + 183 \langle a d \rangle \langle c g \rangle \langle d f \rangle \langle e f \rangle [c d] [d f] \\
& + 32 \langle a f \rangle \langle c d \rangle \langle d f \rangle \langle e g \rangle [c d] [d f] - 24 \langle a f \rangle \langle c g \rangle \langle d f \rangle \langle e f \rangle [c f] [d f] \\
& - 16 \langle a f \rangle \langle c f \rangle \langle d g \rangle \langle e f \rangle [c f] [d f] + 40 \langle a f \rangle \langle c f \rangle \langle d f \rangle \langle e g \rangle [c f] [d f] \\
& + 16 \langle a f \rangle \langle c g \rangle \langle d g \rangle \langle e f \rangle [c g] [d f] - 16 \langle a f \rangle \langle c g \rangle \langle d f \rangle \langle e g \rangle [c g] [d f] \\
& - 8 \langle a f \rangle \langle c f \rangle \langle d g \rangle \langle e g \rangle [c g] [d f] + 32 \langle a f \rangle \langle d f \rangle^2 \langle e g \rangle [d f]^2 \\
& + 8 \langle a g \rangle \langle b f \rangle \langle d g \rangle \langle e d \rangle [b d] [d g] - 32 \langle a f \rangle \langle b d \rangle \langle d g \rangle \langle e g \rangle [b d] [d g] \\
& + 32 \langle a g \rangle \langle b g \rangle \langle d f \rangle \langle e f \rangle [b f] [d g] - 24 \langle a f \rangle \langle b f \rangle \langle d g \rangle \langle e g \rangle [b f] [d g] \\
& - 24 \langle a f \rangle \langle c g \rangle \langle d g \rangle \langle e f \rangle [c f] [d g] + 32 \langle a f \rangle \langle c g \rangle \langle d f \rangle \langle e g \rangle [c f] [d g] \\
& + 32 \langle a f \rangle \langle d f \rangle \langle d g \rangle \langle e g \rangle [d f] [d g] - 506 \langle a f \rangle \langle b d \rangle \langle e d \rangle \langle e g \rangle [b d] [e d] \\
& - 180 \langle a d \rangle \langle b d \rangle \langle e f \rangle \langle e g \rangle [b d] [e d] - 491 \langle a f \rangle \langle b e \rangle \langle e d \rangle \langle e g \rangle [b e] [e d] \\
& + 334 \langle a d \rangle \langle b e \rangle \langle e f \rangle \langle e g \rangle [b e] [e d] + 832 \langle a f \rangle \langle b f \rangle \langle e d \rangle \langle e g \rangle [b f] [e d] \quad (4.103)
\end{aligned}$$

and

$$\begin{aligned}
G_{7:4}^4 = & 32 \langle a f \rangle \langle d f \rangle \langle d g \rangle \langle e g \rangle [d f] [d g] - 506 \langle a f \rangle \langle b d \rangle \langle e d \rangle \langle e g \rangle [b d] [e d] \\
& - 180 \langle a d \rangle \langle b d \rangle \langle e f \rangle \langle e g \rangle [b d] [e d] - 491 \langle a f \rangle \langle b e \rangle \langle e d \rangle \langle e g \rangle [b e] [e d] \\
& + 334 \langle a d \rangle \langle b e \rangle \langle e f \rangle \langle e g \rangle [b e] [e d] + 832 \langle a f \rangle \langle b f \rangle \langle e d \rangle \langle e g \rangle [b f] [e d] \\
& + 6 \langle a f \rangle \langle b d \rangle \langle e f \rangle \langle e g \rangle [b f] [e d] + 54 \langle a f \rangle \langle b d \rangle \langle e g \rangle^2 [b g] [e d] \\
& - 203 \langle a e \rangle \langle c g \rangle \langle e d \rangle \langle e f \rangle [c e] [e d] - 87 \langle a d \rangle \langle c e \rangle \langle e f \rangle \langle e g \rangle [c e] [e d] \\
& - 199 \langle a f \rangle \langle c g \rangle \langle e d \rangle \langle e f \rangle [c f] [e d] + 167 \langle a d \rangle \langle c g \rangle \langle e f \rangle^2 [c f] [e d] \\
& + 40 \langle a f \rangle \langle c f \rangle \langle e d \rangle \langle e g \rangle [c f] [e d] - 24 \langle a f \rangle \langle c d \rangle \langle e f \rangle \langle e g \rangle [c f] [e d] \\
& - 668 \langle a d \rangle \langle c g \rangle \langle e f \rangle \langle e g \rangle [c g] [e d] + 24 \langle a f \rangle \langle c d \rangle \langle e g \rangle^2 [c g] [e d] \\
& + 48 \langle a d \rangle \langle d f \rangle \langle e f \rangle \langle e g \rangle [d f] [e d] + 48 \langle a f \rangle \langle d g \rangle \langle e d \rangle \langle e g \rangle [d g] [e d] \\
& - 48 \langle a d \rangle \langle d f \rangle \langle e g \rangle^2 [d g] [e d] + 16 \langle a g \rangle \langle e d \rangle^2 \langle e f \rangle [e d]^2 \\
& - 192 \langle a f \rangle \langle e d \rangle^2 \langle e g \rangle [e d]^2 + 89 \langle a d \rangle \langle e d \rangle \langle e f \rangle \langle e g \rangle [e d]^2 \\
& - 682 \langle a f \rangle \langle b f \rangle \langle e d \rangle \langle e g \rangle [b d] [e f] - 764 \langle a f \rangle \langle b d \rangle \langle e f \rangle \langle e g \rangle [b d] [e f] \\
& - 70 \langle a f \rangle \langle b e \rangle \langle e f \rangle \langle e g \rangle [b e] [e f] + 78 \langle a f \rangle \langle b f \rangle \langle e f \rangle \langle e g \rangle [b f] [e f] \\
& - 658 \langle a f \rangle \langle b f \rangle \langle e g \rangle^2 [b g] [e f] + 32 \langle a d \rangle \langle c g \rangle \langle e f \rangle^2 [c d] [e f] \\
& + 32 \langle a f \rangle \langle c f \rangle \langle e d \rangle \langle e g \rangle [c d] [e f] - 48 \langle a f \rangle \langle c d \rangle \langle e f \rangle \langle e g \rangle [c d] [e f] \\
& + 195 \langle a e \rangle \langle c g \rangle \langle e f \rangle^2 [c e] [e f] - 740 \langle a f \rangle \langle c g \rangle \langle e f \rangle \langle e g \rangle [c g] [e f] \\
& + 160 \langle a f \rangle \langle c f \rangle \langle e g \rangle^2 [c g] [e f] - 24 \langle a f \rangle \langle d g \rangle \langle e f \rangle^2 [d f] [e f] \\
& - 24 \langle a f \rangle \langle d g \rangle \langle e f \rangle \langle e g \rangle [d g] [e f] - 87 \langle a d \rangle \langle e f \rangle^2 \langle e g \rangle [e d] [e f] \\
& - 740 \langle a f \rangle \langle b d \rangle \langle e g \rangle^2 [b d] [e g] - 70 \langle a f \rangle \langle b e \rangle \langle e g \rangle^2 [b e] [e g] \\
& + 736 \langle a f \rangle \langle b f \rangle \langle e g \rangle^2 [b f] [e g] - 601 \langle a f \rangle \langle c g \rangle \langle e d \rangle \langle e g \rangle [c d] [e g] \\
& + 1269 \langle a d \rangle \langle c g \rangle \langle e f \rangle \langle e g \rangle [c d] [e g] - 24 \langle a f \rangle \langle c d \rangle \langle e g \rangle^2 [c d] [e g] \\
& + 1175 \langle a e \rangle \langle c g \rangle \langle e f \rangle \langle e g \rangle [c e] [e g] + 692 \langle a f \rangle \langle c g \rangle \langle e f \rangle \langle e g \rangle [c f] [e g] \\
& - 112 \langle a f \rangle \langle c f \rangle \langle e g \rangle^2 [c f] [e g] - 87 \langle a d \rangle \langle e f \rangle \langle e g \rangle^2 [e d] [e g] \\
& + 32 \langle a f \rangle \langle d f \rangle \langle e g \rangle \langle f g \rangle [d f] [f g] - 48 \langle a f \rangle \langle e g \rangle^2 \langle f g \rangle [e g] [f g]. \quad (4.104)
\end{aligned}$$

4.5.9 $R_{7:1,1}$

The first new exclusively $U(N_c)$ partial amplitude to be calculated is $R_{7:1,1}$. Although it is a structure not present in the $SU(N_c)$ theory, we chose to reference it in the statement of the $R_{7:3}$ rational piece because it is the simpler of the two structures. As

with the other partial amplitudes, the result produced by augmented recursion was analytic, but not very compact. Simplifying manipulations were therefore carried out, with details in Chapter 6, yielding the form:

$$R_{7:1,1}(a; b; c, d, e, f, g) = \sum_{\mathcal{P}_{7:1,1}} B_{7:1,1}(a, b, c, d, e, f, g), \quad (4.105)$$

with a basis function

$$\begin{aligned} B_{7:1,1}(a, b, c, d, e, f, g) = & B_{7:1,1}^{(tt)}(a, b, c, d, e, f, g) + B_{7:1,1}^{(ts)}(a, b, c, d, e, f, g) \\ & + B_{7:1,1}^{(s)}(a, b, c, d, e, f, g) \end{aligned} \quad (4.106)$$

containing the structures

$$\begin{aligned} B_{7:1,1}^{(tt)}(a, b, c, d, e, f, g) = & \frac{i}{t_{aef} t_{bcd}} \frac{G_{7:1,1}^1}{\langle a e \rangle \langle a f \rangle \langle a g \rangle \langle b c \rangle \langle c d \rangle \langle e f \rangle} \\ & + \frac{i}{t_{aef} t_{bcd}} \frac{[a|k_{ef}|b][g|k_{bcd}|d][a e][b d]}{\langle b c \rangle \langle b d \rangle \langle c d \rangle \langle e f \rangle \langle f g \rangle}, \end{aligned} \quad (4.107)$$

$$B_{7:1,1}^{(ts)}(a, b, c, d, e, f, g) = \frac{i}{t_{aef}} \frac{G_{7:1,1}^2}{\langle a e \rangle \langle a f \rangle \langle a g \rangle \langle b c \rangle \langle b d \rangle \langle b g \rangle \langle c d \rangle \langle c g \rangle \langle e f \rangle \langle f g \rangle} \quad (4.108)$$

and

$$B_{7:1,1}^{(s)}(a, b, c, d, e, f, g) = \frac{G_{7:1,1}^3 + G_{7:1,1}^4 + G_{7:1,1}^5}{\langle c d \rangle \langle d e \rangle \langle e f \rangle \langle f g \rangle \langle g c \rangle} \frac{1}{\langle b c \rangle \langle b d \rangle} \frac{1}{\langle a e \rangle \langle a f \rangle}. \quad (4.109)$$

The numerators are

$$\begin{aligned} G_{7:1,1}^1 = & -[b|k_{bcd}|a][d|k_{bcd}|a][g|k_{bcd}|e][a e] \\ & - [e|k_{bcd}|g] s_{ag} \langle a e \rangle [b g] [d g], \end{aligned} \quad (4.110)$$

4 The Seven Gluon Two-Loop Amplitude

$$\begin{aligned}
G_{7:1,1}^2 = & -[a|k_{aef}|a][b|k_{bcd}|a][d|k_{bcd}|c] \langle b d \rangle \langle b g \rangle \langle f g \rangle \\
& + [b|k_{bcd}|a][d|k_{aef}|a] \langle b d \rangle \langle b g \rangle \langle c e \rangle \langle f g \rangle [a e] \\
& + [a|k_{aef}|b][f|k_{aef}|d] \langle a f \rangle \langle a g \rangle \langle b g \rangle \langle c f \rangle [b d] \\
& + [b|k_{bcd}|a] \langle a f \rangle \langle b c \rangle \langle b d \rangle \langle b g \rangle \langle f g \rangle [a f] [b d] \\
& + [a|k_{aef}|b][f|k_{aef}|g] \langle a f \rangle \langle a g \rangle \langle b c \rangle \langle f g \rangle [b g] \\
& + [d|k_{aef}|a] \langle a g \rangle \langle b d \rangle \langle b g \rangle \langle c g \rangle \langle f g \rangle [a g] [b g] \\
& + \langle a e \rangle \langle a g \rangle \langle b d \rangle \langle b g \rangle \langle c g \rangle \langle f g \rangle [a g] [b g] [d e] \\
& + [b|k_{aef}|c] \langle a f \rangle \langle a g \rangle \langle b d \rangle \langle b g \rangle \langle f g \rangle [a g] [d f] \\
& + [a|k_{aef}|c][f|k_{aef}|b] \langle a f \rangle \langle a g \rangle \langle d g \rangle \langle f g \rangle [d g] \\
& - [a|k_{aef}|b][f|k_{aef}|c] \langle a f \rangle \langle a g \rangle \langle d g \rangle \langle f g \rangle [d g] \\
& - [b|k_{bcd}|a] \langle a e \rangle \langle b d \rangle \langle b g \rangle \langle c g \rangle \langle f g \rangle [a e] [d g] \\
& + \langle a f \rangle \langle a g \rangle \langle b d \rangle \langle b g \rangle \langle c d \rangle \langle f g \rangle [a g] [b d] [f d] \\
& + \langle a f \rangle \langle a g \rangle \langle b d \rangle \langle b g \rangle \langle c d \rangle \langle f g \rangle [a d] [b d] [f g] \\
& + [a|k_{aef}|d][f|k_{aef}|c] \langle a f \rangle \langle a g \rangle \langle b g \rangle \langle f g \rangle [g d] \\
& - [a|k_{aef}|c][f|k_{aef}|d] \langle a f \rangle \langle a g \rangle \langle b g \rangle \langle f g \rangle [g d] \\
& + [f|k_{aef}|c] \langle a f \rangle \langle a g \rangle \langle b d \rangle \langle b g \rangle \langle f g \rangle [a b] [g d], \tag{4.111}
\end{aligned}$$

$$\begin{aligned}
 G_{7;1,1}^3 = & \frac{123}{10} \langle ac \rangle \langle ad \rangle \langle be \rangle \langle bf \rangle [ab]^2 + \frac{27}{10} \langle ab \rangle \langle ae \rangle \langle bc \rangle \langle df \rangle [ab]^2 \\
 & - \frac{11}{5} \langle ab \rangle \langle ad \rangle \langle bc \rangle \langle ef \rangle [ab]^2 - \frac{3}{2} \langle ac \rangle^2 \langle be \rangle \langle df \rangle [ab] [ac] \\
 & - \frac{3}{2} \langle ac \rangle \langle ad \rangle \langle bc \rangle \langle ef \rangle [ab] [ac] - \frac{17}{2} \langle ac \rangle^2 \langle bd \rangle \langle ef \rangle [ab] [ac] \\
 & + \frac{29}{2} \langle ac \rangle \langle ad \rangle \langle be \rangle \langle df \rangle [ab] [ad] - \frac{7}{2} \langle ac \rangle \langle ad \rangle \langle bd \rangle \langle ef \rangle [ab] [ad] \\
 & + \frac{29}{2} \langle ac \rangle \langle ad \rangle \langle be \rangle \langle ef \rangle [ab] [ae] - \frac{9}{2} \langle ac \rangle \langle ae \rangle \langle bf \rangle \langle df \rangle [ab] [af] \\
 & - \frac{84}{5} \langle ab \rangle \langle bd \rangle \langle ce \rangle \langle cf \rangle [ab] [bc] + \frac{9}{5} \langle ab \rangle \langle bc \rangle \langle cf \rangle \langle de \rangle [ab] [bc] \\
 & + \frac{21}{2} \langle ab \rangle \langle bc \rangle \langle ce \rangle \langle df \rangle [ab] [bc] - \frac{29}{2} \langle ab \rangle \langle cd \rangle \langle ce \rangle \langle cf \rangle [ac] [bc] \\
 & - \frac{15}{2} \langle ab \rangle \langle cd \rangle \langle ce \rangle \langle ef \rangle [ae] [bc] + \frac{51}{2} \langle ab \rangle \langle bd \rangle \langle ce \rangle \langle df \rangle [ab] [bd] \\
 & - \frac{33}{2} \langle ab \rangle \langle bc \rangle \langle de \rangle \langle df \rangle [ab] [bd] + \frac{33}{2} \langle ab \rangle \langle cd \rangle \langle de \rangle \langle df \rangle [ad] [bd] \\
 & - \frac{39}{2} \langle ab \rangle \langle cd \rangle \langle df \rangle \langle ef \rangle [af] [bd] - \frac{33}{2} \langle ab \rangle \langle cd \rangle \langle df \rangle \langle eg \rangle [ag] [bd] \\
 & - \frac{11}{5} \langle ab \rangle \langle be \rangle \langle ce \rangle \langle df \rangle [ab] [be] + \frac{36}{5} \langle ab \rangle \langle bd \rangle \langle ce \rangle \langle ef \rangle [ab] [be] \\
 & + \frac{19}{5} \langle ab \rangle \langle bc \rangle \langle de \rangle \langle ef \rangle [ab] [be] - \frac{9}{2} \langle ac \rangle \langle bd \rangle \langle ce \rangle \langle ef \rangle [ac] [be] \\
 & - \frac{9}{2} \langle ac \rangle \langle bd \rangle \langle de \rangle \langle ef \rangle [ad] [be] + \frac{47}{2} \langle ab \rangle \langle ce \rangle \langle de \rangle \langle fg \rangle [ag] [be] \\
 & + \frac{19}{5} \langle ab \rangle \langle be \rangle \langle cf \rangle \langle df \rangle [ab] [bf] - \frac{9}{2} \langle ac \rangle \langle bd \rangle \langle df \rangle \langle ef \rangle [ad] [bf] \\
 & + \frac{29}{2} \langle ab \rangle \langle ce \rangle \langle df \rangle \langle fg \rangle [ag] [bf] - \frac{11}{5} \langle ab \rangle \langle be \rangle \langle cf \rangle \langle dg \rangle [ab] [bg] \\
 & + \frac{29}{2} \langle ab \rangle \langle ce \rangle \langle dg \rangle \langle fg \rangle [ag] [bg] + \frac{3}{2} \langle ac \rangle \langle bd \rangle \langle cf \rangle \langle de \rangle [ab] [cd] \\
 & - \frac{21}{2} \langle ac \rangle \langle bc \rangle \langle de \rangle \langle df \rangle [ab] [cd] - \frac{3}{2} \langle ac \rangle \langle bd \rangle \langle cf \rangle \langle ef \rangle [ab] [cf], \quad (4.112)
 \end{aligned}$$

4 The Seven Gluon Two-Loop Amplitude

$$\begin{aligned}
G_{7:1,1}^4 = & 16 \langle ac \rangle \langle ad \rangle \langle be \rangle \langle cf \rangle [ab] [ac] - 6 \langle ad \rangle^2 \langle bc \rangle \langle ef \rangle [ab] [ad] \\
& + 3 \langle ad \rangle^2 \langle ce \rangle \langle cf \rangle [ac] [ad] - 3 \langle ac \rangle \langle ad \rangle \langle ce \rangle \langle df \rangle [ac] [ad] \\
& + 6 \langle ac \rangle^2 \langle de \rangle \langle df \rangle [ac] [ad] + 3 \langle ac \rangle \langle ad \rangle \langle cd \rangle \langle ef \rangle [ac] [ad] \\
& - 6 \langle ad \rangle^2 \langle ce \rangle \langle df \rangle [ad]^2 + 6 \langle ac \rangle \langle ad \rangle \langle de \rangle \langle df \rangle [ad]^2 \\
& + 6 \langle ad \rangle^2 \langle cd \rangle \langle ef \rangle [ad]^2 - 9 \langle ac \rangle \langle ae \rangle \langle be \rangle \langle df \rangle [ab] [ae] \\
& + 3 \langle ad \rangle \langle ae \rangle \langle ce \rangle \langle cf \rangle [ac] [ae] - 3 \langle ac \rangle \langle ae \rangle \langle ce \rangle \langle df \rangle [ac] [ae] \\
& + 3 \langle ac \rangle \langle ad \rangle \langle ce \rangle \langle ef \rangle [ac] [ae] - 3 \langle ac \rangle^2 \langle de \rangle \langle ef \rangle [ac] [ae] \\
& - 6 \langle ad \rangle \langle ae \rangle \langle ce \rangle \langle df \rangle [ad] [ae] + 6 \langle ac \rangle \langle ae \rangle \langle de \rangle \langle df \rangle [ad] [ae] \\
& + 6 \langle ad \rangle^2 \langle ce \rangle \langle ef \rangle [ad] [ae] - 6 \langle ac \rangle \langle ad \rangle \langle de \rangle \langle ef \rangle [ad] [ae] \\
& + 3 \langle ad \rangle \langle ae \rangle \langle cf \rangle^2 [ac] [af] - 3 \langle ac \rangle \langle ae \rangle \langle cf \rangle \langle df \rangle [ac] [af] \\
& - 4 \langle ab \rangle \langle cd \rangle \langle cf \rangle \langle de \rangle [ad] [bc] + 6 \langle ab \rangle \langle ce \rangle \langle cf \rangle \langle df \rangle [af] [bc] \\
& + 4 \langle ab \rangle \langle cd \rangle \langle cf \rangle \langle ef \rangle [af] [bc] + 4 \langle ab \rangle \langle cd \rangle \langle cg \rangle \langle ef \rangle [ag] [bc] \\
& - 18 \langle ab \rangle \langle bd \rangle \langle cf \rangle \langle de \rangle [ab] [bd] + 6 \langle ac \rangle \langle bd \rangle \langle cf \rangle \langle de \rangle [ac] [bd] \\
& - 3 \langle ac \rangle \langle bd \rangle \langle ce \rangle \langle df \rangle [ac] [bd] - 3 \langle ac \rangle \langle bd \rangle \langle de \rangle \langle df \rangle [ad] [bd] \\
& + 6 \langle ab \rangle \langle cd \rangle \langle de \rangle \langle ef \rangle [ae] [bd] + 3 \langle ab \rangle \langle ce \rangle \langle df \rangle^2 [af] [bd] \\
& - 3 \langle ac \rangle \langle be \rangle \langle de \rangle \langle ef \rangle [ae] [be] - 6 \langle ab \rangle \langle ce \rangle \langle de \rangle \langle ef \rangle [ae] [be] \\
& - 9 \langle ab \rangle \langle ce \rangle \langle df \rangle \langle ef \rangle [af] [be] + 6 \langle ab \rangle \langle cd \rangle \langle ef \rangle^2 [af] [be] \\
& - 9 \langle ab \rangle \langle ce \rangle \langle df \rangle \langle eg \rangle [ag] [be] + 6 \langle ab \rangle \langle cd \rangle \langle ef \rangle \langle eg \rangle [ag] [be] \tag{4.113}
\end{aligned}$$

and

$$\begin{aligned}
 G_{7:1,1}^5 = & 7 \langle ab \rangle \langle bd \rangle \langle cf \rangle \langle ef \rangle [ab] [bf] - 6 \langle ac \rangle \langle bd \rangle \langle cf \rangle \langle ef \rangle [ac] [bf] \\
 & - 6 \langle ab \rangle \langle cf \rangle \langle df \rangle \langle ef \rangle [af] [bf] - 6 \langle ab \rangle \langle cf \rangle \langle df \rangle \langle eg \rangle [ag] [bf] \\
 & + 12 \langle ac \rangle \langle bd \rangle \langle ce \rangle \langle df \rangle [ab] [cd] + 6 \langle ad \rangle \langle cf \rangle^2 \langle de \rangle [af] [cd] \\
 & - 6 \langle ac \rangle \langle cg \rangle \langle de \rangle \langle df \rangle [ag] [cd] - 3 \langle ac \rangle \langle bc \rangle \langle de \rangle \langle ef \rangle [ab] [ce] \\
 & - 3 \langle ad \rangle \langle ce \rangle \langle cf \rangle \langle de \rangle [ad] [ce] + 3 \langle ac \rangle \langle cf \rangle \langle de \rangle^2 [ad] [ce] \\
 & + 3 \langle ad \rangle \langle ce \rangle^2 \langle df \rangle [ad] [ce] - 3 \langle ac \rangle \langle ce \rangle \langle de \rangle \langle df \rangle [ad] [ce] \\
 & + 3 \langle ad \rangle \langle ce \rangle^2 \langle ef \rangle [ae] [ce] - 3 \langle ac \rangle \langle ce \rangle \langle de \rangle \langle ef \rangle [ae] [ce] \\
 & + 6 \langle ac \rangle \langle be \rangle \langle cf \rangle \langle df \rangle [ab] [cf] - 6 \langle ac \rangle \langle cf \rangle \langle de \rangle \langle df \rangle [ad] [cf] \\
 & + 3 \langle ad \rangle \langle ce \rangle \langle cf \rangle \langle ef \rangle [ae] [cf] - 3 \langle ac \rangle \langle cf \rangle \langle de \rangle \langle ef \rangle [ae] [cf] \\
 & - 3 \langle ad \rangle \langle ce \rangle \langle cf \rangle \langle cg \rangle [ac] [cg] + 3 \langle ac \rangle \langle cf \rangle \langle cg \rangle \langle de \rangle [ac] [cg] \\
 & + 6 \langle ad \rangle \langle cf \rangle \langle cg \rangle \langle de \rangle [ad] [cg] + 9 \langle ac \rangle \langle bd \rangle \langle de \rangle \langle ef \rangle [ab] [de] \\
 & + 3 \langle ad \rangle \langle ce \rangle \langle cf \rangle \langle de \rangle [ac] [de] - 3 \langle ac \rangle \langle cf \rangle \langle de \rangle^2 [ac] [de] \\
 & + 6 \langle ac \rangle \langle ce \rangle \langle de \rangle \langle df \rangle [ac] [de] - 6 \langle ad \rangle \langle cf \rangle \langle de \rangle^2 [ad] [de] \\
 & - 6 \langle ae \rangle \langle cd \rangle \langle de \rangle \langle df \rangle [ad] [de] + 6 \langle ad \rangle \langle ce \rangle \langle de \rangle \langle df \rangle [ad] [de] \\
 & + 6 \langle ac \rangle \langle be \rangle \langle df \rangle^2 [ab] [df] + 3 \langle ad \rangle \langle ce \rangle \langle cf \rangle \langle df \rangle [ac] [df] \\
 & + 9 \langle ac \rangle \langle cf \rangle \langle de \rangle \langle df \rangle [ac] [df] - 6 \langle ad \rangle \langle cf \rangle \langle de \rangle \langle df \rangle [ad] [df] \\
 & - 6 \langle ae \rangle \langle cd \rangle \langle df \rangle^2 [ad] [df] + 6 \langle ad \rangle \langle ce \rangle \langle df \rangle^2 [ad] [df] \\
 & + 6 \langle ae \rangle \langle cf \rangle \langle de \rangle \langle df \rangle [ae] [df] - 6 \langle ae \rangle \langle ce \rangle \langle df \rangle^2 [ae] [df] \\
 & - 6 \langle ad \rangle \langle cf \rangle \langle de \rangle \langle ef \rangle [ae] [df] + 6 \langle ad \rangle \langle ce \rangle \langle df \rangle \langle ef \rangle [ae] [df]. \quad (4.114)
 \end{aligned}$$

4.5.10 $R_{7:1,2}$

The second new exclusively $U(N_c)$ rational piece can be expressed in terms of the new $SU(N_c)$ structures via a decoupling identity,

$$\begin{aligned}
 R_{7:1,2}(a; b, c; d, e, f, g) = & -R_{7:3}(b, c; a, d, e, f, g) - R_{7:3}(b, c; a, e, f, g, d) \\
 & - R_{7:3}(b, c; a, f, g, d, e) - R_{7:3}(b, c; a, g, d, e, f) \\
 & - R_{7:4}(a, b, c; d, e, f, g) - R_{7:4}(a, c, b; d, e, f, g)
 \end{aligned}$$

4 The Seven Gluon Two-Loop Amplitude

$$= - \sum_{Z_4(defg)} R_{7:3}(b, c; a, d, e, f, g) - \sum_{Z_2(bc)} R_{7:4}(a, b, c; d, e, f, g). \quad (4.115)$$

4.5.11 $R_{7:1,3}$

From the decoupling identity, the new $U(N_c)$ rational piece $R_{7:1,3}$ can be expressed solely in terms of $R_{7:4}$,

$$\begin{aligned} R_{7:1,3}(a; b, c, d; e, f, g) &= - R_{7:4}(b, c, d; a, e, f, g) - R_{7:4}(b, c, d; a, f, g, e) \\ &\quad - R_{7:4}(b, c, d; a, g, e, f) - R_{7:4}(e, f, g; a, b, c, d) \\ &\quad - R_{7:4}(e, f, g; a, c, d, b) - R_{7:4}(e, f, g; a, d, b, c) \\ &= - \sum_{Z_3(efg)} R_{7:4}(b, c, d; a, e, f, g) - \sum_{Z_3(bcd)} R_{7:4}(e, f, g; a, b, c, d). \end{aligned} \quad (4.116)$$

4.5.12 $R_{7:2,2}$

The final new $SU(N_c)$ rational piece can be expressed in terms of the previous two $U(N_c)$ structures,

$$\begin{aligned} R_{7:2,2}(a, b; c, d; e, f, g) &= - R_{7:1,2}(b; c, d; a, e, f, g) - R_{7:1,2}(b; c, d; a, f, g, e) \\ &\quad - R_{7:1,2}(b; c, d; a, g, e, f) - R_{7:1,3}(b; a, c, d; e, f, g) \\ &\quad - R_{7:1,3}(b; a, d, c; e, f, g) \\ &= - \sum_{Z_3(efg)} R_{7:1,2}(b; c, d; a, e, f, g) - \sum_{Z_2(cd)} R_{7:1,3}(b; a, c, d; e, f, g). \end{aligned} \quad (4.117)$$

4.5.13 $R_{7:1B}$

Lastly is $R_{7:1B}$, the $SU(N_c)$ partial amplitude that appears with a single colour trace and no factors of N_c in the colour decomposition. (This differs from $R_{7:1}$, which appears multiplied by N_c^2 and a single trace.) The augmented recursion result calculated here finds agreement with the n -point postulate in ref. [63]. We reconstruct a version matching that form. The function has cyclic symmetry in the momenta, but unlike other colour structures does not appear with an explicit $\mathcal{P}_{7:\lambda}$ sum.

For compactness, the Parke–Taylor denominator is defined with

$$C_{PT}(a, b, c, d, e, f, g) = \frac{1}{\langle ab \rangle \langle bc \rangle \langle cd \rangle \langle de \rangle \langle ef \rangle \langle fg \rangle \langle ga \rangle}. \quad (4.118)$$

Also useful is the epsilon function

$$\begin{aligned} \epsilon(a, b, c, d) &= [a|b|c|d|a] - \langle a|b|c|d|a \rangle \\ &= [a b] \langle b c \rangle [c d] \langle d a \rangle - \langle a b \rangle [b c] \langle c d \rangle [d a], \end{aligned} \quad (4.119)$$

with a further compact notation

$$\epsilon(\{a_1, \dots, a_x\}, b, c, \{d_1, \dots, d_y\}) = \sum_{i=1}^x \sum_{j=1}^y \epsilon(a_i, b, c, d_j). \quad (4.120)$$

With these identifications, the partial amplitude can be written in two pieces,

$$R_{7:1B}(a, b, c, d, e, f, g) = R_{7:1B}^A(a, b, c, d, e, f, g) + R_{7:1B}^B(a, b, c, d, e, f, g), \quad (4.121)$$

where

$$\begin{aligned} R_{7:1B}^A(a, b, c, d, e, f, g) &= -2i C_{PT}(a, b, c, d, e, f, g) \times \\ &\quad \left(\epsilon(\{a, b, c\}, d, f, g) + \epsilon(\{a, b\}, c, e, \{f, g\}) \right. \\ &\quad + \epsilon(\{a, b\}, c, f, g) + \epsilon(a, b, d, \{e, f, g\}) \\ &\quad \left. + \epsilon(a, b, e, \{f, g\}) + \epsilon(a, b, f, g) \right) \end{aligned} \quad (4.122)$$

4 The Seven Gluon Two-Loop Amplitude

and

$$\begin{aligned}
R_{7:1B}^B(a, b, c, d, e, f, g) = & \\
+4i \left(& C_{PT}(a, b, c, e, f, d, g) \epsilon(\{a, b, c\}, e, d, g) - C_{PT}(a, b, c, f, e, d, g) \epsilon(\{a, b, c\}, f, d, g) \right. \\
& + C_{PT}(a, b, c, f, d, e, g) \epsilon(\{a, b, c\}, f, e, g) + C_{PT}(a, b, d, e, c, f, g) \epsilon(\{a, b\}, d, c, \{f, g\}) \\
& + C_{PT}(a, b, d, e, f, c, g) \epsilon(\{a, b\}, d, c, g) - C_{PT}(a, b, e, d, c, f, g) \epsilon(\{a, b\}, e, c, \{f, g\}) \\
& - C_{PT}(a, b, e, d, f, c, g) \epsilon(\{a, b\}, e, c, g) - C_{PT}(a, b, e, f, d, c, g) \epsilon(\{a, b\}, e, c, g) \\
& + C_{PT}(a, b, e, c, d, f, g) \epsilon(\{a, b\}, e, d, \{f, g\}) + C_{PT}(a, b, e, c, f, d, g) \epsilon(\{a, b\}, e, d, g) \\
& + C_{PT}(a, b, e, f, c, d, g) \epsilon(\{a, b\}, e, d, g) + C_{PT}(a, b, f, e, d, c, g) \epsilon(\{a, b\}, f, c, g) \\
& - C_{PT}(a, b, f, c, e, d, g) \epsilon(\{a, b\}, f, d, g) - C_{PT}(a, b, f, e, c, d, g) \epsilon(\{a, b\}, f, d, g) \\
& + C_{PT}(a, b, f, c, d, e, g) \epsilon(\{a, b\}, f, e, g) + C_{PT}(a, c, d, b, e, f, g) \epsilon(a, c, b, \{e, f, g\}) \\
& + C_{PT}(a, c, d, e, b, f, g) \epsilon(a, c, b, \{f, g\}) + C_{PT}(a, c, d, e, f, b, g) \epsilon(a, c, b, g) \\
& - C_{PT}(a, d, c, b, e, f, g) \epsilon(a, d, b, \{e, f, g\}) - C_{PT}(a, d, c, e, b, f, g) \epsilon(a, d, b, \{f, g\}) \\
& - C_{PT}(a, d, e, c, b, f, g) \epsilon(a, d, b, \{f, g\}) - C_{PT}(a, d, c, e, f, b, g) \epsilon(a, d, b, g) \\
& - C_{PT}(a, d, e, c, f, b, g) \epsilon(a, d, b, g) - C_{PT}(a, d, e, f, c, b, g) \epsilon(a, d, b, g) \\
& + C_{PT}(a, d, b, c, e, f, g) \epsilon(a, d, c, \{e, f, g\}) + C_{PT}(a, d, b, e, c, f, g) \epsilon(a, d, c, \{f, g\}) \\
& + C_{PT}(a, d, e, b, c, f, g) \epsilon(a, d, c, \{f, g\}) + C_{PT}(a, d, b, e, f, c, g) \epsilon(a, d, c, g) \\
& + C_{PT}(a, d, e, b, f, c, g) \epsilon(a, d, c, g) + C_{PT}(a, d, e, f, b, c, g) \epsilon(a, d, c, g) \\
& + C_{PT}(a, e, d, c, b, f, g) \epsilon(a, e, b, \{f, g\}) + C_{PT}(a, e, d, c, f, b, g) \epsilon(a, e, b, g) \\
& + C_{PT}(a, e, d, f, c, b, g) \epsilon(a, e, b, g) + C_{PT}(a, e, f, d, c, b, g) \epsilon(a, e, b, g) \\
& - C_{PT}(a, e, b, d, c, f, g) \epsilon(a, e, c, \{f, g\}) - C_{PT}(a, e, d, b, c, f, g) \epsilon(a, e, c, \{f, g\}) \\
& - C_{PT}(a, e, b, d, f, c, g) \epsilon(a, e, c, g) - C_{PT}(a, e, b, f, d, c, g) \epsilon(a, e, c, g) \\
& - C_{PT}(a, e, d, b, f, c, g) \epsilon(a, e, c, g) - C_{PT}(a, e, d, f, b, c, g) \epsilon(a, e, c, g) \\
& - C_{PT}(a, e, f, b, d, c, g) \epsilon(a, e, c, g) - C_{PT}(a, e, f, d, b, c, g) \epsilon(a, e, c, g) \\
& + C_{PT}(a, e, b, c, d, f, g) \epsilon(a, e, d, \{f, g\}) + C_{PT}(a, e, b, c, f, d, g) \epsilon(a, e, d, g) \\
& + C_{PT}(a, e, b, f, c, d, g) \epsilon(a, e, d, g) + C_{PT}(a, e, f, b, c, d, g) \epsilon(a, e, d, g) \\
& - C_{PT}(a, f, e, d, c, b, g) \epsilon(a, f, b, g) + C_{PT}(a, f, b, e, d, c, g) \epsilon(a, f, c, g) \\
& + C_{PT}(a, f, e, b, d, c, g) \epsilon(a, f, c, g) + C_{PT}(a, f, e, d, b, c, g) \epsilon(a, f, c, g) \\
& - C_{PT}(a, f, b, c, e, d, g) \epsilon(a, f, d, g) - C_{PT}(a, f, b, e, c, d, g) \epsilon(a, f, d, g) \\
& \left. - C_{PT}(a, f, e, b, c, d, g) \epsilon(a, f, d, g) + C_{PT}(a, f, b, c, d, e, g) \epsilon(a, f, e, g) \right). \quad (4.123)
\end{aligned}$$

4.6 Collinear Momentum Limits

As a final validity check on the results, collinear limits are tested.

Collinear limits are those where two momenta are taken to be collinear, meaning that $a \rightarrow zK$ and $b \rightarrow (1-z)K$. In this limit, we expect the amplitude to factorise into splitting functions and lower-point amplitudes. This behaviour is a useful and common test of the validity of newly derived amplitudes. For example, the process is shown explicitly in [52], where it is applied to $A_{5;1}^{(2)}(a^+, b^+, c^+, d^+, e^+)$.

In general, a two-loop amplitude factorises as [68]

$$\mathcal{A}_n^{(2)}(\dots, a^{\lambda_a}, b^{\lambda_b}, \dots) \xrightarrow{a\parallel b} \sum_{\lambda=\pm} \left(\text{Split}_{-\lambda}^{(0)}(z; a^{\lambda_a}, b^{\lambda_b}) \mathcal{A}_{n-1}^{(2)}(\dots, K^\lambda, \dots) \right. \\ \left. + \text{Split}_{-\lambda}^{(1)}(z; a^{\lambda_a}, b^{\lambda_b}) \mathcal{A}_{n-1}^{(1)}(\dots, K^\lambda, \dots) \right. \\ \left. + \text{Split}_{-\lambda}^{(2)}(z; a^{\lambda_a}, b^{\lambda_b}) \mathcal{A}_{n-1}^{(0)}(\dots, K^\lambda, \dots) \right). \quad (4.124)$$

In our all-plus helicity case, the $\mathcal{A}_{n-1}^{(0)}$ tree amplitudes are vanishing, so we do not need any two-loop splitting functions.

The validity of the epsilon and polylogarithmic structures have been previously confirmed, so let us focus only on the rational piece collinear limits. We will make use of the splitting functions [68]

$$\text{Split}_+^{(0)}(z; a^+, b^+) = 0, \\ \text{Split}_-^{(0)}(z; a^+, b^+) = \frac{1}{\sqrt{z(1-z)} \langle ab \rangle} \quad (4.125)$$

and

$$\text{Split}_+^{(0)}(z; a^+, b^+) |_{rat} = -\frac{\sqrt{z(1-z)} [ab]}{3 \langle ab \rangle^2}, \\ \text{Split}_-^{(0)}(z; a^+, b^+) |_{rat} = \frac{\sqrt{z(1-z)}}{3 \langle ab \rangle}, \quad (4.126)$$

where only the rational pieces have been kept in the one-loop functions.

Numerical evaluation shows that the augmented recursion results are consistent with

4 The Seven Gluon Two-Loop Amplitude

the collinear limit relations:

$$A_{7:1,1}^{(2)}(a; b; c, d, e, f, g) \xrightarrow{f||g} \text{Split}_-^{(0)}(z; f^+, g^+) A_{6:1,1}^{(2)}(a; b; c, d, e, K^-), \quad (4.127)$$

$$\begin{aligned} A_{7:1,1}^{(2)}(a; b; c, d, e, f, g) &\xrightarrow{a||b} 0, \\ A_{7:1,1}^{(2)}(a; b; c, d, e, f, g) &\xrightarrow{b||c} 0, \\ A_{7:1,1}^{(2)}(a; b; c, d, e, f, g) &\xrightarrow{c||e} 0, \end{aligned} \quad (4.128)$$

$$\begin{aligned} A_{7:4}^{(2)}(a, b, c; d, e, f, g) &\xrightarrow{a||b} \text{Split}_-^{(0)}(z; a^+, b^+) A_{6:3}^{(2)}(K^+, c; d, e, f, g) \\ &\quad + \text{Split}_+^{(1)}(z; a^+, b^+) A_{6:3}^{(1)}(K^-, c; d, e, f, g) \\ &\quad + \text{Split}_-^{(1)}(z; a^+, b^+) A_{6:3}^{(1)}(K^+, c; d, e, f, g), \\ A_{7:4}^{(2)}(a, b, c; d, e, f, g) &\xrightarrow{f||g} \text{Split}_-^{(0)}(z; f^+, g^+) A_{6:4}^{(2)}(a, b, c; d, e, K^+) \\ &\quad + \text{Split}_+^{(1)}(z; f^+, g^+) A_{6:4}^{(1)}(a, b, c; d, e, K^-) \\ &\quad + \text{Split}_-^{(1)}(z; f^+, g^+) A_{6:4}^{(1)}(a, b, c; d, e, K^+) \end{aligned} \quad (4.129)$$

and

$$\begin{aligned} A_{7:4}^{(2)}(a, b, c; d, e, f, g) &\xrightarrow{c||d} 0, \\ A_{7:4}^{(2)}(a, b, c; d, e, f, g) &\xrightarrow{d||f} 0. \end{aligned} \quad (4.130)$$

Checking these two partial amplitudes is sufficient, as $A_{7:1}^{(2)}$ and $A_{7:1B}^{(2)}$ have been checked previously. Together with the decoupling identities, this confirms the collinear structure of the whole amplitude.

4.7 Conclusions

Using the techniques of four-dimensional unitarity cutting and augmented recursion, we have obtained the two-loop seven gluon all-plus helicity Yang–Mills amplitude in a compact, analytic form. By separating the procedure into two parts, by the type of function involved, we have avoided the need for a more difficult D -dimensional unitarity approach. Our method has only required evaluation of one-loop integrals, to obtain a

two-loop result.

The final result for the amplitude is gauge invariant, as is required for its use in experimentally testable observables. The technique of four-dimensional unitarity is manifestly gauge invariant throughout, involving on-shell amplitudes which are themselves gauge invariant, as well as box integrals. Working in four dimensions allows the spinor-helicity formalism to be used straightforwardly. Helicity considerations greatly constrain the number of diagrams that contribute to the unitarity.

The BCFW recursion is also manifestly gauge invariant. The only ingredients are gauge-invariant lower-point amplitudes. Although the process introduces a new reference momentum to allow the amplitude to be treated as a complex function, the result is independent of this reference and it is not a gauge choice.

Some gauge dependence occurs in intermediate steps of the augmented recursion portion. To ensure that both leading and sub-leading poles are accounted for, we carry out explicit loop integrals involving currents. Internal off-shell legs are treated in the spinor-helicity setup with an axial gauge formalism, which introduces a reference momentum gauge choice. Despite the individual contributions being gauge dependent, the overall result is independent of the reference momentum, which is a powerful consistency check. The particular choice of axial gauge for the gauge-dependent step is also convenient because ghosts decouple from gluons in this gauge, meaning they did not appear in our diagrams.

Our calculation finds agreement with two n -point conjectures, firstly for the two-loop all-plus polylogarithmic piece $P_{n:\lambda}^{(2)}(1^+, 2^+, \dots, n^+)$ [62], and also for the N_c -independent single-trace rational piece $R_{n:B}^{(2)}(1^+, 2^+, \dots, n^+)$ [63]. These were both found by extrapolating from patterns in compact analytic amplitude expressions, demonstrating the value of calculating such objects. With the seven-point amplitude now available in a simple form, general expressions for other partial amplitudes may become apparent.

This thesis continues with discussions of currents and their integration in Chapter 5 and amplitude reconstruction in Chapter 6. (Including the detailed procedure omitted from this chapter.) The successful application of these techniques to the two-loop seven-point amplitude identifies them as valuable tools in whichever amplitude calculation is pursued next, be it of a different helicity choice, or a greater loop or gluon number.

5 Currents and their Integration

5.1 Introduction

BCFW recursion [19] allows an amplitude to be constructed from knowledge of its pole structure. At tree level, diagrams showing factorisation into two amplitudes connected by the desired propagator suffice to capture all pole information. However at loop level, the possibility of non-simple (double etc.) poles means that factorisations are not sufficient. They can provide all leading pole information, but pole-under-the-pole behaviour is missed.

Augmented recursion [52] was devised to overcome this limitation. New diagrams, featuring loop integrals involving currents, are introduced to the procedure. Contained is both the leading and sub-leading pole information.

We illustrate this with an example from the recursion process for the seven-point all-plus two-loop rational piece. Naively, we might draw factorisations involving two one-loop amplitudes such as

$$R_3^{(1)}(a, b, k^-) - \frac{i}{s_{ab}} - R_6^{(1)}(k^+, c, d, e, f, g), \quad (5.1)$$

as shown in Figure 4.5 on page 92, and conclude that we have identified the pole structure. However, this only contains $1/s_{ab}^2$ terms.

Instead, we can draw

$$-R_3^{(0)}(\beta^-, b, l^+) - \frac{i}{l^2} - R_3^{(0)}(l^-, a, \alpha^+) - \frac{i}{\alpha^2} - \tau_7^{(1)}(\alpha^-, \beta^+, c, d, e, f, g) - \frac{i}{\beta^2} \quad (5.2)$$

as depicted in Figure 4.6 on page 92.

It is easy to see that part of the domain of this loop integration corresponds to the previous diagram. However, the rest of the integration contains extra information, including terms with sub-leading $1/s_{ab}$ poles that are required for the recursion.

In the following sections, we will discuss the derivation of currents and present a new, more intuitive perspective. We will derive the currents necessary for the calculation

of the seven-point amplitude in Chapter 4. Finally, we will consider the integration of current diagrams to obtain the contributions to the augmented recursion procedure.

5.2 Deriving Currents

Currents are similar structures to amplitudes, but where external momenta are allowed to be off-shell. For our purposes, we are interested in doubly off-shell currents for use in augmented recursion diagrams.

In the spinor-helicity formalism, we can represent null momenta p_i^μ with spinors $\lambda_i \tilde{\lambda}_i$, which automatically encode the on-shell condition $p_i^2 = \langle i i \rangle = [i i] = 0$. Off-shell momentum requires a different treatment, for which we use the axial gauge formalism [66, 41, 67]. A null reference momentum q is introduced, so that any non-null momentum K can be represented as a sum of a null momentum K^b and a piece proportional to q . Momentum K is said to be “nullified” according to

$$K^b = K - \frac{K^2}{[q|K|q]} q, \quad (5.3)$$

where $(K^b)^2 = 0$, $q^2 = 0$ and $K^2 \neq 0$. The spinors relating to $K^b = \lambda_K \tilde{\lambda}_K$ can be written

$$\begin{aligned} \lambda_K &= K|q], \\ \tilde{\lambda}_K &= \frac{K|q\rangle}{[q|K|q]}. \end{aligned} \quad (5.4)$$

We note that a superscript (b) will be used to denote the nullified form of off-shell momenta when they appear in our calculations. However, spinor labels will not use these superscripts as there is no ambiguity – spinors are on-shell objects and any spinor we use could be considered to be nullified.

As such, an easy algebraic mistake to make would be to incorrectly apply the relation

$$[b a] \langle a c \rangle = [b|a|c], \quad (5.5)$$

which applies for null momenta $\{a, b, c\}$, to a case involving non-null momenta. In the case of non-null K , the equivalent expression is

$$[b K] \langle K c \rangle = [b|K^b|c] = [b|K|c] - K^2 \frac{[b|q|c]}{[q|K|q]}. \quad (5.6)$$

The extra term resulting from a non-null momentum often appears in manipulations involving currents, so should be treated with care.

It will be helpful to use axial gauge forms for the three-point tree amplitudes, incorporating the reference momentum q [67],

$$\begin{aligned} A_{3,q}^{(0)}(a^-, b^+, c^+) &= -i \frac{[bc] \langle aq \rangle^2}{\langle bq \rangle \langle cq \rangle}, \\ A_{3,q}^{(0)}(a^+, b^-, c^-) &= i \frac{\langle bc \rangle [aq]^2}{[bq] [cq]}, \end{aligned} \tag{5.7}$$

as these can simplify expressions involving nullified momenta. In an object such as $[a|K|q\rangle$, the term needed to nullify K vanishes and we can interchange $[a|K|q\rangle = [a|K^\flat|q\rangle$ whenever that aids manipulation.

We do not need to derive the entire current, because only those terms with poles in relevant momenta contribute to the recursion process. Therefore we can derive a simpler “good enough” current approximation that contains only necessary structures. Two conditions on these structures have been identified previously, which allow them to be generated [52, 70]. For a current with legs $\{\alpha, \beta\}$ that are in general off-shell, we have the rules:

- (C1) The current must reproduce the leading $s_{\alpha\beta}$ singularities as $s_{\alpha\beta} \rightarrow 0$, for any choices of momenta $\{\alpha, \beta\}$ with $\alpha^2, \beta^2 \neq 0$.
- (C2) The current must reproduce the appropriate amplitude when $\alpha^2, \beta^2 \rightarrow 0$ and $s_{\alpha\beta}$ takes a general value (which can be $s_{\alpha\beta} \neq 0$).

By following these rules, the terms involving poles in $s_{\alpha\beta}$ are specified, but various other contributions can be omitted.

In the recursion procedure, the $s_{\alpha\beta}$ become $s_{\alpha\beta} = s_{ab} = \langle ab \rangle [ba]$ and we consider residues of the pole introduced by shifting momenta in $\langle ab \rangle$. Therefore we are justified in only deriving $\tau_n^{(1)}(\alpha, \dots, \beta, \dots)$, where the full current,

$$\tau_n^{(1),full}(\alpha, \dots, \beta, \dots) = \tau_n^{(1)}(\alpha, \dots, \beta, \dots) + \mathcal{O}(s_{\alpha\beta}^0), \tag{5.8}$$

contains additional pieces that have no bearing on the augmented recursion procedure.

5.2.1 Note about poles

The following current derivation requires that the rules C1 and C2 refer to $s_{\alpha\beta}$ as the structure that leads to poles. Although $\langle\alpha\beta\rangle$ or $[\alpha\beta]$ may also be present, treating these as also equivalent to poles would be erroneous.

Expanding $s_{\alpha\beta}$ for general off-shell α, β , we obtain

$$\begin{aligned} s_{\alpha\beta} &= (\alpha + \beta)^2 = \left(\alpha^b + \frac{\alpha^2}{2\alpha \cdot q} q + \beta^b + \frac{\beta^2}{2\beta \cdot q} q \right)^2 \\ &= \langle\alpha\beta\rangle [\beta\alpha] + \left(\frac{\alpha^2}{2\alpha \cdot q} + \frac{\beta^2}{2\beta \cdot q} \right) 2q \cdot (\alpha + \beta), \end{aligned} \quad (5.9)$$

where α^b, β^b are null, q is a suitable (i.e. not a function of $\{\alpha, \beta\}$) null reference momentum and we interpret all momenta in spinor products as referring to the nullified versions.

Crucially, the condition $\alpha^2, \beta^2 \neq 0$ (appearing in C1) means that $\langle\alpha\beta\rangle [\alpha\beta]$ must remain non-zero when $s_{\alpha\beta} \rightarrow 0$. In other words, $1/\langle\alpha\beta\rangle, 1/[\alpha\beta]$ factors do not become poles in the limit where $1/s_{\alpha\beta}$ diverges and can safely be treated as finite throughout the derivation.

In the following sections, denominator factors of $s_{\alpha\beta}$ will be referred to as “poles”. Strictly speaking, this is a shorthand for “the structure that leads to poles”, because the complex shift of the recursion process has not yet been applied. Anticipating how the various current structures will contribute to the recursion step, or not, allows effort to be devoted to only developing the pieces that will survive into the result.

5.2.2 A systematic method

Existing literature does not tend to present an intuitive procedure for deriving currents. We present a new systematic approach to derive the “good enough” current satisfying C1 and C2:

1. Start by writing the “good enough” current as

$$\tau_n^{(1)}(\alpha, \beta, \dots) = A_n^{(1)}|_{\alpha^2, \beta^2=0}(\alpha, \beta, \dots) + \mathcal{O}(\alpha^2, \beta^2),$$

where $A_n^{(1)}|_{\alpha^2, \beta^2=0}$ represents the amplitude $A_n^{(1)}$, with nullified α^b and β^b as arguments. Any instances of $s_{\alpha\beta}$ have been replaced by $\langle\alpha\beta\rangle [\beta\alpha]$.

The justification for this step is that it is clear that a current must contain some version of the corresponding amplitude, extended for off-shell legs. This is encoded in condition C2. It is also required that only the amplitude remains when α and β go on-shell, so the extension must be of $\mathcal{O}(\alpha^2, \beta^2)$. However, there is ambiguity about how to adapt an on-shell amplitude to off-shell momenta. Where spinors appear, they can only refer to null momenta, but where momenta themselves appear (eg. in $[a|b|c]$ or $s_{ab} = (a+b)^2$) a choice must be made whether these should be replaced by the full off-shell or nullified momenta.

We choose to interpret all occurrences of the momentum to be taken off-shell inside the amplitude as being the nullified form, including when the momentum itself appears. By doing this, any apparent s -pole of α and β will appear as

$$s_{\alpha^b \beta^b} = (\alpha^b + \beta^b)^2 = \langle \alpha \beta \rangle [\beta \alpha], \quad (5.10)$$

which does not contribute a pole for the purposes of our derivation. (Our poles are $s_{\alpha\beta}$ only, where $(\alpha^b + \beta^b)^2 \neq s_{\alpha\beta}$ for general $\alpha^2, \beta^2 \neq 0$.)

Therefore we have satisfied C2 – the current will reduce to the regular on-shell amplitude when all momenta are on-shell. We have also avoided introducing any $s_{\alpha\beta}$ singularities in the $\alpha^2, \beta^2 \neq 0$ case, so have had no impact on C1.

2. Add the leading singularities to the current. These are given by all the lower-point amplitude factorisations where the propagator is $s_{\alpha\beta}$. In this case, it is the full off-shell $s_{\alpha\beta}$ that should be written. We denote the contribution $\tau_{LS}^{(1)}$.

This satisfies condition C1 straightforwardly. Because we avoided including singularities in step 1, there is no risk of double counting. The only issue left to correct is that C2 no longer holds, because $\tau_{LS}^{(1)}$ gives some extra contribution to the current in the $\alpha^2, \beta^2 \rightarrow 0$ limit.

3. Subtract the piece $\tau_{LS}^{(1)}|_{\alpha^2, \beta^2=0}$, which represents the leading singularity terms with off-shell momenta replaced by the nullified forms $\alpha \rightarrow \alpha^b$ and $\beta \rightarrow \beta^b$. (In particular, $s_{\alpha\beta} \rightarrow \langle \alpha \beta \rangle [\beta \alpha]$.)

5 Currents and their Integration

Doing so cancels those unwanted contributions when $\alpha^2, \beta^2 \rightarrow 0$ (because $\tau_{LS}^{(1)}$ and $\tau_{LS}^{(1)}|_{\alpha^2, \beta^2=0}$ are equivalent in that limit), meaning that C2 holds once again. The subtraction does not contain any $s_{\alpha\beta}$ singularities, by construction, so C1 continues to hold.

Recalling equation 5.10, we see that

$$\tau_{LS}^{(1)} - \tau_{LS}^{(1)}|_{\alpha^2, \beta^2=0} \in \mathcal{O}(\alpha^2, \beta^2) \quad (5.11)$$

is required in order for the derivation to be consistent. Indeed, algebraic manipulation of the difference gives the identity

$$\tau_{LS}^{(1)} - \tau_{LS}^{(1)}|_{\alpha^2, \beta^2=0} \propto \frac{1}{s_{\alpha\beta}} - \frac{1}{\langle \alpha \beta \rangle [\beta \alpha]} = - \left(\frac{\alpha^2}{2\alpha \cdot q} + \frac{\beta^2}{2\beta \cdot q} \right) \frac{2k \cdot q}{s_{\alpha\beta} \langle \alpha \beta \rangle [\beta \alpha]}, \quad (5.12)$$

where $k = \alpha + \beta$. As expected, the structure is explicitly $\mathcal{O}(\alpha^2, \beta^2)$, providing a $1/s_{\alpha\beta}$ pole contribution only when $\alpha^2, \beta^2 \neq 0$.

4. Identifying the $\mathcal{O}(\alpha^2, \beta^2)$ piece of step 1 with $\tau_{LS}^{(1)} - \tau_{LS}^{(1)}|_{\alpha^2, \beta^2=0}$, the entire “good enough” current, satisfying both conditions C1 and C2, can be written as

$$\tau_n^{(1)}(\alpha, \beta, \dots) = A_n^{(1)}|_{\alpha^2, \beta^2=0}(\alpha, \beta, \dots) + \tau_{LS}^{(1)} - \tau_{LS}^{(1)}|_{\alpha^2, \beta^2=0}. \quad (5.13)$$

In this form, writing down a current is a straightforward algorithmic procedure, assuming the relevant amplitudes are known.

5.3 The Two-Loop Five-Point Current

We will illustrate our derivation method by re-deriving the one-loop five-point single-minus current $\tau_{5:1}^{(1)}(\alpha^-, \beta^+, a^+, b^+, c^+)$, used in the calculation of the two-loop all-plus amplitude [52].

To match the notation used in that original derivation, the off-shell legs $\{\alpha, \beta\}$ are chosen such that $\alpha + \beta = d + e$. Therefore the poles of interest to augmented recursion are those in $\langle de \rangle$ in this example, which will become relevant when simplifying the result.

5.3.1 Previous result

The current in question was previously presented in [52], following significant algebra, as

$$\begin{aligned}
 \tau_{5:1}^{(1)}(\alpha^-, \beta^+, a^+, b^+, c^+) = & \\
 & \mathcal{F}_{dp} \left[1 + s_{\alpha\beta} \left(\frac{[qc]}{[ac][qP_{\alpha\beta}|a]} + \frac{[a|q|b]}{[q|P_{\alpha\beta}|q][a|c|b]} + \frac{[c|q|b]}{[q|P_{\alpha\beta}|q][c|a|b]} \right) \right] \\
 & + \frac{i}{3} \frac{\langle \alpha q \rangle^2}{\langle ab \rangle^2} \frac{\langle \alpha q \rangle^2}{\langle \beta q \rangle^2} \left[\frac{\langle da \rangle [a|\beta|b]}{\langle bc \rangle \langle cd \rangle} + \frac{\langle ac \rangle [bc]}{\langle bc \rangle^2} \left(\frac{[q|P_{\alpha\beta}|b]^3 \langle qa \rangle \langle qd \rangle [q|\alpha|q]}{[q|P_{\alpha\beta}|q]^3 \langle da \rangle [q|P_{\alpha\beta}|a]} \right. \right. \\
 & \left. \left. - 3 \frac{\langle qb \rangle [q|P_{\alpha\beta}|b]^2 [q|\beta|q]}{[q|P_{\alpha\beta}|q]^2 [q|P_{\alpha\beta}|a]} \right) \right] \\
 & + \mathcal{F}_{sb} + \frac{i}{3} \frac{1}{\langle ab \rangle^2} \left(-\frac{[\beta c]^2 [qc]}{[c\alpha][\alpha q]} + [c|q|\alpha] \frac{([c\beta][\beta q][kq] + [\beta q]^2 [ck])}{[\alpha q][kq] 2k \cdot q} \right), \quad (5.14)
 \end{aligned}$$

where $k = P_{\alpha\beta} = \alpha + \beta$. The pieces written as

$$\mathcal{F}_{dp} = \frac{i}{3} \frac{\langle \alpha q \rangle^2 \langle q|\alpha\beta|q \rangle}{\langle \beta q \rangle^2} \frac{\langle ca \rangle [ac]^3}{s_{\alpha\beta} \langle ab \rangle \langle bc \rangle [c|P_{\alpha\beta}|q][a|P_{\alpha\beta}|q]} \quad (5.15)$$

and

$$\mathcal{F}_{sb} = -\frac{i}{3} \frac{\langle \alpha k \rangle [\beta q]^2}{[\alpha q][kq]} \frac{1}{s_{\alpha\beta}} \frac{[ck]^2}{\langle ab \rangle^2} \quad (5.16)$$

come from leading pole factorisations in that derivation and will also appear in our new derivation.

5.3.2 New derivation

Following the steps outlined earlier, we first write down the appropriate amplitude,

$$A_{5:1}^{(1)}(\alpha^-, \beta^+, a^+, b^+, c^+) = \frac{i}{3} \frac{1}{\langle ab \rangle^2} \left[-\frac{[\beta c]^3}{[\alpha\beta][c\alpha]} + \frac{\langle \alpha b \rangle^3 \langle ac \rangle [bc]}{\langle \alpha\beta \rangle \langle \beta a \rangle \langle bc \rangle^2} + \frac{\langle \alpha a \rangle^3 [a\beta] \langle b\beta \rangle}{\langle \alpha c \rangle \langle bc \rangle \langle a\beta \rangle^2} \right]. \quad (5.17)$$

This contains no $s_{\alpha\beta}$, so can be included in the current as it is, therefore satisfying C2 without affecting C1.

Now consider the leading $s_{\alpha\beta}$ poles when $\alpha^2, \beta^2 \neq 0$. These are given in full by the factorisations involving an $s_{\alpha\beta}$ propagator. Labelling according to the previous scheme,

5 Currents and their Integration

the factorisations we find are

$$\begin{aligned}\mathcal{F}_{dp} &= A_{3,q}^{(0)}(\alpha^+, -k_{\alpha\beta}^+, \beta^-) \frac{i}{s_{\alpha\beta}} A_4^{(1)}(k_{\alpha\beta}^-, a^+, b^+, c^+), \\ \mathcal{F}_{sb} &= A_{3,q}^{(0)}(\alpha^+, -k_{\alpha\beta}^-, \beta^-) \frac{i}{s_{\alpha\beta}} A_4^{(1)}(k_{\alpha\beta}^+, a^+, b^+, c^+),\end{aligned}\quad (5.18)$$

which differ only by the helicity assignment on the propagator. No further $s_{\alpha\beta}$ pole factorisations can be found.

Subtract the piece with $s_{\alpha\beta}$ replaced by $\langle\alpha\beta\rangle[\alpha\beta]$ to obtain the $\mathcal{O}(\alpha^2, \beta^2)$ contribution. Explicitly,

$$\begin{aligned}\tau_{5:1}^{(1)}|_{\mathcal{O}(\alpha^2, \beta^2)} &= \frac{i}{3} \frac{\langle\alpha q\rangle^2}{\langle\beta q\rangle^2} \langle q|\alpha\beta|q\rangle \left(\frac{1}{s_{\alpha\beta}} - \frac{1}{\langle\alpha\beta\rangle[\beta\alpha]} \right) \frac{\langle ca\rangle [ac]^3}{\langle ab\rangle \langle bc\rangle [c|P_{\alpha\beta}|q][a|P_{\alpha\beta}|q]} \\ &\quad - \frac{i}{3} \frac{\langle\alpha k\rangle [\beta q]^2}{[\alpha q][kq]} \left(\frac{1}{s_{\alpha\beta}} - \frac{1}{\langle\alpha\beta\rangle[\beta\alpha]} \right) \frac{[ck]^2}{\langle ab\rangle^2}.\end{aligned}\quad (5.19)$$

Hence, the total current is

$$\tau_{5:1}^{(1)}(\alpha^-, \beta^+, a^+, b^+, c^+) = A_{5:1}^{(1)} + (\mathcal{F}_{dp} + \mathcal{F}_{sb}) \left(1 - \frac{s_{\alpha\beta}}{\langle\alpha\beta\rangle[\beta\alpha]} \right), \quad (5.20)$$

or, in full,

$$\begin{aligned}\tau_{5:1}^{(1)}(\alpha^-, \beta^+, a^+, b^+, c^+) &= \frac{i}{3} \frac{1}{\langle ab\rangle^2} \left[-\frac{[\beta c]^3}{[\alpha\beta][c\alpha]} + \frac{\langle\alpha b\rangle^3 \langle ac\rangle [bc]}{\langle\alpha\beta\rangle \langle\beta a\rangle \langle bc\rangle^2} + \frac{\langle\alpha a\rangle^3 [a\beta] \langle b\beta\rangle}{\langle\alpha c\rangle \langle bc\rangle \langle a\beta\rangle^2} \right] \\ &\quad + \frac{i}{3} \frac{\langle\alpha q\rangle^2}{\langle\beta q\rangle^2} \langle q|\alpha\beta|q\rangle \left(\frac{1}{s_{\alpha\beta}} - \frac{1}{\langle\alpha\beta\rangle[\beta\alpha]} \right) \frac{\langle ca\rangle [ac]^3}{\langle ab\rangle \langle bc\rangle [c|P_{\alpha\beta}|q][a|P_{\alpha\beta}|q]} \\ &\quad - \frac{i}{3} \frac{\langle\alpha k\rangle [\beta q]^2}{[\alpha q][kq]} \left(\frac{1}{s_{\alpha\beta}} - \frac{1}{\langle\alpha\beta\rangle[\beta\alpha]} \right) \frac{[ck]^2}{\langle ab\rangle^2}.\end{aligned}\quad (5.21)$$

Note that some manipulations are needed before this current can be integrated, so we have not avoided all the non-trivial steps of the earlier derivation. However, our method follows a straightforward logic, which streamlines the derivation and makes errors less likely to occur.

5.3.3 Checks with simplifying reference momentum

The current we have derived does not match the exact form of the previous result. This is not unexpected, as the ‘‘good enough’’ current is defined up to some $\mathcal{O}(\alpha^2, \beta^2)$ piece

that does not contribute to the recursion process. Therefore to validate our derivation process, we should perform manipulations to explicitly confirm that our current is the same as the previous derivation to $\mathcal{O}(\alpha^2, \beta^2)$. Some of these steps relate to the process of preparing the current for integration, although others are added complexity that our new method avoids.

As a first test, we choose a convenient reference momentum, $q = \lambda_b \tilde{\lambda}_c$, that we expect to lead to significant simplification. The old current reduces to

$$\begin{aligned} \tau_{5:1}^{(1),old} = & \mathcal{F}_{dp} + \frac{i}{3} \frac{1}{\langle ab \rangle^2} \frac{\langle \alpha b \rangle^2}{\langle \beta b \rangle^2} \frac{\langle bd \rangle \langle ac \rangle [c|\alpha|b]}{\langle da \rangle \langle bc \rangle^2} \\ & + \frac{i}{3} \frac{1}{\langle ab \rangle^2} \frac{\langle \alpha b \rangle^2}{\langle \beta b \rangle^2} \frac{\langle da \rangle [a|\beta|b]}{\langle bc \rangle \langle cd \rangle} + \mathcal{F}_{sb}. \end{aligned} \quad (5.22)$$

The new current becomes

$$\begin{aligned} \tau_{5:1}^{(1),new} = & \frac{i}{3} \frac{1}{\langle ab \rangle^2} \frac{\langle \alpha b \rangle^3}{\langle \beta b \rangle \langle \beta a \rangle \langle bc \rangle^2} \frac{[\alpha c] \langle ac \rangle}{\langle \beta a \rangle} \\ & + \frac{i}{3} \frac{1}{\langle ab \rangle^2} \frac{\langle \alpha a \rangle^3}{\langle \alpha c \rangle \langle bc \rangle \langle a \beta \rangle^2} \frac{[a \beta] \langle b \beta \rangle}{\langle a \beta \rangle^2} + \mathcal{F}_{dp} + \mathcal{F}_{sb}. \end{aligned} \quad (5.23)$$

Terms 1 and 7 in eq. 5.21 cancel to give no $1/[\alpha \beta]$ piece in eq. 5.23. Terms 2 and 5 in eq. 5.21 combine to form term 1 in eq. 5.23 and no $1/\langle \alpha \beta \rangle$ piece.

To prepare $\tau_{5:1}^{(1),new}$ for integration:

- Multiply term 1 by $\langle \beta b \rangle \langle \alpha a \rangle$ top and bottom.
- Apply a Schouten identity to $\langle \beta b \rangle \langle \alpha a \rangle$ in the numerator, discarding the $\mathcal{O}(\langle \alpha \beta \rangle)$ piece.
- Multiply term 2 by $\langle \beta b \rangle^2$ top and bottom.
- Apply a Schouten identity to $\langle \beta b \rangle^2 \langle \alpha a \rangle^2$ in the numerator, discarding the $\mathcal{O}(\langle \alpha \beta \rangle)$ pieces.
- Apply the approximation

$$\frac{\langle X \alpha \rangle}{\langle Y \alpha \rangle} = \frac{\langle X \alpha \rangle \langle Y d \rangle}{\langle Y \alpha \rangle \langle Y d \rangle} = \frac{\langle X d \rangle}{\langle Y d \rangle} + \mathcal{O}(\langle \alpha d \rangle). \quad (5.24)$$

- Discard pieces of $\mathcal{O}(\langle \alpha d \rangle)$. (These factors will integrate to $\langle de \rangle$. In the derivation of ref. [52], it is $\langle de \rangle$ poles that are the target of recursion, which we copy here

5 Currents and their Integration

for the comparison. Therefore $\mathcal{O}(\langle d\epsilon \rangle)$ terms do not give contributions and can be discarded from the “good enough” current.)

Following these steps, we obtain an identical expression to $\tau_{5:1}^{(1),old}$, demonstrating the required agreement for a specific choice of reference momentum.

5.3.4 Checks with a general reference momentum

Following the success with a specific reference momentum, we complete the comparison by considering a general reference momentum. Again, consider the newly derived current in eq. 5.21. This should match the older version in eq. 5.14 (once manipulations to prepare for integration have been carried out).

Terms 4 and 6 in eq. 5.21 are already in a matching form, being \mathcal{F}_{dp} and \mathcal{F}_{sb} . We now group terms in the new current by their $1/\langle\alpha\beta\rangle$ or $1/[\alpha\beta]$ structures. It should be possible to remove these factors by manipulation to obtain the form of the old current.

Piece with $1/[\alpha\beta]$ factor

The new current contains the terms

$$\mathcal{P}^{sb} = \mathcal{P}_1^{sb} + \mathcal{P}_2^{sb} \equiv -\frac{i}{3\langle ab \rangle^2} \frac{[\beta c]^3}{[\alpha\beta][c\alpha]} + \frac{i}{3\langle ab \rangle^2} \frac{\langle\alpha k\rangle[\beta q]^2}{[\alpha q][kq]} \frac{[ck]^2}{\langle\alpha\beta\rangle[\beta\alpha]}. \quad (5.25)$$

Expand the first of these using

$$\begin{aligned} \mathcal{P}_1^{sb} &= -\frac{i}{3\langle ab \rangle^2} \frac{[\beta c]^2}{[\alpha\beta][c\alpha][\alpha q]} [\alpha q][\beta c] \\ &= -\frac{i}{3\langle ab \rangle^2} \frac{[\beta c]^2[qc]}{[c\alpha][\alpha q]} - \frac{i}{3\langle ab \rangle^2} \frac{[\beta c]^2[q\beta]}{[\alpha\beta][\alpha q]} \equiv \mathcal{P}_{1a}^{sb} + \mathcal{P}_{1b}^{sb}, \end{aligned} \quad (5.26)$$

where we recognise \mathcal{P}_{1a}^{sb} as term 9 in the old current. The remaining terms now combine,

$$\begin{aligned}
 \mathcal{P}_{1b}^{sb} + \mathcal{P}_2^{sb} &= \frac{i}{3 \langle ab \rangle^2} \left(-\frac{[\beta c]^2 [q \beta]}{[\alpha \beta] [\alpha q]} + \frac{\langle k \alpha \rangle [\beta q]^2 [ck]^2}{[\alpha q] [k q] \langle \alpha \beta \rangle [\alpha \beta]} \right) \\
 &= \frac{i}{3 \langle ab \rangle^2} \frac{1}{[\alpha q] [\alpha \beta]} \left(-[\beta c]^2 [q \beta] - \frac{[\beta q]^3 [ck]^2}{[k q]^2} \right) \\
 &= \frac{i}{3 \langle ab \rangle^2} \frac{\langle k q \rangle [\beta q]}{[k q] [q|k|q] [\alpha q] [\alpha \beta]} (-[k q]^2 [\beta c]^2 + [\beta q]^2 [ck]^2) \\
 &= \frac{i}{3 \langle ab \rangle^2} \frac{\langle k q \rangle [\beta q]}{[k q] [\alpha q] [\alpha \beta] 2k \cdot q} ([k q] [c \beta] + [\beta q] [ck]) (-[k q] [c \beta] + [\beta q] [ck]) \\
 &= \frac{i}{3 \langle ab \rangle^2} \frac{\langle k q \rangle [\beta q] [\beta k] [cq]}{[k q] [\alpha q] [\alpha \beta] 2k \cdot q} ([k q] [c \beta] + [\beta q] [ck]) \\
 &= \frac{i}{3 \langle ab \rangle^2} \frac{[\beta \alpha | q] [cq]}{[\alpha q] [k q] [\alpha \beta] 2k \cdot q} ([c \beta] [\beta q] [k q] + [\beta q]^2 [ck]) \\
 &= \frac{i}{3 \langle ab \rangle^2} [c|q|\alpha] \frac{([c \beta] [\beta q] [k q] + [\beta q]^2 [ck])}{[\alpha q] [k q] 2k \cdot q}, \tag{5.27}
 \end{aligned}$$

yielding term 10 in the old current.

Piece with $1/\langle \alpha \beta \rangle$ factor

The new current contains the terms

$$\begin{aligned}
 \mathcal{P}^{ab} = \mathcal{P}_1^{ab} + \mathcal{P}_2^{ab} &\equiv \frac{i}{3} \frac{1}{\langle ab \rangle^2} \frac{\langle \alpha b \rangle^3 \langle ac \rangle [bc]}{\langle \alpha \beta \rangle \langle \beta a \rangle \langle bc \rangle^2} \\
 &\quad - \frac{i}{3} \frac{\langle \alpha q \rangle^2}{\langle \beta q \rangle^2} \langle q|\alpha\beta|q \rangle \left(\frac{1}{\langle \alpha \beta \rangle [\beta \alpha]} \right) \frac{\langle ca \rangle [ac]^3}{\langle ab \rangle \langle bc \rangle [c|P_{\alpha\beta}|q] [a|P_{\alpha\beta}|q]}. \tag{5.28}
 \end{aligned}$$

To begin, consider \mathcal{P}_1^{ab} and apply the identity

$$\frac{1}{\langle \alpha \beta \rangle \langle \beta a \rangle} = \frac{1}{\langle \alpha q \rangle \langle \beta q \rangle^2} \left(\frac{\langle q|\alpha\beta|q \rangle [q|P_{\alpha\beta}|q]}{\langle \alpha \beta \rangle [\beta \alpha] [q|P_{\alpha\beta}|a]} + \frac{\langle q \beta \rangle \langle qa \rangle [q|\alpha|q]}{\langle \beta a \rangle [q|P_{\alpha\beta}|a]} \right) \tag{5.29}$$

to obtain

$$\mathcal{P}_1^{ab} = \frac{i}{3} \frac{1}{\langle ab \rangle^2} \frac{\langle ac \rangle [bc] \langle \alpha q \rangle^2 \langle \alpha b \rangle^3}{\langle bc \rangle^2 \langle \beta q \rangle^2 \langle \alpha q \rangle^3} \left(\frac{\langle q|\alpha\beta|q \rangle [q|P_{\alpha\beta}|q]}{\langle \alpha \beta \rangle [\beta \alpha] [q|P_{\alpha\beta}|a]} + \frac{\langle q \beta \rangle \langle qa \rangle [q|\alpha|q]}{\langle \beta a \rangle [q|P_{\alpha\beta}|a]} \right). \tag{5.30}$$

5 Currents and their Integration

We can expand the factor $\langle \alpha b \rangle / \langle \alpha q \rangle$ to remove unwanted spinor α as follows:

$$\begin{aligned}
\frac{\langle \alpha b \rangle}{\langle \alpha q \rangle} &= \frac{[\beta \alpha] \langle \alpha b \rangle}{[\beta \alpha] \langle \alpha q \rangle} = \frac{[\beta | \alpha^b | b]}{[\beta | \alpha | q]} = \frac{[\beta | \alpha^b + \beta^b | b]}{[\beta | P_{\alpha\beta} | q]} \\
&= \frac{[\beta | \alpha^b + \beta^b | b] [q | P_{\alpha\beta} | q]}{[\beta | P_{\alpha\beta} | q] [q | P_{\alpha\beta} | q]} = \frac{[\beta | \alpha^b + \beta^b | b] [q | \alpha^b + \beta^b | q]}{[\beta | P_{\alpha\beta} | q] [q | P_{\alpha\beta} | q]} \\
&= \frac{[q | P_{\alpha\beta} | b] [\beta | P_{\alpha\beta} | q] + (\alpha^b + \beta^b)^2 \langle q b \rangle [\beta q]}{[\beta | P_{\alpha\beta} | q] [q | P_{\alpha\beta} | q]} \\
&= \frac{[q | P_{\alpha\beta} | b]}{[q | P_{\alpha\beta} | q]} + \frac{\langle \alpha \beta \rangle [\beta \alpha] \langle q b \rangle [\beta q]}{[\beta | P_{\alpha\beta} | q] [q | P_{\alpha\beta} | q]}, \tag{5.31}
\end{aligned}$$

where we have used a Schouten identity and been careful with $\alpha^b + \beta^b \neq P_{\alpha\beta}^b$ (specifically, $(\alpha^b + \beta^b)^2 = \langle \alpha \beta \rangle [\beta \alpha]$ vs. $(P_{\alpha\beta}^b)^2 = 0$). This factor appears cubed in \mathcal{P}_1^{ab} , but we can ignore pieces of $\mathcal{O}(\langle \alpha \beta \rangle)$ which will not contribute when we eventually take residues. The terms of interest are

$$\begin{aligned}
\mathcal{P}_1^{ab} &= \frac{i}{3} \frac{1}{\langle a b \rangle^2} \frac{\langle a c \rangle [b c]}{\langle b c \rangle^2} \frac{\langle \alpha q \rangle^2 [q | P_{\alpha\beta} | b]^3}{\langle \beta q \rangle^2 [q | P_{\alpha\beta} | q]^3} \left(\frac{\langle q | \alpha \beta | q \rangle [q | P_{\alpha\beta} | q]}{\langle \alpha \beta \rangle [\beta \alpha] [q | P_{\alpha\beta} | a]} + \frac{\langle q \beta \rangle \langle q a \rangle [q | \alpha | q]}{\langle \beta a \rangle [q | P_{\alpha\beta} | a]} \right) \\
&\quad + \frac{i}{3} \frac{1}{\langle a b \rangle^2} \frac{\langle a c \rangle [b c]}{\langle b c \rangle^2} \frac{\langle \alpha q \rangle^2 [q | P_{\alpha\beta} | b]^2}{\langle \beta q \rangle^2 [q | P_{\alpha\beta} | q]^2} \left(3 \frac{\langle q b \rangle [\beta q] \langle q | \alpha \beta | q \rangle}{[\beta | P_{\alpha\beta} | q] [q | P_{\alpha\beta} | a]} \right) + \mathcal{O}(\langle \alpha \beta \rangle) \\
&\equiv \mathcal{P}_{1a}^{ab} + \mathcal{P}_{1b}^{ab} + \mathcal{P}_{1c}^{ab} + \mathcal{O}(\langle \alpha \beta \rangle). \tag{5.32}
\end{aligned}$$

We can immediately see that

$$\mathcal{P}_{1b}^{ab} = \frac{i}{3} \frac{1}{\langle a b \rangle^2} \frac{\langle \alpha q \rangle^2 \langle a c \rangle [b c]}{\langle \beta q \rangle^2 \langle b c \rangle^2} \left(\frac{[q | P_{\alpha\beta} | b]^3 \langle q d \rangle \langle q a \rangle [q | \alpha | q]}{[q | P_{\alpha\beta} | q]^3 \langle d a \rangle [q | P_{\alpha\beta} | a]} \right) + \mathcal{O}(\langle \beta d \rangle), \tag{5.33}$$

which gives term 6 in the old current. It is also trivial to rewrite

$$\begin{aligned}
\mathcal{P}_{1c}^{ab} &= \frac{i}{3} \frac{1}{\langle a b \rangle^2} \frac{\langle a c \rangle [b c]}{\langle b c \rangle^2} \frac{\langle \alpha q \rangle^2 [q | P_{\alpha\beta} | b]^2}{\langle \beta q \rangle^2 [q | P_{\alpha\beta} | q]^2} \left(3 \frac{\langle q b \rangle [\beta q] \langle q | \alpha \beta | q \rangle}{[\beta | \alpha | q] [q | P_{\alpha\beta} | a]} \right) \\
&= \frac{i}{3} \frac{1}{\langle a b \rangle^2} \frac{\langle \alpha q \rangle^2 \langle a c \rangle [b c]}{\langle \beta q \rangle^2 \langle b c \rangle^2} \left(-3 \frac{[q | P_{\alpha\beta} | b]^2 \langle q b \rangle [q | \beta | q]}{[q | P_{\alpha\beta} | q]^2 [q | P_{\alpha\beta} | a]} \right), \tag{5.34}
\end{aligned}$$

which is term 7 in the old current.

Further expanding \mathcal{P}_{1a}^{ab} with its unwanted denominator, using

$$[b c] [q | P_{\alpha\beta} | b] = [q | P_{\alpha\beta} b | c] = -[q | P_{\alpha\beta} (a + c + P_{\alpha\beta}) | c] = -[a c] [q | P_{\alpha\beta} | a] - s_{\alpha\beta} [q c], \tag{5.35}$$

leads to

$$\begin{aligned}
 \mathcal{P}_{1a}^{ab} &= \frac{i}{3} \frac{1}{\langle ab \rangle^2} \frac{\langle \alpha q \rangle^2}{\langle \beta q \rangle^2} \frac{\langle q | \alpha \beta | q \rangle}{\langle \alpha \beta \rangle [\beta \alpha]} \frac{\langle ac \rangle [bc]}{\langle bc \rangle^2} \frac{[q P_{\alpha\beta} | b]^3}{[q P_{\alpha\beta} | q]^2 [q P_{\alpha\beta} | a]} \\
 &= \frac{i}{3} \frac{\langle \alpha q \rangle^2}{\langle \beta q \rangle^2} \frac{\langle q | \alpha \beta | q \rangle}{\langle \alpha \beta \rangle [\beta \alpha]} \frac{\langle ca \rangle}{\langle ab \rangle \langle bc \rangle} \\
 &\quad \times \left(\frac{[ac] [q P_{\alpha\beta} | b]^2}{\langle ab \rangle \langle bc \rangle [q P_{\alpha\beta} | q]^2} + s_{\alpha\beta} \frac{[qc] [q P_{\alpha\beta} | b]^2}{\langle ab \rangle \langle bc \rangle [q P_{\alpha\beta} | q]^2 [q P_{\alpha\beta} | a]} \right) \\
 &= \frac{i}{3} \frac{\langle \alpha q \rangle^2}{\langle \beta q \rangle^2} \frac{\langle q | \alpha \beta | q \rangle}{\langle \alpha \beta \rangle [\beta \alpha]} \frac{\langle ca \rangle}{\langle ab \rangle \langle bc \rangle} \\
 &\quad \times \frac{[ac]^2}{[ac]^2} \left(\frac{[ac] [q P_{\alpha\beta} | b]^2}{\langle ab \rangle \langle bc \rangle [q P_{\alpha\beta} | q]^2} + s_{\alpha\beta} \frac{[qc] [q P_{\alpha\beta} | b]^2}{\langle ab \rangle \langle bc \rangle [q P_{\alpha\beta} | q]^2 [q P_{\alpha\beta} | a]} \right) \\
 &= \frac{i}{3} \frac{\langle \alpha q \rangle^2}{\langle \beta q \rangle^2} \frac{\langle q | \alpha \beta | q \rangle}{\langle \alpha \beta \rangle [\beta \alpha]} \frac{\langle ca \rangle}{\langle ab \rangle \langle bc \rangle} \\
 &\quad \times \left(\frac{[ac]^3 [q P_{\alpha\beta} | b]^2}{[a P_{\alpha\beta} | b] [c P_{\alpha\beta} | b] [q P_{\alpha\beta} | q]^2} + s_{\alpha\beta} \frac{[ac]^2 [qc] [q P_{\alpha\beta} | b]^2}{[a P_{\alpha\beta} | b] [c P_{\alpha\beta} | b] [q P_{\alpha\beta} | q]^2 [q P_{\alpha\beta} | a]} \right). \tag{5.36}
 \end{aligned}$$

Multiply numerator and denominator by $[a P_{\alpha\beta} | q] [c P_{\alpha\beta} | q]$, then use the Schouten identities

$$\begin{aligned}
 [a P_{\alpha\beta} | q] [q P_{\alpha\beta} | b] &= [q P_{\alpha\beta} | q] [a P_{\alpha\beta} | b] + s_{\alpha\beta} [qa] \langle qb \rangle, \\
 [c P_{\alpha\beta} | q] [q P_{\alpha\beta} | b] &= [q P_{\alpha\beta} | q] [c P_{\alpha\beta} | b] + s_{\alpha\beta} [qc] \langle qb \rangle, \tag{5.37}
 \end{aligned}$$

to reach the form

$$\begin{aligned}
 \mathcal{P}_{1a}^{ab} &= \frac{i}{3} \frac{\langle \alpha q \rangle^2}{\langle \beta q \rangle^2} \frac{\langle q | \alpha \beta | q \rangle}{\langle \alpha \beta \rangle [\beta \alpha]} \frac{\langle ca \rangle [ac]^3}{\langle ab \rangle \langle bc \rangle} \frac{1}{[a P_{\alpha\beta} | q] [c P_{\alpha\beta} | q]} \\
 &\quad \times \left[1 + s_{\alpha\beta} \left(\frac{[qc]}{[ac] [q P_{\alpha\beta} | a]} + \frac{[a|qb]}{[q P_{\alpha\beta} | q] [a|c|b]} + \frac{[c|qb]}{[q P_{\alpha\beta} | q] [c|a|b]} \right) + \mathcal{O}(s_{\alpha\beta}^2) \right], \tag{5.38}
 \end{aligned}$$

where the $\mathcal{O}(s_{\alpha\beta}^2)$ terms will not contribute to the eventual $\langle de \rangle$ poles.

5 Currents and their Integration

Notice that the first term here cancels \mathcal{P}_2^{ab} . The remaining three can be written

$$\begin{aligned}
\mathcal{P}_{1a}^{ab} + \mathcal{P}_2^{ab} &= \mathcal{F}_{dp} \frac{s_{\alpha\beta}}{\langle \alpha \beta \rangle [\beta \alpha]} \\
&\times \left[s_{\alpha\beta} \left(\frac{[q c]}{[a c] [q | P_{\alpha\beta} | a]} + \frac{[a | q | b]}{[q | P_{\alpha\beta} | q] [a | c | b]} + \frac{[c | q | b]}{[q | P_{\alpha\beta} | q] [c | a | b]} \right) + \mathcal{O}(s_{\alpha\beta}^2) \right] \\
&= \mathcal{F}_{dp} (1 + \mathcal{O}(\alpha^2 s_{\alpha\beta}, \beta^2 s_{\alpha\beta})) \\
&\times \left[s_{\alpha\beta} \left(\frac{[q c]}{[a c] [q | P_{\alpha\beta} | a]} + \frac{[a | q | b]}{[q | P_{\alpha\beta} | q] [a | c | b]} + \frac{[c | q | b]}{[q | P_{\alpha\beta} | q] [c | a | b]} \right) + \mathcal{O}(s_{\alpha\beta}^2) \right] \\
&= \mathcal{F}_{dp} \left[s_{\alpha\beta} \left(\frac{[q c]}{[a c] [q | P_{\alpha\beta} | a]} + \frac{[a | q | b]}{[q | P_{\alpha\beta} | q] [a | c | b]} + \frac{[c | q | b]}{[q | P_{\alpha\beta} | q] [c | a | b]} \right) \right] \\
&\quad + \mathcal{O}(s_{\alpha\beta}, \alpha^2 s_{\alpha\beta}, \beta^2 s_{\alpha\beta}), \tag{5.39}
\end{aligned}$$

where we have obtained terms 2, 3 and 4 in the old current. The pieces of $\mathcal{O}(\alpha^2 s_{\alpha\beta}, \beta^2 s_{\alpha\beta})$ do not contribute to either the leading pole, or when $\alpha^2, \beta^2 = 0$, so can be discarded.

Piece without $1/[\alpha\beta]$ or $1/[\alpha\beta]$ factor

The new current contains the term

$$\mathcal{P}^{w/o} \equiv \frac{i}{3} \frac{1}{\langle a b \rangle^2} \frac{\langle \alpha a \rangle^3 [a \beta] \langle b \beta \rangle}{\langle \alpha c \rangle \langle b c \rangle \langle a \beta \rangle^2}. \tag{5.40}$$

Using the same methods as in the specific q case, we have

$$\begin{aligned}
\mathcal{P}^{w/o} &= \frac{i}{3} \frac{1}{\langle a b \rangle^2} \frac{\langle \beta q \rangle^2 \langle \alpha a \rangle^3 [a \beta] \langle b \beta \rangle}{\langle \beta q \rangle^2 \langle \alpha c \rangle \langle b c \rangle \langle a \beta \rangle^2} \\
&= \frac{i}{3} \frac{1}{\langle a b \rangle^2} \frac{(\langle \beta a \rangle \langle \alpha q \rangle + \langle a q \rangle \langle \alpha \beta \rangle)^2 \langle \alpha a \rangle [a \beta] \langle b \beta \rangle}{\langle \beta q \rangle^2 \langle \alpha c \rangle \langle b c \rangle \langle a \beta \rangle^2} \\
&= \frac{i}{3} \frac{1}{\langle a b \rangle^2} \frac{\langle \alpha q \rangle^2 \langle \alpha a \rangle [a | \beta | b]}{\langle \beta q \rangle^2 \langle b c \rangle \langle c \alpha \rangle} + \mathcal{O}(\langle \alpha \beta \rangle) \\
&= \frac{i}{3} \frac{1}{\langle a b \rangle^2} \frac{\langle \alpha q \rangle^2 \langle d a \rangle [a | \beta | b]}{\langle \beta q \rangle^2 \langle b c \rangle \langle c d \rangle} + \mathcal{O}(\langle \alpha \beta \rangle) + \mathcal{O}(\langle \alpha d \rangle), \tag{5.41}
\end{aligned}$$

which gives us term 5 in the old current.

This completes the demonstration that the new current-derivation method reproduces the version derived in [52]. We have shown that our new method is valid, and allows currents to be derived rapidly in an intuitive way.

5.4 The Two-Loop Seven-Point Currents

We derive the new currents required for the augmented recursion step of the seven-point two-loop amplitude derivation. These were used during the procedure of Chapter 4.

Our derivation is in full colour, so the augmented recursion diagrams must be dressed with colour to obtain the various contributions to each seven-point colour structure. The colour-dressed current contains “partial currents” associated with each possible trace structure that occurs at one loop, denoted by $\tau_{7;\lambda}^{(1)}$ in an analogous way to the colour decomposition of an amplitude. There are also two allowed helicity layouts represented on the diagram, which must both be taken into account. In total, all currents of the following forms appear:

$$\begin{aligned}
 &\tau_{7;\lambda}^{(1)}(\cdots, \alpha^-, \cdots, \beta^+, \cdots), \\
 &\tau_{7;\lambda}^{(1)}(\cdots, \alpha^+, \cdots, \beta^-, \cdots), \\
 &\tau_{7;\lambda}^{(1)}(\cdots, \beta^-, \cdots, \alpha^+, \cdots), \\
 &\tau_{7;\lambda}^{(1)}(\cdots, \beta^+, \cdots, \alpha^-, \cdots),
 \end{aligned} \tag{5.42}$$

for $\lambda = \{1, 2, 3, 4\}$. Out of the structures listed, only the current with adjacent off-shell legs, $\tau_{7;1}^{(1)}(\alpha^-, \beta^+, c^+, d^+, e^+, f^+, g^+)$, has been previously derived. This was done as part of the derivation of the leading in colour partial amplitude $A_{7;1}^{(2)}$ in ref. [60], for which this was the only required current.

The other currents are new. We can reduce the number that must be determined to a smaller set by exploiting symmetries. Because currents are colour decomposed in the same way as amplitudes, decoupling identities exist between partial currents, and the arguments of each colour structure obey the same sets of cyclic and flip symmetries as the arguments of an amplitude.

First, the one-loop seven-point decoupling identities can be used to express all sub-leading in colour partial currents $\tau_{7;2}^{(1)}$, $\tau_{7;3}^{(1)}$, $\tau_{7;4}^{(1)}$ in terms of the leading in colour structure $\tau_{7;1}^{(1)}$. An elegant expression for this relation was presented in ref. [7], which for our situation is written as

$$\tau_{n;r}^{(1)}(1, \cdots, r-1; r, \cdots, n) = (-1)^{r+1} \sum_{\sigma \in COP\{\alpha\}\{\beta\}} \tau_{n;1}^{(1)}(\sigma), \tag{5.43}$$

where $\alpha = \{r-1, \cdots, 1\}$, $\beta = \{r, \cdots, n\}$ and the function $COP\{\alpha\}\{\beta\}$ provides all permutations of $\{1, 2, \cdots, n\}$ for which n is fixed, and the cyclic orderings of the sets

5 Currents and their Integration

α and β are preserved.

The resulting set, now containing only leading in colour partial amplitudes, has a large range of leg arrangements. The flip symmetry of the arguments

$$\tau_{7:1}^{(1)}(a, b, c, d, e, f, g) = -\tau_{7:1}^{(1)}(g, f, e, d, c, b, a) \quad (5.44)$$

allows the momentum α to be placed before β . We can also make use of the $\mathcal{P}_{7:1}$ symmetry in the momenta,

$$\tau_{7:1}^{(1)}(a, b, c, d, e, f, g) = \tau_{7:1}^{(1)}(b, c, d, e, f, g, a) = \cdots = \tau_{7:1}^{(1)}(g, a, b, c, d, e, f), \quad (5.45)$$

to bring α to the first position. The set of currents now contains only six different structures, up to an unimportant relabelling of the on-shell legs. These are

$$\begin{aligned} &\tau_{7:1}^{(1)}(\alpha^-, \beta^+, c^+, d^+, e^+, f^+, g^+), \tau_{7:1}^{(1)}(\alpha^+, \beta^-, c^+, d^+, e^+, f^+, g^+), \\ &\tau_{7:1}^{(1)}(\alpha^-, c^+, \beta^+, d^+, e^+, f^+, g^+), \tau_{7:1}^{(1)}(\alpha^+, c^+, \beta^-, d^+, e^+, f^+, g^+), \\ &\tau_{7:1}^{(1)}(\alpha^-, c^+, d^+, \beta^+, e^+, f^+, g^+), \tau_{7:1}^{(1)}(\alpha^+, c^+, d^+, \beta^-, e^+, f^+, g^+). \end{aligned} \quad (5.46)$$

A final insight is that the two different helicity assignments can also be related by a momentum relabelling. In this case, the reassignment affects the whole augmented recursion diagram. We exchange the α and β labels on the current, which must be matched by a relabelling of the α and β in the three-point amplitudes. A flip symmetry and rotation of the arguments allows the current to be placed in the standard (α^- first) arrangement. Therefore, if a particular helicity choice on an augmented recursion diagram integrates to give a contribution $F(a, b, c, d, e, f, g)$, then the contribution from the other helicity choice can be seen to be $-F(b, a, g, f, e, d, c)$.

We can continue by choosing a principal helicity arrangement for the current of $\{\alpha^-, \beta^+\}$. After integration, we account for the other helicity configuration by also including $F(a, b, c, d, e, f, g) \rightarrow -F(b, a, g, f, e, d, c)$ contributions.

Three independent currents remain as requirements for the augmented recursion procedure. Of these, one is the known current

$$\tau_{7:1}^{(1)}(\alpha^-, \beta^+, c^+, d^+, e^+, f^+, g^+). \quad (5.47)$$

The two new currents which must be derived are

$$\begin{aligned}\tau_7^{(1)}(\alpha^-, c^+, \beta^+, d^+, e^+, f^+, g^+), \\ \tau_7^{(1)}(\alpha^-, c^+, d^+, \beta^+, e^+, f^+, g^+).\end{aligned}\tag{5.48}$$

We see that the difference between these structures is the degree of separation between the two off-shell legs. Referencing this fact, we name the currents the ‘‘adjacent’’, ‘‘singly non-adjacent’’ and ‘‘doubly non-adjacent’’ currents, respectively.

5.4.1 The adjacent current

We re-derive the adjacent current $\tau_{7:1}^{(1)}(\alpha^-, \beta^+, c^+, d^+, e^+, f^+, g^+)$ as a check of our method and that of the previous derivation [60].

Following the procedure set out in Section 5.2.2, we identify the one-loop seven-point single-minus amplitude [37] as the basis for our current. Condition C2 is satisfied by

$$\tau_{7:1}^{(1)}(\alpha^-, \beta^+, c^+, d^+, e^+, f^+, g^+) = A_{7:1}^{(1)}(\alpha^-, \beta^+, c^+, d^+, e^+, f^+, g^+) + \mathcal{O}(\alpha^2, \beta^2).\tag{5.49}$$

We write down the leading $s_{\alpha\beta}$ poles for $\alpha^2, \beta^2 \neq 0$, which come from all the allowed factorisations involving an $s_{\alpha\beta}$ propagator. Labelling them for convenience,

$$\begin{aligned}\mathcal{F}_1 &= A_{3,q}^{(0)}(\alpha^-, \beta^+, -k_{\alpha\beta}^+) \frac{i}{s_{\alpha\beta}} A_6^{(1)}(k_{\alpha\beta}^-, c^+, d^+, e^+, f^+, g^+), \\ \mathcal{F}_2 &= A_{3,q}^{(0)}(\alpha^-, \beta^+, -k_{\alpha\beta}^-) \frac{i}{s_{\alpha\beta}} A_6^{(1)}(k_{\alpha\beta}^+, c^+, d^+, e^+, f^+, g^+),\end{aligned}\tag{5.50}$$

which differ by the helicity arrangement along the propagator. Subtracting the unwanted $\alpha^2, \beta^2 \rightarrow 0$ contribution, we satisfy C1. Therefore the total current can be written

$$\begin{aligned}\tau_{7:1}^{(1)}(\alpha^-, \beta^+, c^+, d^+, e^+, f^+, g^+) &= A_{7:1}^{(1)}(\alpha^-, \beta^+, c^+, d^+, e^+, f^+, g^+) \\ &\quad + (\mathcal{F}_1 + \mathcal{F}_2) \left(1 - \frac{s_{\alpha\beta}}{\langle \alpha \beta \rangle [\beta \alpha]} \right).\end{aligned}\tag{5.51}$$

Which (after integration) finds agreement with the previous result.

5.4.2 The singly non-adjacent current

We derive the singly non-adjacent current $\tau_7^{(1)}(\alpha^-, c^+, \beta^+, d^+, e^+, f^+, g^+)$ by following the procedure set out in Section 5.2.2.

The basis of the current is the seven-point amplitude, with the off-shell momenta inserted on non-adjacent legs, $A_{7;1}^{(1)}(\alpha^-, c^+, \beta^+, d^+, e^+, f^+, g^+)$, to satisfy C2. In a change from previous currents, we find that there are no factorisations involving $s_{\alpha\beta}$ poles. Should any propagator contain both α and β , we would expect it to also contain c due to the arrangement of the external legs. (Factorisations where the order of external legs does not match the desired current also cannot contribute, because their colour structures do not combine to give the correct overall structure.)

Therefore the full singly non-adjacent current can be written

$$\begin{aligned} \tau_7^{(1)}(\alpha^-, c^+, \beta^+, d^+, e^+, f^+, g^+) &= \hat{\tau}_7^{basis}(\alpha^-, c^+, \beta^+, d^+, e^+, f^+, g^+) \\ &\quad - \hat{\tau}_7^{basis}(\alpha^-, g^+, f^+, e^+, d^+, \beta^+, c^+), \end{aligned} \quad (5.52)$$

where we define

$$\begin{aligned} \hat{\tau}_7^{basis}(\alpha^-, c^+, \beta^+, d^+, e^+, f^+, g^+) &= \\ &\frac{i}{3} \left(- \frac{\langle \alpha | k_{c\beta} | d \rangle \langle \beta e \rangle \langle \alpha d \rangle^3}{\langle \beta d \rangle^2 \langle c \beta \rangle \langle d e \rangle^2 \langle e f \rangle \langle f g \rangle \langle g \alpha \rangle \langle \alpha c \rangle} \right. \\ &\quad + \frac{\langle \alpha | k_{ef} | g \rangle^3}{\langle d | k_{ef} | g \rangle \langle \beta d \rangle \langle c \beta \rangle \langle e f \rangle^2 \langle \alpha c \rangle t_{efg}} \\ &\quad - \frac{1}{2} \frac{\langle \alpha | k_{c\beta} k_{de} | \alpha \rangle^3}{\langle \alpha | k_{c\beta} k_{de} | f \rangle \langle \alpha | k_{fg} k_{de} | \beta \rangle \langle c \beta \rangle \langle d e \rangle^2 \langle f g \rangle \langle g \alpha \rangle \langle \alpha c \rangle} \\ &\quad - \frac{\langle c d \rangle \langle \alpha \beta \rangle^3 [c \beta]}{\langle \beta d \rangle^2 \langle c \beta \rangle^2 \langle d e \rangle \langle e f \rangle \langle f g \rangle \langle g \alpha \rangle} \\ &\quad + \frac{[c g]^3}{\langle \beta d \rangle \langle d e \rangle \langle e f \rangle [g \alpha] [\alpha c] t_{g\alpha c}} \left(\frac{1}{2} [\beta f] - \frac{[c | k_{\beta d} k_{ef} | g] s_{de}}{2 \langle \beta | k_{\alpha c} | g \rangle \langle f | k_{g\alpha} | c \rangle} + \frac{[f | k_{de} k_{ef} | g]}{\langle \beta | k_{\alpha c} | g \rangle} \right) \\ &\quad \left. + \frac{\langle \alpha | k_{c\beta} | g \rangle^3}{\langle \beta | k_{\alpha c} | g \rangle \langle c \beta \rangle \langle d e \rangle \langle e f \rangle \langle \alpha c \rangle t_{def} t_{\alpha\beta}} \left(\frac{\langle \alpha | k_{c\beta} | d \rangle s_{de}}{\langle \alpha | k_{c\beta} k_{de} | f \rangle} + \frac{[f | k_{de} k_{ef} | g]}{\langle d | k_{ef} | g \rangle} \right) \right). \end{aligned} \quad (5.53)$$

We integrate this current in the following section, to obtain its contribution to the augmented recursion procedure. Because the current itself does not contain any $s_{\alpha\beta}$, the only poles will come from the loop integration and will be at most simple poles.

5.4.3 The doubly non-adjacent current

The doubly non-adjacent current $\tau_7^{(1)}(\alpha^-, c^+, d^+, \beta^+, e^+, f^+, g^+)$ is derived by again following the procedure set out in Section 5.2.2.

The current is based on the amplitude $A_{7;1}^{(1)}(\alpha^-, c^+, d^+, \beta^+, e^+, f^+, g^+)$, with the off-shell momenta placed with two on-shell legs between them. As a non-adjacent current, again there are no factorisations containing $s_{\alpha\beta}$ poles.

Re-using the function defined in eq. 5.53, we can write the current as

$$\begin{aligned} \tau_7^{(1)}(\alpha^-, c^+, d^+, \beta^+, e^+, f^+, g^+) &= \hat{\tau}_7^{basis}(\alpha^-, c^+, \beta^+, d^+, e^+, f^+, g^+) \\ &\quad - \hat{\tau}_7^{basis}(\alpha^-, g^+, f^+, e^+, \beta^+, d^+, c^+). \end{aligned} \quad (5.54)$$

Having obtained all required currents, we can now progress to integrating the augmented recursion diagrams which they are used to construct.

5.5 Integrating Currents

After deriving expressions for the currents (or “good enough” versions that contain all the relevant structures), the next stage in the procedure is to carry out the loop integral in the augmented recursion diagram.

With the standard leg arrangement of Figure 4.6 on page 92, the momenta on the 3-point corners are $\{a, b\}$ and the internal off-shell momenta are defined to be $\alpha = a + \ell$ and $\beta = b - \ell$. The integrals take the form

$$\begin{aligned} \mathcal{I}_n &= \int \frac{d^D \ell}{(2\pi)^D} \frac{i}{\beta^2} A_{3,q}^{(0)}(-\beta^-, b, -\ell^+) \frac{i}{\ell^2} A_{3,q}^{(0)}(\ell^-, a, -\alpha^+) \frac{i}{\alpha^2} \tau_n^{(1)}(\alpha^-, \dots, \beta^+, \dots) \\ &= - \frac{i}{(2\pi)^D} \int \frac{d^D \ell}{\ell^2 \alpha^2 \beta^2} \frac{[b\ell] \langle \beta q \rangle^2}{\langle b q \rangle \langle \ell q \rangle} \frac{[a\alpha] \langle \ell q \rangle^2}{\langle a q \rangle \langle \alpha q \rangle} \tau_n^{(1)}(\alpha^-, \dots, \beta^+, \dots) \\ &= - \frac{i}{(2\pi)^D} \frac{1}{\langle a q \rangle \langle b q \rangle} \int \frac{d^D \ell}{\ell^2 \alpha^2 \beta^2} [a|\ell|q] [b|\ell|q] \frac{\langle \beta q \rangle^2}{\langle \alpha q \rangle^2} \tau_n^{(1)}(\alpha^-, \dots, \beta^+, \dots), \end{aligned} \quad (5.55)$$

for the α^-, β^+ choice of helicities.

We can relate this form to that of the alternative helicity choice by relabelling $\alpha \leftrightarrow \beta$ and permuting the arguments of the current. The form used for the three-point trees is the axial gauge version defined in eq. 5.7, which makes possible the manipulation $[a\alpha] \langle \alpha q \rangle = [a|\alpha|q] = [a|\ell|q]$ in the third line.

5 Currents and their Integration

For future reference, we will use the more concise notation

$$\mathcal{I}_n = \int d\Lambda \left[\frac{\langle \beta q \rangle^2}{\langle \alpha q \rangle^2} \tau_n^{(1)}(\alpha^-, \dots, \beta^+, \dots) \right], \quad (5.56)$$

with the definition

$$d\Lambda = -\frac{i}{(2\pi)^D} \frac{1}{\langle a q \rangle \langle b q \rangle} \frac{d^D \ell}{\ell^2 \alpha^2 \beta^2} [a|\ell|q][b|\ell|q]. \quad (5.57)$$

We may refer to this as “integrating the current”, although strictly speaking it is the whole augmented recursion diagram that is being integrated.

The expressions \mathcal{I}_n give rise to Feynman loop integrals, but generally with some inconvenient dependency on the nullified loop momentum appearing inside spinor products. It is necessary to manipulate the integrand into a form without these, at which point the integration can follow standard techniques.

5.5.1 Manipulations to aid integration

We would like to manipulate our integrals \mathcal{I}_n , so that they are in a form that we recognise how to integrate. A barrier to this is that the nullified forms of loop momenta ℓ , $\alpha(\ell)$, $\beta(\ell)$ can appear in spinor products, giving the integrand a complicated dependence on ℓ . If possible we would like to remove these, leaving only full off-shell momentum factors.

The following manipulations may be useful when dealing with spinors of nullified momenta, allowing reduction to an easily integrated form. That we only need to identify rational terms containing $s_{\alpha\beta} = s_{ab}$ poles also allows for some contributions to be discarded.

Firstly, some loop momentum dependence in the denominator can be simplified by expanding in powers of $\langle \alpha \beta \rangle$, such as in

$$\begin{aligned} \frac{1}{[X|\beta + Y|\alpha]} &= \frac{1}{[X|\beta|\alpha] + [X|Y|\alpha]} \\ &= \frac{1}{[X|Y|\alpha]} \left(1 - \frac{[X|\beta|\alpha]}{[X|Y|\alpha]} + \dots \right) = \frac{1}{[X|Y|\alpha]} + \mathcal{O}(\langle \alpha \beta \rangle). \end{aligned} \quad (5.58)$$

This should be carried out where possible, since the $\mathcal{O}(\langle \alpha \beta \rangle)$ piece can cancel an explicit $\langle \alpha \beta \rangle$ in the denominator, if one is present.

After simplifying the denominators, remaining $\langle \alpha \beta \rangle, [\alpha \beta]$ factors can be converted to propagators via

$$\frac{1}{\langle \alpha \beta \rangle} = \frac{[q \alpha] [\beta q]}{[q | \alpha \beta | q]} = \frac{[q \alpha] [\beta q]}{[q | \alpha (a+b) | q]} = \frac{[q \alpha] [\beta q]}{[q | \alpha | k] [k q]} = \frac{[q \alpha] [\beta q]}{(\alpha + \chi)^2 [k q]} + \mathcal{O}(\alpha^2) \quad (5.59)$$

and

$$\frac{1}{[\alpha \beta]} = \frac{\langle q \alpha \rangle \langle \beta q \rangle}{\langle q | \alpha \beta | q \rangle} = \frac{\langle q \alpha \rangle \langle \beta q \rangle}{\langle q | \alpha (a+b) | q \rangle} = \frac{\langle q \alpha \rangle \langle \beta q \rangle}{\langle q | \alpha | k \rangle \langle k q \rangle} = \frac{\langle q \alpha \rangle \langle \beta q \rangle}{(\alpha + \bar{\chi})^2 \langle k q \rangle} + \mathcal{O}(\alpha^2), \quad (5.60)$$

where $k = k_{ab} = a + b$ and we define new on-shell momenta $\chi \equiv \lambda_k \tilde{\lambda}_q$ and $\bar{\chi} \equiv \lambda_q \tilde{\lambda}_k$. The denominator spinor containing k_{ab}^b that we introduce may cancel a factor in the numerator, or survive to influence the recursion result, but is no longer a concern for the integration process.

Numerator factors can also be modified so that loop momenta are accompanied by a q spinor, by expanding

$$[X | \alpha | Y] = [X | \alpha^b | Y] + \mathcal{O}(\alpha^2) = [X | \alpha | q] \frac{\langle \alpha Y \rangle}{\langle \alpha q \rangle} + \mathcal{O}(\alpha^2). \quad (5.61)$$

This can be helpful because the loop momentum can now be considered to be q -nullified or not, depending on which is more convenient. The q spinor will also tend to cause cancellations with the Feynman shift we apply to the loop momentum when performing the integration.

In the previous two steps, terms containing additional factors of α^2, β^2 can usually be discarded when they occur, as these cancel a propagator factor and reduce the resulting power of $\langle a b \rangle$ obtained from the integration. We are only interested in the residue, so terms that only contribute to $\mathcal{O}(\langle a b \rangle^0)$ have no effect and can be discarded whenever they are identified. The exception occurs when an explicit factor of $s_{\alpha\beta} = s_{ab}$ is already present in the denominator before integration. In that case, even those integral contributions that produce no s_{ab} themselves form part of the residue. Care should be taken not to discard these pieces erroneously.

An additional manipulation which clears some loop momentum spinors is

$$\frac{\langle X \alpha \rangle}{\langle Y \alpha \rangle} = \frac{\langle X \alpha \rangle \langle Y a \rangle}{\langle Y \alpha \rangle \langle Y a \rangle} = \frac{\langle X a \rangle}{\langle Y a \rangle} + \mathcal{O}(\langle \alpha a \rangle). \quad (5.62)$$

Generally, $\langle \alpha a \rangle$ can be combined with other numerator factors to produce factors of $\langle a b \rangle$. (For example, the sequence of manipulations may be $\langle \alpha a \rangle [\alpha q] = \langle a | \alpha | q] =$

5 Currents and their Integration

$\langle a|\ell|q\rangle$, with a Feynman shift used in the integration process itself introducing b where the loop momentum appears.) These terms can be discarded if the overall result would be $\mathcal{O}(\langle ab\rangle^0)$, which occurs when there are no explicit denominator factors of $\langle ab\rangle$ to cancel the effect of $\langle \alpha a\rangle$.

Various trivial substitutions can also be made, based on the relationship between $\alpha + \beta = k = a + b$, such as

$$[X|\beta|Y] = [X|k|Y] - [X|\alpha|Y], \quad (5.63)$$

where k is constant with respect to the integral.

Following the above substitutions, we reduce the denominators of our currents to a series of propagator factors. The numerators are constant spinor structures, or contain factors of the loop momentum ℓ^μ . We recognise this form as one which can be integrated using the method of Feynman parameters.

5.5.2 Feynman integration

We follow a standard procedure to integrate the currents once prepared in the appropriate form. Firstly, the denominator is put in a symmetric form using Feynman parametrisation. The loop momentum integral is carried out, then the Feynman parameter integrals are interpreted in terms of gamma functions. For the purposes of augmented recursion, we are only interested in the rational, $\mathcal{O}(\epsilon^0)$ pieces of the results.

1. Introduce Feynman parameters to combine propagator factors into single denominator,

$$\frac{1}{D_1 D_2 \cdots D_N} = \Gamma(N) \int_0^1 \prod_{i=1}^N dz_i \frac{\delta(1 - \sum_{j=1}^N z_j)}{(z_1 D_1 + z_2 D_2 + \cdots + z_N D_N)^N}. \quad (5.64)$$

2. Complete the square in the denominator, to yield a form $((l + A)^2 + M)^N$.
3. Redefine the loop momentum, $\ell \rightarrow \ell - A$, to obtain the symmetric denominator form $(\ell^2 + M)^N$.
4. Looking at the numerator, discard vanishing terms that are antisymmetric in ℓ . Even powers of ℓ , where both are contracted with $|q\rangle$, will also vanish due to the Fierz rearrangement formula $[i|\gamma^\mu|j][k|\gamma_\mu|l] = 2[ik]\langle lj\rangle$ yielding $\langle q q\rangle = 0$.

5. Perform the momentum integral. We derive the general result, which can be applied straightforwardly:

$$\int d^D \ell \frac{1}{(\ell^2 - R^2)^N} = (-1)^N i\pi^{\frac{D}{2}} \frac{\Gamma(N - \frac{D}{2})}{\Gamma(N)} (R^2)^{-N + \frac{D}{2}}. \quad (5.65)$$

6. Perform the x_i integrals. This tends to produce gamma functions, defined as

$$\Gamma(z) = \int_0^\infty x^{z-1} e^{-x} dx. \quad (5.66)$$

Applying the beta function definition,

$$B(x, y) = \int_0^1 t^{x-1} (1-t)^{y-1} dt, \quad (5.67)$$

for $\text{Re}(x) > 0, \text{Re}(y) > 0$, followed by the relationship

$$B(x, y) = \frac{\Gamma(x)\Gamma(y)}{\Gamma(x+y)}, \quad (5.68)$$

may be appropriate.

7. Expand the gamma functions in powers of ϵ and keep the rational piece.

To illustrate the process, let us pick a particular current structure to show the integration steps in detail. Choosing

$$\tilde{\tau}_n^{(1)}(\alpha^-, \dots, \beta^+, \dots) = \frac{\langle \alpha q \rangle^2}{\langle \beta q \rangle^2}, \quad (5.69)$$

the integration to evaluate is

$$\begin{aligned} \tilde{\mathcal{I}}_n &= \int d\Lambda[1] \\ &= -\frac{i}{(2\pi)^D} \frac{1}{\langle a q \rangle \langle b q \rangle} \int \frac{d^D \ell}{\ell^2 \alpha^2 \beta^2} [a|\ell|q][b|\ell|q]. \end{aligned} \quad (5.70)$$

To proceed with the integration, use Feynman parametrisation. Recalling that $\alpha =$

5 Currents and their Integration

$a + \ell$ and $\beta = b - \ell$, we have

$$\begin{aligned}
\frac{1}{\ell^2 \alpha^2 \beta^2} &= \Gamma(3) \int_0^1 \int_0^1 \int_0^1 dx_1 dx_2 dx_3 \frac{\delta(1 - x_1 - x_2 - x_3)}{(x_1 \alpha^2 + x_2 \beta^2 + x_3 \ell^2)^3} \\
&= \Gamma(3) \int_0^1 \int_0^{1-x_2} dx_1 dx_2 \frac{1}{(\ell^2 + 2\ell \cdot (x_1 a - x_2 b))^3} \\
&= \Gamma(3) \int_0^1 \int_0^{1-x_2} dx_1 dx_2 \frac{1}{((\ell + x_1 a - x_2 b)^2 + x_1 x_2 s_{ab})^3}. \tag{5.71}
\end{aligned}$$

Using the substitution $\ell \rightarrow \ell - x_1 a + x_2 b$, the denominator reaches a convenient form.

This substitution must also be applied to the rest of the integrand. We have

$$\begin{aligned}
\tilde{\mathcal{I}}_n &= \frac{i}{(2\pi)^D} \frac{\Gamma(3)}{\langle a q \rangle \langle b q \rangle} \int d^D \ell \int_0^1 \int_0^{1-x_2} dx_1 dx_2 \frac{x_2 [a|b|q] x_1 [b|a|q]}{(\ell^2 + x_1 x_2 s_{ab})^3} \\
&= -\frac{i}{(2\pi)^D} \Gamma(3) [ab]^2 \int d^D \ell \int_0^1 \int_0^{1-x_2} dx_1 dx_2 \frac{x_1 x_2}{(\ell^2 + x_1 x_2 s_{ab})^3}, \tag{5.72}
\end{aligned}$$

which after momentum integration with $R^2 = x_1 x_2 s_{ab}$ becomes

$$\begin{aligned}
\tilde{\mathcal{I}}_n &= -\frac{\pi^{\frac{D}{2}}}{(2\pi)^D} \Gamma\left(3 - \frac{D}{2}\right) [ab]^2 \int_0^1 \int_0^{1-x_2} dx_1 dx_2 x_1 x_2 (x_1 x_2 s_{ab})^{-3+\frac{D}{2}} \\
&= -\frac{\pi^{\frac{D}{2}}}{(2\pi)^D} \Gamma\left(3 - \frac{D}{2}\right) [ab]^2 s_{ab}^{-3+\frac{D}{2}} \int_0^1 \int_0^{1-x_2} dx_1 dx_2 (x_1 x_2)^{\frac{D}{2}-2}. \tag{5.73}
\end{aligned}$$

The integral over Feynman parameters becomes

$$\begin{aligned}
&\int_0^1 \int_0^{1-x_2} dx_1 dx_2 x_1^{\frac{D}{2}-2} x_2^{\frac{D}{2}-2} \\
&= \int_0^1 dx x^{\frac{D}{2}-2} (1-x)^{\frac{D}{2}-1} \left(\frac{1}{\frac{D}{2}-1}\right) \\
&= B\left(\frac{D}{2}-1, \frac{D}{2}\right) \frac{2}{D-2} = \frac{\Gamma(\frac{D}{2}-1)\Gamma(\frac{D}{2})}{\Gamma(D-1)} \frac{2}{D-2} \\
&= \frac{\Gamma(1-\epsilon)\Gamma(2-\epsilon)}{\Gamma(3-2\epsilon)} \frac{1}{1-\epsilon} = \frac{1}{2} + \mathcal{O}(\epsilon), \tag{5.74}
\end{aligned}$$

where we have made use of the fact that $D = 4 - 2\epsilon$ to expand in powers of ϵ .

Therefore overall,

$$\tilde{\mathcal{I}}_n = \frac{1}{2} \frac{1}{(4\pi)^2} \frac{[ab]}{\langle ab \rangle} + \mathcal{O}(\epsilon) \tag{5.75}$$

The denominator factor of $(4\pi)^2$, or $(4\pi)^{2-\epsilon}$ in the all- ϵ form, is part of the constant factor $a = g^2 e^{-\epsilon\gamma_E} / (4\pi)^{2-\epsilon}$ that accompanies loop amplitudes $\mathcal{A}_n^{(\ell)}$ in the overall decomposition of an amplitude (equation 2.1 on page 21). The loop integration has created a two-loop structure from a one-loop structure, so an additional factor of a was expected to arise. Strictly speaking, we should also expect factors of the coupling constant g^2 to emerge from the calculation, so that

$$\tilde{\mathcal{I}}_n = \frac{1}{2} a \frac{[a b]}{\langle a b \rangle} + \mathcal{O}(\epsilon). \quad (5.76)$$

Noting that each of the three-point tree amplitudes should be accompanied by a factor of g in the full expansion, but have not been here, shows where these factors have been omitted from our derivation.

For the results that follow, we will state only the functional form relevant to the augmented recursion procedure. For example,

$$\tilde{\mathcal{I}}_n = \frac{1}{2} \frac{[a b]}{\langle a b \rangle} + \mathcal{O}(\epsilon). \quad (5.77)$$

Factors of $1/(4\pi)^2$ (and g^2) can be assumed to have been absorbed into the correct definition of the loop amplitude expansion.

5.5.3 Integration results

We carry out the integration of currents piece-wise, recording the results of each structure encountered here.

Triangle integrals, or those involving three propagator factors, take the forms:

$$\int d\Lambda [1] = \frac{1}{2} \frac{[a b]}{\langle a b \rangle} + \mathcal{O}(\epsilon), \quad (5.78)$$

$$\int d\Lambda [[X|\alpha|q\rangle] = \frac{1}{6} \frac{[a b]}{\langle a b \rangle} [X|b + 2a|q\rangle + \mathcal{O}(\epsilon), \quad (5.79)$$

$$\int d\Lambda [[X|\beta|q\rangle] = \frac{1}{6} \frac{[a b]}{\langle a b \rangle} [X|2b + a|q\rangle + \mathcal{O}(\epsilon), \quad (5.80)$$

$$\int d\Lambda [[X|\beta|q\rangle^2] = \frac{1}{12} \frac{[a b]}{\langle a b \rangle} ([X|a|q\rangle^2 + 3[X|a|q\rangle[X|b|q\rangle + 3[X|b|q\rangle^2) + \mathcal{O}(\epsilon), \quad (5.81)$$

$$\int d\Lambda [\langle q|\alpha\beta|q\rangle] = \frac{1}{6} \frac{[a b]}{\langle a b \rangle} \langle q|ab|q\rangle + \mathcal{O}(\epsilon), \quad (5.82)$$

5 Currents and their Integration

$$\int d\Lambda [\alpha^2] = \int d\Lambda [\beta^2] = 0. \quad (5.83)$$

Four-propagator integrals occur when a denominator factor is promoted to propagator. The results contain transcendental functions (logarithms) and only some contain rational pieces. For the following box integrals we state only the rational terms (denoted with $|\mathbb{Q}$), as these give the contribution to augmented recursion:

$$\int d\Lambda \left[\frac{1}{(\alpha + X)^2} \right] \Big|_{\mathbb{Q}} = 0, \quad (5.84)$$

$$\int d\Lambda \left[\frac{[X|l|q]}{(\beta + Y)^2} \right] \Big|_{\mathbb{Q}} = -\frac{1}{2} \frac{[a|b]}{\langle a|b \rangle} \frac{[X|a|q]}{[a|Y|a]}, \quad (5.85)$$

$$\int d\Lambda \left[\frac{[X|l|q]^2}{(\beta + Y)^2} \right] \Big|_{\mathbb{Q}} = \frac{1}{6} \frac{[a|b]}{\langle a|b \rangle} \frac{[X|a|q]}{[a|Y|a]} \left([X|a|q] \left(1 - 2 \frac{[b|Y|b]}{[a|Y|a]} \right) - [X|b|q] \right). \quad (5.86)$$

When two denominator factors are promoted to propagators, we obtain pentagon integrals. In the following two cases, there are no rational contributions:

$$\int d\Lambda \left[\frac{1}{(\alpha + X)^2(\beta + Y)^2} \right] \Big|_{\mathbb{Q}} = 0, \quad (5.87)$$

$$\int d\Lambda \left[\frac{[W|l|Z]}{(\alpha + X)^2(\beta + Y)^2} \right] \Big|_{\mathbb{Q}} = 0. \quad (5.88)$$

When calculating integrals with higher numbers of propagators, it can be useful to expand the structure inside $d\Lambda$ as

$$[a|l|q][b|l|q] = \frac{\alpha^2 \langle q|bl|q \rangle + \beta^2 \langle q|al|q \rangle + l^2 \langle q|K_{ab}(b-l)|q \rangle}{\langle a|b \rangle} \quad (5.89)$$

to produce a sum of simpler integrals. This manipulation pulls out an explicit $\langle a|b \rangle$ pole, so a further factor is not expected from the integration step.

For integrals with more than five propagators, the integral reduction described by Passarino and Veltman [29] is useful. Any integral greater than a pentagon can be reduced to a linear combination of pentagons, by following the logic:

- We have for $N > 5$,

$$I_N = \prod_{i=1}^N \frac{1}{d_i}, \quad (5.90)$$

where $d_i = (\ell + p_i)^2 - m_i^2$.

- It is possible to choose $N > 5$ unknowns α_i such that the equations $\sum_{i=1}^N \alpha_i = 0$, $\sum_{i=1}^N \alpha_i q_i^\mu = 0$ have at least one non-trivial solution.
- With these α_i chosen,

$$\sum_{i=1}^N \alpha_i d_i = \sum_{i=1}^N \alpha_i (\ell^2 + 2\ell \cdot p_i + p_i^2 - m_i^2) = \sum_{i=1}^N \alpha_i (p_i^2 - m_i^2), \quad (5.91)$$

so

$$1 = \frac{\sum_{i=1}^N \alpha_i d_i}{\sum_{i=1}^N \alpha_i (p_i^2 - m_i^2)}. \quad (5.92)$$

- The α_i and denominator are independent of the loop momentum, so multiplying I_N by this factor produces a sum of I_{N-1} -type integrals with known coefficients.

Hence, hexagons and above can be reduced to pentagons, of which we have calculated two commonly occurring types. Hexagons which reduce to the two pentagons calculated above contribute no rational piece.

With all current integrals carried out, we collect the integrated pieces and sum over the momentum configurations required for each partial amplitude colour structure. Both helicity configurations in the diagram are accounted for by including relabelled integrals as previously described. We divide by z , apply the shift, then take the residues to obtain the augmented recursion contributions to the partial amplitudes.

5.6 Conclusions

The inclusion of currents with off-shell legs is the development that separates augmented recursion from the original recursive method of BCFW for calculating rational amplitude pieces. By integrating current diagrams, Laurent coefficients can be obtained for the sub-leading poles in the rational part of an amplitude, an improvement on factorisation diagrams which provide only the leading pole information. This allows the whole of the rational piece to be determined by its analytic structure.

Calculating the necessary currents is a difficult task, but certain simplifications can be made because it is known that the current is only required for its contributions to a complex residue. Imposing two conditions that ensure the correct residue is later obtained, the current can be determined up to some terms that do not affect the procedure. An algorithmic way of writing down such a current was presented in this

5 *Currents and their Integration*

chapter, and its validity demonstrated by reproducing an earlier result. New currents used in the successful derivation of the two-loop seven-point all-plus helicity amplitude, the subject of Chapter 4, were then presented.

Integrating currents presents its own challenges, as spinor structures can bear quite complicated relations to the loop momentum of interest. However, there are often manipulations that can be applied in a systematic way to each type of term, of which we list a number. Existing Feynman integral results can also be used in new problems, reducing the burden in future calculations.

The next chapter describes a procedure for reconstructing analytic amplitudes in a simpler, more symmetric form. This can be applied directly to the complicated expressions produced by integrating currents, to produce a more compact result. Or it can be used on the amplitudes that form the initial ingredients of currents themselves, so that the simplification filters through the entire process.

6 Reconstruction of Rational Functions

6.1 Introduction

Various techniques exist for generating the rational pieces of amplitudes. Perhaps the most conceptually straightforward is to write down and evaluate all Feynman diagrams for the desired interaction. However, the drawback is that the number of diagrams to draw grows rapidly with the number of external particles involved, making the approach unfeasible for deriving more complicated amplitudes on typical computers [5].

Augmented recursion offers a way to obtain the rational pieces, by building them from residues of a small number of factorisations and non-factorising current diagrams [38, 39, 40]. As part of this process, a reference momentum is introduced to control the analytic behaviour. The final result produced will tend to contain factors of this reference momentum, but does not have any dependence on it overall. Therefore we are motivated to find a way to reconstruct the rational piece result so that it is explicitly free of this temporary inclusion. At the same time, we can also aim for a structure where other symmetries are manifest, for example the cyclic symmetries in the momentum labelling.

As we consider amplitudes of higher numbers of gluons, particularly those partial amplitudes appearing in the full colour form, we also see an increase in the complexity of the initial augmented recursion result. Although still more efficient than a Feynman diagram approach, the result can require tens of factorisations and current diagrams. The inclusion of multiple current diagrams can quickly cause expressions to become (notationally) large, due to the complicated nature of currents, and their sizes being at least as large as the corresponding one-loop amplitude from which they are built. The issue is compounded for sub-leading in colour structures, which would tend to contain integrals of sub-leading in colour currents. To avoid having to separately calculate these sub-leading currents, they are re-expressed in terms of the leading in colour structure using decoupling identities. The result is a further multiplication of the terms appearing in the augmented recursion process and results.

More generally, our processes (such as forming factorisations and current-building)

often rely on the form of one-loop amplitudes. Unnecessary complexity in these structures carries through to any new result we wish to find, making the interpretation and tidy presentation of results more difficult. It can therefore be desirable to reconstruct not only two-loop results, but existing one-loop results when they are inefficient.

Given a complicated analytic form for (the rational piece of) a partial amplitude, we have established our desire to be able to reconstruct it in some way. Doing so, we wish to remove reference momenta which the expression is independent of, and produce human-readable results that showcase the symmetries of the theory. Simpler reconstructed amplitudes are also a valuable ingredient to any future recursion or factorisation technique.

In the next section, we present our method for reconstructing the rational pieces of amplitudes. In the sections following it, we carry out reconstruction on certain one-loop amplitudes which are useful to the reconstruction of two-loop amplitudes, but have not previously been written in an efficient form. Lastly, we devote sections to the reconstruction of the two-loop seven-point amplitude results, obtained in an analytic, but complicated, form using augmented recursion in Chapter 4.

6.2 Overview of the Method

To reconstruct amplitudes, we adopt an approach of dividing a given partial amplitude's rational piece into two parts, according to the pole structures present. For this procedure, a "pole" has a slightly different meaning to in the recursion step, because there is no longer a complex shift involved. We refer to denominator factors of t_{ijk} , s_{ij} , $\langle ij \rangle$ and $[ij]$ as t -poles, s -poles, angle bracket poles and square bracket poles, because of the divergence caused when those factors become small.

Those terms with leading poles can be reconstructed by considering possible factorisations into smaller amplitudes. The remaining sub-leading poles are then fitted to an ansatz with as many manifest symmetries as possible.

6.2.1 Leading poles

Our method is to divide a given partial amplitude's rational piece into two pieces, according to the pole structures present. In this section we reconstruct those terms with leading poles, by inspecting factorisations which give rise to the leading poles in the propagator. The procedure differs from BCFW recursion in that we do not apply a momentum shift or take residues. Identifying the leading poles by hand this way

allows them to be written in a compact form, with symmetries manifest. However, the approach can introduce “spurious poles” into the expressions, which are spinor structures that appear to relate to propagators not present in the overall amplitude. For example, amplitudes will not contain poles of the type

$$\frac{1}{[a|b+c|d]} = \frac{1}{(b+c+X)^2} + \mathcal{O}(s_{bc}), \quad (6.1)$$

where $X \equiv |d\rangle[a|$, because X is not an external momentum. But such structures can occur when viewing factorisations, as a result of the momentum sum in the propagator. We do not want spurious poles polluting the compact form for the amplitude, because this would obscure its symmetries and imply greater complexity, so a strategy for dealing with them will be required.

For amplitudes of up to six gluons, spurious poles can be removed quite simply, if they occur. This is done by performing manipulations that only introduce new terms which are sub-leading in the factorisation pole, so can be discarded. Schematically, for a factorisation about a t_{abc} pole, in six-point momentum, spurious pole structures such as

$$\frac{1}{t_{abc}[a|k_{abc}|f]} \quad (6.2)$$

may appear. Recalling that k_{abc} is non-null as a momentum, but must be nullified when treated as a spinor, we can separate the spurious pole into spinor products. Each can be paired with a new spinor product, chosen to lead to a convenient cancellation. Also recalling that external momenta must sum to zero, a typical spurious pole may be removed following a procedure such as

$$\begin{aligned} \frac{1}{t_{abc}[a|k_{abc}|f]} &= \frac{1}{t_{abc}[a|k_{abc}]\langle k_{abc}|f\rangle} + \mathcal{O}(t_{abc}^0) \\ &= \frac{\langle k_{abc}|c\rangle[d|k_{abc}]}{t_{abc}[a|k_{abc}]\langle k_{abc}|c\rangle[d|k_{abc}]\langle k_{abc}|f\rangle} + \mathcal{O}(t_{abc}^0) \\ &= \frac{[d|k_{abc}|c]}{t_{abc}[a|k_{abc}|c][d|k_{abc}|f]} + \mathcal{O}(t_{abc}^0) \\ &= -\frac{[d|k_{abc}|c]}{t_{abc}[a|k_{abc}|c][d|k_{def}|f]} + \mathcal{O}(t_{abc}^0) \\ &= -\frac{[d|k_{abc}|c]}{t_{abc}[a|b|c][d|e|f]} + \mathcal{O}(t_{abc}^0), \end{aligned} \quad (6.3)$$

6 Reconstruction of Rational Functions

where the momentum sum has been used to exchange some denominator arguments in the fourth step. Because this derivation only aims to find the leading pole terms, those pieces of $\mathcal{O}(t_{abc}^0)$ can be neglected.

A similar manipulation can be applied for all spurious poles that appear, so their treatment with six-point momenta and below is straightforward.

However for seven-point amplitudes and above, this type of manipulation no longer succeeds in removing all spurious poles. Consider how the above example plays out with seven-point momenta. The condition on the momenta is now

$$\sum_{i=1}^7 p_i = 0, \tag{6.4}$$

so the momentum swap used in step four no longer yields a non-spurious structure. We instead obtain a factor of

$$[d|k_{abc}|f\rangle = -[d|k_{defg}|f\rangle = -[d|k_{eg}|f\rangle \tag{6.5}$$

and there is no simple manipulation to remove structures of this type. These structures are not present in the overall amplitude, so the only remaining strategy is to collect all the terms containing a particular spurious pole, which we infer must undergo some sort of cancellation. The poles can be removed by applying manipulations that make their overall cancellation under the sum manifest at an earlier stage, but this is a considerably more difficult process than the six-point manipulation.

Note that when applying this technique to a two-loop amplitude, the ability to find a simple result, free of spurious poles, is affected by the simplicity of the one-loop amplitudes that are fed into the factorisations. Often, one-loop amplitudes for sub-leading colour structures have not been explicitly derived previously, because all one-loop partial amplitudes can be represented in terms of the leading structure via decoupling identities [7]. However, the decoupling identity form tends not to be the simplest possible statement of a partial amplitude, as a result of it containing structures that cancel in the overall sum. In particular, it is often the case that a pole present in the leading in colour partial amplitude is not present in the sub-leading in colour structure, so these represent spurious poles in the decoupling identity form.

The outcome is that in order to find simple forms for two-loop amplitudes, we may first have to find simpler forms for one-loop amplitudes.

6.2.2 Sub-leading poles

After the leading poles of a rational piece are obtained from factorisations and made manifestly free of spurious poles, they can be subtracted from the large, notationally inefficient expression that we wish to simplify. What remains is an expression, still large, but that contains only the sub-leading pole terms. We can now attempt to fit an ansatz to the sub-leading piece based on which poles are still present.

In principle, we could have started by attempting to fit an ansatz to the entire expression. However, the leading pole structures would be additional possible factors that could appear in the ansatz denominators, leading to a far larger ansatz being required than for the sub-leading terms alone. By restricting our search to the smaller set of sub-leading poles, we face a problem that is far more tractable with typically available computing power. Deriving the leading poles by hand is also beneficial when trying to make symmetries manifest. Although this is harder to do with ansatz fitting, we can ensure some symmetries of the result are explicit by building them into the ansatz. For example, when trying to fit a rational piece with a $\mathcal{P}_{n;\lambda}$ symmetry in its arguments, we can restrict the form of our ansatz to some basis function with unknown coefficients, under a $\mathcal{P}_{n;\lambda}$ sum.

To be able to choose an appropriate ansatz, we must know which poles are present in an expression. Checking by eye is not sufficient, as structures that appear to be present can cancel between terms, so that the overall result does not depend on them. A technique of numerical pole testing is employed, where we evaluate our amplitude on a particular kinematic point (a numerical choice for each external momentum), chosen so that certain pole structures become large. Methodically testing which combinations of poles are allowed to coincide in a term can greatly constrain the possible numerators needed in the ansatz. A limitation of this procedure is that due to momentum considerations, certain collections of spinor products becoming small require others to do so, so some combinations of poles cannot be tested alone. For example, testing for $\langle ab \rangle$ and $\langle bc \rangle$ poles automatically involves $\langle ac \rangle$ poles too.

With a knowledge of the allowed pole combinations, we select denominators that are representative of all the required poles. Then choosing sets of independent numerator terms, each with unknown coefficients, we obtain an ansatz that is relatively small, but should be guaranteed to contain all the structures of the target amplitude. Or in the case that the complete ansatz would still contain too many terms to work with, simpler non-guaranteed subsets of the terms can be postulated and tested to look for

a successful fit.

The ansatz fitting itself proceeds by setting the ansatz equal to the amplitude, and numerically evaluating on multiple kinematic points, to create a system of equations for the unknowns of the ansatz. As many evaluations are needed as there are unknowns, so smaller ansatzes are desirable to reduce computation time. This is particularly true when the amplitude we wish to fit is a large, inefficient expression. We use Mathematica’s `Solve` function to solve for the ansatz unknowns. If the ansatz is complete and contains all the structures of the amplitude, we expect an integer (or rational, depending on normalisation) solution for the unknowns, where most are zero. The solving stage presents another reason to desire a small ansatz, as the manipulations carried out on the equation matrix can exceed computer memory if too large an ansatz is chosen.

6.3 One-Loop Partial Amplitudes

The augmented recursion procedure makes use of factorisations into one-loop amplitudes. For recursion of leading in colour partial amplitudes, those factorisations tend to involve leading in colour amplitudes, but when working at full colour, the factorisations also involve sub-leading in colour structures. As previously mentioned, these do not always exist in an efficient form, because they can always be obtained from the one-loop decoupling relations [7] and this is sufficient for most applications. However, expressions free of spurious poles are useful for our purposes.

In the following subsections, we reconstruct a number of one-loop amplitudes. The forms produced are better suited for use in recursion processes, or in constructing the leading pole factorisations for a two-loop amplitude that we wish to simplify.

6.3.1 Single-minus helicity $A_{5;2}^{(1)}(a^+; b^-, c^+, d^+, e^+)$

In determining the leading pole factorisation for the two-loop six-point full colour amplitude, we require the one-loop partial amplitude $A_{5;2}^{(1)}(a^+; b^-, c^+, d^+, e^+)$.

This can be obtained from a decoupling identity

$$\begin{aligned}
 A_{5;2}^{(1)}(a^+; b^-, c^+, d^+, e^+) &= -A_{5;1}^{(1)}(b^-, a^+, c^+, d^+, e^+) - A_{5;1}^{(1)}(b^-, c^+, a^+, d^+, e^+) \\
 &\quad - A_{5;1}^{(1)}(b^-, c^+, d^+, a^+, e^+) - A_{5;1}^{(1)}(b^-, c^+, d^+, e^+, a^+) \quad (6.6)
 \end{aligned}$$

involving the leading-in-colour partial amplitude with a single negative helicity [71],

$$A_{5:1}^{(1)}(a^-, b^+, c^+, d^+, e^+) = \frac{i}{3} \frac{1}{\langle cd \rangle^2} \left(-\frac{[be]^3}{[ab][ea]} + \frac{\langle ad \rangle^3 \langle ce \rangle [de]}{\langle ab \rangle \langle bc \rangle \langle de \rangle^2} - \frac{\langle ac \rangle^3 \langle db \rangle [cb]}{\langle ae \rangle \langle cb \rangle^2 \langle ed \rangle} \right). \quad (6.7)$$

The decoupling expression contains apparent double poles of the type $1/\langle cd \rangle^2$, originating in the $A_{5:1}^{(1)}$ partial amplitude. However, pole tests show that this type of pole is not present in $A_{5:2}^{(1)}(a^+; b^-, c^+, d^+, e^+)$ once the sum has taken place – they are spurious. We will reconstruct an expression for $A_{5:2}^{(1)}(a^+; b^-, c^+, d^+, e^+)$ that is explicitly free of spurious poles, so that these are not inherited by the two-loop factorisation we wish to determine. The target amplitude only contains simple poles, so we can move directly to ansatz fitting, rather than inspecting leading pole factorisations.

Pole tests on $A_{5:2}^{(1)}(a^+; b^-, c^+, d^+, e^+)$ show that it contains poles in the following spinor products:

$$\langle ac \rangle, \langle ad \rangle, \langle ae \rangle, \langle bc \rangle, \langle be \rangle, \langle cd \rangle, \langle de \rangle, [bc], [be]. \quad (6.8)$$

This allows us to postulate an ansatz of the form

$$\frac{G}{s_{bc}s_{be} \langle ac \rangle \langle ad \rangle \langle ae \rangle \langle cd \rangle \langle de \rangle}, \quad (6.9)$$

where G contains a linearly independent sum of numerator terms with unknown coefficients, chosen to give the amplitude the correct overall spinor weight and little group scaling in each momentum.

The ansatz fit is successful, yielding the result

$$A_{5:2}^{(1)}(a^+; b^-, c^+, d^+, e^+) = \frac{iG_{5:2}^{sm2}}{s_{bc}s_{be} \langle ac \rangle \langle ad \rangle \langle ae \rangle \langle cd \rangle \langle de \rangle}, \quad (6.10)$$

where

$$\begin{aligned}
G_{5:2}^{sm2} = & \langle ac \rangle \langle ad \rangle^2 \langle bd \rangle \langle be \rangle [ad]^2 [ce] + 2 \langle ac \rangle \langle ad \rangle^2 \langle be \rangle^2 [ad] [ae] [ce] \\
& + \langle ac \rangle \langle ad \rangle \langle ae \rangle \langle be \rangle^2 [ae]^2 [ce] - \langle ac \rangle^2 \langle bd \rangle^2 \langle de \rangle [ad] [cd] [ce] \\
& + \langle ac \rangle \langle bc \rangle \langle bd \rangle \langle cd \rangle \langle de \rangle [cd]^2 [ce] - 2 \langle ac \rangle^2 \langle bd \rangle \langle be \rangle \langle de \rangle [ad] [ce]^2 \\
& + 3 \langle ac \rangle \langle bc \rangle \langle bd \rangle \langle ce \rangle \langle de \rangle [cd] [ce]^2 - 2 \langle ac \rangle \langle bc \rangle^2 \langle de \rangle^2 [cd] [ce]^2 \\
& + \langle ad \rangle^3 \langle bd \rangle \langle be \rangle [ad]^2 [de] + 3 \langle ad \rangle^3 \langle be \rangle^2 [ad] [ae] [de] \\
& + 2 \langle ad \rangle^2 \langle ae \rangle \langle be \rangle^2 [ae]^2 [de] - \langle ac \rangle \langle ad \rangle \langle bd \rangle^2 \langle de \rangle [ad] [cd] [de] \\
& + \langle ad \rangle \langle bc \rangle \langle bd \rangle \langle cd \rangle \langle de \rangle [cd]^2 [de] + 2 \langle ad \rangle^2 \langle bd \rangle \langle be \rangle \langle ce \rangle [ad] [ce] [de] \\
& - 5 \langle ac \rangle \langle ad \rangle \langle bd \rangle \langle be \rangle \langle de \rangle [ad] [ce] [de] + 2 \langle ad \rangle^2 \langle be \rangle^2 \langle ce \rangle [ae] [ce] [de] \\
& - 2 \langle ac \rangle \langle ad \rangle \langle be \rangle^2 \langle de \rangle [ae] [ce] [de] + \langle ad \rangle \langle bd \rangle^2 \langle ce \rangle^2 [cd] [ce] [de] \\
& + 3 \langle ad \rangle \langle bc \rangle \langle bd \rangle \langle ce \rangle \langle de \rangle [cd] [ce] [de] - \langle ac \rangle \langle bd \rangle^2 \langle ce \rangle \langle de \rangle [cd] [ce] [de] \\
& - 3 \langle ad \rangle \langle bc \rangle^2 \langle de \rangle^2 [cd] [ce] [de] + \langle ac \rangle \langle bc \rangle \langle bd \rangle \langle de \rangle^2 [cd] [ce] [de] \\
& + \langle ad \rangle \langle bd \rangle \langle be \rangle \langle ce \rangle^2 [ce]^2 [de] - 3 \langle ac \rangle \langle bd \rangle \langle be \rangle \langle ce \rangle \langle de \rangle [ce]^2 [de] \\
& + 2 \langle ac \rangle \langle bc \rangle \langle be \rangle \langle de \rangle^2 [ce]^2 [de] - \langle ad \rangle^2 \langle bd \rangle \langle be \rangle \langle ce \rangle [ae] [de]^2 \\
& - 2 \langle ad \rangle^2 \langle bd \rangle \langle be \rangle \langle de \rangle [ad] [de]^2 - \langle ad \rangle \langle bd \rangle^2 \langle ce \rangle \langle de \rangle [cd] [de]^2 \\
& + \langle ad \rangle \langle bc \rangle \langle bd \rangle \langle de \rangle^2 [cd] [de]^2 - 3 \langle ad \rangle \langle bd \rangle \langle be \rangle \langle ce \rangle \langle de \rangle [ce] [de]^2 \\
& + 3 \langle ad \rangle \langle bc \rangle \langle be \rangle \langle de \rangle^2 [ce] [de]^2. \tag{6.11}
\end{aligned}$$

This expression contains 31 terms, compared to the 12 terms present in the decoupling identity expression, so is less compact. However, the new form contains no spurious poles so is better suited for use in recursion and factorisations of larger amplitudes.

6.3.2 All-plus helicity $A_{5:2}^{(1)}(a^+, b^+, c^+, d^+, e^+)$

The five-point one-loop all-plus helicity amplitude $A_{5:2}^{(1)}(a^+, b^+, c^+, d^+, e^+)$ appears when writing down the leading poles of the seven-point two-loop amplitude.

An all- n expression for this partial amplitude was obtained in ref. [54], derived by considering applying decoupling identities to the all- n leading-in-colour partial ampli-

tude of ref. [31]. It can be written as

$$\begin{aligned}
 A_{5:2}^{(1)}(a^+; b^+, c^+, d^+, e^+) &= -i \frac{1}{\langle bc \rangle \langle cd \rangle \langle de \rangle \langle eb \rangle} \sum_{b \leq i < j \leq e} [ai] \langle ij \rangle [ja] \\
 &= -i \frac{1}{\langle bc \rangle \langle cd \rangle \langle de \rangle \langle eb \rangle} ([a|bc|a] + [a|bd|a] + [a|be|a] \\
 &\quad + [a|cd|a] + [a|ce|a] + [a|de|a]).
 \end{aligned} \tag{6.12}$$

However, a simplification can be made by exploiting the linear dependence of the momenta appearing in numerator structures. We can write the amplitude in a smaller form,

$$A_{5:2}^{(1)}(a^+; b^+, c^+, d^+, e^+) = -i \frac{1}{\langle bc \rangle \langle cd \rangle \langle de \rangle \langle eb \rangle} ([a|bc|a] + [a|de|a]), \tag{6.13}$$

which helps to reduce complexity in later steps of a recursion procedure. In fact, the use of linear dependence to eliminate terms in amplitudes is more generally applicable whenever such a sum of terms occurs.

Directly building in the linear dependence where possible can yield an n -point expression with fewer terms, making it more convenient as an ingredient for larger amplitudes. For example, we can write

$$A_{n:2}^{(1)}(1^+; 2^+, \dots, n^+) = -i \frac{1}{\langle 23 \rangle \langle 34 \rangle \dots \langle n2 \rangle} \left(-[1|2n|1] + \sum_{2 < i < j < n} [1|ij|1] \right), \tag{6.14}$$

where the summation indices now exclude the two extreme values. This is an expression with $\frac{1}{2}(n-3)(n-4) + 1$ terms, compared to $\frac{1}{2}(n-1)(n-2)$ in the original version.

6.3.3 Single-minus helicity $A_{5:2}^{(1)}(a^-; b^+, c^+, d^+, e^+)$

The five-point one-loop single-minus helicity amplitude $A_{5:2}^{(1)}(a^-; b^+, c^+, d^+, e^+)$ appears when writing down the leading poles of the seven-point two-loop amplitude.

An all- n expression for this partial amplitude was derived in ref. [54]. It bears strong

6 Reconstruction of Rational Functions

resemblance to the all-plus helicity expression. Specialising to our case, we have

$$\begin{aligned}
 A_{5:2}^{(1)}(a^-; b^+, c^+, d^+, e^+) &= -i \frac{1}{\langle bc \rangle \langle cd \rangle \langle de \rangle \langle eb \rangle} \sum_{b \leq i < j \leq e} \langle ai \rangle [ij] \langle ja \rangle \\
 &= -i \frac{1}{\langle bc \rangle \langle cd \rangle \langle de \rangle \langle eb \rangle} (\langle a|bc|a \rangle + \langle a|bd|a \rangle + \langle a|be|a \rangle \\
 &\quad + \langle a|cd|a \rangle + \langle a|ce|a \rangle + \langle a|de|a \rangle).
 \end{aligned} \tag{6.15}$$

Again, linear dependence between the external momenta allows terms to be eliminated, yielding the smaller form

$$A_{5:2}^{(1)}(a^-; b^+, c^+, d^+, e^+) = -i \frac{1}{\langle bc \rangle \langle cd \rangle \langle de \rangle \langle eb \rangle} (\langle a|bc|a \rangle + \langle a|de|a \rangle), \tag{6.16}$$

which we find more convenient for the recursion procedure.

As done in the previous subsection, if we wish to explore factorisations of larger amplitudes then we can build the linear dependence relation into the all- n expression with

$$A_{n:2}^{(1)}(1^-; 2^+, \dots, n^+) = -i \frac{1}{\langle 23 \rangle \langle 34 \rangle \dots \langle n2 \rangle} \left(-\langle 1|2n|1 \rangle + \sum_{2 < i < j < n} \langle 1|ij|1 \rangle \right), \tag{6.17}$$

which reduces the number of terms in the sum.

6.3.4 Single-minus helicity $A_{6:4}^{(1)}(a^-, b^+, c^+; d^+, e^+, f^+)$

The one-loop single-minus partial amplitude $A_{6:4}^{(1)}(a^-, b^+, c^+; d^+, e^+, f^+)$ is of interest when building the leading pole piece of the two-loop seven-point amplitude.

This partial amplitude has not been written in a simple form previously, but can be obtained in terms of the leading-in-colour partial amplitude using decoupling identities.

The expression obtained is

$$\begin{aligned}
 A_{6:4}^{(1)}(a^-, b^+, c^+; d^+, e^+, f^+) = & \\
 & - (A_{6:1}^{(1)}(a, c, b, d, e, f) + A_{6:1}^{(1)}(a, c, d, b, e, f) + A_{6:1}^{(1)}(a, c, d, e, b, f) \\
 & + A_{6:1}^{(1)}(a, d, c, b, e, f) + A_{6:1}^{(1)}(a, d, c, e, b, f) + A_{6:1}^{(1)}(a, d, e, c, b, f) \\
 & + A_{6:1}^{(1)}(a, c, d, e, f, b) + A_{6:1}^{(1)}(a, d, c, e, f, b) + A_{6:1}^{(1)}(a, d, e, c, f, b) \\
 & + A_{6:1}^{(1)}(a, c, e, f, b, d) + A_{6:1}^{(1)}(a, e, c, f, b, d) + A_{6:1}^{(1)}(a, c, f, b, d, e) \\
 & + A_{6:1}^{(1)}(a, d, e, f, c, b) + A_{6:1}^{(1)}(a, e, f, c, b, d) + A_{6:1}^{(1)}(a, f, c, b, d, e) \\
 & + A_{6:1}^{(1)}(a, e, f, c, d, b) + A_{6:1}^{(1)}(a, f, c, d, b, e) + A_{6:1}^{(1)}(a, f, c, d, e, b) \\
 & + A_{6:1}^{(1)}(a, c, b, e, f, d) + A_{6:1}^{(1)}(a, c, e, b, f, d) + A_{6:1}^{(1)}(a, e, c, b, f, d) \\
 & + A_{6:1}^{(1)}(a, c, e, f, d, b) + A_{6:1}^{(1)}(a, e, c, f, d, b) + A_{6:1}^{(1)}(a, c, f, d, b, e) \\
 & + A_{6:1}^{(1)}(a, e, f, d, c, b) + A_{6:1}^{(1)}(a, f, d, c, b, e) + A_{6:1}^{(1)}(a, f, d, c, e, b) \\
 & + A_{6:1}^{(1)}(a, c, b, f, d, e) + A_{6:1}^{(1)}(a, c, f, d, e, b) + A_{6:1}^{(1)}(a, f, d, e, c, b)),
 \end{aligned} \tag{6.18}$$

where the leading in colour (originally obtained in ref. [72]) is

$$\begin{aligned}
 A_{6:1}^{(1)}(a^-, b^+, c^+, d^+, e^+, f^+) = & \\
 & \frac{i}{3} \left(\frac{[f|k_{bc}|a]^3}{[f|k_{ab}|c] \langle ab \rangle \langle bc \rangle \langle de \rangle^2 t_{abc}} + \frac{[b|k_{cd}|a]}{[b|k_{cd}|e] \langle cd \rangle^2 \langle ef \rangle \langle fa \rangle t_{bcd}} \right. \\
 & + \frac{[bf]^3}{[ab][fa] t_{cde}} \left(\frac{[bc][cd]}{[b|k_{cd}|e] \langle de \rangle} - \frac{[de][ef]}{[f|k_{ab}|c] \langle cd \rangle} + \frac{[ce]}{\langle cd \rangle \langle de \rangle} \right) \\
 & - \frac{\langle ac \rangle^3 \langle bd \rangle [bc]}{\langle bc \rangle^2 \langle cd \rangle^2 \langle de \rangle \langle ef \rangle \langle fa \rangle} + \frac{\langle ae \rangle^3 \langle df \rangle [ef]}{\langle ab \rangle \langle bc \rangle \langle cd \rangle \langle de \rangle^2 \langle ef \rangle^2} \\
 & \left. - \frac{[d|k_{bc}|a] \langle ad \rangle^3 \langle ce \rangle}{\langle ab \rangle \langle bc \rangle \langle cd \rangle^2 \langle de \rangle^2 \langle ef \rangle \langle fa \rangle} \right).
 \end{aligned} \tag{6.19}$$

Overall, this representation of the partial amplitude contains many terms and various spurious poles, making it unhelpful as an ingredient in building simple forms of larger amplitudes. In particular, the double poles and t -poles inherited from the leading-in-colour expression are spurious when they appear in $A_{6:4}^{(1)}(a^-, b^+, c^+; d^+, e^+, f^+)$, which does not show those structures under pole tests.

We can carry out pole tests to determine which structures are permitted in a form of the partial amplitude free of spurious poles. Testing individual spinor products, we

6 Reconstruction of Rational Functions

find poles in

$$\langle ab \rangle, \langle bc \rangle, \langle cd \rangle, \langle de \rangle, \langle ef \rangle, \langle ac \rangle, \langle bd \rangle, \langle be \rangle, \langle bf \rangle, \langle ce \rangle, \langle cf \rangle, \langle df \rangle, \\ [ab], [ac], \quad (6.20)$$

appearing as simple poles at most. There are no t -poles present and for a six-point one-loop amplitude, we require an overall weight of -2 in spinor products. Inspecting symmetries, we note that

$$A_{6:4}^{(1)}(a^-, b^+, c^+; d^+, e^+, f^+) = -A_{6:4}^{(1)}(a^-, c^+, b^+; d^+, e^+, f^+), \\ A_{6:4}^{(1)}(a^-, b^+, c^+; d^+, e^+, f^+) = -A_{6:4}^{(1)}(a^-, b^+, c^+; e^+, d^+, f^+). \quad (6.21)$$

There is also the usual cyclic symmetry of the (second) momentum set

$$A_{6:4}^{(1)}(a^-, b^+, c^+; d^+, e^+, f^+) = A_{6:4}^{(1)}(a^-, b^+, c^+; e^+, f^+, d^+) = A_{6:4}^{(1)}(a^-, b^+, c^+; f^+, d^+, e^+). \quad (6.22)$$

To make these symmetries manifest in the simplified amplitude, we will build them into the ansatz as sums over an appropriate basis function.

In theory, the ansatz basis could be chosen to include all the types of pole found in the amplitude, guaranteeing it would find a match to the structure. However, this ansatz would be impractically large - to reach the correct overall spinor weight, the numerator terms would each need to contain 12 spinor products to account for the 14 in the denominator. An ansatz containing all the linearly independent numerator terms of this size, which satisfy the little group scaling, would be tens of thousands of terms long and could not be evaluated in any reasonable time on a standard computer. Solving the system of ansatz equations for the unknowns would also require excessive memory usage.

Instead of this, we will choose simpler ansatz bases, consisting of one or more denominator choices that do not contain every individual pole. This can still represent every pole overall, because many poles are equivalent under the sums that we apply to the basis to enforce symmetries. However, we no longer have a guarantee that the ansatz will capture the amplitude so will in general have to test multiple ansatz denominator choices. One principle that helps when picking denominators is to look to the structures of known compact amplitudes for common patterns, then incorporating these into the

Diverging poles:	$\langle 1 2 \rangle \langle 1 3 \rangle \langle 2 3 \rangle$	$\langle 1 2 \rangle \langle 3 4 \rangle$	$\langle 1 2 \rangle [1 2]$
Weight -2	$\langle b c \rangle \langle b d \rangle \langle c d \rangle$ $\langle c d \rangle \langle c e \rangle \langle d e \rangle$ $\langle d e \rangle \langle d f \rangle \langle e f \rangle$ $\langle b d \rangle \langle b e \rangle \langle d e \rangle$	$\langle a b \rangle \langle c d \rangle$ $\langle a b \rangle \langle d e \rangle$ $\langle b c \rangle \langle d e \rangle$	
Weight -1	$\langle a b \rangle \langle a d \rangle \langle b d \rangle$ $\langle a d \rangle \langle a e \rangle \langle d e \rangle$	$\langle a d \rangle \langle b e \rangle$ $\langle b d \rangle \langle c f \rangle$	$\langle a b \rangle [a b]$
Weight 0	$\langle a b \rangle \langle a c \rangle \langle b c \rangle$		

Table 6.1: Results of numerical pole tests on $A_{6:4}^{(1)}(a^-, b^+, c^+; d^+, e^+, f^+)$, to find coinciding poles. Column headings indicate the type of poles that are taken to be small. Each entry is a specific group of poles and their greatest total weight in the amplitude. For example, an entry with “weight -1 ” means that of that group of spinor products, only one can occur as a pole in a given term, or two can occur as poles if the third group member (where applicable) is in the numerator.

ansatz. An example of this would be to try the Parke–Taylor denominator,

$$\frac{1}{\langle 1 2 \rangle \langle 2 3 \rangle \cdots \langle (n-1) n \rangle \langle n 1 \rangle}, \quad (6.23)$$

which is a common denominator for leading in colour partial amplitudes, but can also occur over a cyclic subset of the momenta $\{1, 2, \dots, n\}$ in a sub-leading in colour partial amplitude.

To constrain which poles appear together in a term, we can also run numerical pole tests where multiple spinor products become small simultaneously. Those combinations which do not appear together can then be removed from the denominator choice without accidentally excluding any required structures.

The symmetries in the arguments of the amplitude mean that only a subset of all the possible pole combinations must be tested, the results of which are recorded in Table 6.1. We are unable to check some combinations without other spinor products also being made small, which is why the three spinor product combination $\langle 1 2 \rangle \langle 2 3 \rangle \langle 1 3 \rangle$ is used. The strongest constraint found is the “weight 0” on the group $\langle a b \rangle \langle a c \rangle \langle b c \rangle$, meaning that one of these poles can appear in a term only if it is accompanied by at least one of the other group members as a numerator factor. In comparison, the “weight -2 ” result for $\langle a b \rangle \langle c d \rangle$ means that these poles can and do occur together in some terms of the amplitude.

6 Reconstruction of Rational Functions

Various ansatz denominators can be chosen that are in keeping with this set of rules. The following five ansatzes were tested against the amplitude:

$$\begin{aligned}
& \sum_{Z_3(def)} \sum_{[bc]} \sum_{[de]} \frac{G_1}{\langle ab \rangle \langle bc \rangle \langle cd \rangle \langle de \rangle \langle ef \rangle [ac]}, \\
& \sum_{Z_3(def)} \sum_{[bc]} \sum_{[de]} \frac{G_2}{\langle ab \rangle \langle bd \rangle \langle bf \rangle \langle cd \rangle \langle de \rangle \langle ef \rangle [ac]}, \\
& \sum_{Z_3(def)} \sum_{[bc]} \sum_{[de]} \frac{G_3}{\langle ab \rangle \langle bc \rangle \langle bd \rangle \langle cd \rangle \langle de \rangle \langle ef \rangle \langle fb \rangle [ac]}, \\
& \sum_{Z_3(def)} \sum_{[bc]} \sum_{[de]} \frac{G_4}{\langle ab \rangle \langle bc \rangle \langle cd \rangle \langle de \rangle \langle ef \rangle \langle fd \rangle [ac]}, \\
& \sum_{Z_3(def)} \sum_{[bc]} \sum_{[de]} \frac{G_5}{\langle ab \rangle \langle bc \rangle \langle cd \rangle \langle de \rangle \langle ef \rangle [ab] [ac]}, \tag{6.24}
\end{aligned}$$

where the sums are over the antisymmetric and cyclic momentum symmetries identified in equations 6.21 and 6.22. The antisymmetric sum notation,

$$\sum_{[bc]} f(\dots, b, c, \dots) \equiv f(\dots, b, c, \dots) - f(\dots, c, b, \dots), \tag{6.25}$$

is introduced as a shorthand for the former type of symmetry. Each G represents a complete linearly independent set of spinor product numerators with unknown coefficients, satisfying overall momentum weight and little group requirements. The ansatzes are not exhaustive – some combinations of poles occurring together are not represented. However, they do contain every non-spurious pole identified in the amplitude, either explicitly or as a result of the summation.

The first four ansatzes do not give rational coefficient solutions, which we interpret as a sign that the ansatz is missing pole structures present in the amplitude. The fifth ansatz succeeds, needing only a relatively small basis of 45 terms.

We write the partial amplitude, using the results of ansatz fitting, as

$$A_{6:4}^{(1)}(a^-, b^+, c^+; d^+, e^+, f^+) = \sum_{Z(def)} \sum_{[bc]} \sum_{[de]} \frac{iG_{6:1}^{sm}}{\langle ab \rangle \langle bc \rangle \langle cd \rangle \langle de \rangle \langle ef \rangle [ab] [ac]}, \tag{6.26}$$

where

$$\begin{aligned}
 G_{6:4}^{sm} = & -2[b|c|a\rangle \langle b d| [b f] [c d] - 2[c|k_{ef}|c\rangle \langle a d| [b f] [c d] \\
 & - 2[c|k_{de}|a\rangle \langle c d| [b d] [c f] + [c|k_{bef}|a\rangle \langle c d| [b c] [d f] \\
 & - [c|e|a\rangle \langle c d| [b d] [c f].
 \end{aligned} \tag{6.27}$$

The new expression is very compact and contains only genuine poles – the spurious poles of the decoupling version have been removed. The symmetries have been made manifest, in the form of summations over a basis. The pole structure now takes a simple, almost Parke–Taylor form. These are useful features for an amplitude used as a recursion ingredient, but also interesting in their own right as the structure of the partial amplitude is seen more clearly. An n -point form for this type of partial amplitude appears quite achievable given the form seen here.

6.4 Seven-Point Two-Loop Rational Pieces

The augmented recursion procedure used to find the rational part of the full colour two-loop seven-point all-plus amplitude $R_{7:\lambda}^{(2)}(a^+, b^+, c^+, d^+, e^+, f^+, g^+)$ was described in Chapter 4. The outcome of this is a set of analytic, but large, expressions for each partial amplitude. There is also a reference momentum q present in the expressions, although the overall function has no dependence on it, so we refer to the rational pieces as $R_{7:\lambda}^{(2),q}$.

We would like to reconstruct the $R_{7:\lambda}^{(2),q}$ in new, compact forms for several reasons:

- The amplitude should be written in a human-readable way, so that symmetries of the theory are manifest.
- The expressions are large and unwieldy, occupying large amounts of computer memory when loaded and taking significant time to evaluate numerically on a single kinematic point.
- The functions have no overall dependence on the reference momentum q , but factors of q appear in the detailed forms of $R_{7:\lambda}^{(2),q}$. Such a dependence is spurious and should not appear.

The approximate sizes of the $R_{7:\lambda}^{(2),q}$ can be found in Table 6.2. The six-point amplitude could be expressed analytically in a few pages [59], so we infer that something similar

6 Reconstruction of Rational Functions

	$R_{7:1}^{(2),q}$	$R_{7:2}^{(2),q}$	$R_{7:3}^{(2),q}$	$R_{7:4}^{(2),q}$	$R_{7:1,1}^{(2),q}$	$R_{7:1,2}^{(2),q}$	$R_{7:1,3}^{(2),q}$	$R_{7:2,2}^{(2),q}$	$R_{7:1B}^{(2),q}$
File size / MB	4.64	28.8	50.6	115	116	349	406	345	162
Memory usage / MB	38.8	240	414	976	960	2920	3400	2810	1290
LeafCount/ 10^6	1.44	8.94	15.5	35.9	35.7	108	126	104	48.5
Evaluation time / s	13.3	77.5	146	436	323	1110	1270	1030	434

Table 6.2: Approximate expression sizes for the seven-point rational pieces calculated using augmented recursion. Recorded are the size for a Mathematica file storing each expression in terms of spinor products, the size of that function when loaded into memory, and the Mathematica `LeafCount` value. Evaluation time for one choice of numerical momentum values is also checked. (To a precision of 70 figures, using a 2.60 GHz processor.)

should be possible for the seven-point amplitude. It is clear that what the augmented recursion process outputs is not the most efficient description of an amplitude possible. Rather, recursion builds expressions from many contributions, each one being a potentially complicated object like an integrated current diagram. When increasing the number of gluons considered, even by a modest step of six to seven, the size of results can increase by orders of magnitude due to the compounded effects of needing to include more recursion contributions, and the greater complexity of each of those contributions.

We confirm that the rational pieces $R_{7:\lambda}^{(2),q}$ satisfy the decoupling identities of Section 4.2.1. With that, we can sidestep having to do further work on the worst partial amplitude expressions, instead expressing them via those identities, in terms of the other structures. For example, we could express all the $U(N_c)$ partial amplitudes in terms of the subset of the purely $SU(N_c)$ structures

$$R_{7:1}^{(2),q}, R_{7:3}^{(2),q}, R_{7:4}^{(2),q}, R_{7:1B}^{(2),q}, \quad (6.28)$$

so that it is only necessary to reconstruct these four in compact forms to obtain the whole amplitude.

In fact, we choose to reconstruct the $U(N_c)$ partial amplitude $R_{7:1,1}^{(2)}$ instead of $R_{7:3}^{(2)}$. Pole tests show that $R_{7:3}^{(2)}$ contains t -poles as well as double angle bracket poles, but $R_{7:1,1}^{(2)}$ is simpler with only t -poles and simple angle bracket poles. We can write $R_{7:3}^{(2)}$ in terms of $R_{7:1}^{(2)}$ and $R_{7:1,1}^{(2)}$ via a decoupling identity, so the two are equivalent for our

purposes. The set of interest is then

$$R_{7:1}^{(2),q}, R_{7:1,1}^{(2),q}, R_{7:4}^{(2),q}, R_{7:1B}^{(2),q}. \quad (6.29)$$

A compact form for $R_{7:1}^{(2)}$ was already found in ref. [60] and a compact form for $R_{7:1B}^{(2)}$ can be written down from the n -point postulate of ref. [63]. Therefore we focus our attention on reconstructing $R_{7:1,1}^{(2),q}$ and $R_{7:4}^{(2),q}$, detailed in the two sections that follow.

6.5 Seven-Point Rational Piece $R_{7:1,1}^{(2)}$

We aim to fit the reference-momentum-containing rational piece $R_{7:1,1}^{(2),q}$ to a compact, symmetric form. To simplify the problem, we first deal with the leading poles by hand, which can be written down from factorisations. The sub-leading poles are fitted to an ansatz.

6.5.1 Augmented recursion output

The output of augmented recursion is an analytic expression for $R_{7:1,1}^{(2),q}$, but in a large and inefficient form that makes investigating its properties difficult. The Mathematica code used to generate the expression can be modified to not expand terms all the way down to their constituent spinors, to create a somewhat smaller result written in terms of spinor products. For the case of $R_{7:1,1}^{(2),q}$, this leads to a 116 MB Mathematica file. This version of the expression contains 6782 terms and occupies 960 MB when in memory.

Given the number of recursion contributions involved, it is likely that the result contains various repeated terms, which may not have been condensed in the summation, inflating its apparent size. Checking for these reveals more than half of the expression consists of duplicate terms. Once condensed, only 3032 terms remain in the expression.

Another possibility is that some collections of terms cancel completely, so can be removed from the expression entirely. Checking for and removing cancelling pairs further reduces the expression to 2528 terms. The possibility of a Schouten identity taking place suggests that groups of three terms could experience cancellation, however no such sets are found. Checking for larger cancelling sets is too computationally expensive, because the search time scales exponentially with the number of terms.

The new $R_{7:1,1}^{(2),q}$ has a file size of 27 MB, or occupies 231 MB in memory. One numerical evaluation (on an i7, 2.60 GHz processor) takes one minute, which is an improvement on the five minutes taken by the larger expression in proportion with the reduction in file size.

6 Reconstruction of Rational Functions

We briefly perform the same expression size checks on $R_{7:3}^{(2),q}$. Given its close relationship with $R_{7:1,1}^{(2),q}$ via decoupling identities, there may be some benefit to using it in some tasks if it has a more efficient form. The initial spinor product expression for the rational piece is a 50.6 MB file, containing 2824 terms and occupying 414 MB in memory. After condensing repeated terms, 1326 terms remain. Finally, removing three cancelling pairs leaves 1320 terms, in an expression for $R_{7:3}^{(2),q}$ that is 25 MB on file and occupies 200 MB in memory. One numerical evaluation of the new expression takes one minute, compared to the two minutes taken by the original.

6.5.2 Pole tests

Numerical tests are run on $R_{7:1,1}^{(2),q}$ to identify the types of pole which are present. By arranging multiple spinor products to become small simultaneously, information on which combinations of permitted poles occur in the same terms of the amplitude can also be tested.

The partial amplitude has an overall $\mathcal{P}_{7:1,1}$ symmetry, meaning that if a pole such as $\langle bc \rangle$ is present, then so is $\langle ac \rangle$, $\langle bd \rangle$, etc. We can make use of this fact to reduce the number of pole tests that need to be run, and express the results in a simple way where we record only one of each equivalent pole or combination type, leaving the rest as implied.

The poles present are

$$t_{bcd}, \langle bc \rangle, \langle cd \rangle \tag{6.30}$$

and those which are as equivalent under the $\mathcal{P}_{7:1,1}$ symmetry. As mentioned previously, this set of poles is significantly simpler than that of $R_{7:3}^{(2),q}$. There are no double poles present, and poles in $\langle ab \rangle$ also do not occur. Multi-pole tests show that up to two t -poles can occur in the same term, in a specific configuration $t_{aef}t_{bcd}$ where the momenta sets involved do not overlap. Other configurations are not permitted.

6.5.3 Leading pole factorisations

The leading poles in $R_{7:1,1}^{(2),q}$ can be obtained from factorisations involving $R_4^{(1)} - R_5^{(1)}$, where the propagator creates a t -pole.

Those amplitudes must be colour dressed and multiplied, joining the colour traces using matrix identities. Terms that contain the overall colour structure of interest are selected, which in this case are the factorisations accompanying the $U(N_c)$ structure

$\text{Tr}[T^a]\text{Tr}[T^b]\text{Tr}[T^cT^dT^eT^fT^g]$.

We will work with basis expressions, which then have a $\mathcal{P}_{7:1,1}$, or $Z_2(a, b)Z_5(c, d, e, f, g)$, sum applied to reproduce the known symmetry of the amplitude. In this case, the leading t -poles are denoted by

$$F_{7:1,1} = \sum_{\mathcal{P}_{7:1,1}} B_{7:1,1}, \quad (6.31)$$

where the basis function built from factorisations is

$$\begin{aligned} B_{7:1,1} = & A_{4:2}^{(1),ap}(b, c, d, -k_{bcd}^+) \frac{i}{t_{bcd}} A_{5:2}^{(1),sm}(a, k_{bcd}^-, e, f, g) \\ & + A_{4:2}^{(1),sm}(b, -k_{bcd}^-, c, d) \frac{i}{t_{bcd}} A_{5:2}^{(1),ap}(a, k_{bcd}^+, e, f, g). \end{aligned} \quad (6.32)$$

Testing the factorisations

Pole tests confirm that $F_{7:1,1}$ contains the desired t -poles, which are what we consider to be the leading poles in this case. It is also likely that spurious poles have been introduced by the factorisation, which are not present in the amplitude itself.

Inserting the amplitudes into the factorisation, spinor products containing nullified k_{bcd}^b appear. Joining these into larger spinor structures such as $[x|k_{bcd}|y\rangle$ allows the k to be expressed in its non-nullified form. The extra piece from the nullification identity contains a $k_{bcd}^2 = t_{bcd}$ factor which cancels the pole, so can be ignored.

Where $[x|k_{bcd}|y\rangle$ appear in the denominator, they represent spurious poles, which we must identify and attempt to remove. The $A_{4:2}^{(1),sm}(b, -k_{bcd}^-, c, d)$ piece in particular introduces spurious poles stemming from $[b|k_{bcd}]$, $[c|k_{bcd}]$ and $[d|k_{bcd}]$. Some of these happen to be removable by using four-point manipulations, such as

$$s_{bd} = -[c|k_{bcd}]\langle k_{bcd}|c\rangle + \mathcal{O}(t_{bcd}), \quad (6.33)$$

to express new factors of the spurious structure in the numerator, keeping only the terms relevant to the leading poles. However, it can be seen that removing this spurious pole type is in fact trivial wherever it appears, by using a manipulation such as

$$\frac{1}{[b|k_{bcd}]} = \frac{\langle k_{bcd}|d\rangle}{[b|k_{bcd}]\langle k_{bcd}|d\rangle} = \frac{\langle k_{bcd}|d\rangle}{[b|k_{bcd}|d]} + \mathcal{O}(t_{bcd}) = \frac{\langle k_{bcd}|d\rangle}{[b|c]\langle c|d\rangle} + \mathcal{O}(t_{bcd}). \quad (6.34)$$

This way of removing spurious poles is guaranteed to be applicable for any number of gluons up to six-point amplitudes.

However, we see that it fails for some spurious poles in the seven-point factorisation,

6 Reconstruction of Rational Functions

due to the additional momentum in the zero total momentum sum. Specifically, spurious poles occur in the factorisation basis that are of the type $[g|k_{bcd}|g\rangle$ and $[e|k_{bcd}|e\rangle$. These spurious poles are non-trivial to remove, in a way that has not occurred previously in our derivations. Attempting a manipulation like in eq. 6.34 on one of the problematic spinor products,

$$\frac{1}{[g|k_{bcd}]} = \frac{\langle k_{bcd}|e\rangle}{[g|k_{bcd}]\langle k_{bcd}|e\rangle} = \frac{\langle k_{bcd}|e\rangle}{[g|k_{bcd}|e]} + \mathcal{O}(t_{bcd}) = -\frac{\langle k_{bcd}|e\rangle}{[g|k_{af}|e]} + \mathcal{O}(t_{bcd}), \quad (6.35)$$

we are unable to create a non-spurious denominator. New approaches will be needed to remove these factors.

After performing some simplifying manipulations, including removing all spurious poles of a trivial type, the basis containing the t_{bcd} poles can be written as

$$B_{7:1,1} = B_{711}^{nsp} + B_{711}^{spE} + B_{711}^{spG}, \quad (6.36)$$

where the remaining spurious poles have been separated as much as possible and collected by type.

We have

$$B_{711}^{nsp} = i \frac{num_{nsp}}{t_{bcd} \langle bc \rangle \langle cd \rangle \langle ef \rangle \langle fg \rangle \langle ae \rangle \langle af \rangle \langle ag \rangle} - i \frac{([be][dg] + [bg][de])[ag]}{t_{bcd} \langle af \rangle \langle bc \rangle \langle cd \rangle \langle ef \rangle}, \quad (6.37)$$

$$B_{711}^{spE} = \frac{i}{[e|k_{bcd}|e]} \frac{[ag][bd][a|k_{bcde}|b][e|k_{bcd}|d]}{t_{bcd} \langle bc \rangle \langle cd \rangle \langle ef \rangle \langle fg \rangle} \frac{1}{\langle db \rangle} + \frac{i}{[e|k_{bcd}|e]} \frac{num_{spE}}{t_{bcd} \langle bc \rangle \langle cd \rangle \langle ef \rangle \langle fg \rangle} \frac{1}{\langle ae \rangle \langle af \rangle \langle ag \rangle} \quad (6.38)$$

and

$$B_{711}^{spG} = \frac{i}{[g|k_{bcd}|g]} \frac{[ae][bd][a|k_{bcdg}|b][g|k_{bcd}|d]}{t_{bcd} \langle bc \rangle \langle cd \rangle \langle ef \rangle \langle fg \rangle} \frac{1}{\langle db \rangle} + \frac{i}{[g|k_{bcd}|g]} \frac{num_{spG}}{t_{bcd} \langle bc \rangle \langle cd \rangle \langle ef \rangle} \frac{1}{\langle ae \rangle \langle af \rangle \langle ag \rangle}, \quad (6.39)$$

with numerators

$$\begin{aligned}
 num_{nsp} = & - [b|k_{bcd}|a\rangle [d|k_{bcd}|e\rangle \langle a f \rangle [a e] \\
 & - [b|k_{bcd}|f\rangle [d|k_{bcd}|a\rangle \langle e g \rangle [e g] \\
 & + [b|k_{bcd}|f\rangle [d|k_{bcd}|g\rangle \langle a e \rangle [e g], \tag{6.40}
 \end{aligned}$$

$$\begin{aligned}
 num_{spE} = & - [g|k_{bcd}|e\rangle [b e] [d e] \langle a e \rangle \langle f g \rangle s_{ag} \\
 & - [b|k_{bcd}|a\rangle [d|k_{bcd}|a\rangle \langle e f \rangle s_{eg} [a e] \\
 & - [b|k_{bcd}|a\rangle [d|k_{bcd}|e\rangle \langle f g \rangle s_{ae} [e g] \\
 & - [b|k_{bcd}|a\rangle [d|k_{bcd}|f\rangle \langle a e \rangle \langle f g \rangle [a f] [e g] \\
 & - [b|k_{bcd}|a\rangle [d|k_{bcd}|e\rangle \langle f g \rangle s_{eg} [e g] \\
 & - [b|k_{bcd}|g\rangle [d|k_{bcd}|e\rangle \langle a e \rangle \langle f g \rangle [e g]^2 \\
 & - [b|k_{bcd}|a\rangle [d|k_{bcd}|f\rangle [g|k_{bcd}|g\rangle s_{ae} \tag{6.41}
 \end{aligned}$$

and

$$\begin{aligned}
 num_{spG} = & - [e|k_{bcd}|g\rangle \langle a e \rangle [b g] [d g] s_{ag} \\
 & - [b|k_{bcd}|a\rangle [d|k_{bcd}|a\rangle [g|k_{bcd}|e\rangle [a e]. \tag{6.42}
 \end{aligned}$$

A notable detail is that although the full rational piece contains pole structures like $t_{bcd}t_{aef}$, and numerical tests confirm that our factorisation captures the leading pole behaviour, we do not see any explicit factors of $t_{bcd}t_{aef}$ in the denominators. Instead, we see structures like $t_{bcd}[g|k_{bcd}|g\rangle$, which contain only one explicit t -pole and one spurious pole.

Why this still gives the correct pole behaviour for t_{bcd} is that as t_{bcd} becomes small,

$$[g|k_{bcd}|g\rangle = t_{bcdg} - t_{bcd} = t_{aef} - t_{bcd} \rightarrow t_{aef}, \tag{6.43}$$

the spurious poles behave like regular t -poles.

Separating spurious poles from leading poles

It is found that the factorisation basis contains terms of the form

$$B_{7:1,1} \sim \frac{1}{t_{bcd}[g|k_{bcd}|g\rangle}, \tag{6.44}$$

6 Reconstruction of Rational Functions

which reproduce the t -pole behaviour without containing the expected pairs of t -poles explicitly.

The factorisation must reproduce all the same (t -pole containing) terms that appear in the amplitude itself, so there must exist a way of re-expressing the summed factorisation so that it contains manifest double t -pole terms. Hence, it can be inferred that the total factorisation is equivalent to a form schematically written as

$$F_{7:1,1} \sim \sum_{\mathcal{P}_{7:1,1}} \left(\frac{1}{t_{bcd}t_{aef}} + \frac{1}{t_{bcd}} + \frac{1}{[g|k_{bcd}|g]} \right), \quad (6.45)$$

with appropriate numerators. There must be terms that explicitly contain two t -pole structures, as well as terms containing only one, which can be identified with the terms detected in the amplitude. Spurious poles do not appear in the amplitude, so any spurious poles in $F_{7:1,1}$ must appear in separate terms to the t -poles.

How this separation comes about is of interest to us. We would like to identify whatever cancellations take place after the sum is applied, then use manipulations that allow them to take place at the basis stage. With that, the spurious poles can be discarded to leave only a compact form for the leading poles. And those poles would appear underneath an explicit sum in the overall expression, making the symmetry of the structure manifest.

The equivalence of the spurious poles to differences of t -poles, such as $[g|k_{bcd}|g] = t_{aef} - t_{bcd}$, offers a potential removal method. Series expanding in the leading t_{bcd} pole, which we consider to be small, gives

$$\begin{aligned} \frac{1}{t_{bcd}[g|k_{bcd}|g]} &= \frac{1}{t_{bcd}(t_{aef} - t_{bcd})} = \frac{1}{t_{bcd}t_{aef}} \left(1 - \frac{t_{bcd}}{t_{aef}} \right)^{-1} \\ &= \frac{1}{t_{bcd}t_{aef}} \left(1 + \frac{t_{bcd}}{t_{aef}} + \frac{t_{bcd}^2}{t_{aef}^2} + \dots \right) \\ &= \frac{1}{t_{bcd}t_{aef}} + \frac{1}{t_{aef}^2} + \frac{t_{bcd}}{t_{aef}^3} + \dots \\ &= \frac{1}{t_{bcd}t_{aef}} + \mathcal{O}(t_{bcd}^0). \end{aligned} \quad (6.46)$$

It is tempting to discard the terms of $\mathcal{O}(t_{bcd}^0)$ in the final step, leaving only the non-spurious structure. This does maintain the correct pole behaviour in the basis when t_{bcd} becomes small, but at the expense of incorrect pole behaviour in the summed

factorisation $F_{7:1,1}$. This happens because the $\mathcal{O}(t_{bcd}^0)$ terms contain poles in t_{aef} , which is also leading. Once the $\mathcal{P}_{7:1,1}$ sum is applied, there are terms where t_{aef} poles become t_{bcd} poles with the rotated momentum assignment. So removing any specific t -pole from the basis amounts to modifying the behaviour of all t -poles in the summed factorisation, which we cannot do if we wish to retain agreement with the amplitude.

Various ansatzes are also tested, where an attempt is made to fit the factorisation $F_{7:1,1}$ to a structure with separated spurious poles, of the form shown in eq. 6.45. The presence of up to two t -poles in a term leads to very large ansatzes being required, on account of there being many possible permutations of the numerator factor needed to balance the high spinor weight in the denominator. Even running ansatzes with on the order of 10 000 terms, a successful fit is not found, likely because those ansatzes still omit many pole combinations.

The importance of, and complications introduced by, the presence of $t_{bcd}t_{aef}$ pole structures in the amplitude motivates us to consider whether our choice to have the basis contain all t_{bcd} poles is the most appropriate. A more symmetric basis might contain the $t_{bcd}t_{aef}$ term and equal parts t_{bcd} and t_{aef} terms, at the expense of not fully capturing the pole behaviour for either structure. The full behaviour at each pole would then only be regained after all the contributions to the $\mathcal{P}_{7:1,1}$ sum are collected.

A separate line of logic also leads to such a structure. In order for the spurious pole terms to separate from the t -pole terms, as in eq. 6.45, then in general some interaction must take place between all terms containing a certain type of spurious pole. Therefore if we want this separation to be manifest at the basis level, then we must collect all the spurious poles of a particular type in one basis. The overall sum allows us to freely rotate the arguments of any given term in the basis according to the $\mathcal{P}_{7:1,1}$ symmetry. Doing so will cause the basis to no longer represent the full t_{bcd} pole behaviour, but will allow us to arrange for only one spurious structure to appear in the denominator of the basis.

Choosing $[g|k_{bcd}|g\rangle$ to be the spurious pole we wish to target, a change of

$$B_{7:1,1}^{spE} \rightarrow B_{7:1,1}^{spG2} \equiv B_{7:1,1}^{spE}(b, a, e, f, g, c, d) \quad (6.47)$$

is made under the sum. The new basis contains only one type of spurious pole, which is exclusive to this part of the overall sum. Numerical tests confirm that even without applying the overall $\mathcal{P}_{7:1,1}$ factorisation sum, the pieces containing the spurious pole,

$$B_{711}^{2-t} = B_{711}^{spG} + B_{711}^{spG2}, \quad (6.48)$$

6 Reconstruction of Rational Functions

resolve to something of the form

$$B_{711}^{2-t} \sim \frac{1}{t_{bcd}t_{aef}} + \frac{1}{t_{bcd}} + \frac{1}{t_{aef}} + \frac{1}{[g|k_{bcd}|g]} \quad (6.49)$$

with appropriate factors in the numerators and denominators. The desired separation of spurious poles from t -poles that occurred in $F_{7:1,1}$ has been arranged to take place at the earlier stage of the basis $B_{7:1,1}$. Tests show that $B_{7:1,1}$ contains the two t -pole term, but no longer captures all t_{bcd} poles, instead mixing t_{bcd} and t_{aef} . The remaining task is to perform this manipulation explicitly, to obtain the leading poles of the rational piece in a symmetric form, manifestly free of spurious poles.

The new basis, written out in full, is

$$B_{711} = B_{711}^{nsp} + B_{711}^{spG} + B_{711}^{spG2}, \quad (6.50)$$

where

$$B_{711}^{nsp} = i \frac{num_{nsp}}{t_{bcd} \langle bc \rangle \langle cd \rangle \langle ef \rangle \langle fg \rangle \langle ae \rangle \langle af \rangle \langle ag \rangle} - i \frac{([be][dg] + [bg][de])[ag]}{t_{bcd} \langle af \rangle \langle bc \rangle \langle cd \rangle \langle ef \rangle}, \quad (6.51)$$

$$B_{711}^{spG} = \frac{i}{[g|k_{bcd}|g]} \frac{[ae][bd][a|k_{bcdg}|b][g|k_{bcd}|d]}{t_{bcd} \langle bc \rangle \langle cd \rangle \langle ef \rangle \langle fg \rangle \langle db \rangle} + \frac{i}{[g|k_{bcd}|g]} \frac{num_{spG}}{t_{bcd} \langle bc \rangle \langle cd \rangle \langle ef \rangle \langle ae \rangle \langle af \rangle \langle ag \rangle} \quad (6.52)$$

and

$$B_{711}^{spG2} = \frac{i}{t_{aef}[g|k_{aef}|g]} \frac{[af][bd][b|k_{aefg}|a][g|k_{aef}|f]}{\langle ae \rangle \langle af \rangle \langle cd \rangle \langle ef \rangle \langle gc \rangle} + \frac{i}{t_{aef}[g|k_{aef}|g]} \frac{num_{spG2}}{\langle ae \rangle \langle bc \rangle \langle bd \rangle \langle bg \rangle \langle cd \rangle \langle ef \rangle \langle gc \rangle}, \quad (6.53)$$

with numerators

$$\begin{aligned}
 num_{nsp} = & - [b|k_{bcd}|a][d|k_{bcd}|e] \langle a f \rangle [a e] \\
 & - [b|k_{bcd}|f][d|k_{bcd}|a] \langle e g \rangle [e g] \\
 & + [b|k_{bcd}|f][d|k_{bcd}|g] \langle a e \rangle [e g], \tag{6.54}
 \end{aligned}$$

$$\begin{aligned}
 num_{spG} = & - [e|k_{bcd}|g] \langle a e \rangle [b g] [d g] s_{ag} \\
 & - [b|k_{bcd}|a][d|k_{bcd}|a][g|k_{bcd}|e] [a e] \tag{6.55}
 \end{aligned}$$

and

$$\begin{aligned}
 num_{spG2} = & - s_{bd} \langle b g \rangle \langle c d \rangle [a g] [f g] [d|k_{aef}|g] \\
 & - s_{gd} \langle g c \rangle [b g] [a|k_{aef}|b][f|k_{aef}|b] \\
 & - \langle b g \rangle \langle c d \rangle [b c] [g d] [a|k_{aef}|b][f|k_{aef}|c] \\
 & - s_{bg}[a|k_{aef}|b][d|k_{aef}|d][f|k_{aef}|c] \\
 & - s_{bg} \langle c d \rangle [g d] [a|k_{aef}|b][f|k_{aef}|g] \\
 & - s_{gd} \langle c d \rangle [g d] [a|k_{aef}|b][f|k_{aef}|g] \\
 & - \langle b g \rangle \langle c d \rangle [g d]^2 [a|k_{aef}|d][f|k_{aef}|g]. \tag{6.56}
 \end{aligned}$$

Leading poles t_{bcd} and t_{aef} are present, although their overlap term containing a $t_{bcd}t_{aef}$ denominator factor is not yet explicit. The spurious poles present are all of the same type, $[g|k_{bcd}|g] = -[g|k_{aef}|g]$.

Manipulations to clear spurious poles

Manipulations are carried out to express the basis in a clear, spurious-pole-free form. By inserting an expression equivalent to the identity into B_{711}^{spG} ,

$$1 = \frac{t_{aef}}{t_{aef}} = \frac{t_{bcd} + [g|k_{bcd}|g]}{t_{aef}}, \tag{6.57}$$

that basis piece yields terms explicitly containing two t -poles. Other terms produced containing one spurious pole and one t -pole are of the same type as appear in B_{711}^{spG2} , namely their denominators contain $t_{aef}[g|k_{bcd}|g]$.

Redefining the pieces of the basis, we collect all those spurious poles in the same

6 Reconstruction of Rational Functions

piece with

$$B_{711} = B_{711}^{nsp} + B_{711}^{nsp t} + B_{711}^{sp}, \quad (6.58)$$

where

$$B_{711}^{nsp} = i \frac{num_{nsp}}{t_{bcd} \langle bc \rangle \langle cd \rangle \langle ef \rangle \langle fg \rangle \langle ae \rangle \langle af \rangle \langle ag \rangle} - i \frac{([be][dg] + [bg][de])[ag]}{t_{bcd} \langle af \rangle \langle bc \rangle \langle cd \rangle \langle ef \rangle}, \quad (6.59)$$

$$B_{711}^{nsp t} = \frac{i}{t_{aef} t_{bcd}} \frac{[ae][bd][a|k_{bcd}g|b][g|k_{bcd}|d]}{\langle bc \rangle \langle cd \rangle \langle ef \rangle \langle fg \rangle} \frac{1}{\langle db \rangle} + \frac{i}{t_{aef} t_{bcd}} \frac{num_{spG}}{\langle bc \rangle \langle cd \rangle \langle ef \rangle \langle ae \rangle \langle af \rangle \langle ag \rangle} \frac{1}{\langle db \rangle} \quad (6.60)$$

and

$$B_{711}^{sp} = - \frac{i}{t_{aef}[g|k_{bcd}|g]} \frac{[af][bd][b|k_{aefg}|a][g|k_{aef}|f]}{\langle ae \rangle \langle af \rangle \langle cd \rangle \langle ef \rangle \langle gc \rangle} - \frac{i}{t_{aef}[g|k_{bcd}|g]} \frac{num_{spG2}}{\langle ae \rangle \langle bc \rangle \langle bd \rangle \langle bg \rangle \langle cd \rangle \langle ef \rangle \langle gc \rangle} + \frac{i}{t_{aef}[g|k_{bcd}|g]} \frac{[ae][bd][a|k_{bcd}g|b][g|k_{bcd}|d]}{\langle bc \rangle \langle cd \rangle \langle ef \rangle \langle fg \rangle} \frac{1}{\langle db \rangle} + \frac{i}{t_{aef}[g|k_{bcd}|g]} \frac{num_{spG}}{\langle bc \rangle \langle cd \rangle \langle ef \rangle \langle ae \rangle \langle af \rangle \langle ag \rangle} \frac{1}{\langle db \rangle}. \quad (6.61)$$

Numerical tests confirm that the t -poles and spurious poles in B_{711}^{sp} separate fully, once all terms are taken into account. To help in finding that separation explicitly, the spurious piece B_{711}^{sp} can be written over one denominator as

$$B_{711}^{sp} = \frac{i}{t_{aef}[g|k_{bcd}|g]} \frac{num_{sp}}{\langle ae \rangle \langle af \rangle \langle ag \rangle \langle bc \rangle \langle bd \rangle \langle bg \rangle \langle cd \rangle \langle cg \rangle \langle ef \rangle \langle fg \rangle}, \quad (6.62)$$

with a large number of numerator factors,

$$\begin{aligned}
 num_{sp} = & - [a e] [b d] \langle a e \rangle \langle a f \rangle \langle a g \rangle \langle b g \rangle \langle c g \rangle [a | k_{bcd} | b] [g | k_{bcd} | d] \\
 & - \langle a e \rangle [b g] [d g] s_{ag} \langle b d \rangle \langle b g \rangle \langle c g \rangle \langle f g \rangle [e | k_{bcd} | g] \\
 & - [a e] \langle b d \rangle \langle b g \rangle \langle c g \rangle \langle f g \rangle [b | k_{bcd} | a] [d | k_{bcd} | a] [g | k_{bcd} | e] \\
 & - s_{bd} \langle b g \rangle \langle c d \rangle [a g] [f g] \langle a f \rangle \langle a g \rangle \langle f g \rangle [d | k_{aef} | g] \\
 & - s_{gd} \langle g c \rangle [b g] \langle a f \rangle \langle a g \rangle \langle f g \rangle [a | k_{aef} | b] [f | k_{aef} | b] \\
 & - \langle b g \rangle \langle c d \rangle [b c] [g d] \langle a f \rangle \langle a g \rangle \langle f g \rangle [a | k_{aef} | b] [f | k_{aef} | c] \\
 & - s_{bg} \langle a f \rangle \langle a g \rangle \langle f g \rangle [a | k_{aef} | b] [d | k_{aef} | d] [f | k_{aef} | c] \\
 & - s_{bg} \langle c d \rangle [g d] \langle a f \rangle \langle a g \rangle \langle f g \rangle [a | k_{aef} | b] [f | k_{aef} | g] \\
 & - s_{gd} \langle c d \rangle [g d] \langle a f \rangle \langle a g \rangle \langle f g \rangle [a | k_{aef} | b] [f | k_{aef} | g] \\
 & - \langle b g \rangle \langle c d \rangle [g d]^2 \langle a f \rangle \langle a g \rangle \langle f g \rangle [a | k_{aef} | d] [f | k_{aef} | g] \\
 & + [a f] [b d] \langle a g \rangle \langle b c \rangle \langle b d \rangle \langle b g \rangle \langle f g \rangle [b | k_{aefg} | a] [g | k_{aef} | f]. \tag{6.63}
 \end{aligned}$$

To eliminate spurious poles from the basis $B_{7:1,1}$, we must separate the parts of B_{711}^{sp} with t_{aef} poles from those spurious $[g | k_{bcd} | g]$ pieces. Numerical tests show this to be possible, meaning that there exist manipulations to place the numerator terms into the form

$$num_{sp} = A t_{aef} + B [g | k_{bcd} | g] \tag{6.64}$$

for some spinor functions A and B to be found. Then cancellations against the denominator factors create a t -pole piece free of spurious poles and a spurious pole piece free of t -poles. The latter can be discarded.

A strategy for finding the desired form for num_{sp} involves numerical evaluation. Suppose that each term is numerically evaluated, using a kinematic point where both $[g | k_{bcd} | g]$ and t_{aef} are small. As a result of the structure in eq 6.64, the total value of num_{sp} will be small. However, individual terms in num_{sp} , where the pole factors are not explicit, will not necessarily be small. Since the larger terms must partially cancel to produce the small total, we can inspect those large terms which show similar magnitudes for ways in which they can be combined algebraically, to produce a single new large term and/or small terms involving explicit pole factors. By repeatedly matching and combining those terms of the greatest magnitude, the whole of num_{sp} can be converted to only small terms containing explicit poles, as required for the structure in eq. 6.64.

Performing the manipulations, the end result is a form for num_{sp} where the t_{aef} and $[g | k_{bcd} | g]$ factors are separated, leading to separable t -pole and spurious pole parts. In

6 Reconstruction of Rational Functions

full, the numerator sum is expanded into approximately twice as many terms,

$$\begin{aligned}
num_{sp} = & - [g|k_{aef}|g][a|k_{aef}|b][f|k_{aef}|c]s_{dg} \langle a f \rangle \langle a g \rangle \langle f g \rangle \\
& - [g|k_{bcd}|g][a|k_{aef}|a][b|k_{bcd}|a][d|k_{bcd}|c] \langle b d \rangle \langle b g \rangle \langle f g \rangle \\
& + [g|k_{bcd}|g][b|k_{bcd}|a][d|k_{aef}|a] \langle b d \rangle \langle b g \rangle \langle c e \rangle \langle f g \rangle [a e] \\
& - [g|k_{bcd}|g][b|g|c][d|k_{aef}|a] \langle a g \rangle \langle b d \rangle \langle b g \rangle \langle f g \rangle [a g] \\
& + [g|k_{bcd}|g][a|k_{aef}|b][f|k_{aef}|d] \langle a f \rangle \langle a g \rangle \langle b g \rangle \langle c f \rangle [b d] \\
& + [g|k_{bcd}|g][b|k_{bcd}|a] \langle a f \rangle \langle b c \rangle \langle b d \rangle \langle b g \rangle \langle f g \rangle [a f] [b d] \\
& + [g|k_{bcd}|g] \langle a e \rangle \langle a g \rangle \langle b d \rangle \langle b g \rangle \langle c g \rangle \langle f g \rangle [a g] [b g] [d e] \\
& + [g|k_{bcd}|g][b|k_{aef}|c] \langle a f \rangle \langle a g \rangle \langle b d \rangle \langle b g \rangle \langle f g \rangle [a g] [d f] \\
& - [g|k_{bcd}|g][b|k_{bcd}|a] \langle a e \rangle \langle b d \rangle \langle b g \rangle \langle c g \rangle \langle f g \rangle [a e] [d g] \\
& + [g|k_{bcd}|g][a|k_{aef}|d][f|k_{aef}|c] \langle a f \rangle \langle a g \rangle \langle b g \rangle \langle f g \rangle [g d] \\
& + [g|k_{bcd}|g][f|k_{aef}|c] \langle a f \rangle \langle a g \rangle \langle b d \rangle \langle b g \rangle \langle f g \rangle [a b] [g d] \\
& - t_{aef}[a|k_{aef}|b][g|k_{bcd}|d] \langle a f \rangle \langle a g \rangle \langle b g \rangle \langle c g \rangle [b d] \\
& - t_{aef}[b|k_{bcd}|a] \langle a g \rangle \langle b d \rangle \langle b g \rangle \langle c e \rangle \langle f g \rangle [a e] [d g] \\
& + t_{aef}[b|k_{bcd}|a] \langle a e \rangle \langle b d \rangle \langle b g \rangle \langle c g \rangle \langle f g \rangle [a e] [d g] \\
& + t_{aef}[b|g|c](\langle a g \rangle)^2 \langle b d \rangle \langle b g \rangle \langle f g \rangle [a g] [d g] \\
& - t_{aef}[b|k_{bcd}|a][d|k_{bcd}|c] \langle a g \rangle \langle b d \rangle \langle b g \rangle \langle f g \rangle [g a] \\
& - t_{aef}[a|k_{aef}|d] \langle a f \rangle \langle a g \rangle \langle b g \rangle \langle c g \rangle \langle f g \rangle [f g] [g d] \\
& - t_{aef} \langle a f \rangle \langle a g \rangle \langle b d \rangle \langle b g \rangle \langle c g \rangle \langle f g \rangle [a b] [f g] [g d] \\
& + t_{aef}[a|k_{aef}|b]s_{dg} \langle a f \rangle \langle a g \rangle \langle c g \rangle \langle f g \rangle [g f] \\
& + t_{aef}[a|k_{aef}|b] \langle a f \rangle \langle a g \rangle \langle b g \rangle \langle c f \rangle \langle d g \rangle [b d] [g f]. \tag{6.65}
\end{aligned}$$

However, only those that contain a $[g|k_{bcd}|g]$ factor to cancel the spurious pole will contribute to the leading pole behaviour overall.

The clean basis

We can discard the num_{sp} numerators containing t_{aef} factors, as these correspond to terms containing spurious poles but not t -poles once the denominator is considered.

Finally, we are also free to rotate the arguments of any part of the basis under the $\mathcal{P}_{7:1,1}$ sum. Performing

$$B_{711}^{nsp}(a, b, c, d, e, f, g) \rightarrow B_{711}^{nsp}(b, a, e, f, g, c, d) \tag{6.66}$$

brings all the single t -pole basis terms over the same t_{aef} factor. Combining and tidying up, the basis for the t -pole part of R_{711} can be written in terms of single t -pole (st) and dual t -pole (dt) parts

$$B_{711} = B_{711}^{dt} + B_{711}^{st}, \quad (6.67)$$

where

$$B_{711}^{dt} = \frac{i}{t_{aef}t_{bcd}} \frac{num_{dt}}{\langle a e \rangle \langle a f \rangle \langle a g \rangle \langle b c \rangle \langle c d \rangle \langle e f \rangle} + \frac{i}{t_{aef}t_{bcd}} \frac{[a|k_{ef}|b][g|k_{bcd}|d][a e][b d]}{\langle b c \rangle \langle b d \rangle \langle c d \rangle \langle e f \rangle \langle f g \rangle} \quad (6.68)$$

and

$$B_{711}^{st} = \frac{i}{t_{aef}} \frac{num_{st}}{\langle a e \rangle \langle a f \rangle \langle a g \rangle \langle b c \rangle \langle b d \rangle \langle b g \rangle \langle c d \rangle \langle c g \rangle \langle e f \rangle \langle f g \rangle}, \quad (6.69)$$

with numerators

$$num_{dt} = - [b|k_{bcd}|a][d|k_{bcd}|a][g|k_{bcd}|e][a e] - [e|k_{bcd}|g]s_{ag} \langle a e \rangle [b g][d g] \quad (6.70)$$

and

$$\begin{aligned}
 num_{st} = & - [a|k_{aef}|a][b|k_{bcd}|a][d|k_{bcd}|c] \langle b d \rangle \langle b g \rangle \langle f g \rangle \\
 & + [b|k_{bcd}|a][d|k_{aef}|a] \langle b d \rangle \langle b g \rangle \langle c e \rangle \langle f g \rangle [a e] \\
 & + [a|k_{aef}|b][f|k_{aef}|d] \langle a f \rangle \langle a g \rangle \langle b g \rangle \langle c f \rangle [b d] \\
 & + [b|k_{bcd}|a] \langle a f \rangle \langle b c \rangle \langle b d \rangle \langle b g \rangle \langle f g \rangle [a f] [b d] \\
 & + [a|k_{aef}|b][f|k_{aef}|g] \langle a f \rangle \langle a g \rangle \langle b c \rangle \langle f g \rangle [b g] \\
 & + [d|k_{aef}|a] \langle a g \rangle \langle b d \rangle \langle b g \rangle \langle c g \rangle \langle f g \rangle [a g] [b g] \\
 & + \langle a e \rangle \langle a g \rangle \langle b d \rangle \langle b g \rangle \langle c g \rangle \langle f g \rangle [a g] [b g] [d e] \\
 & + [b|k_{aef}|c] \langle a f \rangle \langle a g \rangle \langle b d \rangle \langle b g \rangle \langle f g \rangle [a g] [d f] \\
 & + [a|k_{aef}|c][f|k_{aef}|b] \langle a f \rangle \langle a g \rangle \langle d g \rangle \langle f g \rangle [d g] \\
 & - [a|k_{aef}|b][f|k_{aef}|c] \langle a f \rangle \langle a g \rangle \langle d g \rangle \langle f g \rangle [d g] \\
 & - [b|k_{bcd}|a] \langle a e \rangle \langle b d \rangle \langle b g \rangle \langle c g \rangle \langle f g \rangle [a e] [d g] \\
 & + \langle a f \rangle \langle a g \rangle \langle b d \rangle \langle b g \rangle \langle c d \rangle \langle f g \rangle [a g] [b d] [f d] \\
 & + \langle a f \rangle \langle a g \rangle \langle b d \rangle \langle b g \rangle \langle c d \rangle \langle f g \rangle [a d] [b d] [f g] \\
 & + [a|k_{aef}|d][f|k_{aef}|c] \langle a f \rangle \langle a g \rangle \langle b g \rangle \langle f g \rangle [g d] \\
 & - [a|k_{aef}|c][f|k_{aef}|d] \langle a f \rangle \langle a g \rangle \langle b g \rangle \langle f g \rangle [g d] \\
 & + [f|k_{aef}|c] \langle a f \rangle \langle a g \rangle \langle b d \rangle \langle b g \rangle \langle f g \rangle [a b] [g d]. \tag{6.71}
 \end{aligned}$$

Numerical tests confirm this expression to be correct and to contain all leading t -pole terms.

We can now move on to fitting the sub-leading poles of $R_{7:1,1}^{(2),q}$, to complete the compact form.

6.5.4 Sub-leading pole fitting

The leading poles (meaning the t -poles) of the $R_{7:1,1}^{(2)}$ rational piece have been identified. By subtracting these from the full $R_{7:1,1}^{(2),q}$ result obtained by augmented recursion, we are left with only terms with sub-leading (angle bracket) poles. We now fit those poles to an appropriate compact form via ansatz fitting.

We may investigate the pole content of our sub-leading piece by choosing specific numerical points on which to evaluate it. Choosing momenta close to a particular pole can be expected to cause the output to become large, if that pole is present in the

Diverging poles:	$\langle 12 \rangle \langle 13 \rangle \langle 23 \rangle$	$\langle 12 \rangle \langle 34 \rangle$
Weight -3	$\langle bc \rangle \langle bd \rangle \langle cd \rangle$	
Weight -2	$\langle cd \rangle \langle de \rangle (\langle ce \rangle)$	$\langle ac \rangle \langle bd \rangle$ $\langle ac \rangle \langle be \rangle$ $\langle bc \rangle \langle de \rangle$ $\langle bc \rangle \langle ef \rangle$ $\langle cd \rangle \langle ef \rangle$
Weight -1	$\langle ac \rangle \langle bc \rangle (\langle ab \rangle)$ $\langle bc \rangle \langle be \rangle (\langle ce \rangle)$	

Table 6.3: Results of numerical pole tests on $R_{7:4}^{(2)}(a^+, b^+, c^+; d^+, e^+, f^+)$, to find coinciding poles. Headings indicate the type of poles that are chosen to become small simultaneously. Each entry is a specific group of poles, associated with the lowest total weight they appear as in the amplitude. For example, an entry with “weight -1 ” means that of the group indicated, there can be at most one more member of the group in the denominator than the numerator. Spinor products in parentheses are those that do not appear as poles, so can only be in the numerator if present.

expression. As the leading and sub-leading pieces separately obey the $\mathcal{P}_{7:1,1}$ symmetry, any insight into one pole structure can be applied directly to any of those equivalent under the symmetry.

Individual pole tests confirm that no t -poles remain in the sub-leading piece, leaving only the simple poles $\langle bc \rangle$, $\langle cd \rangle$ and those equivalent. The results of applying pole tests to multiple poles simultaneously are recorded in Table 6.3.

Ansatz fitting

Only the two entries with weight -1 represent restrictions beyond those of the individual pole tests, for example $\langle ac \rangle \langle bc \rangle (\langle ab \rangle)$ shows that a particular sub-leading term may contain at most one of the structures

$$\left\{ \frac{1}{\langle ac \rangle}, \frac{1}{\langle bc \rangle}, \frac{\langle ab \rangle}{\langle ac \rangle \langle bc \rangle} \right\}. \quad (6.72)$$

Given knowledge of the poles present, we can construct an ansatz function that encompasses any possible term in the sub-leading piece. Ideally, this ansatz will contain as few terms as possible, so that when fitted to the large expression generated by recursion we will see significant simplification. Starting with the denominator, all the poles that might be expected to coincide in a term are selected.

6 Reconstruction of Rational Functions

A first proposal might be

$$\frac{1}{\langle cd \rangle \langle de \rangle \langle ef \rangle \langle fg \rangle \langle gc \rangle} \frac{1}{\langle bc \rangle \langle bd \rangle} \frac{1}{\langle ae \rangle \langle af \rangle}, \quad (6.73)$$

which is one of the largest allowed structures if (for now) we assume the more complicated structures like the third term of eq. 6.72 do not occur.

Filling in the numerator with terms with unknown coefficients, satisfying spinor weight requirements, the basis for an ansatz is formed. These conditions are firstly that the overall weight of spinor products should be -3 for a seven-point two-loop amplitude, so each term must contain six spinor products. For correct little group scaling, we also require an overall spinor weight of -2 for each positive helicity momentum present. (An angle product is worth $+1$ in the numerator and -1 in the denominator. For square bracket products the values are reversed.)

While choosing basis numerators, we must be aware of linear dependence between terms, which can be caused by Schouten relations and the zero momentum sum. Using matrix reduction, the full list of possible numerator permutations can be reduced to a linearly independent set. Note that this reduction step is computationally difficult, involving a matrix of size (number of numerators)². As a result, it is not always feasible to choose the largest possible ansatz denominator.

The ansatz basis is placed under a $\mathcal{P}_{7:1,1}$ sum, ensuring symmetry matching the target expression, and meaning that other allowed poles not present in the basis will be explored by the rest of the ansatz. Further linear dependence could also occur between terms after we apply the $\mathcal{P}_{7:1,1}$ sum over the ansatz basis. We will be cautious of how this may affect the fitting result.

Selecting numerators, the ansatz basis is

$$B_{7:1,1} = \frac{G}{\langle cd \rangle \langle de \rangle \langle ef \rangle \langle fg \rangle \langle gc \rangle \langle bc \rangle \langle bd \rangle \langle ae \rangle \langle af \rangle}, \quad (6.74)$$

where G contains 2625 linearly independent numerators and unknowns. Mathematica is used to evaluate the equation where the summed ansatz is set equal to the sub-leading part of $R_{7:1,1}^{(2),q}$ on as many kinematic points as there are unknowns.

The resulting system of linear equations has a clean solution of zeroes and rational values, showing that an appropriate ansatz was chosen. Of the initial 2625 unknowns, all but 108 terms take a value of zero. The effect of linear dependence between terms in the ansatz manifests itself as linear dependence in the solution for the unknowns. However, those undetermined coefficients can be set to zero to obtain a valid solution.

The compact sub-leading piece

The successful ansatz result, containing 108 terms, has a manifest $\mathcal{P}_{7:1,1}$ symmetry and is free of factors of the reference momentum q . In full, the sub-leading pole terms for $R_{7:1,1}^{(2)}$ can be written

$$R_{7:1,1}^{(sub)} = \sum_{\mathcal{P}_{7:1,1}} B_{7:1,1}^{(sub)}, \quad (6.75)$$

where the basis is

$$B_{711}^{(sub)} = \frac{num_{sub}^{(1)} + num_{sub}^{(2)} + num_{sub}^{(3)}}{\langle cd \rangle \langle de \rangle \langle ef \rangle \langle fg \rangle \langle gc \rangle} \frac{1}{\langle bc \rangle \langle bd \rangle} \frac{1}{\langle ae \rangle \langle af \rangle}. \quad (6.76)$$

6 Reconstruction of Rational Functions

The numerator terms are

$$\begin{aligned}
num_{sub}^{(1)} = & \frac{123}{10} \langle a c \rangle \langle a d \rangle \langle b e \rangle \langle b f \rangle [a b]^2 + \frac{27}{10} \langle a b \rangle \langle a e \rangle \langle b c \rangle \langle d f \rangle [a b]^2 \\
& - \frac{11}{5} \langle a b \rangle \langle a d \rangle \langle b c \rangle \langle e f \rangle [a b]^2 - \frac{3}{2} \langle a c \rangle^2 \langle b e \rangle \langle d f \rangle [a b] [a c] \\
& - \frac{3}{2} \langle a c \rangle \langle a d \rangle \langle b c \rangle \langle e f \rangle [a b] [a c] - \frac{17}{2} \langle a c \rangle^2 \langle b d \rangle \langle e f \rangle [a b] [a c] \\
& + \frac{29}{2} \langle a c \rangle \langle a d \rangle \langle b e \rangle \langle d f \rangle [a b] [a d] - \frac{7}{2} \langle a c \rangle \langle a d \rangle \langle b d \rangle \langle e f \rangle [a b] [a d] \\
& + \frac{29}{2} \langle a c \rangle \langle a d \rangle \langle b e \rangle \langle e f \rangle [a b] [a e] - \frac{9}{2} \langle a c \rangle \langle a e \rangle \langle b f \rangle \langle d f \rangle [a b] [a f] \\
& - \frac{84}{5} \langle a b \rangle \langle b d \rangle \langle c e \rangle \langle c f \rangle [a b] [b c] + \frac{9}{5} \langle a b \rangle \langle b c \rangle \langle c f \rangle \langle d e \rangle [a b] [b c] \\
& + \frac{21}{2} \langle a b \rangle \langle b c \rangle \langle c e \rangle \langle d f \rangle [a b] [b c] - \frac{29}{2} \langle a b \rangle \langle c d \rangle \langle c e \rangle \langle c f \rangle [a c] [b c] \\
& - \frac{15}{2} \langle a b \rangle \langle c d \rangle \langle c e \rangle \langle e f \rangle [a e] [b c] + \frac{51}{2} \langle a b \rangle \langle b d \rangle \langle c e \rangle \langle d f \rangle [a b] [b d] \\
& - \frac{33}{2} \langle a b \rangle \langle b c \rangle \langle d e \rangle \langle d f \rangle [a b] [b d] + \frac{33}{2} \langle a b \rangle \langle c d \rangle \langle d e \rangle \langle d f \rangle [a d] [b d] \\
& - \frac{39}{2} \langle a b \rangle \langle c d \rangle \langle d f \rangle \langle e f \rangle [a f] [b d] - \frac{33}{2} \langle a b \rangle \langle c d \rangle \langle d f \rangle \langle e g \rangle [a g] [b d] \\
& - \frac{11}{5} \langle a b \rangle \langle b e \rangle \langle c e \rangle \langle d f \rangle [a b] [b e] + \frac{36}{5} \langle a b \rangle \langle b d \rangle \langle c e \rangle \langle e f \rangle [a b] [b e] \\
& + \frac{19}{5} \langle a b \rangle \langle b c \rangle \langle d e \rangle \langle e f \rangle [a b] [b e] - \frac{9}{2} \langle a c \rangle \langle b d \rangle \langle c e \rangle \langle e f \rangle [a c] [b e] \\
& - \frac{9}{2} \langle a c \rangle \langle b d \rangle \langle d e \rangle \langle e f \rangle [a d] [b e] + \frac{47}{2} \langle a b \rangle \langle c e \rangle \langle d e \rangle \langle f g \rangle [a g] [b e] \\
& + \frac{19}{5} \langle a b \rangle \langle b e \rangle \langle c f \rangle \langle d f \rangle [a b] [b f] - \frac{9}{2} \langle a c \rangle \langle b d \rangle \langle d f \rangle \langle e f \rangle [a d] [b f] \\
& + \frac{29}{2} \langle a b \rangle \langle c e \rangle \langle d f \rangle \langle f g \rangle [a g] [b f] - \frac{11}{5} \langle a b \rangle \langle b e \rangle \langle c f \rangle \langle d g \rangle [a b] [b g] \\
& + \frac{29}{2} \langle a b \rangle \langle c e \rangle \langle d g \rangle \langle f g \rangle [a g] [b g] + \frac{3}{2} \langle a c \rangle \langle b d \rangle \langle c f \rangle \langle d e \rangle [a b] [c d] \\
& - \frac{21}{2} \langle a c \rangle \langle b c \rangle \langle d e \rangle \langle d f \rangle [a b] [c d] - \frac{3}{2} \langle a c \rangle \langle b d \rangle \langle c f \rangle \langle e f \rangle [a b] [c f], \quad (6.77)
\end{aligned}$$

$$\begin{aligned}
 num_{sub}^{(2)} = & 16 \langle a c \rangle \langle a d \rangle \langle b e \rangle \langle c f \rangle [a b] [a c] - 6 \langle a d \rangle^2 \langle b c \rangle \langle e f \rangle [a b] [a d] \\
 & + 3 \langle a d \rangle^2 \langle c e \rangle \langle c f \rangle [a c] [a d] - 3 \langle a c \rangle \langle a d \rangle \langle c e \rangle \langle d f \rangle [a c] [a d] \\
 & + 6 \langle a c \rangle^2 \langle d e \rangle \langle d f \rangle [a c] [a d] + 3 \langle a c \rangle \langle a d \rangle \langle c d \rangle \langle e f \rangle [a c] [a d] \\
 & - 6 \langle a d \rangle^2 \langle c e \rangle \langle d f \rangle [a d]^2 + 6 \langle a c \rangle \langle a d \rangle \langle d e \rangle \langle d f \rangle [a d]^2 \\
 & + 6 \langle a d \rangle^2 \langle c d \rangle \langle e f \rangle [a d]^2 - 9 \langle a c \rangle \langle a e \rangle \langle b e \rangle \langle d f \rangle [a b] [a e] \\
 & + 3 \langle a d \rangle \langle a e \rangle \langle c e \rangle \langle c f \rangle [a c] [a e] - 3 \langle a c \rangle \langle a e \rangle \langle c e \rangle \langle d f \rangle [a c] [a e] \\
 & + 3 \langle a c \rangle \langle a d \rangle \langle c e \rangle \langle e f \rangle [a c] [a e] - 3 \langle a c \rangle^2 \langle d e \rangle \langle e f \rangle [a c] [a e] \\
 & - 6 \langle a d \rangle \langle a e \rangle \langle c e \rangle \langle d f \rangle [a d] [a e] + 6 \langle a c \rangle \langle a e \rangle \langle d e \rangle \langle d f \rangle [a d] [a e] \\
 & + 6 \langle a d \rangle^2 \langle c e \rangle \langle e f \rangle [a d] [a e] - 6 \langle a c \rangle \langle a d \rangle \langle d e \rangle \langle e f \rangle [a d] [a e] \\
 & + 3 \langle a d \rangle \langle a e \rangle \langle c f \rangle^2 [a c] [a f] - 3 \langle a c \rangle \langle a e \rangle \langle c f \rangle \langle d f \rangle [a c] [a f] \\
 & - 4 \langle a b \rangle \langle c d \rangle \langle c f \rangle \langle d e \rangle [a d] [b c] + 6 \langle a b \rangle \langle c e \rangle \langle c f \rangle \langle d f \rangle [a f] [b c] \\
 & + 4 \langle a b \rangle \langle c d \rangle \langle c f \rangle \langle e f \rangle [a f] [b c] + 4 \langle a b \rangle \langle c d \rangle \langle c g \rangle \langle e f \rangle [a g] [b c] \\
 & - 18 \langle a b \rangle \langle b d \rangle \langle c f \rangle \langle d e \rangle [a b] [b d] + 6 \langle a c \rangle \langle b d \rangle \langle c f \rangle \langle d e \rangle [a c] [b d] \\
 & - 3 \langle a c \rangle \langle b d \rangle \langle c e \rangle \langle d f \rangle [a c] [b d] - 3 \langle a c \rangle \langle b d \rangle \langle d e \rangle \langle d f \rangle [a d] [b d] \\
 & + 6 \langle a b \rangle \langle c d \rangle \langle d e \rangle \langle e f \rangle [a e] [b d] + 3 \langle a b \rangle \langle c e \rangle \langle d f \rangle^2 [a f] [b d] \\
 & - 3 \langle a c \rangle \langle b e \rangle \langle d e \rangle \langle e f \rangle [a e] [b e] - 6 \langle a b \rangle \langle c e \rangle \langle d e \rangle \langle e f \rangle [a e] [b e] \\
 & - 9 \langle a b \rangle \langle c e \rangle \langle d f \rangle \langle e f \rangle [a f] [b e] + 6 \langle a b \rangle \langle c d \rangle \langle e f \rangle^2 [a f] [b e] \\
 & - 9 \langle a b \rangle \langle c e \rangle \langle d f \rangle \langle e g \rangle [a g] [b e] + 6 \langle a b \rangle \langle c d \rangle \langle e f \rangle \langle e g \rangle [a g] [b e] \tag{6.78}
 \end{aligned}$$

and

$$\begin{aligned}
 num_{sub}^{(3)} = & 7 \langle ab \rangle \langle bd \rangle \langle cf \rangle \langle ef \rangle [ab] [bf] - 6 \langle ac \rangle \langle bd \rangle \langle cf \rangle \langle ef \rangle [ac] [bf] \\
 & - 6 \langle ab \rangle \langle cf \rangle \langle df \rangle \langle ef \rangle [af] [bf] - 6 \langle ab \rangle \langle cf \rangle \langle df \rangle \langle eg \rangle [ag] [bf] \\
 & + 12 \langle ac \rangle \langle bd \rangle \langle ce \rangle \langle df \rangle [ab] [cd] + 6 \langle ad \rangle \langle cf \rangle^2 \langle de \rangle [af] [cd] \\
 & - 6 \langle ac \rangle \langle cg \rangle \langle de \rangle \langle df \rangle [ag] [cd] - 3 \langle ac \rangle \langle bc \rangle \langle de \rangle \langle ef \rangle [ab] [ce] \\
 & - 3 \langle ad \rangle \langle ce \rangle \langle cf \rangle \langle de \rangle [ad] [ce] + 3 \langle ac \rangle \langle cf \rangle \langle de \rangle^2 [ad] [ce] \\
 & + 3 \langle ad \rangle \langle ce \rangle^2 \langle df \rangle [ad] [ce] - 3 \langle ac \rangle \langle ce \rangle \langle de \rangle \langle df \rangle [ad] [ce] \\
 & + 3 \langle ad \rangle \langle ce \rangle^2 \langle ef \rangle [ae] [ce] - 3 \langle ac \rangle \langle ce \rangle \langle de \rangle \langle ef \rangle [ae] [ce] \\
 & + 6 \langle ac \rangle \langle be \rangle \langle cf \rangle \langle df \rangle [ab] [cf] - 6 \langle ac \rangle \langle cf \rangle \langle de \rangle \langle df \rangle [ad] [cf] \\
 & + 3 \langle ad \rangle \langle ce \rangle \langle cf \rangle \langle ef \rangle [ae] [cf] - 3 \langle ac \rangle \langle cf \rangle \langle de \rangle \langle ef \rangle [ae] [cf] \\
 & - 3 \langle ad \rangle \langle ce \rangle \langle cf \rangle \langle cg \rangle [ac] [cg] + 3 \langle ac \rangle \langle cf \rangle \langle cg \rangle \langle de \rangle [ac] [cg] \\
 & + 6 \langle ad \rangle \langle cf \rangle \langle cg \rangle \langle de \rangle [ad] [cg] + 9 \langle ac \rangle \langle bd \rangle \langle de \rangle \langle ef \rangle [ab] [de] \\
 & + 3 \langle ad \rangle \langle ce \rangle \langle cf \rangle \langle de \rangle [ac] [de] - 3 \langle ac \rangle \langle cf \rangle \langle de \rangle^2 [ac] [de] \\
 & + 6 \langle ac \rangle \langle ce \rangle \langle de \rangle \langle df \rangle [ac] [de] - 6 \langle ad \rangle \langle cf \rangle \langle de \rangle^2 [ad] [de] \\
 & - 6 \langle ae \rangle \langle cd \rangle \langle de \rangle \langle df \rangle [ad] [de] + 6 \langle ad \rangle \langle ce \rangle \langle de \rangle \langle df \rangle [ad] [de] \\
 & + 6 \langle ac \rangle \langle be \rangle \langle df \rangle^2 [ab] [df] + 3 \langle ad \rangle \langle ce \rangle \langle cf \rangle \langle df \rangle [ac] [df] \\
 & + 9 \langle ac \rangle \langle cf \rangle \langle de \rangle \langle df \rangle [ac] [df] - 6 \langle ad \rangle \langle cf \rangle \langle de \rangle \langle df \rangle [ad] [df] \\
 & - 6 \langle ae \rangle \langle cd \rangle \langle df \rangle^2 [ad] [df] + 6 \langle ad \rangle \langle ce \rangle \langle df \rangle^2 [ad] [df] \\
 & + 6 \langle ae \rangle \langle cf \rangle \langle de \rangle \langle df \rangle [ae] [df] - 6 \langle ae \rangle \langle ce \rangle \langle df \rangle^2 [ae] [df] \\
 & - 6 \langle ad \rangle \langle cf \rangle \langle de \rangle \langle ef \rangle [ae] [df] + 6 \langle ad \rangle \langle ce \rangle \langle df \rangle \langle ef \rangle [ae] [df]. \quad (6.79)
 \end{aligned}$$

We present the complete compact, analytic expression for $R_{7:1,1}^{(2)}$, of which this is a component, in Section 4.5.9 on page 100.

6.6 Seven-Point Rational Piece $R_{7:4}^{(2)}$

We aim to fit the reference momentum-containing rational piece $R_{7:4}^{(2),q}$ to a compact ansatz. To simplify the problem, we first deal with the leading poles by hand, which can be written down from the factorisations.

6.6.1 Augmented recursion output

The output of augmented recursion is an analytic, but very large, expression for $R_{7:4}^{(2),q}$. Generated using code that avoids expanding terms all the way down to their constituent spinors, the expression is written in terms of spinor products and can be written as a 115 MB Mathematica file. The expression contains 4155 terms and occupies 976 MB when in memory.

As was the case for $R_{7:3}^{(2),q}$ and $R_{7:1,1}^{(2),q}$, immediate improvements can be made by checking for duplicate terms. Condensing these, we are left with 1959 terms.

An additional small improvement can be made by checking for terms that cancel in the overall expression. Twenty-four cancelling pairs are found, reducing the total number of terms in the expression to 1911. No cancelling sets of three are found and a search for larger sets is too computationally expensive.

The new $R_{7:4}^{(2),q}$ is a 56 MB file, or 480 MB in memory. One numerical evaluation of the expression (on an i7, 2.60 GHz machine) takes 4 min, in comparison to the 8 min taken by the larger expression. The long time taken by even a single evaluation highlights the need to keep the ansatz fitting portion of the reconstruction as small as possible, so that fewer evaluations are needed. It demonstrates why attempting to fit the leading poles as well as the sub-leading poles would be unworkable.

6.6.2 Pole tests

We can run numerical tests on $R_{7:4}^{(2),q}$ to identify which poles are present. Tests involving multiple spinor products becoming small can be used to find combinations of permitted poles.

The $\mathcal{P}_{7:4}$ symmetry of the partial amplitude means that if a pole such as $\langle ab \rangle$ is present, then so is $\langle bc \rangle$ etc. For simplicity, we will tend to record only one of each equivalent pole or combination type, but the rest are implied.

The (leading) poles present are

$$t_{abc}, t_{def}, \langle ab \rangle^2, \langle de \rangle^2, \langle ad \rangle \quad (6.80)$$

and all those which appear as equivalent to these under the $\mathcal{P}_{7:4}$ symmetry.

Checking the extent to which collections of poles are allowed to occur together in the same term, we find the following constraints:

- At most one t -pole occurs per term.
- At most one double angle bracket pole occurs per term.

6 Reconstruction of Rational Functions

- There is no overlap between t_{abc} and any double pole.
- Overlap between t_{def} and $\langle de \rangle^2$ is permitted.
- Overlap between t_{def} and $\langle ab \rangle^2$ is not permitted.

6.6.3 Leading pole factorisations

The leading poles emerge from factorisations involving $R_4^{(1)} - R_5^{(1)}$ (t -poles relating to the propagator) and $R_3^{(1)} - R_6^{(1)}$ (double s -poles from the propagator and a factor in $R_3^{(1)}$).

We colour dress those amplitudes and perform the multiplication, joining the colour traces using identities. Those terms containing the overall colour structure of interest are selected. In this case, the factorisations relating to $R_{7:4}^{(2)}$ are those that multiply the traces $\text{Tr}[T^a T^b T^c] \text{Tr}[T^d T^e T^f T^g]$.

Let us work with basis expressions, which must be summed under the $\mathcal{P}_{7:4}$, or $Z_3(a, b, c)Z_4(d, e, f, g)$, symmetry to give the full factorisation,

$$F_{7:4} = \sum_{\mathcal{P}_{7:4}} B_{7:4}. \quad (6.81)$$

The t -poles occur in the factorisations

$$\begin{aligned} B_{7:4}^{tp}(a, b, c, d, e, f, g) = & \frac{1}{3} A_{4:2}^{(1),ap}(-k_{abc}^+; a, b, c) \frac{i}{t_{abc}} A_{5:1}^{(1),sm}(k_{abc}^-, d, e, f, g) \\ & + \frac{1}{3} A_{4:2}^{(1),sm}(-k_{abc}^-; a, b, c) \frac{i}{t_{abc}} A_{5:1}^{(1),ap}(k_{abc}^+, d, e, f, g) \\ & + \frac{1}{12} A_{4:2}^{(1),ap}(-k_{abc}^+; a, b, c) \frac{i}{t_{abc}} A_{5:2}^{(1),sm}(k_{abc}^-; d, e, f, g) \\ & + \frac{1}{12} A_{4:2}^{(1),sm}(-k_{abc}^-; a, b, c) \frac{i}{t_{abc}} A_{5:2}^{(1),ap}(k_{abc}^+; d, e, f, g) \\ & + \frac{1}{4} A_{4:1}^{(1),ap}(a, b, c, -k_{abc}^+) \frac{i}{t_{abc}} A_{5:2}^{(1),sm}(k_{abc}^-; d, e, f, g) \\ & + \frac{1}{4} A_{4:1}^{(1),sm}(a, b, c, -k_{abc}^-) \frac{i}{t_{abc}} A_{5:2}^{(1),ap}(k_{abc}^+; d, e, f, g) \\ & + \frac{1}{3} A_{4:1}^{(1),ap}(e, f, g, -k_{efg}^+) \frac{i}{t_{efg}} A_{5:3}^{(1),sm}(k_{efg}^-, d; a, b, c) \\ & + \frac{1}{3} A_{4:1}^{(1),sm}(e, f, g, -k_{efg}^-) \frac{i}{t_{efg}} A_{5:3}^{(1),ap}(k_{efg}^+, d; a, b, c), \end{aligned} \quad (6.82)$$

where these are all one-loop partial amplitudes, either all-plus helicity (ap) or single-minus helicity (sm) and the helicity of the propagator momenta are explicitly stated.

Double s -poles occur in

$$\begin{aligned}
 B_{7:4}^s(a, b, c, d, e, f, g) = & \frac{1}{4} A_{3:1}^{(1),ap}(a, b, -k_{ab}^+) \frac{i}{s_{ab}} A_{6:3}^{(1),sm}(k_{ab}^-, c; d, e, f, g) \\
 & + \frac{1}{3} A_{3:1}^{(1),ap}(f, g, -k_{fg}^+) \frac{i}{s_{fg}} A_{6:4}^{(1),sm}(a, b, c; k_{fg}^-, d, e). \quad (6.83)
 \end{aligned}$$

The partial amplitude $A_{6:4}^{(1),sm}$ is one for which a simple compact expression does not exist in other literature. A functional but complicated expression is available by applying decoupling identities to $A_{6:1}^{(1),sm}$; however, pole tests show that $A_{6:1}^{(1),sm}$ contains many types of pole not present in $A_{6:4}^{(1),sm}$. These unwanted poles appear to be present in the decoupling expression, but must actually cancel overall. The presence of such “apparent” double s -poles and t -poles in particular obstructs our work on factorisations, because they make it harder to see which leading poles are present. So we would prefer a form for $A_{6:4}^{(1)}$ that is explicitly free of apparent poles. This is achieved using ansatz fitting in Section 6.3.4.

Testing the factorisations

We perform pole tests on the factorisations to confirm that they match $R_{7:4}^{(2),q}$ to leading order. In addition to the leading and sub-leading poles, there may be spurious poles in some factorisations that do not appear in the full augmented recursion expression. Accidental overlap can occur between the t -pole and double s -pole pieces (i.e. the t -pole piece also contains some double s -poles, or vice versa), which should also be checked for.

We write out the factorisations explicitly to check for unwanted pole types. Note that the transition from spinor products containing complicated objects like k_{abc} (such as $\langle k_{abc} g \rangle$), to terms involving the external momenta only (such as $[g|k_{abc}|g]$), can often give rise to spurious poles.

Using the same term ordering as in equations 6.82 and 6.83, we assign some labels for convenience,

$$B_{7:4}^{tp}(a, b, c, d, e, f, g) = pt_1 + pt_2 + pt_3 + pt_4 + pt_5 + pt_6 + pt_7 + pt_8 \quad (6.84)$$

and

$$B_{7:4}^{sp}(a, b, c, d, e, f, g) = pt_9 + pt_{10}. \quad (6.85)$$

Each factorisation is written out in terms of its amplitudes, then spinor products con-

6 Reconstruction of Rational Functions

taining nullified sums of momenta k^b are joined together so that they can be promoted to non-nullified momenta k . The extra piece created when moving from $k^b \rightarrow k$ contains an additional factor of k^2 , which cancels with the leading pole the factorisation aims to capture. Discarding these pieces, we obtain

$$\begin{aligned}
 pt_1 = & \frac{i}{9} \frac{1}{t_{abc}} \frac{1}{\langle bc \rangle \langle ca \rangle} \\
 & \left(- \frac{[a|k_{abc}|e][b|k_{abc}|e][e|k_{abc}|e] \langle df \rangle}{\langle de \rangle^2 \langle ef \rangle^2 \langle fg \rangle \langle gd \rangle} \right. \\
 & + \frac{[ag][bg]}{[g|k_{abc}|g]} \left(\frac{[dg]}{\langle ef \rangle^2} [d|k_{abc}|g] + \frac{[gf]}{\langle de \rangle^2} [f|k_{abc}|g] \right) \\
 & \left. - \frac{[dg]}{\langle ef \rangle^2} ([ag][bd] + [ad][bg]) \right), \tag{6.86}
 \end{aligned}$$

$$\begin{aligned}
 pt_2 = & \frac{1}{9} \frac{i}{t_{abc}} \frac{[ab]}{\langle ab \rangle \langle bc \rangle \langle ca \rangle} \frac{1}{\langle de \rangle \langle dg \rangle \langle ef \rangle \langle fg \rangle} \frac{1}{[g|k_{abc}|g]} \\
 & ([g|k_{abc}|b]s_{de}s_{ef} \langle ag \rangle - [g|k_{abc}|b]s_{ef}s_{fg} \langle ag \rangle \\
 & + [f|k_{abc}|b][g|k_{abc}|a] \langle dg \rangle \langle ef \rangle [de]) \\
 & - \frac{1}{9} \frac{i}{t_{abc}} \frac{[ab]}{\langle ab \rangle \langle bc \rangle \langle ca \rangle} \frac{1}{\langle de \rangle \langle dg \rangle \langle ef \rangle \langle fg \rangle} \\
 & ([d|k_{abc}|a][g|k_{abc}|b] \langle dg \rangle), \tag{6.87}
 \end{aligned}$$

$$\begin{aligned}
 pt_3 = & \frac{1}{12} \frac{i}{t_{abc}} \frac{1}{\langle bc \rangle \langle ca \rangle} \frac{1}{\langle de \rangle \langle ef \rangle \langle fg \rangle \langle gd \rangle} \\
 & ([a|k_{abc}|d][b|k_{abc}|e] [de] + [a|k_{abc}|f][b|k_{abc}|g] [fg]), \tag{6.88}
 \end{aligned}$$

$$\begin{aligned}
 pt_4 = & \frac{1}{12} \frac{i}{t_{abc}} \frac{1}{\langle ab \rangle \langle bc \rangle \langle ca \rangle} \frac{[ab]}{\langle de \rangle \langle ef \rangle \langle fg \rangle \langle gd \rangle} \\
 & ([d|k_{abc}|a][e|k_{abc}|b] \langle de \rangle + [f|k_{abc}|a][g|k_{abc}|b] \langle fg \rangle), \tag{6.89}
 \end{aligned}$$

$$\begin{aligned}
 pt_5 = & - \frac{1}{12} \frac{i}{t_{abc}} \frac{1}{\langle bc \rangle \langle ca \rangle} \frac{1}{\langle de \rangle \langle ef \rangle \langle fg \rangle \langle gd \rangle} \\
 & ([a|k_{abc}|d][b|k_{abc}|e] [de] + [a|k_{abc}|f][b|k_{abc}|g] [fg]), \tag{6.90}
 \end{aligned}$$

$$pt_6 = -\frac{1}{12} \frac{i}{t_{abc}} \frac{1}{\langle ab \rangle \langle bc \rangle \langle ca \rangle} \frac{[ab]}{\langle de \rangle \langle ef \rangle \langle fg \rangle \langle gd \rangle} ([d|k_{abc}|a][e|k_{abc}|b] \langle de \rangle + [f|k_{abc}|a][g|k_{abc}|b] \langle fg \rangle), \quad (6.91)$$

$$pt_7 = \frac{1}{9} \frac{i}{t_{efg}} \frac{1}{\langle ef \rangle \langle fg \rangle} \left(\frac{([e|k_{efg}|b][g|k_{efg}|c] [bc] + [e|k_{efg}|a][g|k_{efg}|d] [da])}{\langle ab \rangle \langle bc \rangle \langle cd \rangle \langle da \rangle} + \frac{([e|k_{efg}|a][g|k_{efg}|c] [ca] + [e|k_{efg}|b][g|k_{efg}|d] [db])}{\langle ad \rangle \langle bc \rangle \langle ca \rangle \langle db \rangle} + \frac{([e|k_{efg}|a][g|k_{efg}|b] [ab] + [e|k_{efg}|c][g|k_{efg}|d] [dc])}{\langle ab \rangle \langle bd \rangle \langle ca \rangle \langle dc \rangle} \right), \quad (6.92)$$

$$pt_8 = -\frac{2}{9} \frac{i}{t_{efg}} \frac{1}{\langle ab \rangle \langle bc \rangle \langle ca \rangle} \frac{[d|k_{efg}|f] [eg]}{\langle ef \rangle \langle fg \rangle} \left(\frac{[d|k_{efg}|g]}{\langle fg \rangle} + \frac{[d|k_{efg}|e]}{\langle ef \rangle} \right), \quad (6.93)$$

$$pt_9 = -\frac{i}{3} \frac{[ab]}{\langle ab \rangle^2} \frac{1}{\langle cd \rangle \langle de \rangle \langle ef \rangle \langle fg \rangle \langle gc \rangle} (-\langle b|c|g|a \rangle + \langle b|d|e|a \rangle + \langle b|d|f|a \rangle + \langle b|e|f|a \rangle), \quad (6.94)$$

and

$$pt_{10} = 3 \sum_{[ab]} \sum_{[de]} pt_{10}^{(basis)}, \quad (6.95)$$

which makes use of the notation for antisymmetric sums defined in eq. 6.25, to sum

6 Reconstruction of Rational Functions

over the basis

$$\begin{aligned}
 pt_{10}^{(basis)} = & \frac{i}{9} \frac{1}{\langle fg \rangle^2} \frac{\langle ef \rangle}{\langle ab \rangle \langle bc \rangle \langle de \rangle \langle ea \rangle} \frac{1}{[d|k_{fg}|d][e|k_{fg}|e]} \\
 & (-2[f|g|a] \langle da \rangle [da] [dc] [ea] - 2[f|g|b] \langle da \rangle [db] [dc] [ea] \\
 & - 2[f|g|c] \langle da \rangle [dc]^2 [ea] - [f|g|a] \langle ea \rangle [dc] [ea]^2 \\
 & + 2[f|g|a] \langle eb \rangle [dc] [ea] [eb] + 3[f|g|a] \langle ea \rangle [da] [ea] [ec] \\
 & + 2[f|g|a] \langle ec \rangle [dc] [ea] [ec] + 3[f|g|b] \langle ea \rangle [da] [eb] [ec]). \quad (6.96)
 \end{aligned}$$

Immediately, we see that $pt_3 + pt_5 = 0$ and $pt_4 + pt_6 = 0$. Spurious poles, of the type $[x|k|x]$, are present in pt_1 and pt_2 . The piece pt_8 contains both double angle bracket poles and t -poles. The double angle bracket poles are not spurious because they are of a type present in the amplitude, even though they appear in a t -pole factorisation. What they represent is an overlap between the two types of pole factorisation, so we expect some double counting of these poles overall, which should be identified and removed. Similarly, the denominator $[x|k|x]$ factors in pt_{10} are equivalent to t -poles and form another overlap. The double poles in pt_1 can be considered spurious, because the factor $t_{abc} \langle de \rangle^2$ does not appear as a denominator in the amplitude.

Clearing spurious poles

First, we clear the spurious poles appearing in pt_1 and pt_2 .

We know that after applying the $\mathcal{P}_{7,4}$ sum to all the factorisations, we must obtain the leading pole structure as it appears in the amplitude, plus sub-leading parts which we can discard. Since the spurious poles do not appear in the amplitude, by algebraic manipulation it should be possible to move them out of the leading terms, to sub-leading terms of our factorisations.

Applying Schouten identities, rotations of momentum labels under the sum, the zero total momentum, etc. we can create numerator factors to cancel either the spurious pole or a t -pole (and discard non-leading terms).

Begin with the spurious pole $[g|k_{abc}|g]$ in pt_1 . This pole is also present in pt_2 , so in general its removal may require cancellation between the two pieces. In this case, no

such cancellations are necessary and we obtain

$$\begin{aligned}
 pt_1 = & \frac{1}{9} \frac{i}{t_{abc}} \frac{1}{\langle bc \rangle \langle ca \rangle} \\
 & \left(- \frac{[a|k_{abc}|e][b|k_{abc}|e][e|k_{abc}|e] \langle df \rangle}{\langle de \rangle^2 \langle ef \rangle^2 \langle fg \rangle \langle gd \rangle} \right. \\
 & - \frac{[dg]}{\langle ef \rangle^2} ([ag][bd] + [ad][bg]) \\
 & \left. + [ag][bg] \left(\frac{[d|k_{abc}|e]}{\langle de \rangle \langle ef \rangle^2} + \frac{\langle eg \rangle [fg]}{\langle de \rangle^2 \langle ef \rangle} \right) \right), \tag{6.97}
 \end{aligned}$$

after successfully removing $[x|k|x]$ -type poles. Spurious double poles are still present. With that, the clearing of pt_2 should also be possible, without cancellations between pieces. Indeed, we find

$$\begin{aligned}
 pt_2 = & \frac{1}{9} \frac{i}{t_{abc}} \frac{[ab]}{\langle ab \rangle \langle bc \rangle \langle ca \rangle} \frac{1}{\langle de \rangle \langle dg \rangle \langle ef \rangle \langle fg \rangle} \\
 & ([f|k_{abc}|b] \langle ag \rangle \langle ef \rangle [eg] - [f|k_{abc}|b] \langle ad \rangle \langle ef \rangle [de] \\
 & + [g|k_{abc}|b] s_{ef} \langle ag \rangle - [d|k_{abc}|a] [g|k_{abc}|b] \langle dg \rangle), \tag{6.98}
 \end{aligned}$$

which is free of all spurious poles.

Returning to pt_1 , there are two spurious double poles $\langle de \rangle^2$ and $\langle ef \rangle^2$. To proceed, we should attempt to separate them and rotate one under the $\mathcal{P}_{7:4}$ sum to match the other. This will shift the cancellation from between different versions of pt_1 under the sum to within the one basis pt_1 .

Doing so, we obtain

$$\begin{aligned}
 pt_1 = & - \frac{1}{9} \frac{i}{t_{abc}} \frac{1}{\langle bc \rangle \langle ca \rangle} \frac{1}{\langle de \rangle \langle ef \rangle \langle fg \rangle \langle gd \rangle} \\
 & ([a|k_{abc}|e][b|k_{abc}|d] [de] + [a|k_{abc}|e] s_{fg} [be] \\
 & + [b|k_{fg}|d] s_{fg} [ad] + s_{fg} \langle fg \rangle [ag][bf] \\
 & + \langle ef \rangle \langle fg \rangle [af][bf][eg]), \tag{6.99}
 \end{aligned}$$

which is now free of spurious poles.

Overlap between factorisations

Having cleared the spurious poles, we have expressions for the amplitude terms containing t -poles and for the amplitude terms containing double angle bracket poles. Due to the full amplitude containing terms with both t -poles and double poles, there is overlap between our two expressions.

The (summed) t -pole factorisation $F_{7:4}^{tp}$ contains all the required t -poles, but also $\langle de \rangle^2$ -type double poles (in pt_8).

The (summed) double s -pole factorisation $F_{7:4}^{sp}$ contains all the required double angle bracket poles, but also t_{def} -type t -poles (in pt_{10}). When the basis is written as

$$\begin{aligned}
 pt_{10}^{(basis)} = & \frac{i}{9} \frac{1}{\langle fg \rangle^2} \frac{\langle ef \rangle}{\langle ab \rangle \langle bc \rangle \langle de \rangle \langle ea \rangle} \frac{1}{t_{efg} t_{fgd}} \\
 & (-2[f|g|a] \langle da \rangle [da] [dc] [ea] - 2[f|g|b] \langle da \rangle [db] [dc] [ea] \\
 & - 2[f|g|c] \langle da \rangle [dc]^2 [ea] - [f|g|a] \langle ea \rangle [dc] [ea]^2 \\
 & + 2[f|g|a] \langle eb \rangle [dc] [ea] [eb] + 3[f|g|a] \langle ea \rangle [da] [ea] [ec] \\
 & + 2[f|g|a] \langle ec \rangle [dc] [ea] [ec] + 3[f|g|b] \langle ea \rangle [da] [eb] [ec]), \quad (6.100)
 \end{aligned}$$

this becomes evident.

The presence of two t -poles in the same denominator complicates things, as t -poles should only appear alone in the amplitude. Pole tests confirm that after all sums are taken into account, this structure reduces to one involving at most one t -pole. Before we can resolve the overlap with pt_8 , it may be necessary to deal with these “spurious” second poles. (We can modify pt_{10} by a piece containing only leading t -poles, without spoiling its agreement with the leading double poles.)

To check for cancellations, we carry out the sum in pt_{10} over its basis, giving

$$pt_{10} = pt_{10}^a + pt_{10}^b, \quad (6.101)$$

where

$$\begin{aligned}
 pt_{10}^a = & \frac{i}{3} \frac{1}{\langle fg \rangle^2} \frac{1}{t_{efg} t_{fgd}} \frac{[fg]}{\langle ab \rangle \langle ac \rangle \langle bc \rangle \langle de \rangle} \\
 & (-2[e|d|g][e|k_{ab}|c] \langle ef \rangle [cd] + 3[e|a|c][e|b|g] \langle ef \rangle [cd] \\
 & + 3[e|a|g][e|b|c] \langle ef \rangle [cd] + 3[c|k_{ab}|c][e|k_{ab}|g] \langle ef \rangle [de] \\
 & - 2[d|e|g][d|k_{ab}|c] \langle df \rangle [ce] + 3[d|a|c][d|b|g] \langle df \rangle [ce] \\
 & + 3[d|a|g][d|b|c] \langle df \rangle [ce] + 3[c|k_{ab}|c][d|k_{ab}|g] \langle df \rangle [ed]) \quad (6.102)
 \end{aligned}$$

and

$$\begin{aligned}
 pt_{10}^b = & \frac{i}{3} \frac{1}{\langle fg \rangle^2} \frac{1}{t_{fgd}} \frac{\langle ef \rangle [fg]}{\langle ab \rangle \langle ac \rangle \langle bc \rangle \langle de \rangle \langle ea \rangle \langle eb \rangle} \\
 & (2 \langle ac \rangle \langle ag \rangle \langle eb \rangle [cd] [ea] + 2 \langle bc \rangle \langle bg \rangle \langle ea \rangle [cd] [eb]) \\
 & + \frac{i}{3} \frac{1}{\langle fg \rangle^2} \frac{1}{t_{efg}} \frac{\langle df \rangle [fg]}{\langle ab \rangle \langle ac \rangle \langle bc \rangle \langle de \rangle \langle da \rangle \langle db \rangle} \\
 & (2 \langle ac \rangle \langle ag \rangle \langle db \rangle [ce] [da] + 2 \langle bc \rangle \langle bg \rangle \langle da \rangle [ce] [db]). \quad (6.103)
 \end{aligned}$$

The piece pt_{10}^a separates out those terms that need further work.

Fitting to an ansatz

We can attempt to fit pt_{10}^a to a basis of non-spurious allowed forms, plus a purely spurious piece containing the two coinciding t -poles. Schematically, we wish to find

$$\frac{A}{\langle fg \rangle^2 t_{efg} t_{fgd}} \rightarrow \frac{B}{\langle fg \rangle^2 t_{efg}} + \frac{C}{\langle fg \rangle^2 t_{fgd}} + \frac{D}{\langle fg \rangle t_{efg} t_{fgd}} \quad (6.104)$$

for some unknown spinor functions B, C, D . The terms containing B and C are leading pole contributions, while term D contains only spurious and sub-leading poles so can be discarded. That this separation takes place is a reasonable prediction, because we know from pole testing that overall, the factorisations reproduce the leading poles of the amplitude and these do not contain spurious poles. In actuality, however, the spurious pole separation may require cancellations to take place with other terms in the $\mathcal{P}_{7:4}$ sum which share a particular t -pole. It may be that

$$\sum_{\mathcal{P}_{7:4}} \frac{A}{\langle fg \rangle^2 t_{efg} t_{fgd}} \rightarrow \sum_{\mathcal{P}_{7:4}} \left(\frac{B}{\langle fg \rangle^2 t_{efg}} + \frac{C}{\langle fg \rangle^2 t_{fgd}} + \frac{D}{\langle fg \rangle t_{efg} t_{fgd}} \right) \quad (6.105)$$

6 Reconstruction of Rational Functions

is the required relation. For this reason we propose ansatz bases, to which a $\mathcal{P}_{7:4}$ sum is applied before comparing to pt_{10}^a under a $\mathcal{P}_{7:4}$ sum.

An initial ansatz basis is tested, containing only the poles present in pt_{10}^a ,

$$\begin{aligned}
 B_1 = & \frac{i}{3} \frac{1}{\langle fg \rangle^2} \frac{1}{t_{efg}} \frac{1}{\langle ab \rangle \langle ac \rangle \langle bc \rangle \langle de \rangle} \frac{ansnum_1}{\langle ab \rangle \langle ac \rangle \langle bc \rangle \langle de \rangle} \\
 & + \frac{i}{3} \frac{1}{\langle fg \rangle^2} \frac{1}{t_{fgd}} \frac{1}{\langle ab \rangle \langle ac \rangle \langle bc \rangle \langle de \rangle} \frac{ansnum_2}{\langle ab \rangle \langle ac \rangle \langle bc \rangle \langle de \rangle} \\
 & + \frac{i}{3} \frac{1}{\langle fg \rangle} \frac{1}{t_{efg} t_{fgd}} \frac{1}{\langle ab \rangle \langle ac \rangle \langle bc \rangle \langle de \rangle} \frac{ansnum_3}{\langle ab \rangle \langle ac \rangle \langle bc \rangle \langle de \rangle}. \tag{6.106}
 \end{aligned}$$

It is unsuccessful, failing to reach a rational solution for the coefficients. This suggests that if manipulations do exist that can separate the two t -poles and double angle bracket poles, they involve new poles entering the denominators. Extending the ansatz to

$$\begin{aligned}
 B_2 = & \frac{i}{3} \frac{1}{\langle fg \rangle^2} \frac{1}{t_{efg}} \frac{1}{\langle ab \rangle \langle ac \rangle \langle bc \rangle \langle de \rangle \langle ef \rangle} \frac{ansnum_1}{\langle ab \rangle \langle ac \rangle \langle bc \rangle \langle de \rangle \langle ef \rangle} \\
 & + \frac{i}{3} \frac{1}{\langle fg \rangle^2} \frac{1}{t_{fgd}} \frac{1}{\langle ab \rangle \langle ac \rangle \langle bc \rangle \langle de \rangle \langle ef \rangle} \frac{ansnum_2}{\langle ab \rangle \langle ac \rangle \langle bc \rangle \langle de \rangle \langle ef \rangle} \\
 & + \frac{i}{3} \frac{1}{\langle fg \rangle} \frac{1}{t_{efg} t_{fgd}} \frac{1}{\langle ab \rangle \langle ac \rangle \langle bc \rangle \langle de \rangle} \frac{ansnum_3}{\langle ab \rangle \langle ac \rangle \langle bc \rangle \langle de \rangle}. \tag{6.107}
 \end{aligned}$$

is also unsuccessful. It is difficult to predict which additional poles are missing from the ansatz, given the wide range that occur in the summed factorisation expression. Having experienced the drawbacks of an ansatz-based approach for this task, we move to a different approach.

Factorisation to find the overlapping leading terms

An alternative route to removing the spurious poles is to use factorisations to directly obtain the overlapping terms containing t_{fgd} and $\langle fg \rangle^2$, rather than attempting to extract them from a larger expression. These terms could be considered the “most leading” pole terms, because they represent the part of the amplitude where both types of leading pole structure occur. It is these “most leading” terms which appear in both pt_8 and pt_{10} as the double counted overlap poles.

We can imagine two such diagrams that give rise to this structure:

$$A_{3:1}^{(1)}(a^+, b^+, -k_{ab}^+) \frac{i}{s_{ab}} A_3^{(0)}(k_{ab}^-, c^+, -k_{abc}^\mp) \frac{i}{t_{abc}} A_5^{(1)}(k_{abc}^\pm, d^+, e^+, f^+, g^+), \tag{6.108}$$

which differ in the helicities across the t -pole propagator. To form the factorisation, we colour dress each factor in this product, then join the colour traces using matrix relations to eliminate repeated k -momenta factors. Then extracting only the coefficients of the relevant colour structure, $\text{Tr}[T^a T^b T^c] \text{Tr}[T^d T^e T^f T^g]$, we obtain a factorisation for the leading parts of $R_{7:4}^{(2)}$:

$$R_{7:4}^{lead} = \sum_{P_{7:4}} B_{7:4}^{lead}, \quad (6.109)$$

where

$$\begin{aligned} B_{7:4}^{lead} = & \frac{1}{4} A_{3:1}^{(1)}(a, b, -k_{ab}^+) \frac{i}{s_{ab}} A_3^{(0)}(k_{ab}^-, c, -k_{abc}^-) \frac{i}{t_{abc}} A_{5:2}^{(1)}(k_{abc}^\pm; d, e, f, g) \\ & + \frac{1}{3} A_{3:1}^{(1)}(f, g, -k_{fg}^+) \frac{i}{s_{fg}} A_3^{(0)}(k_{fg}^-, d, -k_{fgd}^-) \frac{i}{t_{fgd}} A_{5:3}^{(1)}(k_{fgd}^\pm; e, a, b, c) \end{aligned} \quad (6.110)$$

and the two factorisations represented by the second term give rise to our structure of interest. Writing those out in terms of their amplitudes, then eliminating factors of k , we find that the t -pole cancels in the factorisation helicity choice which includes $R_{5:3}^{(1),sm}$. So only the factorisation involving $R_{5:3}^{(1),ap}$ contributes, giving

$$B_{7:4}^{lead} = \frac{2i}{9} \frac{s_{df}}{\langle fg \rangle^2 t_{fgd}} \frac{[de]^2}{\langle ab \rangle \langle bc \rangle \langle ca \rangle} \quad (6.111)$$

as the overlap between t_{fgd} t -poles and $\langle fg \rangle^2$ double angle bracket poles.

In fact, we need to include an additional term in the basis

$$B_{7:4}^{ts^2} = B_{7:4}^{lead} + B_{7:4}^{lead}|_{d \leftrightarrow e} \quad (6.112)$$

to account for overlaps of the type $t_{efg} \langle fg \rangle^2$. Numerical tests that cause both pole types to become large simultaneously confirm that this captures the most leading pole structure of the amplitude. The same test also shows the structure matches the overlap behaviour of both pt_8 and pt_{10} , as expected.

Separating out the overlap poles

Now that we have an expression for the overlapping pole pieces, we want to see what remains of pt_8 and pt_{10} once it is subtracted off.

In principle, we know that summing $pt_8 + pt_{10}$ causes a double counting of $B_{7:4}^{ts^2}$, so just including a factor of $-B_{7:4}^{ts^2}$ in the overall factorisation basis when both t -poles

and double poles are included is sufficient to reproduce all the amplitude's leading pole structures. However, we are interested in results that present the properties of the amplitude as clearly as possible. The separation of the most leading poles from other leading poles will be carried out explicitly, to ensure that no spurious terms remain (for example terms in pt_{10} with two t -poles).

Taking the difference $B_{7:4}^t = pt_8 - B_{7:4}^{ts^2}$, we obtain as a basis

$$B_{7:4}^t = \frac{2i}{9} \frac{1}{t_{efg}} \frac{1}{\langle ab \rangle \langle bc \rangle \langle ca \rangle} \left(\frac{[fg][de]^2}{\langle fg \rangle} + 2 \frac{[eg][dg][de]\langle eg \rangle}{\langle ef \rangle \langle fg \rangle} \right), \quad (6.113)$$

which as usual lives under the $\mathcal{P}_{7:4}$ sum. With this, the terms containing only t -poles (and simple angle bracket poles) have been fully separated from those containing double angle bracket poles.

We would also like to find $pt_{10} - B_{7:4}^{ts^2}$, which would hopefully contain only double angle bracket poles as leading poles and no t -poles, but the expressions are larger and a nice cancellation does not occur between the basis forms. Numerical testing confirms that the subtracted poles only cancel once the $Z(abc)$ part of the overall sum has taken place. Rotating momentum labels of terms of the basis under the sum does not cause the cancellation to take place sooner. (Every possible combination of momentum rotations was applied to each term, but at no point did it lead to full t -pole cancellation.) We might expect there to exist some combination of manipulations that allow the t -poles to cancel before the sum is applied. But without a guiding strategy, searching for it is impractical and unlikely to be successful on an expression of this size.

For now, we will move on from factorisation manipulations. Instead of fitting only the sub-leading poles to an ansatz, we can propose ansatzes for sub-leading and $\langle fg \rangle^2$ -type poles. This leads to an increase in the complexity of ansatzes that must be tested, however it is only of one spinor product so should not be too problematic.

6.6.4 Sub-leading pole fitting

We now perform ansatz fitting on the sub-leading poles, as well as $\langle fg \rangle^2$ -type poles that did not reduce to a clean form in the leading pole factorisation.

By choosing kinematic points near to multiple poles, knowledge of the sub-leading pole structure can be gained. Due to the $\mathcal{P}_{7:4}$ symmetry, testing a particular collection of pole structures also determines those other structures that are equivalent under the

Diverging poles:	$\langle 12 \rangle \langle 13 \rangle \langle 23 \rangle$	$\langle 12 \rangle^2 \langle 13 \rangle \langle 23 \rangle$	$\langle 12 \rangle \langle 34 \rangle$	$\langle 12 \rangle^2 \langle 34 \rangle$
Weight -3	$\langle ab \rangle \langle ac \rangle \langle bc \rangle$	$\langle de \rangle^2 \langle ef \rangle (\langle df \rangle)$		$\langle de \rangle^2 \langle ab \rangle$ $\langle de \rangle^2 \langle fg \rangle$
Weight -2	$\langle ab \rangle \langle ad \rangle \langle bd \rangle$	$\langle de \rangle^2 \langle ad \rangle \langle ae \rangle$	$\langle ab \rangle \langle cd \rangle$	
Weight -1	$\langle ad \rangle \langle af \rangle (\langle df \rangle)$		$\langle ad \rangle \langle be \rangle$ $\langle ad \rangle \langle bf \rangle$	

Table 6.4: Results of numerical pole tests on $R_{7:4}^{(2)}(a^+, b^+, c^+; d^+, e^+, f^+)$, to find coinciding poles. Column headings indicate the type of poles that are chosen to become small. Each entry is a specific group of poles, associated with the lowest total weight they appear as in the amplitude. For example, an entry with “weight -1 ” means that of the group indicated, there can be at most one more spinor product in the denominator than the numerator. Spinor products in parentheses are those that cannot appear as poles, so if present will be in the numerator.

symmetry. We maintain this symmetry in our ansatz by choosing poles to place in a basis under a $\mathcal{P}_{7:4}$ sum. Restrictions found on allowed pole groupings are described in Table 6.4, where one form of each group has been shown as representative of those under the symmetry.

Ansatz fitting

From these pole conditions and the allowed pole types $(\langle ab \rangle \langle ad \rangle \langle de \rangle^2)$, potential pole structures are constructed. Taking a specific example, the pole test result for $\langle ad \rangle \langle af \rangle (\langle df \rangle)$ means that a particular ansatz denominator can contain only one of the structures

$$\left\{ \frac{1}{\langle ad \rangle}, \frac{1}{\langle ad \rangle}, \frac{\langle df \rangle}{\langle ad \rangle \langle af \rangle} \right\}. \quad (6.114)$$

It is not guaranteed that structures with compulsory numerator factors, like the third one here, must occur in the amplitude. However, it is a possibility that cannot be ruled out by pole testing. Assuming these structures do not appear, for the sake of simplicity,

6 Reconstruction of Rational Functions

some initial potential ansatz structures are

$$\begin{aligned}
 & \frac{1}{\langle fg \rangle^2} \frac{1}{\langle ab \rangle \langle bc \rangle \langle ca \rangle} \frac{1}{\langle de \rangle \langle ef \rangle \langle gd \rangle} \frac{1}{\langle ad \rangle}, \\
 & \frac{1}{\langle fg \rangle^2} \frac{1}{\langle ab \rangle \langle bc \rangle \langle ca \rangle} \frac{1}{\langle de \rangle \langle ef \rangle \langle gd \rangle} \frac{1}{\langle ae \rangle}, \\
 & \frac{1}{\langle ab \rangle \langle bc \rangle \langle ca \rangle} \frac{1}{\langle de \rangle \langle ef \rangle \langle fg \rangle \langle gd \rangle} \frac{1}{\langle ad \rangle}.
 \end{aligned} \tag{6.115}$$

Assembling the first two into an ansatz basis, to which a $\mathcal{P}_{7:4}$ sum is applied, forms an ansatz containing all the required poles of the sub-leading (and $\langle ef \rangle^2$ -type) partial amplitude piece. We have the basis

$$\begin{aligned}
 B = & \frac{1}{\langle fg \rangle^2} \frac{G_1}{\langle ab \rangle \langle bc \rangle \langle ca \rangle} \frac{1}{\langle de \rangle \langle ef \rangle \langle gd \rangle} \frac{1}{\langle ad \rangle} \\
 & + \frac{1}{\langle fg \rangle^2} \frac{G_2}{\langle ab \rangle \langle bc \rangle \langle ca \rangle} \frac{1}{\langle de \rangle \langle ef \rangle \langle gd \rangle} \frac{1}{\langle ae \rangle},
 \end{aligned} \tag{6.116}$$

where G_1 and G_2 are chosen as linearly independent sets of numerator terms with the correct spinor weights and unknown coefficients.

The fitting is successful, yielding coefficients that are either zero or simple rational values. This piece completes the compact $R_{7:4}$ expression.

The compact sub-leading piece

The succesful ansatz fit for sub-leading (and double) poles, containing 133 terms, is

$$R_{7:4}^{(sub)} = \sum_{\mathcal{P}_{7:4}} B_{7:4}^{(sub)}, \tag{6.117}$$

where

$$\begin{aligned}
 B_{7:4}^{(sub)} = & \frac{1}{\langle fg \rangle^2} \frac{num_{sub}^{(1)}}{\langle ab \rangle \langle bc \rangle \langle ca \rangle} \frac{1}{\langle de \rangle \langle ef \rangle \langle gd \rangle} \frac{1}{\langle ad \rangle} \\
 & + \frac{1}{\langle fg \rangle^2} \frac{num_{sub}^{(2)}}{\langle ab \rangle \langle bc \rangle \langle ca \rangle} \frac{1}{\langle de \rangle \langle ef \rangle \langle gd \rangle} \frac{1}{\langle ae \rangle},
 \end{aligned} \tag{6.118}$$

with numerator terms

$$\begin{aligned}
 num_{sub}^{(1)} = & 6i(\langle a f \rangle \langle b d \rangle \langle b f \rangle \langle d g \rangle [b d] [b f] + \langle a f \rangle \langle b d \rangle \langle c g \rangle \langle d f \rangle [b f] [c d] \\
 & + \langle a f \rangle \langle b f \rangle \langle c d \rangle \langle d g \rangle [b d] [c f] + \langle a f \rangle \langle c d \rangle \langle c f \rangle \langle d g \rangle [c d] [c f] \\
 & + 2 \langle a f \rangle \langle b f \rangle \langle d e \rangle \langle d g \rangle [b f] [d e] - \langle a f \rangle \langle b e \rangle \langle d f \rangle \langle d g \rangle [b f] [d e] \\
 & + 2 \langle a e \rangle \langle c g \rangle \langle d f \rangle^2 [c f] [d e] - \langle a f \rangle \langle c e \rangle \langle d f \rangle \langle d g \rangle [c f] [d e] \\
 & - \langle a f \rangle \langle b f \rangle \langle d e \rangle \langle d g \rangle [b e] [d f] - \langle a e \rangle \langle c g \rangle \langle d f \rangle^2 [c e] [d f] \\
 & + \langle a e \rangle \langle d f \rangle \langle d g \rangle \langle e f \rangle [d e] [e f]) \tag{6.119}
 \end{aligned}$$

and

$$num_{sub}^{(2)} = num_{sub}^{(2)A} + num_{sub}^{(2)B} + num_{sub}^{(2)C}, \tag{6.120}$$

where

$$\begin{aligned}
 num_{sub}^{(2)A} = & \frac{i}{8} (- 12 \langle a g \rangle \langle b d \rangle \langle b f \rangle \langle c e \rangle [b c] [b d] + 44 \langle a g \rangle \langle b d \rangle \langle b f \rangle \langle e d \rangle [b d]^2 \\
 & - 32 \langle a f \rangle \langle b d \rangle^2 \langle e g \rangle [b d]^2 + 138 \langle a g \rangle \langle b e \rangle \langle b f \rangle \langle c e \rangle [b c] [b e] \\
 & - 138 \langle a g \rangle \langle b e \rangle \langle b f \rangle \langle e d \rangle [b d] [b e] - 740 \langle a f \rangle \langle b d \rangle \langle b e \rangle \langle e g \rangle [b d] [b e] \\
 & - 70 \langle a f \rangle \langle b e \rangle^2 \langle e g \rangle [b e]^2 + 12 \langle a f \rangle \langle b d \rangle \langle b f \rangle \langle e g \rangle [b d] [b f] \\
 & + 646 \langle a f \rangle \langle b e \rangle \langle b f \rangle \langle e g \rangle [b e] [b f] + 8 \langle a g \rangle \langle b f \rangle \langle b g \rangle \langle e d \rangle [b d] [b g] \\
 & - 32 \langle a g \rangle \langle b d \rangle \langle b g \rangle \langle e f \rangle [b d] [b g] + 36 \langle a g \rangle \langle b d \rangle \langle b f \rangle \langle e g \rangle [b d] [b g] \\
 & - 138 \langle a g \rangle \langle b e \rangle \langle b f \rangle \langle e g \rangle [b e] [b g] + 8 \langle a g \rangle \langle b d \rangle \langle c f \rangle \langle e d \rangle [b d] [c d] \\
 & - 12 \langle a f \rangle \langle b d \rangle \langle c g \rangle \langle e d \rangle [b d] [c d] + 36 \langle a d \rangle \langle b d \rangle \langle c g \rangle \langle e f \rangle [b d] [c d] \\
 & - 32 \langle a f \rangle \langle b d \rangle \langle c d \rangle \langle e g \rangle [b d] [c d] - 54 \langle a f \rangle \langle b d \rangle \langle c e \rangle \langle e g \rangle [b e] [c d] \\
 & - 8 \langle a f \rangle \langle b f \rangle \langle c g \rangle \langle e d \rangle [b f] [c d] - 24 \langle a g \rangle \langle b d \rangle \langle c f \rangle \langle e f \rangle [b f] [c d] \\
 & + 32 \langle a f \rangle \langle b d \rangle \langle c g \rangle \langle e f \rangle [b f] [c d] - 40 \langle a f \rangle \langle c d \rangle \langle c g \rangle \langle e d \rangle [c d]^2 \\
 & + 40 \langle a d \rangle \langle c d \rangle \langle c g \rangle \langle e f \rangle [c d]^2 + 24 \langle a g \rangle \langle b f \rangle \langle c e \rangle^2 [b c] [c e] \\
 & - 48 \langle a g \rangle \langle b e \rangle \langle c f \rangle \langle e d \rangle [b d] [c e] - 106 \langle a f \rangle \langle b e \rangle \langle c g \rangle \langle e d \rangle [b d] [c e] \\
 & + 690 \langle a d \rangle \langle b e \rangle \langle c g \rangle \langle e f \rangle [b d] [c e] - 710 \langle a f \rangle \langle b d \rangle \langle c e \rangle \langle e g \rangle [b d] [c e] \\
 & + 40 \langle a e \rangle \langle b e \rangle \langle c g \rangle \langle e f \rangle [b e] [c e] - 70 \langle a f \rangle \langle b e \rangle \langle c e \rangle \langle e g \rangle [b e] [c e] \\
 & - 40 \langle a g \rangle \langle b e \rangle \langle c f \rangle \langle e f \rangle [b f] [c e] + 560 \langle a f \rangle \langle b e \rangle \langle c g \rangle \langle e f \rangle [b f] [c e]), \tag{6.121}
 \end{aligned}$$

$$\begin{aligned}
 num_{sub}^{(2)B} = & \frac{i}{8} (54 \langle a f \rangle \langle b f \rangle \langle c e \rangle \langle e g \rangle [b f] [c e] - 24 \langle a g \rangle \langle b g \rangle \langle c e \rangle \langle e f \rangle [b g] [c e] \\
 & - 108 \langle a f \rangle \langle b e \rangle \langle c g \rangle \langle e g \rangle [b g] [c e] - 104 \langle a f \rangle \langle c e \rangle \langle c g \rangle \langle e d \rangle [c d] [c e] \\
 & + 108 \langle a e \rangle \langle c f \rangle \langle c g \rangle \langle e d \rangle [c d] [c e] + 664 \langle a d \rangle \langle c e \rangle \langle c g \rangle \langle e f \rangle [c d] [c e] \\
 & - 24 \langle a f \rangle \langle c d \rangle \langle c e \rangle \langle e g \rangle [c d] [c e] - 14 \langle a e \rangle \langle c e \rangle \langle c g \rangle \langle e f \rangle [c e]^2 \\
 & + 706 \langle a f \rangle \langle b f \rangle \langle c e \rangle \langle e g \rangle [b e] [c f] + 44 \langle a f \rangle \langle c f \rangle \langle c g \rangle \langle e d \rangle [c d] [c f] \\
 & + 8 \langle a f \rangle \langle c d \rangle \langle c g \rangle \langle e f \rangle [c d] [c f] - 52 \langle a d \rangle \langle c f \rangle \langle c g \rangle \langle e f \rangle [c d] [c f] \\
 & + 536 \langle a f \rangle \langle c e \rangle \langle c g \rangle \langle e f \rangle [c e] [c f] - 652 \langle a e \rangle \langle c f \rangle \langle c g \rangle \langle e f \rangle [c e] [c f] \\
 & - 16 \langle a f \rangle \langle c e \rangle \langle c f \rangle \langle e g \rangle [c e] [c f] + 8 \langle a g \rangle \langle b g \rangle \langle c f \rangle \langle e d \rangle [b d] [c g] \\
 & - 8 \langle a g \rangle \langle b g \rangle \langle c d \rangle \langle e f \rangle [b d] [c g] - 4 \langle a f \rangle \langle c g \rangle^2 \langle e d \rangle [c d] [c g] \\
 & + 4 \langle a d \rangle \langle c g \rangle^2 \langle e f \rangle [c d] [c g] + 54 \langle a e \rangle \langle c g \rangle^2 \langle e f \rangle [c e] [c g] \\
 & - 108 \langle a f \rangle \langle c e \rangle \langle c g \rangle \langle e g \rangle [c e] [c g] - 32 \langle a f \rangle \langle b f \rangle \langle d g \rangle \langle e d \rangle [b d] [d f] \\
 & - 32 \langle a f \rangle \langle b f \rangle \langle d g \rangle \langle e f \rangle [b f] [d f] + 32 \langle a f \rangle \langle b f \rangle \langle d f \rangle \langle e g \rangle [b f] [d f] \\
 & - 8 \langle a f \rangle \langle b f \rangle \langle d g \rangle \langle e g \rangle [b g] [d f] - 231 \langle a f \rangle \langle c g \rangle \langle d f \rangle \langle e d \rangle [c d] [d f] \\
 & + 8 \langle a f \rangle \langle c f \rangle \langle d g \rangle \langle e d \rangle [c d] [d f] + 183 \langle a d \rangle \langle c g \rangle \langle d f \rangle \langle e f \rangle [c d] [d f] \\
 & + 32 \langle a f \rangle \langle c d \rangle \langle d f \rangle \langle e g \rangle [c d] [d f] - 24 \langle a f \rangle \langle c g \rangle \langle d f \rangle \langle e f \rangle [c f] [d f] \\
 & - 16 \langle a f \rangle \langle c f \rangle \langle d g \rangle \langle e f \rangle [c f] [d f] + 40 \langle a f \rangle \langle c f \rangle \langle d f \rangle \langle e g \rangle [c f] [d f] \\
 & + 16 \langle a f \rangle \langle c g \rangle \langle d g \rangle \langle e f \rangle [c g] [d f] - 16 \langle a f \rangle \langle c g \rangle \langle d f \rangle \langle e g \rangle [c g] [d f] \\
 & - 8 \langle a f \rangle \langle c f \rangle \langle d g \rangle \langle e g \rangle [c g] [d f] + 32 \langle a f \rangle \langle d f \rangle^2 \langle e g \rangle [d f]^2 \\
 & + 8 \langle a g \rangle \langle b f \rangle \langle d g \rangle \langle e d \rangle [b d] [d g] - 32 \langle a f \rangle \langle b d \rangle \langle d g \rangle \langle e g \rangle [b d] [d g] \\
 & + 32 \langle a g \rangle \langle b g \rangle \langle d f \rangle \langle e f \rangle [b f] [d g] - 24 \langle a f \rangle \langle b f \rangle \langle d g \rangle \langle e g \rangle [b f] [d g] \\
 & - 24 \langle a f \rangle \langle c g \rangle \langle d g \rangle \langle e f \rangle [c f] [d g] + 32 \langle a f \rangle \langle c g \rangle \langle d f \rangle \langle e g \rangle [c f] [d g] \\
 & + 32 \langle a f \rangle \langle d f \rangle \langle d g \rangle \langle e g \rangle [d f] [d g] - 506 \langle a f \rangle \langle b d \rangle \langle e d \rangle \langle e g \rangle [b d] [e d] \\
 & - 180 \langle a d \rangle \langle b d \rangle \langle e f \rangle \langle e g \rangle [b d] [e d] - 491 \langle a f \rangle \langle b e \rangle \langle e d \rangle \langle e g \rangle [b e] [e d] \\
 & + 334 \langle a d \rangle \langle b e \rangle \langle e f \rangle \langle e g \rangle [b e] [e d] + 832 \langle a f \rangle \langle b f \rangle \langle e d \rangle \langle e g \rangle [b f] [e d])
 \end{aligned}
 \tag{6.122}$$

and

$$\begin{aligned}
 num_{sub}^{(2)C} = \frac{i}{8} & (32 \langle a f \rangle \langle d f \rangle \langle d g \rangle \langle e g \rangle [d f] [d g] - 506 \langle a f \rangle \langle b d \rangle \langle e d \rangle \langle e g \rangle [b d] [e d] \\
 & - 180 \langle a d \rangle \langle b d \rangle \langle e f \rangle \langle e g \rangle [b d] [e d] - 491 \langle a f \rangle \langle b e \rangle \langle e d \rangle \langle e g \rangle [b e] [e d] \\
 & + 334 \langle a d \rangle \langle b e \rangle \langle e f \rangle \langle e g \rangle [b e] [e d] + 832 \langle a f \rangle \langle b f \rangle \langle e d \rangle \langle e g \rangle [b f] [e d] \\
 & + 6 \langle a f \rangle \langle b d \rangle \langle e f \rangle \langle e g \rangle [b f] [e d] + 54 \langle a f \rangle \langle b d \rangle \langle e g \rangle^2 [b g] [e d] \\
 & - 203 \langle a e \rangle \langle c g \rangle \langle e d \rangle \langle e f \rangle [c e] [e d] - 87 \langle a d \rangle \langle c e \rangle \langle e f \rangle \langle e g \rangle [c e] [e d] \\
 & - 199 \langle a f \rangle \langle c g \rangle \langle e d \rangle \langle e f \rangle [c f] [e d] + 167 \langle a d \rangle \langle c g \rangle \langle e f \rangle^2 [c f] [e d] \\
 & + 40 \langle a f \rangle \langle c f \rangle \langle e d \rangle \langle e g \rangle [c f] [e d] - 24 \langle a f \rangle \langle c d \rangle \langle e f \rangle \langle e g \rangle [c f] [e d] \\
 & - 668 \langle a d \rangle \langle c g \rangle \langle e f \rangle \langle e g \rangle [c g] [e d] + 24 \langle a f \rangle \langle c d \rangle \langle e g \rangle^2 [c g] [e d] \\
 & + 48 \langle a d \rangle \langle d f \rangle \langle e f \rangle \langle e g \rangle [d f] [e d] + 48 \langle a f \rangle \langle d g \rangle \langle e d \rangle \langle e g \rangle [d g] [e d] \\
 & - 48 \langle a d \rangle \langle d f \rangle \langle e g \rangle^2 [d g] [e d] + 16 \langle a g \rangle \langle e d \rangle^2 \langle e f \rangle [e d]^2 \\
 & - 192 \langle a f \rangle \langle e d \rangle^2 \langle e g \rangle [e d]^2 + 89 \langle a d \rangle \langle e d \rangle \langle e f \rangle \langle e g \rangle [e d]^2 \\
 & - 682 \langle a f \rangle \langle b f \rangle \langle e d \rangle \langle e g \rangle [b d] [e f] - 764 \langle a f \rangle \langle b d \rangle \langle e f \rangle \langle e g \rangle [b d] [e f] \\
 & - 70 \langle a f \rangle \langle b e \rangle \langle e f \rangle \langle e g \rangle [b e] [e f] + 78 \langle a f \rangle \langle b f \rangle \langle e f \rangle \langle e g \rangle [b f] [e f] \\
 & - 658 \langle a f \rangle \langle b f \rangle \langle e g \rangle^2 [b g] [e f] + 32 \langle a d \rangle \langle c g \rangle \langle e f \rangle^2 [c d] [e f] \\
 & + 32 \langle a f \rangle \langle c f \rangle \langle e d \rangle \langle e g \rangle [c d] [e f] - 48 \langle a f \rangle \langle c d \rangle \langle e f \rangle \langle e g \rangle [c d] [e f] \\
 & + 195 \langle a e \rangle \langle c g \rangle \langle e f \rangle^2 [c e] [e f] - 740 \langle a f \rangle \langle c g \rangle \langle e f \rangle \langle e g \rangle [c g] [e f] \\
 & + 160 \langle a f \rangle \langle c f \rangle \langle e g \rangle^2 [c g] [e f] - 24 \langle a f \rangle \langle d g \rangle \langle e f \rangle^2 [d f] [e f] \\
 & - 24 \langle a f \rangle \langle d g \rangle \langle e f \rangle \langle e g \rangle [d g] [e f] - 87 \langle a d \rangle \langle e f \rangle^2 \langle e g \rangle [e d] [e f] \\
 & - 740 \langle a f \rangle \langle b d \rangle \langle e g \rangle^2 [b d] [e g] - 70 \langle a f \rangle \langle b e \rangle \langle e g \rangle^2 [b e] [e g] \\
 & + 736 \langle a f \rangle \langle b f \rangle \langle e g \rangle^2 [b f] [e g] - 601 \langle a f \rangle \langle c g \rangle \langle e d \rangle \langle e g \rangle [c d] [e g] \\
 & + 1269 \langle a d \rangle \langle c g \rangle \langle e f \rangle \langle e g \rangle [c d] [e g] - 24 \langle a f \rangle \langle c d \rangle \langle e g \rangle^2 [c d] [e g] \\
 & + 1175 \langle a e \rangle \langle c g \rangle \langle e f \rangle \langle e g \rangle [c e] [e g] + 692 \langle a f \rangle \langle c g \rangle \langle e f \rangle \langle e g \rangle [c f] [e g] \\
 & - 112 \langle a f \rangle \langle c f \rangle \langle e g \rangle^2 [c f] [e g] - 87 \langle a d \rangle \langle e f \rangle \langle e g \rangle^2 [e d] [e g] \\
 & + 32 \langle a f \rangle \langle d f \rangle \langle e g \rangle \langle f g \rangle [d f] [f g] - 48 \langle a f \rangle \langle e g \rangle^2 \langle f g \rangle [e g] [f g]).
 \end{aligned} \tag{6.123}$$

We present the full compact expression for $R_{7:4}^{(2)}$, of which this is a piece, in Section 4.5.8 on page 95.

Reconstruction has greatly reduced the sizes of the expressions produced by aug-

6 Reconstruction of Rational Functions

	$R_{7:1}^{(2)}$	$R_{7:2}^{(2)}$	$R_{7:3}^{(2)}$	$R_{7:4}^{(2)}$	$R_{7:1,1}^{(2)}$	$R_{7:1,2}^{(2)}$	$R_{7:1,3}^{(2)}$	$R_{7:2,2}^{(2)}$	$R_{7:1B}^{(2)}$
File size / KB	5	5	16	13	11	29	13	29	6
Memory usage / MB	0.201	1.21	6.78	0.995	0.757	29.1	5.97	99.3	0.135
LeafCount/ 10^3	7.81	46.8	266	41.3	31.8	1150	248	3930	5.32
Evaluation time / s	0.0938	0.516	2.98	0.422	0.297	12.5	2.27	39.7	0.0625

Table 6.5: Approximate expression sizes and evaluation times for the reconstructed seven-point rational pieces. Comparing to the functions produced using augmented recursion (Table 6.2 on page 156), there is an improvement of three orders of magnitude in most cases. (Note the smaller scale choices used on some rows of this table.)

mented recursion. Table 6.5 collects the sizes and evaluation times of the new compact analytic expressions, which can be compared to those of the augmented recursion versions presented in Table 6.2 on page 156.

6.7 Conclusions

Any technique for generating amplitudes out of multiple contributions will tend to produce increasingly complex results as the number of gluons involved rises. Amplitudes can also be expressed in ways where their symmetries are not manifest, their structure contains unnecessary reference momenta, or they contain spurious apparent poles that cancel in the overall expression. These are all reasons why it may be desirable to reconstruct an analytic amplitude expression in a more compact, symmetric form.

We have shown that by understanding the pole structure, it is possible to postulate a simple ansatz to fit to a given amplitude. This was successfully applied to one-loop amplitudes to obtain new forms free of spurious poles. In the two-loop case, the required ansatz would be too large so we first identify the leading pole structures by hand, from factorisations. This was demonstrated on the seven-point all-plus helicity partial amplitudes, obtaining the compact, analytic forms presented in Chapter 4.

A new behaviour was also identified at seven-point in spinor product manipulations. Whereas spurious poles in lower-point factorisations could be trivially removed by a certain manipulation, this fails for seven-point algebra and above. That the removal of spurious poles, and therefore the reconstruction process itself, experiences a discontinuity in difficulty at a particular number of momenta was unexpected. Techniques for addressing this were presented and will be useful in any future work involving amplitudes of at least seven gluons.

7 Conclusions

This thesis presents a number of new results in Yang–Mills amplitude calculations. We use the methods of four dimensional unitarity and augmented recursion to obtain two-loop results, specifying all the structures of a colour decomposition. These techniques give rise to simplification, particularly with the choice of all-plus helicity, because they reduce the problem to an essentially one-loop one. We also make a more general contribution to augmented recursion by describing an intuitive algorithmic way to obtain the currents required by the process. Lastly, there is discussion of amplitude reconstruction, for when the results of a calculation require further manipulation to reach a compact form with manifest symmetry.

In Chapter 3, the method used to derive the full colour six-point two-loop amplitude with all-plus helicity was outlined. The complete amplitude was published in ref. [59] as the outcome of collaboration. This author’s contribution is featured in the chapter, relating to the rational piece and its reconstruction in a compact form.

Chapter 4 follows with the calculation of the full colour seven-point two-loop amplitude, in a compact, analytic form. The polylogarithmic parts are obtained using unitarity cuts and agree with the n -point form described in ref. [62]. The remaining rational parts are then calculated using augmented recursion. The partial amplitude piece $R_{7:1B}^{(2)}$ agrees with the n -point postulate of ref. [63].

In Chapter 5, the currents used in augmented recursion are explored in greater detail. A procedure for deriving currents is proposed, then shown to reproduce a previous five-point result. Two new currents required for the full colour seven-point amplitude are obtained.

Finally, Chapter 6 discusses the algebraic forms taken by amplitude expressions. A number of one-loop partial amplitudes are re-expressed to remove spurious poles, making them more suitable for use in recursive methods. The seven-point two-loop amplitude result of Chapter 4 is also reconstructed using factorisations and ansatzes, to remove reference momenta and bring it to a manifestly symmetric, compact form.

The results obtained in this thesis are not only of theoretical interest, but are also relevant to experimental tests of the Standard Model, such as those undertaken at high-

7 Conclusions

energy particle colliders. The methodology used could also be applied straightforwardly to all-plus helicity amplitudes of greater gluon number. Such calculations would rely increasingly on the reconstruction techniques explored in this thesis, if a compact result is desired. An extension of the procedure to the single-minus helicity is another logical next step. The main difference from an all-plus calculation is that the four-dimensional unitarity step no longer behaves like a one-loop problem, although the algebra remains simpler than in a D -dimensional approach. For the rational structures, augmented recursion is anticipated to apply as before. Ultimately, the goal is to achieve a more general understanding of two-loop Yang–Mills amplitudes, which compact, symmetric results are a step towards.

Bibliography

- [1] A. Huss, J. Huston, S. Jones, and M. Pellen, “Les Houches 2021: Physics at TeV Colliders: Report on the Standard Model Precision Wishlist,” Jul 2022.
- [2] S. Amoroso *et al.*, “Les Houches 2019: Physics at TeV Colliders: Standard Model Working Group Report,” in *11th Les Houches Workshop on Physics at TeV Colliders: PhysTeV Les Houches*, Mar 2020.
- [3] R. L. Workman *et al.*, “Review of Particle Physics: 9. Quantum Chromodynamics,” *PTEP*, vol. 2022, p. 083C01, 2022.
- [4] C.-N. Yang and R. L. Mills, “Conservation of Isotopic Spin and Isotopic Gauge Invariance,” *Phys. Rev.*, vol. 96, pp. 191–195, 1954.
- [5] B. Feng and M. Luo, “An Introduction to On-shell Recursion Relations,” *Front. Phys. (Beijing)*, vol. 7, pp. 533–575, 2012.
- [6] M. L. Mangano, S. J. Parke, and Z. Xu, “Duality and Multi - Gluon Scattering,” *Nucl. Phys. B*, vol. 298, pp. 653–672, 1988.
- [7] Z. Bern and D. A. Kosower, “Color decomposition of one loop amplitudes in gauge theories,” *Nucl. Phys. B*, vol. 362, pp. 389–448, 1991.
- [8] Z. Bern, A. De Freitas, and L. J. Dixon, “Two loop helicity amplitudes for gluon-gluon scattering in QCD and supersymmetric Yang-Mills theory,” *JHEP*, vol. 3, p. 18, 2002.
- [9] S. G. Naculich, “All-loop group-theory constraints for color-ordered SU(N) gauge-theory amplitudes,” *Phys. Lett. B*, vol. 707, pp. 191–197, 2012.
- [10] A. C. Edison and S. G. Naculich, “SU(N) group-theory constraints on color-ordered five-point amplitudes at all loop orders,” *Nucl. Phys. B*, vol. 858, pp. 488–501, 2012.

Bibliography

- [11] V. Del Duca, A. Frizzo, and F. Maltoni, “Factorization of tree QCD amplitudes in the high-energy limit and in the collinear limit,” *Nucl. Phys. B*, vol. 568, pp. 211–262, 2000.
- [12] V. Del Duca, L. J. Dixon, and F. Maltoni, “New color decompositions for gauge amplitudes at tree and loop level,” *Nucl. Phys. B*, vol. 571, pp. 51–70, 2000.
- [13] S. J. Parke and T. R. Taylor, “An Amplitude for n Gluon Scattering,” *Phys. Rev. Lett.*, vol. 56, p. 2459, 1986.
- [14] F. A. Berends and W. T. Giele, “Recursive Calculations for Processes with n Gluons,” *Nucl. Phys. B*, vol. 306, pp. 759–808, 1988.
- [15] P. De Causmaecker, R. Gastmans, W. Troost, and T. T. Wu, “Multiple Bremsstrahlung in Gauge Theories at High-Energies. 1. General Formalism for Quantum Electrodynamics,” *Nucl. Phys. B*, vol. 206, pp. 53–60, 1982.
- [16] F. A. Berends, R. Kleiss, P. De Causmaecker, R. Gastmans, W. Troost, and T. T. Wu, “Multiple Bremsstrahlung in Gauge Theories at High-Energies. 2. Single Bremsstrahlung,” *Nucl. Phys. B*, vol. 206, pp. 61–89, 1982.
- [17] R. Kleiss and W. J. Stirling, “Spinor Techniques for Calculating p anti- $p \rightarrow W^+ / Z^0 + \text{Jets}$,” *Nucl. Phys. B*, vol. 262, pp. 235–262, 1985.
- [18] Z. Xu, D.-H. Zhang, and L. Chang, “Helicity Amplitudes for Multiple Bremsstrahlung in Massless Nonabelian Gauge Theories,” *Nucl. Phys. B*, vol. 291, pp. 392–428, 1987.
- [19] R. Britto, F. Cachazo, B. Feng, and E. Witten, “Direct proof of tree-level recursion relation in Yang-Mills theory,” *Phys. Rev. Lett.*, vol. 94, p. 181602, 2005.
- [20] E. Witten, “Perturbative gauge theory as a string theory in twistor space,” *Commun. Math. Phys.*, vol. 252, pp. 189–258, 2004.
- [21] F. Cachazo, P. Svrcek, and E. Witten, “MHV vertices and tree amplitudes in gauge theory,” *JHEP*, vol. 9, p. 6, 2004.
- [22] R. Britto, F. Cachazo, and B. Feng, “New recursion relations for tree amplitudes of gluons,” *Nucl. Phys. B*, vol. 715, pp. 499–522, 2005.
- [23] K. Risager, “A Direct proof of the CSW rules,” *JHEP*, vol. 12, p. 3, 2005.

- [24] G. 't Hooft and M. J. G. Veltman, “Regularization and Renormalization of Gauge Fields,” *Nucl. Phys. B*, vol. 44, pp. 189–213, 1972.
- [25] Z. Bern, A. De Freitas, L. J. Dixon, and H. L. Wong, “Supersymmetric regularization, two loop QCD amplitudes and coupling shifts,” *Phys. Rev. D*, vol. 66, p. 85002, 2002.
- [26] R. K. Ellis and J. C. Sexton, “QCD Radiative Corrections to Parton Parton Scattering,” *Nucl. Phys. B*, vol. 269, pp. 445–484, 1986.
- [27] Z. Bern and D. A. Kosower, “The Computation of loop amplitudes in gauge theories,” *Nucl. Phys. B*, vol. 379, pp. 451–561, 1992.
- [28] Z. Bern, L. J. Dixon, D. C. Dunbar, and D. A. Kosower, “Fusing gauge theory tree amplitudes into loop amplitudes,” *Nucl. Phys. B*, vol. 435, pp. 59–101, 1995.
- [29] G. Passarino and M. J. G. Veltman, “One Loop Corrections for $e^+ e^-$ Annihilation Into $\mu^+ \mu^-$ in the Weinberg Model,” *Nucl. Phys. B*, vol. 160, pp. 151–207, 1979.
- [30] R. E. Cutkosky, “Singularities and discontinuities of Feynman amplitudes,” *J. Math. Phys.*, vol. 1, pp. 429–433, 1960.
- [31] Z. Bern, L. J. Dixon, D. C. Dunbar, and D. A. Kosower, “One loop n point gauge theory amplitudes, unitarity and collinear limits,” *Nucl. Phys. B*, vol. 425, pp. 217–260, 1994.
- [32] Z. Bern, L. J. Dixon, and D. A. Kosower, “One loop amplitudes for $e^+ e^-$ to four partons,” *Nucl. Phys. B*, vol. 513, pp. 3–86, 1998.
- [33] G. Ossola, C. G. Papadopoulos, and R. Pittau, “Reducing full one-loop amplitudes to scalar integrals at the integrand level,” *Nucl. Phys. B*, vol. 763, pp. 147–169, 2007.
- [34] W. T. Giele, Z. Kunszt, and K. Melnikov, “Full one-loop amplitudes from tree amplitudes,” *JHEP*, vol. 4, p. 49, 2008.
- [35] R. Britto, F. Cachazo, and B. Feng, “Generalized unitarity and one-loop amplitudes in $N=4$ super-Yang-Mills,” *Nucl. Phys. B*, vol. 725, pp. 275–305, 2005.
- [36] S. D. Badger, “Direct Extraction Of One Loop Rational Terms,” *JHEP*, vol. 1, p. 49, 2009.

Bibliography

- [37] Z. Bern, L. J. Dixon, and D. A. Kosower, “On-shell recurrence relations for one-loop QCD amplitudes,” *Phys. Rev. D*, vol. 71, p. 105013, 2005.
- [38] D. C. Dunbar, J. H. Eittle, and W. B. Perkins, “Augmented Recursion For One-loop Amplitudes,” *Nucl. Phys. B Proc. Suppl.*, vol. 205-206, pp. 74–79, 2010.
- [39] S. D. Alston, D. C. Dunbar, and W. B. Perkins, “Complex Factorisation and Recursion for One-Loop Amplitudes,” *Phys. Rev. D*, vol. 86, p. 85022, 2012.
- [40] S. D. Alston, D. C. Dunbar, and W. B. Perkins, “ n -point amplitudes with a single negative-helicity graviton,” *Phys. Rev. D*, vol. 92, no. 6, p. 65024, 2015.
- [41] D. A. Kosower, “Next-to-maximal helicity violating amplitudes in gauge theory,” *Phys. Rev. D*, vol. 71, p. 45007, 2005.
- [42] S. Catani, “The Singular behavior of QCD amplitudes at two loop order,” *Phys. Lett. B*, vol. 427, pp. 161–171, 1998.
- [43] Z. Kunszt, A. Signer, and Z. Trocsanyi, “Singular terms of helicity amplitudes at one loop in QCD and the soft limit of the cross-sections of multiparton processes,” *Nucl. Phys. B*, vol. 420, pp. 550–564, 1994.
- [44] Z. Bern, L. J. Dixon, and D. A. Kosower, “A Two loop four gluon helicity amplitude in QCD,” *JHEP*, vol. 1, p. 27, 2000.
- [45] E. W. N. Glover, C. Oleari, and M. E. Tejeda-Yeomans, “Two loop QCD corrections to gluon-gluon scattering,” *Nucl. Phys. B*, vol. 605, pp. 467–485, 2001.
- [46] T. Ahmed, J. Henn, and B. Mistlberger, “Four-particle scattering amplitudes in QCD at NNLO to higher orders in the dimensional regulator,” *JHEP*, vol. 12, p. 177, 2019.
- [47] S. Badger, H. Frellesvig, and Y. Zhang, “A Two-Loop Five-Gluon Helicity Amplitude in QCD,” *JHEP*, vol. 12, p. 45, 2013.
- [48] C. Cheung and D. O’Connell, “Amplitudes and Spinor-Helicity in Six Dimensions,” *JHEP*, vol. 7, p. 75, 2009.
- [49] S. Badger, G. Mogull, A. Ochirov, and D. O’Connell, “A Complete Two-Loop, Five-Gluon Helicity Amplitude in Yang-Mills Theory,” *JHEP*, vol. 10, p. 64, 2015.
- [50] Z. Bern, J. J. M. Carrasco, and H. Johansson, “New Relations for Gauge-Theory Amplitudes,” *Phys. Rev. D*, vol. 78, p. 85011, 2008.

-
- [51] T. Gehrmann, J. M. Henn, and N. A. Lo Presti, “Analytic form of the two-loop planar five-gluon all-plus-helicity amplitude in QCD,” *Phys. Rev. Lett.*, vol. 116, no. 6, p. 62001, 2016. Erratum: *Phys. Rev. Lett.*, vol. 116, no. 18, p. 189903, 2016.
- [52] D. C. Dunbar and W. B. Perkins, “Two-loop five-point all plus helicity Yang-Mills amplitude,” *Phys. Rev. D*, vol. 93, no. 8, p. 85029, 2016.
- [53] S. Badger, D. Chicherin, T. Gehrmann, G. Heinrich, J. M. Henn, T. Peraro, P. Wasser, Y. Zhang, and S. Zoia, “Analytic form of the full two-loop five-gluon all-plus helicity amplitude,” *Phys. Rev. Lett.*, vol. 123, no. 7, p. 71601, 2019.
- [54] D. C. Dunbar, J. H. Godwin, W. B. Perkins, and J. M. W. Strong, “Color Dressed Unitarity and Recursion for Yang-Mills Two-Loop All-Plus Amplitudes,” *Phys. Rev. D*, vol. 101, no. 1, p. 016009, 2020.
- [55] S. Badger, C. Brønnum-Hansen, H. B. Hartanto, and T. Peraro, “Analytic helicity amplitudes for two-loop five-gluon scattering: the single-minus case,” *JHEP*, vol. 1, p. 186, 2019.
- [56] A. von Manteuffel and R. M. Schabinger, “A novel approach to integration by parts reduction,” *Phys. Lett. B*, vol. 744, pp. 101–104, 2015.
- [57] S. Abreu, J. Dormans, F. Febres Cordero, H. Ita, B. Page, and V. Sotnikov, “Analytic Form of the Planar Two-Loop Five-Parton Scattering Amplitudes in QCD,” *JHEP*, vol. 5, p. 84, 2019.
- [58] D. C. Dunbar, G. R. Jehu, and W. B. Perkins, “Two-loop six gluon all plus helicity amplitude,” *Phys. Rev. Lett.*, vol. 117, no. 6, p. 61602, 2016.
- [59] A. R. Dalgleish, D. C. Dunbar, W. B. Perkins, and J. M. W. Strong, “Full color two-loop six-gluon all-plus helicity amplitude,” *Phys. Rev. D*, vol. 101, no. 7, p. 76024, 2020.
- [60] D. C. Dunbar, J. H. Godwin, G. R. Jehu, and W. B. Perkins, “Analytic all-plus-helicity gluon amplitudes in QCD,” *Phys. Rev. D*, vol. 96, no. 11, p. 116013, 2017.
- [61] D. A. Kosower and S. Pögel, “A Unitarity Approach to Two-Loop All-Plus Rational Terms,” [arXiv:2206.14445 \[hep-ph\]](https://arxiv.org/abs/2206.14445), Jun 2022.
- [62] A. R. Dalgleish, D. C. Dunbar, W. B. Perkins, and J. M. W. Strong, “Full color two-loop seven-gluon all-plus helicity amplitude,” in preparation.

Bibliography

- [63] D. C. Dunbar, W. B. Perkins, and J. M. W. Strong, “ n -point QCD two-loop amplitude,” *Phys. Rev. D*, vol. 101, no. 7, p. 76001, 2020.
- [64] D. C. Dunbar, W. B. Perkins, and E. Warrick, “The Unitarity Method using a Canonical Basis Approach,” *JHEP*, vol. 6, p. 56, 2009.
- [65] D. C. Dunbar, G. R. Jehu, and W. B. Perkins, “The two-loop n -point all-plus helicity amplitude,” *Phys. Rev. D*, vol. 93, no. 12, p. 125006, 2016.
- [66] D. A. Kosower, “Light Cone Recurrence Relations for QCD Amplitudes,” *Nucl. Phys. B*, vol. 335, pp. 23–44, 1990.
- [67] C. Schwinn and S. Weinzierl, “Scalar diagrammatic rules for Born amplitudes in QCD,” *JHEP*, vol. 5, p. 6, 2005.
- [68] Z. Bern, L. J. Dixon, and D. A. Kosower, “Two-loop $g \rightarrow gg$ splitting amplitudes in QCD,” *JHEP*, vol. 8, p. 12, 2004.
- [69] A. C. Edison and S. G. Naculich, “Symmetric-group decomposition of $SU(N)$ group-theory constraints on four-, five-, and six-point color-ordered amplitudes,” *JHEP*, vol. 9, p. 69, 2012.
- [70] D. C. Dunbar and W. B. Perkins, “ $\mathcal{N} = 4$ supergravity next-to-maximally-helicity-violating six-point one-loop amplitude,” *Phys. Rev. D*, vol. 94, no. 12, p. 125027, 2016.
- [71] Z. Bern, L. J. Dixon, and D. A. Kosower, “One loop corrections to five gluon amplitudes,” *Phys. Rev. Lett.*, vol. 70, pp. 2677–2680, 1993.
- [72] G. Mahlon, “Multi - gluon helicity amplitudes involving a quark loop,” *Phys. Rev. D*, vol. 49, pp. 4438–4453, 1994.